

***HvALOG1*, an ALOG Transcription Factor Regulates
Spikelet Meristem Determinacy and Organ Boundary
Formation in Barley Inflorescence**

Dissertation
zur Erlangung des
Doktorgrades der Agrarwissenschaften (Dr. agr.)

der

Naturwissenschaftlichen Fakultät III
Agrar- und Ernährungswissenschaften,
Geowissenschaften und Informatik

der Martin-Luther-Universität
Halle-Wittenberg

vorgelegt von
Herrn M.Sc. Guojing Jiang

Gutachter:

Prof. Dr. Thorsten Schnurbusch

Prof. Dr. Laura Rossini

verteidigt am: 23.01.2023

Contents

Acknowledgments	I
Abbreviations	III
1. Introduction	1
1.1 Morphology and boundary formation of inflorescence.....	2
1.1.1 Inflorescence architecture in plants.....	2
1.1.2 Boundary formation of the inflorescence.....	6
1.2 Inflorescence architecture in grasses	13
1.3 The development of barley inflorescence	16
1.4 The genetic basis of inflorescence architecture in barley	17
1.4.1 Regulation of row-type.....	18
1.4.2 Spikelet meristem identity	22
1.4.3 Spikelet meristem determinacy	25
1.5 Aims of this study	26
2. Materials and Methods	28
2.1 Plant materials	28
2.2 Methods.....	29
2.2.1 Phenotyping	29
2.2.2 Genomic DNA isolation.....	29
2.2.3 Whole-genome sequencing and introgression identification.....	30
2.2.4 Genetic analysis of <i>Flo.a</i> locus in the F2 population	30
2.2.5 Map-based cloning of <i>Flo.a</i>	31
2.2.6 Identification of new <i>flo.a</i> alleles through allelism tests	31
2.2.7 Inducing knock-out (KO) mutation by CRISPR-Cas9 gene-editing system....	31
2.2.8 Construction of GFP report plants	32
2.2.9 Scanning Electron Microscopy (SEM) analysis.....	32
2.2.10 mRNA isolation and qRT-PCR	33
2.2.11 RNA sequencing.....	33
2.2.12 RNA-seq data analysis.....	34
2.2.13 Phylogenetic analysis	34
2.2.14 Phytohormone measurements.....	35
2.2.15 Subcellular localization.....	35
2.2.16 3D-reconstruction.....	35
2.2.17 Light microscopy.....	36
2.2.18 mRNA <i>in situ</i> hybridization.....	36
2.3. Data contribution by the author and the collaborators toward the present thesis	36

3. Results	39
3.1 Morphological differences between wild-type and <i>flo.a</i> mutant	39
3.1.1 <i>flo.a</i> mutant produces extra spikelets.....	39
3.1.2 The development of lateral spikelets is suppressed in <i>flo.a</i> mutant	45
3.1.3 The fertility of extra spikelets in <i>flo.a</i> mutant is inhibited	45
3.1.4 Determinacy loss of the spikelet meristem in <i>flo.a</i> mutant.....	46
3.1.5 The organ boundary and identity of glumes in the central spikelets are affected in <i>flo.a</i> mutant	47
3.1.6 The formation of extra spikelets interferes with the normal vascular patterning.....	49
3.2 Map-based cloning of <i>Flo.a</i>	54
3.2.1 <i>flo.a</i> is a recessive mutant.....	54
3.2.2 Fine-Mapping of the <i>Flo.a</i> locus	54
3.2.3 Validation of <i>Flo.a</i> candidate in allelic <i>flo-like</i> mutants	56
3.3 <i>Flo.a</i> encodes an ALOG protein	58
3.4 Site-directed mutagenesis of <i>HvALOG1</i> and <i>HvALOG2</i> by RNA-guided CRISPR-Cas9	60
3.5 The conserved role of ALOG proteins across grasses and eudicots lineages	63
3.6 <i>HvALOG1</i> protein localizes to the nucleus	66
3.7 Temporal and spatial expression pattern of <i>HvALOG1</i>	67
3.8 <i>HvALOG1</i> involves in the regulation of organ boundary formation and development	71
3.9 <i>HvALOG1</i> represses ectopic activity of cell division in meristems	73
3.10 Potential functional redundancy of ALOG protein family members occurs early during spike development	74
3.11 Dysregulation of hormonal homeostasis involves extra organ formation	76
4. Discussion	79
4.1 <i>flo.a</i> is an ‘extra spikelet’ mutant but not an ‘extra floret’ mutant	79
4.2 <i>HvALOG1</i> is involved in the regulation of spikelet meristem activity and the establishment of floral organ boundary	81
4.2.1 Conserved roles of ALOG genes in the regulation of plant inflorescence formation.....	81
4.2.2 <i>HvALOG1</i> specifies the spikelet meristem determinacy in a non-cell autonomous manner	82
4.2.3 <i>HvALOG1</i> cell autonomously regulates the establishment of floral organ boundary.....	84
4.3 Putative regulatory factors of spikelet meristem determinacy and floral organ boundary formation in barley	86
4.3.1 <i>HvALOG1</i> may integrate the boundary genes to regulate the development of lateral organs.....	86

4.3.2 Putative role for low auxin during barley boundary formation	87
4.3.3 Potential effect of meristem identity/determinacy genes	87
4.3.4 Promotion of organ development genes may induce extra spikelet organs .	89
4.4 Barley ALOG family members are functionally redundant in early spike development.....	90
4.5 Application of extra spikelets in breeding	92
5. Outlook.....	94
6. Summary	96
7. Zusammenfassung	98
8. References	101
9. Appendix	125
10. Curriculum Vitae	142
11. Eidesstattliche Erklärung/Declaration under Oath	144
12. Erklärung über bestehende Vorstrafen und anhängige Ermittlungsverfahren/Declaration concerning Criminal Record and Pending Investigations	145

Acknowledgments

This work has been carried out in the research group Plant Architecture (PBP) at the Leibniz Institute of Plant Genetics and Crop Plant Research, Gatersleben, Germany since September 2017.

First and foremost, I would like to express my gratitude to Prof. Dr. Thorsten Schnurbusch for allowing me to join his team, and for his constant advice, support, and constructive discussions. As my supervisor, Thorsten has provided me with instruction that goes beyond my Ph.D. thesis. He is providing me with a stimulating and energetic environment rich in opportunities, challenges, and freedoms to grow as a scientist. During these five years of training, not only did I learn the logic of plant science and honed my thinking skills, but also strengthened my belief in continuing to engage in scientific research.

Also, I would like to thank the postdocs of the PBP group, Dr. Ravi Koppolu, and Dr. Yongyu Huang, for supervising and supporting my research. Dr. Koppolu introduced this project and suggested the study direction to me. Dr. Huang provided careful and enthusiastic guidance in experiments. I appreciate their readiness for scientific discussions, stimulating ideas and constructive suggestions.

I'd like to express my sincere thanks to everyone who assisted me in completing my experiments. Especially for Dr. Twan Rutten, who helped me with most of the imaging work and broadened my thinking about the function of the *HvALOG1* gene. Also, I would like to thank Dr. Jochen Kumlehn, Dr. Götz Hensel, Robert Hoffie, and the PRB barley transformation team; the functional analysis for *HvALOG1* is inseparable from a precise and efficient plant transformation system. I also appreciate Dr. Jeyaraman Rajaraman for his great work on cellular localization experiments and Dr. Shuangshuang Zhao for her excellent contribution to mRNA *in situ* hybridization assays. Many thanks to Dr. Naser Poursarebani for sharing the sequence information and primers regarding the *flo.a* mutant. Special thanks are given to Dr. Yudelsy Antonia Tandron Moya and the MPE team for supporting hormone measurement and analysis. The advancement of this research is inextricably linked to good plant cultivation management; a special thank you to all the gardeners for their hard work to take care of barley plants.

I especially thank Prof. Dr. Nicolaus von Wirén, Dr. Zhongtao Jia, and Dr. Ying Liu for their helpful advice on hormone measurement. Also, I would like to give my special thanks to Dr. Martin Mascher, Yu Guo, and Anne Fiebig for bioinformatics analysis. Thanks to Prof. Dr. Ganggang Guo for his patience and detailed guidance on my projects. In addition, I would like to thank my office colleague and my friend Nandhakumar Shanmugaraj, Roop Kamal, and Constanze Schmidt for supporting and encouraging each other in the process of exploring the unknown journey of plants.

Many thanks to all members of the PBP team for the lively talks and innovative ideas at the laboratory meeting. Thanks to everyone at the IPK who helped with this project.

Thanks to all staff at the IPK administration, especially to Dr. Britt Leps, who made the daily life of my family in Germany more convenient.

Finally, my deepest and sincere gratitude to my family for their endless support and companionship, and for giving me great freedom and energy to continue pursuing my dreams.

Abbreviations

%	Percent
°C	degree Celsius
µg	Microgram
µl	Microliter
µM	Micromolar
AA	Amino Acid
ABA	Abscisic acid
AxM	Axillary Meristem
AP	Awn Primordium
AdS	Additional Spikelet
Bd	Brachypodium distachyon
BIM	Branch Inflorescence Meristem
BLAST	Basic Local Alignment Search Tool
BLASTN	Nucleotide BLAST
BLASTP	Protein BLAST
BM	Branch Meristem
bp	base pair
BR	Brassinosteroid
BW	Bowman
cDNA	Complementary DNA
CDS	Coding sequence
CHIP	Chromatin Immunoprecipitation
CK	Cytokinins
cM	centi Morgan
cm	Centimeter
CRISPR	Clustered Regularly Interspaced Short Palindromic Repeats
CS	Central Spikelet
CSM	Central Spikelet Meristem
cv	Cultivar
ddH ₂ O	Double distilled water
DEPC	Diethylpyrocarbonate
DNA	Deoxyribonucleic acid
DR	Double Ridge

EDTA	Ethylenediaminetetraacetic acid
EMS	Ethyl Methanesulfonate
F1	First filial generation
F2	Second filial generation
F3	Third filial generation
FAO	The Food and Agriculture Organization
FDR	False discovery rate
FM	Floral Meristem
g	Gram
GA	Gibberellins
GrA	Green Anther
GFP	Green Fluorescent Protein
Gb	Gigabase
GO	Gene ontology
GP	Glume Primordium
gRNA	Guide RNA
GWAS	Genome-Wide Association Study
H	Hour
HC	High Confidence
Hv	Hordeum vulgare
IAA	Indole-3-acetic acid
IM	Inflorescence Meristem
INDEL	Insertion and Deletion
IPK	Leibniz Institute of Plant Genetics and Crop Plant Research
Kb	Kilobase pairs
LBD	LOB (Lateral Organ Boundary) Domain
LC	Low Confidence
LC-MS	Liquid Chromatography-Mass Spectrometry
LOB	Lateral Organ Boundary
LP	Lemma Primordium
LR	Leaf ridge
LS	Lateral Spikelet
LSM	Lateral Spikelet Meristem
mRNA	messenger RNA

miRNA	micro RNA
Mb	Megabase pairs
mg	Milligram
ml	Milliliter
ML	maximum likelihood
mM	Millimolar
NCBI	National Centre for Biotechnology Information
ng	Nanogram
NGS	Next Generation Sequencing
NIL	Nearly isogenic lines
NN	Node Number Per Spike
NordGen	Nordic Genetic Resource Center
ORF	Open Reading Frame
<i>Os</i>	<i>Oryza sativa</i>
PBM	Primary Branch Meristems
P-value	Probability value
PCR	Polymerase Chain Reaction
QC	Quality Control
qRT-PCR	quantitative Real Time-Polymerase Chain Reaction
RIN	RNA Integrity Number
RNA	Ribonucleic acid
RNAi	RNA interference
RNA-seq	RNA sequencing
SAM	Shoot Apical Meristem
SBM	Secondary Branch Meristem
SEM	Scanning Electron Microscopy
SIM	Secondary Inflorescence Meristem
SM	Spikelet Meristem
SNP	Single Nucleotide Polymorphism
SP	Stamen Primordium
SPM	Spikelet Pair Meristem
SR	Spikelet Ridge
TF	Transcription Factor
TILLING	Targeting Induced Local Lesions IN Genomes

TM	Triple Mound
TSM	Triple Spikelet Meristem
USDA–ARS	United States Department of Agriculture-Agricultural Research Service
UTRs	Untranslated Region
WGS	Whole-genome sequencing
WA	White Anther
WT	Wild type
<i>Zm</i>	<i>Zea mays</i>

1. Introduction

Barley (*Hordeum vulgare* L.) is an important cereal crop produced in the world and total output is ranked 4th after maize, rice, and wheat (Figure 1.1) (<https://www.fao.org/faostat/en/#data/QCL/visualize>). Its major uses are as food, for brewing and feeding, and to a further extent, for human nutrition (Geng *et al.*, 2022). In the face of the ever-increasing dietary demands of humans and their livestock, high-grain yield is the main breeding goal in developing cultivars. Studying the regulation mechanism of complex agronomic traits in barley may provide a greater contribution to genetic improvement for yield, which is very critical to global food security (Bailey-Serres *et al.*, 2019; Liu *et al.*, 2021; Yu and Li, 2021).

The grain-producing flowers (or florets) of cereals, such as wheat, maize, rice, and barley, form on reproductive branches known as spikelets, which group together on a structure known as an inflorescence. Inflorescence structure is one of the most important traits of plants because it determines the number of seeds/grains produced (Hake, 2008). Grass inflorescences show significant diversity in the number and arrangement of spikelets and florets. This particularity is fully utilized in the domesticated process to increase yields and promote harvest. A better understanding of the developmental processes that determine potential seed/grain numbers could enhance the efficiency of breeding programs aimed at improving grain yield.

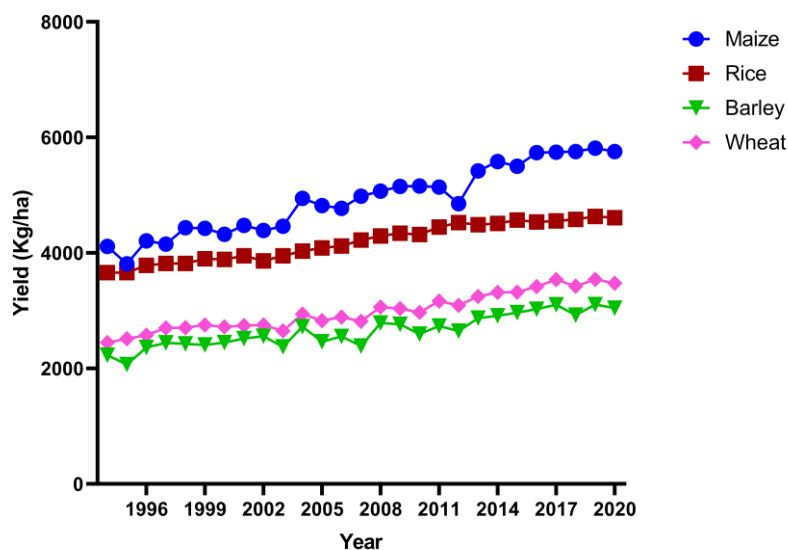


Figure 1.1. The yield Trends of the world's four most important cereal crops. Data was obtained from The Food and Agriculture Organization (FAO, 2022).

1.1 Morphology and boundary formation of inflorescence

1.1.1 Inflorescence architecture in plants

A distinctive feature of plants is the wide variety of forms that exist in nature. This wide morphological diversity comes from the types, shapes, proportions, and positions of different plant organs. The number and arrangement of plant organs (mainly shoots, leaves, flowers and following fruits) are the basis of plant architecture (Benlloch *et al.*, 2007). The area where the flowers cluster on the plant and are regularly arranged in a certain way is called the inflorescence (Weberling, 1992). Inflorescence morphology varies greatly among different plant species. Because of the strong influence on pollination and fruit-set, inflorescence forms most likely have a determining role in the success of reproduction (Benlloch *et al.*, 2007; Wyatt, 1982).

Plant development is controlled by the activity of the shoot apical meristem (SAM) and the root apical meristem (RAM), which are both formed during embryogenesis (Xue *et al.*, 2020). All aerial parts of the plants, such as shoots, leaves, and flowers, are formed from the SAM, while roots are formed from the RAM (Teo *et al.*, 2014). The post-embryo development depends on the function and activity of the meristems (Xue *et al.*, 2020). Therefore, the fate and maintenance of meristematic organizations are vital to plant growth. The formation of inflorescences originates from the continuous activity of the SAM, which is a group of stem cells existing at the tip of the growth axis (Barlow, 2002). In different developmental stages of the plant, the specific identity of the SAM is changed according to the timing and position of its occurrence (Kaufmann *et al.*, 2010a). In the vegetative phase, the SAM continuously generates aerial organs, such as shoots and leaves (Xue *et al.*, 2020). When the vegetative growth reaches a certain stage, upon appropriate environmental signals, plants enter the reproductive stage, which is specifically manifested as the transformation of the SAM into the inflorescence meristem (IM) (Xue *et al.*, 2020). The various patterns of the IM during reproductive growth in different species produce diverse inflorescence architectures (Han *et al.*, 2014). Ongoing activity of the IM produces branches or flowers. In turn, the branching pattern and flower position determine the basic shape of the inflorescence (Benlloch *et al.*, 2007; Teo *et al.*, 2014).

In the process of reproductive growth, the inflorescence morphology of plants is diverse. The inflorescence architecture can be divided into determinate or indeterminate and simple or compound (Zhu and Wagner, 2020). Specifically, if the IM

ends with a terminal flower, the inflorescences are classified as determinate, and conversely, it is indeterminate; a simple inflorescence shows flowers produced on the main rachis but a compound inflorescence shows flowers produced on branches (Zhu and Wagner, 2020). For example, *Tulipa* sp. plants have an extremely determinate and simple inflorescence architecture, whereas *Arabidopsis* and *Antirrhinum* have indeterminate and simple inflorescences; many *Leguminosae* species, such as pea (*Pisum sativum* L.) and *Medicago truncatula*, form indeterminate and compound inflorescences; but the inflorescence of tomato (*Solanum lycopersicum* L.) is determinate and compound (Figure 1.2) (Benlloch *et al.*, 2015; Benlloch *et al.*, 2007; Zhu and Wagner, 2020). In addition to these four typical inflorescence structures, there are other more diverse and complex inflorescence types in the plant kingdom (Benlloch *et al.*, 2007).

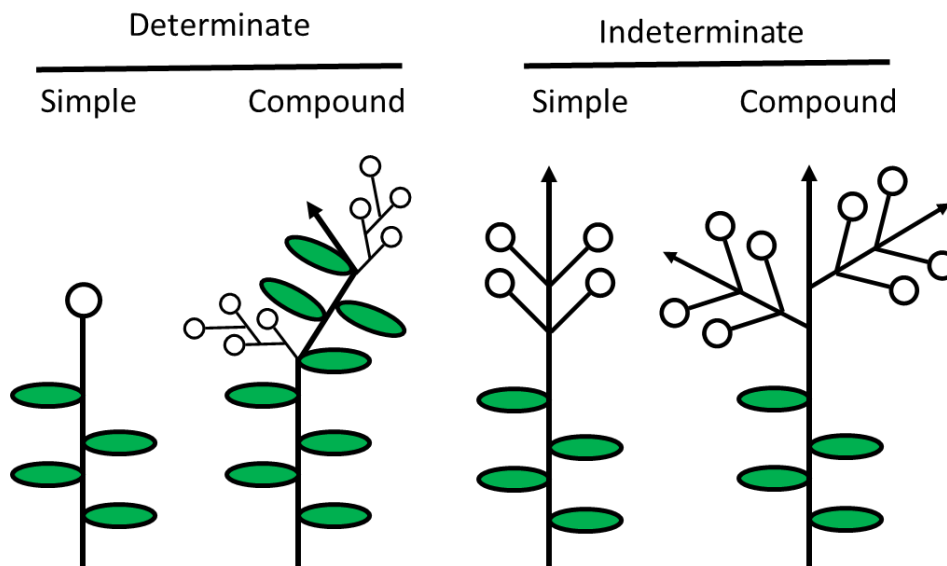


Figure 1.2. Different types of inflorescence architecture. Diagrams of classical architecture of inflorescences in plants. Circles represent flowers; arrows represent indeterminate shoots. The figure was modified from (Benlloch *et al.*, 2015).

The establishment of the inflorescence architecture is majorly derived from the activity and development of the axillary meristem (AxM), which is a type of meristem that produces axillary bud and axillary shoot in leaf axils, thereby determining the branching degree and the number of flowers being formed (Wang *et al.*, 2018; Zhu and Wagner, 2020). During the phase transition, the vegetative SAM is first transformed into an IM, and next AxMs are either transformed into branches or differentiated into flowers (Wang *et al.*, 2018). In the inflorescences of *Arabidopsis*, the floral meristem (FM) is directly produced by the IM; whereas in rice panicles, the IM firstly forms multiple

primary and secondary branch meristems (PBM and SBM), which continue producing spikelet meristems (SMs) (Li *et al.*, 2021b). The spikelet is the basic unit of inflorescence in grasses, featured by sterile bracts and a spikelet axis bearing one to multiple florets; in tomato, new IMs emerge at the flank of each previous sympodial IM before being differentiated into FMs (Benlloch *et al.*, 2015; Kellogg, 2022; Teo *et al.*, 2014; Wang *et al.*, 2018). The branching pattern that initiates SMs or FMs determines the diversity of plant inflorescence shape.

The unique architecture of the plant inflorescence largely determines the reproduction success and yield of wild and cultivated plants (Zhu and Wagner, 2020). An in-depth understanding of the underlying regulatory mechanisms of inflorescence formation makes it possible to optimize the plant architecture of crop species in an ideal way and finally increase crop yields. The genetic regulation of inflorescence structure has been widely reported (Benlloch *et al.*, 2015; Teo *et al.*, 2014; Wang *et al.*, 2018; Yuan *et al.*, 2020; Zhu and Wagner, 2020). Here, we briefly summarize a simplified model and corresponding key genes that control the maturation of meristems and regulate the architecture of inflorescences in the model plant *Arabidopsis*.

In *Arabidopsis*, the classic CLAVATA3 (CLV3)-WUSCHEL (WUS) feedback regulation loop regulates SAM activity and size, as well as IM formation and differentiation (Wang *et al.*, 2021). The *WUS* gene, encoding a homeodomain transcription factor (TF), plays a role in promoting the expression of the *CLV3*. In turn, as a secreted peptide, the *CLV3* is recognized by receptor complexes, leucine-rich repeats (LRRs) kinases *CLV1* and *CLV2*, which, when activated, signals back to suppress *WUS* expression to stabilize the stem cell population (Wang *et al.*, 2018; Wang *et al.*, 2021). Mutations in *CLV1*, *CLV2*, or *CLV3* drive over-proliferation of stem cells, leading to enlargement of IM and FM, increasing the number of flowers and floral organs (Clark *et al.*, 1997; Fletcher, 1999; Jeong *et al.*, 1999). Mechanisms of conserved CLV signaling underlying meristem size regulation and inflorescence specification have also been discovered in rice and maize (Fletcher, 2018).

Inflorescence branching is influenced by growth patterns of determinate and indeterminate (Wang *et al.*, 2018). In *Arabidopsis*, *FLOWERING LOCUS T (FT)* is a critical flower-promoting gene, whereas *TERMINAL FLOWER 1 (TFL1)* is an inhibitor of flowering. *TFL1* encodes a phosphatidyl-ethanolamine-binding protein and plays an important role in promoting indeterminacy of the AxMs and the IMs (Bradley *et al.*,

1997; Conti and Bradley, 2007). Mutations in the *TFL1* cause the conversion of *Arabidopsis* inflorescence from indeterminate to determinate fate (IM to FM), resulting in a terminal flower produced in the main inflorescence stem and replacement of lateral branches by solitary axillary flowers (Benlloch *et al.*, 2015).

In opposition to *TFL1* to maintain the IM fate, *LEAFY* (*LFY*) and the *APETALA1* (*AP1*) are essential to specify FM identity in *Arabidopsis*. *LFY* is a plant-specific TF expressed in the flanks of the IM at a very early developing stage and promotes the formation of FM (Benlloch *et al.*, 2015; Blazquez *et al.*, 1997; Maizel *et al.*, 2005; Weigel *et al.*, 1992). Mutants of *lfy* lose the FM identity, meaning that FM is converted back into IM, resulting in a substitution of first flowers by shoots (Benlloch *et al.*, 2015). *AP1* encodes a MADS-box TF, which has a function in the specification of FM identity together with *LFY*. Up-regulation of expression of *AP1* is later than *LFY* and limited to the young floral primordium that has determined the floral fate (Alejandra Mandel *et al.*, 1992; Bowman *et al.*, 1993; Hempel *et al.*, 1997; Weigel and Meyerowitz, 1993). The transcriptional level of *AP1* is directly up-regulated by *LFY* (Wagner *et al.*, 1999). In *ap1* mutants, the flowers are partially converted into inflorescence shoots and floral organs such as sepal and petal have severe morphological and homeotic alterations (Bowman *et al.*, 1993). Moreover, other related MADS-box TFs, such as *CAULIFLOWER* (*CAL*) and *FRUITFULL* (*FUL*) play redundant functions to *AP1* to promote FM identity (Ferrandiz *et al.*, 2000).

The interactions of *TFL1*, *LFY*, and *AP1* constitute the basic model of controlling meristem identity during the development of *Arabidopsis* inflorescence (Benlloch *et al.*, 2015). In this model, *TFL1* plays a critical role in promoting and maintaining IM indeterminacy. *TFL1* is expressed in the IM and suppresses the expression of *AP1* and *LFY* in the IM, preventing premature conversion and termination of the inflorescence. In fact, *AP1* and *LFY* are ectopically expressed in the IMs of *tfl1* mutants, and as a result, these meristems take on the floral identity and generate terminal and axillary flowers (Alejandra Mandel *et al.*, 1992; Bradley *et al.*, 1997; Weigel *et al.*, 1992). On the contrary, *LFY* and *AP1* specify the FM identity and promote the formation of flowers (Benlloch *et al.*, 2015). *LFY* and *AP1* genes are expressed in meristems formed at the flanks of the IM and repress the expression *TFL1*, promoting FMs to acquire floral identity and flower formation by up-regulating floral organ identity genes (Kaufmann *et al.*, 2010b; Liljegren *et al.*, 1999; Parcy *et al.*, 1998; Wagner *et al.*, 1999). This mutual

inhibitory effect between *TFL1* and *LFY/AP1* explains the maintenance of an indeterminate IM and the formation of flanking FMs in *Arabidopsis* (Benlloch *et al.*, 2015; Wagner, 2017; Zhu and Wagner, 2020).

1.1.2 Boundary formation of the inflorescence

Plant organogenesis depends on the formation of boundaries, which are domains where growth is restricted, separating cells with different identities (Žádníková and Simon, 2014). Boundary cells exist between the meristem and the newly formed primordium and maintain a different orientational developmental balance by forming an interface to separate the meristem and the growing primordium (Hepworth and Pautot, 2015). The boundary can be divided into two types: between meristems and organs (M-O), and between organs and organs (O-O) (Yu and Huang, 2016). In flower development, the M-O boundaries are required for the initiation of flower primordium from the IM, whereas the establishment of the O-O boundaries are dependent on the development of the floral organ (Figure 1.3) (Aida and Tasaka, 2006; Yu and Huang, 2016). During the development of plant inflorescence, the formation of boundary is a complex process that requires the integration of intercellular signals and gene regulatory networks, including precise control of cell division, expansion, and differentiation (Žádníková and Simon, 2014). Here, we briefly summarize the regulation network and critical genes that control the boundary formation in inflorescences.

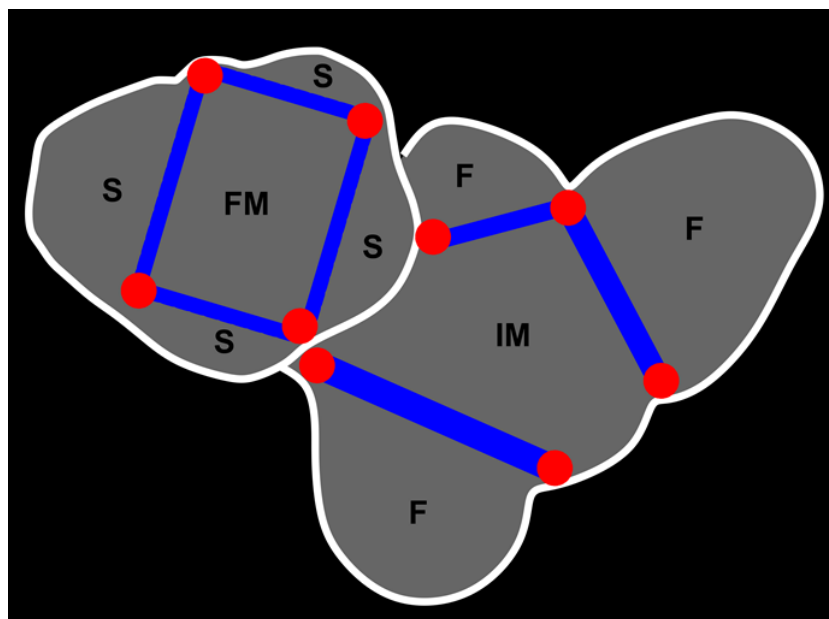


Figure 1.3. Organ boundaries in the *Arabidopsis* inflorescence apex. The boundary positions are marked with colors. The blue lines represent the M–O boundary; the red dots represent the O–O the

boundary. IM, inflorescence meristem; F, floral primordium; FM, floral meristem; S, sepal primordium. The figure is modified from (Aida and Tasaka, 2006).

During the development of the *Arabidopsis* inflorescence, the SAM initially transits into an IM, which further differentiates into FM, which finally develops into a complete flower. Several floral fate genes, such as *LFY* and *AP1*, are up-regulated in response to flowering-inducing signals, for example, the *FT* pathway, to promote the formation of FM and floral organ primordia (Irish, 2010). The formation of flowers firstly requires the establishment of an M-O boundary, which results in the separation of the central and peripheral domains in the IM (Yu and Huang, 2016). Restriction of cell division within the boundary is controlled by a gene regulatory network. The key regulatory genes include *SHOOT MERISTEMLESS (STM)*, *CUP-SHAPED COTYLEDON (CUC)* and *Lateral Organ Boundary (LOB)* (Bell *et al.*, 2012; Borghi *et al.*, 2007; Jasinski *et al.*, 2005; Luo *et al.*, 2021; Richardson and Hake, 2019; Wang *et al.*, 2016a). These genes are specifically expressed at boundaries to retard growth, thereby driving boundary formation. Loss or down-regulation of the boundary genes usually leads to organ fusion and AxMs defects, whereas overexpression of that leads to the ectopic formation of AxMs (Gómez-Mena and Sablowski, 2008; Greb *et al.*, 2003; Hepworth and Pautot, 2015; Hibara *et al.*, 2006; Lee *et al.*, 2009; Luo *et al.*, 2021; Raman *et al.*, 2008; Spinelli *et al.*, 2011; Vroemen *et al.*, 2003).

Arabidopsis STM encodes a class-I KNOTTED1-LIKE HOMEODOMAIN (KNOXI) TF which plays an important role in the formation and maintenance of the SAM as well as AxM by preventing cell differentiation (Endrizzi *et al.*, 1996; Hay and Tsiantis, 2010; Lenhard *et al.*, 2002; Long *et al.*, 1996). *STM* is expressed throughout the SAM, but down-regulated in primordial cells on the periphery of the SAM, which differentiate into the earliest lateral organ primordium (Endrizzi *et al.*, 1996; Hay and Tsiantis, 2010; Long and Barton, 2000; Long *et al.*, 1996). Loss-of-function mutants of *STM* cannot produce a SAM, failing to form lateral organs (Barton and Poethig, 1993; Long *et al.*, 1996). In addition to controlling the fate of the SAM, *STM* also plays a critical role in boundary regulation together with *CUC* genes (Balkunde *et al.*, 2017; Scofield *et al.*, 2018).

Arabidopsis CUC genes, including *CUC1*, *CUC2* and *CUC3*, which belong to the NAC-domain TF family, function redundantly in controlling the initiation of the SAM and formation of shoot organ boundaries during the entire development processes, including M-O and O-O boundary formation (Aida *et al.*, 1997; Aida *et al.*, 1999; Raman

et al., 2008; Vroemen *et al.*, 2003). Loss-of-function of *CUC* genes typically causes the absence of boundary, which results in failing initiation of AxM or fusion of organs. *CUC* genes are expressed at the domain of boundaries and are required to activate *STM* expression to promote initiation meristems (Aida *et al.*, 1999; Takada *et al.*, 2001). Overexpression of *CUC1* leads to the initiation of ectopic meristems, supporting *STM* expression induced by *CUC1* and *CUC2* (Takada *et al.*, 2001). In turn, *STM* activates the expression of the *CUC1/2/3* at the boundaries to separate meristems with different fates (Spinelli *et al.*, 2011). *STM* and *CUC1* constitute a direct attenuated positive transcriptional feedback loop, driving *STM* to activate the expression of *CUC1*-targeted *miR164c*, which explains that *STM* and *CUC1* have different expressions patterns on meristem and organ boundaries, respectively (Balkunde *et al.*, 2017; Scofield *et al.*, 2018).

Other class-I KNOX genes include *BREVIPEDICELLUS (BP)/KNAT1*, *KNAT2* and *KNAT6*. *KNAT2* has no direct effect on the activity of meristems (Belles-Boix *et al.*, 2006; Byrne *et al.*, 2002). *BP* and *KNAT6* work in conjunction with *STM* to maintain the activity of the SAM and the formation of boundaries (Belles-Boix *et al.*, 2006; Byrne *et al.*, 2002; Nidhi *et al.*, 2021). *BP* participates in regulating the development of internode and promotes SAM maintenance together with *STM* (Byrne *et al.*, 2002; Douglas *et al.*, 2002; Smith and Hake, 2003; Venglat *et al.*, 2002). *KNAT6* contributes to SAM maintenance and boundary establishment during embryogenesis by the *STM-CUC* module (Belles-Boix *et al.*, 2006). The residual activity of meristem in *stm* mutants was eliminated by the inactivation of *KNAT6*. Meanwhile, *KNAT6* and *STM* work together with other regulators *BELLRINGER (BLR)* and *LATERAL SUPPRESSOR (LAS)* to serve as downstream targets of *CUC1* and *CUC2* to regulate the formation of shoot meristem as well as separation of cotyledons (Aida *et al.*, 2020). In addition, KNOX genes promote Cytokinins (CK) levels and reduce Gibberelline (GA) levels to keep cell division and inhibit cell differentiation to maintain the activity of the meristem (Yu and Huang, 2016). This process is mainly through simultaneously promoting CK biosynthetic gene *isopentenyl transferase 7 (IPT7)* and repressing GA biosynthetic *GA20-oxidases* (Jasinski *et al.*, 2005; Sakamoto *et al.*, 2001; Yanai *et al.*, 2005).

The *Arabidopsis* *LOB* gene is a member of the plant-specific TF family with a highly conserved *LOB* domain and displays specific expression in organ boundaries (Shuai

et al., 2002). Loss-of-function *lob* mutant exhibits organ fusion phenotype, whereas ectopic expression of *LOB* causes changes in the shape and size of leaves and floral organs and infertile phenotype (Bell *et al.*, 2012; Shuai *et al.*, 2002). *LOB* forms a feedback loop with Brassinosteroids (BR) to regulate the accumulation of local BR to limit the growth of the boundary domain (Bell *et al.*, 2012). In maize, *Ramosa2 (RA2)*, encoding a protein with a LOB domain, specifies meristem determinacy by patterning the fate of stem cells in AxMs (Bortiri *et al.*, 2006). *RA2* is expressed in a predicted boundary domain of the AxM formation. Mutants of *ra2* show increased branching with long and indeterminate branches replacing short ones (Bortiri *et al.*, 2006). In addition, barley *Six-rowed spike 4 (VRS4)*, the barley ortholog of the *RA2* gene, plays a critical role in controlling SM determinacy. Mutations in the *VRS4* gene result in the production of supernumerary spikelets and florets (Koppolu *et al.*, 2013).

Arabidopsis BLADE-ON-PETIOLE1 (BOP1) and *BOP2* are another group of important genes for meristem maintenance and organ differentiation that determine the architecture of leaf, inflorescence and flower (Hepworth and Pautot, 2015; Wang *et al.*, 2016a). *BOP1/2* genes encode a NON-EXPRESSOR OF PATHOGENESIS-RELATED GENES1-like TF, containing a BTB/POZ domain and are expressed at lateral organ boundaries (Ha *et al.*, 2004; Norberg *et al.*, 2005). During leaf development, *BOP1/2* genes repress the expression of the class-I KNOX genes to regulate cell differentiation and growth by activating the expression of *ASYMMETRIC LEAVES2 (AS2)*, a gene involved in the establishment of the leaf vein system, at the boundary (Jun *et al.*, 2010). In contrast, *BOP1/2* genes show an opposite model to control inflorescence architecture. The expression of *BOP1/2* is restricted to pedicel axils and promotes the formation of an abscission zone in flower development (McKim *et al.*, 2008). Both *bop1* and *bop2* mutants formed fused and/or fasciated inflorescences and produced multi-flowers on the same node (Ha *et al.*, 2007). *BOP1/2* genes interact with *BP-PENNYWISE (PNY)* to control the architecture of the *Arabidopsis* inflorescence (Khan *et al.*, 2012b). Gain-of-function of *BOP1/2* genes causes the defects of inflorescence architecture in *bp* and *pny* mutants. The BP-PNY module restricts the expression of *BOP1/2*, *KNAT2*, *KNAT6* and *Arabidopsis thaliana homeobox 1* gene (*ATH1*) to boundary domains at the floral shoot base (Khan *et al.*, 2012a; Khan *et al.*, 2012b; Ragni *et al.*, 2008; Zhao *et al.*, 2015). Whereas *BOP1/2* genes promote *ATH1* and *KNAT6* expression, forming a module to opposes BP-PNY activity to regulating inflorescence architecture (Khan *et al.*, 2012a; Khan *et al.*, 2012b).

In addition, *BOP1/2* genes are also involved in *PNY* and *POUND-FOOLISH (PNF)* pathway-mediated flowering regulation (Khan *et al.*, 2015). *PNY* and *PNF*, two related BEL1-like homeobox genes, are essential for flowering by repressing the expression of *BOP1/2* genes and their downstream genes *KNAT6* and *ATH1* to induce flowering. *PNY* directly inhibits *BOP1/2* in the shoot stem and maintains its expression at the boundaries (Khan *et al.*, 2015; Khan *et al.*, 2012a; Khan *et al.*, 2012b). In the *pny* mutant, ectopic expression of *BOP1/2* in the SAM reduces mRNA level of a bZIP TF *FD*, which is a binding partner of *FT*, required for the activation of *LYF* and *AP1* (Andres *et al.*, 2015). The double Mutant of *pny pnf* is unable to produce flowers, driven by misexpression of *BOP1/2*, *KNAT6* and *ATH1*, preventing the accumulation of FM identity genes, such as *LFY*, *CAL* and *AP1*, required for flower production (Khan *et al.*, 2015). Therefore, expressional restriction of *BOP1/2-ATH1-KNAT6* in the lateral boundary is critical for the integrity and specification of FM in the *PNY-PNF* pathway. In barley, *HvLax-a* and *HvCul4*, the orthologs of *Arabidopsis BOP1/2* genes, are involved in inflorescence development, and regulation of the formation of leaf and tillering, respectively (Jost *et al.*, 2016; Tavakol *et al.*, 2015).

Arabidopsis boundary gene *HANABA TARANU (HAN)*, encoding a GATA-3 TF, plays a role in flower development (Ding *et al.*, 2015; Zhao *et al.*, 2004b). *HAN* is specifically expressed at the boundary of inflorescence M-O and floral O-O (Ding *et al.*, 2015; Zhao *et al.*, 2004b). The mutations in *HAN* cause fused sepals and reduce the number of petals and stamens (Zhao *et al.*, 2004b). *HAN* regulates meristem organization by interacting with two meristem regulators *BP* and *ARGONAUTE 10/PINHEAD (PNH)*, a member of the ARGONAUTE family that interacts with *miR166/165* to regulate meristem maintenance (Ding *et al.*, 2015; Ji *et al.*, 2011; Liu *et al.*, 2009; Zhu *et al.*, 2011). Moreover, *HAN* regulates floral organ development by directly promoting the expression of *BOP2* and an organ primordium-specific gene *JAGGED (JAG)*, a putative C2H2 zinc finger TF that shapes lateral organs (Dinneny *et al.*, 2006; Dinneny *et al.*, 2004; Ohno *et al.*, 2004) (Ding *et al.*, 2015; Hepworth *et al.*, 2005; Jun *et al.*, 2010; McKim *et al.*, 2008; Norberg *et al.*, 2005; Xu *et al.*, 2010). In addition, *HAN* directly upregulates the expression of *CYTOKININ OXIDASE 3 (CKX3)* to reduce CK levels at the boundary, suppressing cell division activity (Ding *et al.*, 2015).

Phytohormone gradients determine the formation of the boundary in the inflorescence. Various stage-specific genes are involved in regulating the distribution of growth-

promoting hormones, such as auxin and BR to inhibit cell division or differentiation at the boundary domain (Luo *et al.*, 2021; Yu and Huang, 2016).

The local maximum of auxin determines the initiation of floral primordia in *Arabidopsis*, which originates from the transport of auxin-mediated by auxin efflux transporter gene *PINFORMED1* (*PIN1*) (Zhu and Wagner, 2020). The depletion of auxin driven by directional transport of auxin causes a reduced cell division and growth rate in the presumable boundary between new primordium and meristem, resulting in the establishment of the boundary (Yu and Huang, 2016; Žádníková and Simon, 2014). Mutations in *PIN1* and the auxin-responsive transcription factor *MONOPTEROS* (*MP*) result in naked inflorescence stems lacking flowers, which is related to the incorrect expression of *STM*, *LFY* and *CUC* genes in the peripheral region of SAM (Aida *et al.*, 2002; Przemeck *et al.*, 1996; Vernoux *et al.*, 2000; Yu and Huang, 2016). In the reproductive stage, *MP* responds to auxin and directly activates *LFY*, which in turn directly regulates the auxin pathway through the forward loop (Yamaguchi *et al.*, 2013).

BR plays an important role in plant growth and stress response, and its temporal and spatial distribution pattern affects the formation of the boundary in plant architecture (Bell *et al.*, 2012; Espinosa-Ruiz *et al.*, 2017; Gendron *et al.*, 2012; Li and He, 2020; Nolan *et al.*, 2020). The low-level BR is related to boundary formation. In the *lob* mutant, excessive accumulation of BR contributes to organ fusion phenotype. *LOB* directly activates the expression of *PHYB ACTIVATION TAGGED SUPPRESSOR1* (*BAS1*), a gene encoding cytochrome P450 enzyme related to BR-inactivating, to negatively regulate the accumulation of BR at the boundary domain. In addition, BR regulates the accumulation of *LOB*. Therefore, *LOB* and BR signaling display a negative feedback loop to regulate the accumulation of local BR in organ boundaries (Bell *et al.*, 2012). Two master TFs in responding to BR, *BRASSINAZOLE RESISTANT 1* (*BZR1*) and *BR1EMS-SUPPRESSOR 1* (*BES1*) can directly or indirectly inhibit the expression of boundary genes, such as *CUC* genes, *LOB* and *LATERAL ORGAN FUSION1*, at the boundary domain (Espinosa-Ruiz *et al.*, 2017; Gendron *et al.*, 2012). Low levels of *BZR1* and *BES1* contribute to the formation of boundaries. These data indicate that the BR signaling pathway involved in cell division activities is a key factor in organ boundary formation.

In addition to forming the correct M-O boundary, the development of the flower also requires the establishment of the O-O boundary, to separate the floral organs in the

same and adjacent whorl (Yu and Huang, 2016). The *Arabidopsis* flower consists of four regularly arranged concentric whorls, including sepals, petals, stamens and carpels. Many genes specify M-O boundaries and flower O-O boundaries, such as *CUC* genes (Hibara *et al.*, 2006; Ishida *et al.*, 2000; Takada *et al.*, 2001; Taoka *et al.*, 2004; Vroemen *et al.*, 2003), *BOP1/2* genes (Ha *et al.*, 2007; Hepworth *et al.*, 2005) and *HAN* (Ding *et al.*, 2015; Zhao *et al.*, 2004b). The expression of *CUC* genes is limited in boundaries between organ primordia (Ishida *et al.*, 2000; Takada *et al.*, 2001). Mutants of *CUC* genes display the fusion of floral organs in the adjacent whorl (Takada *et al.*, 2001; Vroemen *et al.*, 2003). *CUC* genes are at the center of the regulatory network for the formation of floral organ boundaries. Several genes that are directly or indirectly regulated by *CUC* genes contribute to the separation of the floral organs and maintain boundaries, including *ATH1*, *LATERAL ORGAN FUSION1 (LOF1)* which is an MYB domain TF (Gendron *et al.*, 2012; Gomez *et al.*, 2011), *ORGAN BOUNDARY1/LIGHT-DEPENDENT SHORT HYPOCOTYLS3 (OBO1/LSH3)*, and *LSH4*, which are two members of the *Arabidopsis* LSH1 and *Oryza* G1 (ALOG) family (Cho and Zambryski, 2011; Takeda *et al.*, 2011).

In *Arabidopsis* flowers, the expression of *CUC1* and *CUC2* were regulated by three *microRNA164* genes (*MIR164a*, *b* and *c*) (Laufs *et al.*, 2004). Among the three *MIR164* genes, *miR164c*, characterized as *Early Extra Petals1 (EEP1)*, performed most of the negative regulation for *CUC1* and *CUC2* to prevent the formation of extra petals in early flower development (Baker *et al.*, 2005). Meanwhile, all three *MIR164* genes were regulated by *RABBIT EARS (RBE)*, encoding a C2H2 zinc finger TF (Huang *et al.*, 2012; Takeda *et al.*, 2004). *RBE* negatively regulates *EEP1* expression via directly interacting with its promoter (Huang *et al.*, 2012). Therefore, *RBE* fine-tunes *miR164* expression to regulate *CUC1* and *CUC2* genes, finally regulating the development of sepal and petal (Huang *et al.*, 2012).

The *Arabidopsis* *HAWAIIAN SKIRT (HWS)* gene, which encodes an F-box TF, regulates organ growth and floral organ abscission (González-Carranza *et al.*, 2007; Levin *et al.*, 1998). The loss-of-function *HWS* results in fused sepals and increased organ size (González-Carranza *et al.*, 2007; González-Carranza *et al.*, 2017; Levin *et al.*, 1998). *HWS* has recently been reported to be involved in the regulation of floral organ number and boundary formation via modulating the transcript levels of *miR164* and *CUC1* (González-Carranza *et al.*, 2017).

The *Arabidopsis SUPERMAN (SUP)* gene encodes a C2H2-type zinc finger protein, playing a critical role in maintaining the boundary between stamen and carpel whorl (third and fourth floral whorl) (Sakai *et al.*, 2000; Sakai *et al.*, 1995). The expression of *SUP* is limited to a ring-like domain at the boundary between the third and fourth whorl, circumventing the expression region of *CLV3* or *WUS*, and affecting floral stem cells in a non-cell autonomous manner (Sakai *et al.*, 2000; Xu *et al.*, 2018). The mutation of *sup* results in the ectopic expression of *APETALA3 (AP3)* and *PISTILATA (PI)* in the fourth whorl and promotes the formation of extra stamens (Bowman *et al.*, 1992; Sakai *et al.*, 2000). The expression of *SUP* is controlled by other flower development regulators, including *LFY*, *AP3*, *PI* and *AGAMOUS (AG)* (Sakai *et al.*, 2000). In addition, *SUP* affects the cell proliferation and growth of stamens and carpels primordia, possibly through its regulation of auxin- and cytokinin-regulated processes (Nibau *et al.*, 2011). Additionally, *SUP* coordinates floral organogenesis and floral meristem size by fine-tuning auxin biosynthesis (Xu *et al.*, 2018). Therefore, *SUP* may regulate the activities of stamen and carpel primordia by coordinating a series of key regulators and hormonal pathways for the development of floral organs, maintaining the correct structure and boundary of the third and fourth whorl.

1.2 Inflorescence architecture in grasses

The grass family contains approximately 12,000 recognized taxa, including a series of important cereals, such as rice (*Oryza sativa* L.), maize (*Zea mays* L.), wheat (*Triticum aestivum* L.), barley (*Hordeum vulgare* L.), and sorghum (*Sorghum bicolor* (L.) Moench) (Kellogg, 2022). The grain yield of cereals is determined by inflorescence architecture, which therefore is one of the most important agricultural traits to be modified for production and harvesting during domestication and breeding (Gibson, 2009; Yuan *et al.*, 2020).

In morphology, the inflorescence architecture of grasses exhibits complex and diverse characteristics, and this is largely derived from the activities of the IM and AxM (Kellogg *et al.*, 2013; Koppolu and Schnurbusch, 2019). In general, according to the developmental pattern of lateral organs, for example, branches and spikelets that originated from AxMs, the inflorescence architectures in grasses are typically classified into three categories, namely "racemes" (spikelets have peduncle on a single central uniaxial axis), "spikes" (spikelets lacking pedicels, for example, wheat, barley, and

Brachypodium distachyon) and "panicles" (with higher-order branches, such as rice and sorghum) (Figure 1.4) (Yuan *et al.*, 2020). Spike and panicle are mainly two types of grass inflorescences. In spike-type inflorescences, all spikelets are attached directly to nodes of the inflorescence stem (Gibson, 2009; Kyozyuka, 2014). The number and density of nodes and spikelets attached determine the basic pattern of spike-type inflorescences. In contrast, the panicle-type inflorescence has primary and secondary, or more advanced branches, ending with one or more spikelets (Harrington, 1977). This inflorescence is generally determined by a branching pattern that involves the number of and relative length of the branches and spikelets per internode (Li *et al.*, 2021b). These two types of complex inflorescence patterns give rise to conspicuous variations among grass taxa (Yuan *et al.*, 2020).

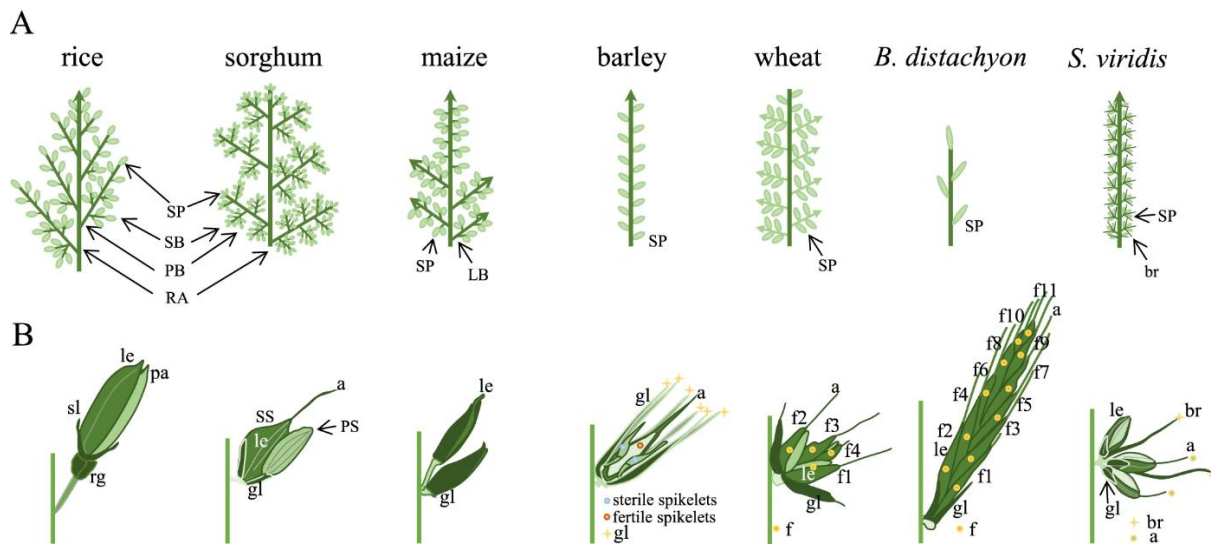


Figure 1.4. Model of the inflorescences (A) and spikelets (B) in grasses. a, awn; br, bristle; le, lemma; f, flower; gl, glume; LB, lateral branch; pa, palea; PB, primary branch; PS, pedicellate spikelet; RA, rachis; rg, rudimentary glume; SB, secondary branch; sl, sterile lemma; SP, spikelet; SS, sessile spikelets. The figure is taken from (Yuan *et al.*, 2020).

From a developmental perspective, the IMs of grasses are not directly transformed into FMs to generate the floret but differentiated into higher-level meristems, for example, branch meristem (BM), which subsequently produce SMs (Kellogg, 2022). After the transition from the vegetative SAM to the reproductive IM, the IM produces bracts and new meristems, which are formed in the axils of the inflorescence (Figure 1.5) (Kellogg, 2022; Tanaka *et al.*, 2013). These new meristems have two developmental fates: one is to initiate a determinate SM and then transform directly to the FM, which produces the floret; another is to keep its indeterminate fate and to initiate the BM, which forms new meristems or the SM (Figure 1.5) (Kellogg, 2022). In this way, new branches give

birth to spikelets, which are formed iteratively to varying degrees, owing to the timing of the transformation and maturation of meristems, and finally display diverse inflorescence shapes.

The spikelet develops from the SM, with two bracts called glumes being firstly produced, followed by one or more florets (Kellogg, 2022). In addition, in some grass species, there are additional peripheral organs, such as the sterile lemma in rice and the bristles of *Setaria* (Yuan *et al.*, 2020). The floret of grasses usually consists of external non-reproductive, bract-like organs (lemma and palea) and internal reproductive organs (stamen, pistil, and ovary) (Kellogg, 2022). The FMs that eventually develop into florets originate from the meristematic transition and further differentiation of the SM (Yuan *et al.*, 2020). In grass species, the timing of the termination of SM activity has a wide range, resulting in one or multiple florets within a single spikelet (Koppolu and Schnurbusch, 2019). Typically, a determinate spikelet produces a fixed number of florets, for example, one floret in the rice panicle and the barley spike and two florets in the maize tassel. In contrast, indeterminate spikelets produce various numbers of florets, for example, the spikelets of wheat and *Brachypodium* show a diverse number of florets. This is mainly due to the interaction of genetics and environment (Figure 1.4) (Bommert *et al.*, 2005; Yuan *et al.*, 2020).

Although there is a huge variation in the number of florets in a spikelet on a scale from 1 to up of 50, the indeterminate growth events within a single spikelet do not have an impact on the whole inflorescence structure (Kyozyuka, 2014). This is mainly because the spikelets are always orderly organized in the spikes or panicles so that they form a sequential inflorescence (Gibson, 2009). Therefore, the spikelet is considered the terminal differentiation unit of the inflorescence, rather than the florets. In short, the IM can differentiate into BMs or SMs on its flanks, and the BMs themselves may produce BMs or differentiate into SMs. The IM itself may eventually transform into SM, or it may become consumed during producing lateral structure (Kellogg *et al.*, 2013).

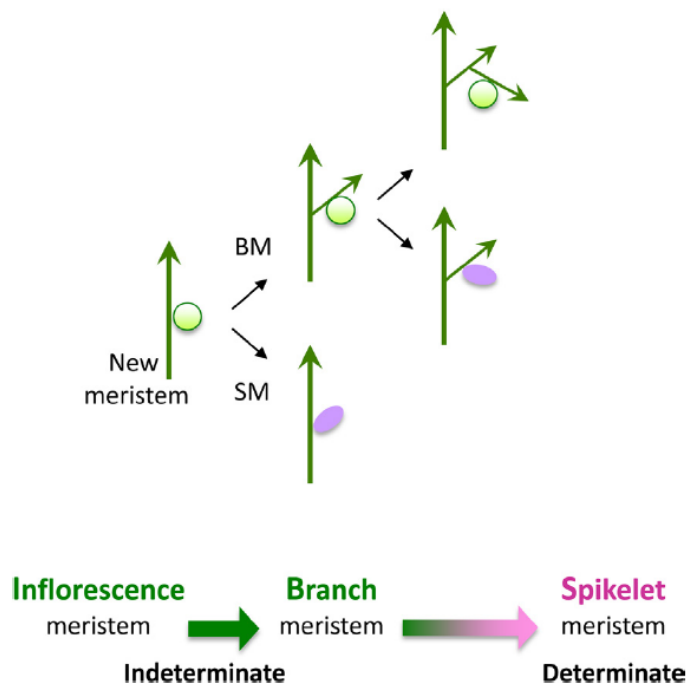


Figure 1.5. Model of Meristem development in grasses. IM, inflorescence meristem; BM, branch meristem; SM, spikelet meristem; FM, floral meristem. The figure is taken from (Kyoizuka, 2014).

1.3 The development of barley inflorescence

The grass tribe *Triticeae* includes approximately 400–500 wild taxa (Sakuma *et al.*, 2011). Most *Triticeae* species, including wheat, barley, and rye (*Secale cereale* L.), display spike-type inflorescence architecture, which is different from other main crop species, such as maize, rice, and sorghum (Larson *et al.*, 2013). Each spike normally forms multiple sessile spikelets that are inserted on one node and can produce one or several florets (Larson *et al.*, 2013). The number of spikelets and florets is different depending on the species. The IM of wheat displays a determinate identity, with a terminal spikelet at the apical end of the inflorescence, but the SM stays indeterminate to typically produce three or four fertile florets and multiple degraded florets (Figure 1.4) (Koppolu and Schnurbusch, 2019). However, all *Hordeum* species, including barley, display opposite phenotypes to the wheat in inflorescence (Koppolu and Schnurbusch, 2019). The IM of barley has an indeterminate fate, resulting in a continuous differentiation of SM. The barley SM has a determinate identity and only produces a single floret (Figure 1.4) (Koppolu and Schnurbusch, 2019).

A key feature of barley spikes is the spikelet triplet (one central spikelet, CS, and two lateral spikelets, LS) emerging on the same rachis node (Kirby and Appleyard, 1984). The triple spikelet meristem (TSM) develops from the rachis nodes in a distichous pattern, giving rise to the row-type of the barley spike (Koppolu and Schnurbusch, 2019; Sakuma and Schnurbusch, 2020). Morphologically, the barley spike can typically be divided into two-rowed and six-rowed (Zwirek *et al.*, 2019). This mainly affects the fertility of LSs. In wild barley and so-called two-rowed cultivars, the development of the floral organs of the two LSs is inhibited, leading to sterile spikelets. However, the development of the CS is not affected and can be fertilized normally to produce mature grains (Komatsuda *et al.*, 2007). Because the fertile CSs and grains are regularly arranged on the opposite sides of the rachis, the spike shows a two-rowed spike phenotype. In contrast, so-called six-rowed barleys have fertile central as well as LSs, and six rows of grains are regularly arranged around the rachis, namely, the six-rowed spike phenotype (Zwirek *et al.*, 2019). Interestingly, six-rowed spikes only exist among cultivated barleys, indicating a transition from two-rowed to six-rowed spike types during the domestication process (Komatsuda *et al.*, 2007; Pourkheirandish *et al.*, 2018).

1.4 The genetic basis of inflorescence architecture in barley

Inflorescence architecture, which is formed from reproductive meristematic activity, has a profound impact on crop production (Tanaka *et al.*, 2013). The formation and transition of IM, BM, SM and FM have a direct effect on the number of spikelets, which in turn decide the final number of mature grains. The various degree of branching reflects the dramatic diversity of grass inflorescences in shape. In “panicle/compound spike”, branching undergoes multiple iterations and ends with the production of spikelets. However, in “spike-like” inflorescences, branching of the inflorescence appears to be inhibited by a gene regulatory network. Studies in cereals have shown that inflorescence branching is a complex trait regulated by multiple genes (Koppolu and Schnurbusch, 2019). Barley has the simplest inflorescence shape, featuring determinate spikelets in addition to an unbranched spike. Thus, the identity and determinacy of the SM greatly affect the morphology of barley inflorescences. In the following sections, we review the responsible genes that help shape the indeterminate, unbranched row-typed spike and the determinate spikelet in barley.

1.4.1 Regulation of row-type

One of the most obvious characteristics of barley inflorescences is the distichously patterned spikelets alternating on the central rachis. According to the size and fertility of the two LSs, the inflorescence can be mainly divided into two types, namely two-rowed and six-rowed (Zwirek *et al.*, 2019). Natural variations, which took place about 12,000–8,000 years before the present, were the main reason to produce the six-rowed type from domesticated two-rowed inflorescence in barley (Dawson *et al.*, 2015; Palmer *et al.*, 2009). At least eleven independent loci were associated with the fertility of the lateral spikelets (Lundqvist, 2014). Among these loci, five genes, which result in variation of the row-type were identified, including *Six-rowed spike 1/vulgare row-type spike 1 (VRS1)*, *VRS2*, *VRS3*, *VRS4*, *VRS5/Intermedium-spike c (Int-c)* (Bull *et al.*, 2017; Komatsuda *et al.*, 2007; Koppolu *et al.*, 2013; Ramsay *et al.*, 2011; Youssef *et al.*, 2017). Mutations of these loci resulted in a variable level of LSs fertility (Koppolu *et al.*, 2013; Koppolu and Schnurbusch, 2019) (Figure 1.6 and Table 1.1).

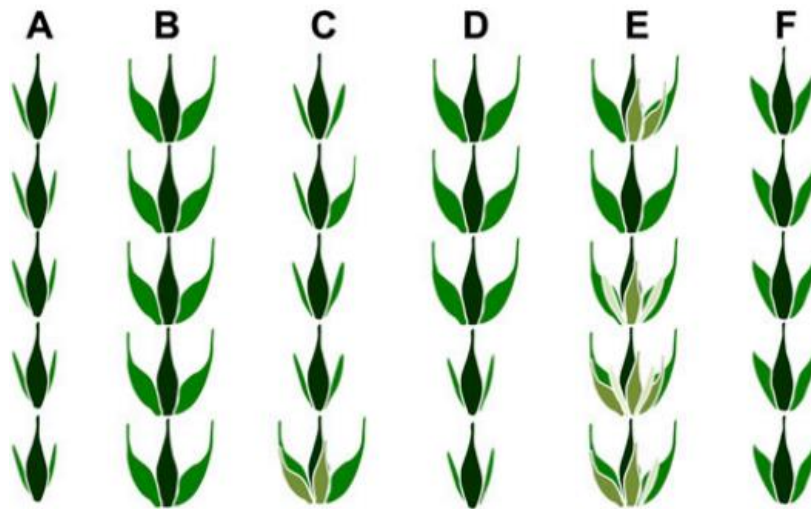


Figure 1.6 Spike morphology of different row-type loci. (A) Two-rowed spike. (B) *vrs1*. (C) *vrs2*. (D) *vrs3*. (E) *vrs4*. (F) *vrs5/int-c*. The figure is taken from (Koppolu *et al.*, 2013).

Table 1.1. List of VRS genes in barley.

Gene	Fertility of LSs in loss of function mutant	Variation	Location	References
<i>VRS1</i>	Fully fertile	Natural alleles; Induced mutants	2HL	(Komatsuda <i>et al.</i> , 2007)
<i>VRS2</i>	Fully fertile in the basal	Induced mutant	5HL	(Youssef <i>et al.</i> , 2017)
<i>VRS3</i>	Fully fertile in the upper	Induced mutant	1HL	(Bull <i>et al.</i> , 2017)
<i>VRS4</i>	Fully fertile	Induced mutant	3HL	(Koppolu <i>et al.</i> , 2013)
<i>VRS5</i> (<i>Int-c</i>)	Fully fertile	Natural alleles; Induced mutants	4HS	(Ramsay <i>et al.</i> , 2011)

VRS1

The *VRS1* gene was firstly identified and considered as a major regulatory factor, which negatively regulates LS fertility to promote the formation of the two-rowed spike in barley (Komatsuda *et al.*, 2007; Sakuma *et al.*, 2013). *VRS1* is located in the long arm of chromosome 2H and encodes a homeodomain-leucine zipper class I TF (*HvHOX1*) (Komatsuda *et al.*, 2007). The homologs of *VRS1* in maize, *GRASSY TILLERS 1 (GT1)*, has a similar function that inhibits tiller bud outgrowth. *VRS1* expression was strictly limited to rachilla, pistil, lemma, palea and lodicule of LSs (Sakuma *et al.*, 2013), suggesting that the *VRS1* protein functions in suppressing the development of the LSs in two-rowed barley. The loss-of-function in *VRS1* (*vrs1.a* alleles) displays fertility restoration in the LSs, resulting in completely fertile -spikelet triplets that form a six-rowed spike (Figure 1.6B) (Komatsuda *et al.*, 2007). During domestication, at different times and in different global regions, six-rowed barley (*vrs1* alleles) originated repeatedly by independent variations in *VRS1* from wild barley or cultivated two-rowed types (Komatsuda *et al.*, 2007; Pourkheirandish *et al.*, 2018).

Another interesting case of *VRS1* inhibiting the development of LS was reported by (Sakuma *et al.*, 2017), who worked on the barley mutant “*deficiens*”. The LSs of the *deficiens* mutant are highly reduced in size compared to regular two-rowed barleys because of a mutation in the putative phosphorylation site of the *VRS1* protein, which might prolong the duration of the inhibitory *VRS1* protein (Sakuma *et al.*, 2017). In addition, *VRS1* has an impact on leaf-related traits, such as leaf primordium size, vein number and subsequently leaf area (Thirulogachandar *et al.*, 2017). In the *vrs1* mutants, cell proliferation might be promoted to enlarge the size of leaf primordia,

enable an increase in leaf width and possibly supports a higher grain number compared with the wild-type (Thirulogachandar *et al.*, 2017).

Interestingly, the wheat *VRS1* orthologs have a similar inhibitory effect. The wheat spike does not produce LS but produces a variable number of florets on each spikelet's rachilla. The orthologous wheat *VRS1* protein, called GRAIN NUMBER INCREASE 1 (*GNI1-A*), acts on apical florets and rachillas to inhibit their development. The missense allele of *GNI1-A* induces an increase in fertile floret and grain number and was therefore selected during domestication (Sakuma *et al.*, 2019).

VRS2

VRS2 regulates hormonal homeostasis and gradients to influence floral organ formation and phase duration during spike development (Youssef *et al.*, 2017). *VRS2* encodes one protein of the plant-specific SHORT INTERNODES (SHI) TF family, involved in regulating floral development, auxin biosynthesis, gibberellin responses and flowering time (Youssef *et al.*, 2017). Mutants of *vrs2* display additional spikelets at the spike base and enlarged and occasionally fertile lateral spikelets, whereas sterile lateral spikelets at its tip (Figure 1.6C). This unique phenotype of a basal-to-apical fertility gradient along the spike indicates that the spike patterning of *vrs2* mutants is affected (Youssef *et al.*, 2017). *VRS2* has a high expression level in tiller buds and immature spikes, displaying a similar trend of auxin gradients in basal–apical spike sections in wild-type plants (Youssef *et al.*, 2017). Interestingly, *VRS2* also regulates developmental phase duration, which is known to be affected by plant hormones and carbohydrates during inflorescence development (Matsoukas, 2014; Su *et al.*, 2011). In wild-type plants, concentrations of auxin and CK display gradient changes in an inverse manner along the basal–apical spike sections; however, *vrs2* mutant plants failed to establish such hormonal gradients (Nordström *et al.*, 2004; Youssef *et al.*, 2017).

VRS3

VRS3 was identified as a regulator for chromatin state to control the development of LS (Bull *et al.*, 2017; van Esse *et al.*, 2017). Unlike other row-type genes, *VRS3* encodes not a TF but an enzyme, a putative Jumonji C-type H3K9me2/3 demethylase, which is orthologous to *OsJMJ706* gene in rice (Bull *et al.*, 2017). The mutant of *OsJMJ706* shows a perturbed inflorescence phenotype (Sun and Zhou, 2008).

Interestingly, *VRS3* appears to positively regulate all genes known to control spike row-type supposedly via clearing repressive chromatin methylation marks (Bull *et al.*, 2017). However, *vrs3* mutants do not exhibit the complete six-rowed but displayed a two-rowed condition in the lower third of the spike (Figure 1.6D). This phenotype of the coexistence of two-rowed and six-rowed indicates that the position-specific effect of spike row-type is driven by the regulation of *VRS3* across the barley spike (Bull *et al.*, 2017).

VRS4

VRS4 was identified as a key regulator not only for LS fertility but also for meristem determinacy (Koppolu *et al.*, 2013). *VRS4* encodes a LATERAL ORGAN BOUNDARY (LOB) domain-containing TF protein, which is orthologous to maize *RAMOSA2 (RA2)* (Bortiri *et al.*, 2006; Koppolu *et al.*, 2013). In maize, the *RAMOSA* pathway is involved in the regulation of inflorescence branching (Bortiri *et al.*, 2006; Gallavotti *et al.*, 2010). Mutants of *vrs4* display a six-rowed spike derived from fertility restoration of LSs, but more interestingly, additional spikelets are randomly produced on one rachis node developing a short branch-like structure (Figure 1.6E). *VRS4* controls the row-type by regulating the expression of *VRS1*. In *vrs4* mutants, *VRS1* is significantly down-regulated. *HvRA2* and *VRS1* are expressed in highly overlapping domains of LSs, suggesting that *VRS1* is regulated at the transcription level by *HvRA2* (Koppolu *et al.*, 2013).

VRS5/Intermedium-spike c

Most six-rowed barleys carry a combination of *vrs1.a* and a missense allele of *VRS5 (Int-c.a)* (Ramsay *et al.*, 2011). *VRS5* is orthologous of maize *TEOSINTE BRANCHED 1 (TB1)*, encoding a TCP (TEOSINTE BRANCHED 1/CYCLOIDEA/PCF1) TF (Ramsay *et al.*, 2011). In modern maize, elevated expression of *TB1* inhibited the growth of AxMs that develop into tillers, thereby promoting apical dominance (Doebley *et al.*, 1997). *TB1* in barley plays a conserved role in lateral growth suppression. In commercial six-rowed varieties, the alleles of *Int-c.a* and *vrs1.a* promote the development of LSs and contribute to the enlargement of lateral grain size (Figure 1.6B and F) (Ramsay *et al.*, 2011).

1.4.2 Spikelet meristem identity

In nature, one distinct feature of grass species is the spikelet structure, considered the basic unit of inflorescence. A spikelet is composed of sterile glumes (generally two) without AxM and one or multiple florets borne on its axis, called rachilla (Kellogg, 2022). Unlike other types of meristems that have the activity to differentiate into higher-order meristems or SMs in grass inflorescences, SM produces glume primordium (GP) and FMs as endpoints of its maturation. This rigorous developmental program is understood as the spikelet acquiring a unique identity, the SM identity (Whipple, 2017). Spikelet formation is regulated by endogenous and environmental signals. This developmental process usually involves a three-stage transition, including the initiation, maintenance, and termination of the SM (Yuan *et al.*, 2020).

When the identity of the SM is absent in grass plants, the SM loses the ability to produce GP and the FM but reverts into other types of meristems such as IM or BM, resulting in extra inflorescence-like structures or branches. A set of TFs has the function to specify SM identity during inflorescence development by using environmental and hormonal interactions (Yuan *et al.*, 2020; Zhu and Wagner, 2020). In grasses, proteins of the APETALA2/ETHYLENE RESPONSIVE FACTOR (AP2/ERF) family were firstly reported to regulate SM identity. Members of this family typically function to affect stress responses and plant development, especially in the process of controlling AxM activity and spikelet pair meristem (SpM) identity by hormone signaling (Bai *et al.*, 2017; Huang *et al.*, 2018; Wang *et al.*, 2019; Yang *et al.*, 2018a).

The *BRANCHED SILKLESS1 (BD1)* gene in maize was firstly identified in the AP2/ERF family as a key regulatory factor for SM identity. The *bd1* mutants give rise to more than two glumes and fail to suppress the AxMs, resulting in the formation of new spikelets from the axils of the glumes (Chuck *et al.*, 2002). The ortholog of *BD1* in rice, *FRIZZY PANICLE (FZP)* inhibits the formation of AxMs and/or promotes the transformation of SM into FM. Mutants of *fzp* produce branches instead of spikelets and rudimentary glumes with AxMs (Komatsu *et al.*, 2003). In short, the *BD1/FZP* gene functions to inhibit the fates of indeterminate lateral BM. Interestingly, *BD1/FZP* is not expressed in the SM, but at the boundary between differentiating lateral organs and the SM (Chuck *et al.*, 2002; Komatsu *et al.*, 2003), indicating that *BD1/FZP* specifies SM function in a non-cell autonomous manner (Whipple, 2017). The variations of wheat *FRIZZY PANICLE (WFZP)* confer supernumerary spikelets produced from

primary SM (Dobrovolskaya *et al.*, 2014; Li *et al.*, 2021c). In *Brachypodium*, *More spikelets1* (*Mos1*), the ortholog of *BD1/FZP*, has a set of AxMs produced from the IM, resulting in branching with the production of higher-order spikelets (Derbyshire and Byrne, 2013). Notably, the change in the expression of *FZP* shows a subtle regulation of the panicle architecture. The decrease in the expression level of *FZP* leads to an increase in the number of branches and spikelets, thereby increasing the yield (Bai *et al.*, 2017; Fujishiro *et al.*, 2018; Huang *et al.*, 2018; Wang *et al.*, 2020). In addition, *MULTI-FLORET SPIKELET 1* (*MFS1*), another member of AP2/ERF family showed a similar function in rice. Mutations of *MFS1* show pleiotropic defective phenotypes in spikelets as a result of delaying the transformation of spikelet meristems to floral meristems (Ren *et al.*, 2013).

In barley, a set of induced mutants called *compositum* (*com*) displays non-canonical spike-branching. SMs of *com* mutants lose their identity and then revert to the IM stage to produce diminutive spikes, or supernumerary spikelets or extra florets (Franckowiak JD, 2011). Two loci, *compositum 1* (*COM1*) on 5HL and *compositum 2* (*COM2*) on 2HS, have been reported (Bossinger *et al.*, 1992). Both *COM1* and *COM2* actively suppress branch formation by specifying SM identity and determinacy. The first *com* gene identified was *COM2*, which is the barley ortholog of *BD1/FZP* (Poursarebani *et al.*, 2015). The mutants of barley *com2* and orthologous tetraploid “*miracle wheats*” (AABB), also called *branched head^t* (*bh^t*), display altered and branched spikes. Here, SMs lose their determinacy and identity and revert to branch- or IM-like meristems, producing further spikelets in a distichous manner, developing florets along a secondary rachis (Poursarebani *et al.*, 2015). Notably, similar to *BD1/FZP* in maize and rice, the expression of *COM2* is also limited at the boundary between CS and LS (Poursarebani *et al.*, 2015), suggesting that this non-cell autonomous manner of regulation for SM identity is conserved across grass species including wheat.

COM1 has been identified recently. The *com1* spike resembles the *com2* mutant phenotype, which displays branch-like structures on the inflorescences, resulting from the deficiency of SM identity. *COM1* encodes a CYC/TB1-type TCP TF (Poursarebani *et al.*, 2020). The TCP TF family plays an important role in boundary formation of grass inflorescence development, especially in branch formation, SM identity and carpel fertility (Dixon *et al.*, 2018; Doebley *et al.*, 1997; Lewis *et al.*, 2014; Lyu *et al.*, 2020; Poursarebani *et al.*, 2020; Ramsay *et al.*, 2011; Yuan *et al.*, 2009). The function of

COM1 involves inhibition of branch formation by regulating cell wall development, hormonal signaling and metabolic processes in the spikelet-rachis boundary region. Like *COM1*, *COM2* may provide signals at the boundary to maintain SM identity in a non-cell autonomous manner. More recently, *BRANCHED AND INDETERMINATE SPIKELET 1 (BDI1)* was found to share the same locus with *COM1* (Poursarebani *et al.*, 2020; Shang *et al.*, 2020).

As a row-type gene, *VRS4* not only controls the fertility of LSs but is also involved in the regulation of SM identity. Loss of function of *VRS4* leads to a severely branched spike phenotype. The *vrs4* mutants display additional spikelet or floret formation or even miniature spikes produced from central SM (Koppolu *et al.*, 2013). Expression analysis showed that *COM2* transcripts were significantly down-regulated in the mutants of *vrs4*. This suggests that *VRS4* may function upstream of *COM2* to maintain SM identity to inhibit branching or extra spikelet/floret formation (Koppolu *et al.*, 2013; Poursarebani *et al.*, 2015). In addition, the expression of *COM2* and *VRS4* overlapped in spikelet primordium domains, supporting a potential interaction. Therefore, the pathway (*VRS4–COM2*) may have the possibility to be co-regulators for inflorescence shape by SM identity and determinacy (Poursarebani *et al.*, 2015).

Recently, the barley SEPALLATA MADS-box gene *HvMADS1* has been reported to have the effect of regulating the inflorescence architecture under high ambient temperature (Li *et al.*, 2021a). The MADS-box gene family has been widely reported as an important transcription factor that regulates plant growth and development, and stress resistance. *MADS1* participates in the regulation of development in all whorls of floral organs and the identity of flowers in plants (Wang *et al.*, 2021). In barley, *HvMADS1* integrates heat response and CK homeostasis to maintain inflorescence structure through *HvCKX3*, which is the direct target of *HvMADS1*. In the absence of *HvMADS1*, *HvCKX3* level is insufficient to maintain CK homeostasis at high temperatures, resulting in a reversion of the identity of SM meristems to IM-like meristems, eventually forming branched inflorescences (Li *et al.*, 2021a).

In addition to the above genes, several other loci have been reported to be involved in the identity of the SM in barley. *Low number of tillers 1 (Lnt1)* encodes a BELL-like homeodomain TF *JuBel2* (Dabbert *et al.*, 2010). *lnt1.a* mutant plants show the reduced tiller number but branched spike phenotype. In the case of *rattail (rtt1.a)* mutant, florets cannot be produced due to a lack in the transition from SM to FM. This is mainly

because the FM within the spikelet repeatedly reverts back to SMs, producing glumes but no floral organs (McKim *et al.*, 2018).

1.4.3 Spikelet meristem determinacy

In general, SM identity specifies the fate of lateral organs produced by an SM, whereas SM determinacy specifies the number of lateral organs (Bommert and Whipple, 2017). After the initiation of the SM, a determinacy decision made by the SM itself is the number of produced florets, which is variable between grasses but typically is strictly controlled (Bommert and Whipple, 2017). As mentioned earlier, in rice and maize, two lateral abortive florets and a single lateral floret (abortive in the ear but fertile in the tassel) are generated before the production of a terminal floret, respectively. In barley, only a single floret is produced on a single spikelet, while other *Triticum* species like wheat and *Brachypodium* display the production of a varied number of florets per spikelet (Bommert and Whipple, 2017; Koppolu and Schnurbusch, 2019).

Many genetic studies indicate that SM determinacy is controlled by the interaction of one *microRNA* (*miR172*) family and its target AP2 TFs. The mechanism of AP2 genes for SM determinacy was first reported in maize (Chuck *et al.*, 1998). Maize *Indeterminate Spikelet 1 (IDS1)*, encoding an AP2 protein, is the direct target of *miR172* encoded by the *Tasselseed 4 (Ts4)* (Chuck *et al.*, 2007). The SM of maize *ids1* mutant loses the determinacy and produces more than two normal florets per spikelet (Chuck *et al.*, 1998). *IDS1* and its close paralog, *SISTER OF IDS 1 (SID1)* are needed for branching of the IM, initiating FMs and controlling SM determinacy (Chuck *et al.*, 2008; Chuck *et al.*, 2007; Chuck *et al.*, 1998). In rice, *IDS1* and *SID1* orthologs, known as rice *INDETERMINATE SPIKELET 1 (OsIDS1)* and *SUPERNUMERARY BRACT (SNB)*, have a redundant role to control inflorescence architecture and FM establishment (Lee and An, 2012; Wang *et al.*, 2015). In single and double mutants of *OsIDS1* and *SNB*, the IM and BMs were converted precociously to spikelets, resulting in a fewer number of both primary and secondary branches (Lee and An, 2012); mutant spikelets are indeterminate and produce extra glumes due to a delay in the floral transition (Lee and An, 2012). In wheat, the ortholog of *IDS1* is known as one important dominant domestication locus, *Q* (Simons *et al.*, 2006), which is also regulated by *miR172*; it specifies SM determinacy by timing rachilla degeneration. The null mutation of the dominant *Q* allele shows an extension of rachilla activity, resulting in more floret production per spikelet. Strikingly, reduced levels of *Q* transcript by over-expressing of

miR172 also promote the additional floret phenotype (Debernardi *et al.*, 2017). In addition to SM determinacy, Q and its paralog *AP2L2* play redundant roles to specify the identity of FM and lemma (Debernardi *et al.*, 2020; Debernardi *et al.*, 2017).

In barley, the cleavage of *AP2* mRNA by *miR172*-mediated regulation has been reported to control spike-related traits (Brown and Bregitzer, 2011; Houston *et al.*, 2013; Nair *et al.*, 2010; Zhong *et al.*, 2021). One *Ds-miR172* mutant containing a 3.6 kb *Ds*-transposon insertion in the region of a putative barley *miR172* gene displays the abnormal spike phenotype, including developed florets converted from glumes in the apical and additional branched spikelets in the basal spike. Barley *HvAP2L-H5* is orthologous to maize *IDS1* and wheat Q; it promotes IM activity and suppresses the identity shift towards the terminal spikelet meristem to achieve spike indeterminacy and spikelet determinacy (Zhong *et al.*, 2021). Mutations in *HvAP2L-H5* lead to wheat-like inflorescence phenotypes, particularly in producing a terminal spikelet at the tip of the spike (determinacy spike) and extra florets per spikelet (indeterminacy spikelet). Interestingly, a high level of *AP2L-H5* activity in wheat delays the transition from IM to terminal spikelet meristem (Zhong *et al.*, 2021). Thus, the *miR172*-*AP2* module is essential for the regulation of the SM determinacy and the function of which is likely conserved in major cereal crops. Given the important role of this regulatory module in the development of inflorescences, the manipulation of the module may provide new insight into improved inflorescence structure and increased grain yields.

1.5 Aims of this study

Increasing grain yields is the most important goal for cereal crop genetic improvement. The inflorescence architecture determines the distribution of the grains and ultimately has a decisive impact on cereal yields. Grass inflorescences show a dramatic diversity concerning their shape, spanning branching patterns to the number of florets. From all of the inflorescence forms in cereals, barley has the most simplified or slimmed-down inflorescence shape, featuring a non-ramified and indeterminate spike with sessile, determinate spikelets bearing only a single floret. However, knowledge of the genetics of barley inflorescence development is still highly limited.

This study aims to have a deeper understanding of the genetic mechanism of the regulation of spikelet development in barley. To this end, a paired-spikelet mutant

called *extra floret.a (flo.a)*, which is deficient in the determinacy of the spikelet meristem, was subjected to this research. The *flo.a* mutant produces extra spikelets abaxially to the central spikelets. To dissect the genetic basis controlling the extra spikelet formation and to reveal the underlying molecular mechanism, this study carried out the following aspects:

- Dissecting developmental details of extra spikelet formation in *flo.a* mutants by morphological observation and histochemical analysis.
- Genetic analysis and map-based cloning of the *Flo.a* locus by scanning segregating populations derived from the *flo.a* mutant and wild-type to identify recombinants.
- Validation of *Flo.a* candidate gene in allelic mutants and transgenic knock-out plants mediated by CRISPR-Cas9 mutagenesis.
- Functional identification of *Flo.a* gene by studying mRNA and protein expression patterns, endogenous hormone levels and potential regulatory pathways.

Thus, the molecular identification and characteristics of the *Flo.a* gene responsible for extra spikelet formation not only show us how barley maintains a simplified inflorescence morphology but also further demonstrates the potential application of extra spikelets for the genetic improvement in barley breeding.

2. Materials and Methods

2.1 Plant materials

Three *flo* (*flo.a*, GSHO 2005; *flo.b*, GSHO 2128; *flo.c*, GSHO 1877) mutants originally used in this study were obtained from the United States Department of Agriculture (USDA–ARS), USA. The original *flo* mutants with the background of spring barley cultivars (*cv.*) Foma was backcrossed with the recurrent parent spring barley *cv.* Bowman (BW) several times to form three near-isogenic lines (NILs) we are investigating, respectively (Druka *et al.*, 2011). In addition, a set of nine *flo-like* mutants were obtained from Nordic Genetic Resources Center (NGRC, NordGen), Sweden.

For genetic analysis and preliminary mapping, one BW NIL of *flo* mutant, namely *flo.a*, was used for the construction of a segregating population: *flo.a* was crossed with recurrent parent BW to generate F1 plants, followed by self-pollinating to form F2 population with 192 plants. Subsequently, the phenotypes were investigated and molecular markers were designed to identify recombinants in the F2 population to determine the linkage relationship between phenotype and genotype. For fine-mapping, the recombinant plants from the F2 population were grown into the next F3 generation to form a segregating population with around 3,800 plants.

The barley plants were initially germinated in 96-well plates. Then, seedlings of two weeks were transferred to the vernalization room for 4 weeks of vernalization. Finally, the plants were transplanted into individual pots (11 cm diameter) under greenhouse conditions (20°C in day / 15°C at night, 16h of light / 8h of dark). In addition, wild-type plants and *flo* mutants were grown in the field. After germinated in greenhouse condition, the seedlings were transplanted in the field in the Leibniz Institute of Plant Genetics and Crop Plant Research, Gatersleben, Germany (51° 49' 23" N, 11° 17' 13" E, altitude 112 m).

For transgenic plants, the clustered regularly interspaced short palindromic repeats (CRISPR)-Cas9 knock-out and green fluorescent protein (GFP)-reporter plants in *cv.* Golden Promise background were generated via the plant transformation platform (Plant Reproductive Biology group) in IPK-Gatersleben. All transgenic plants were grown in IPK greenhouse under the condition mentioned above.

2.2 Methods

2.2.1 Phenotyping

Morphological observation of spikes was performed between wild-type (Bowman) and *flo* mutants at early developing and mature stages. After the transition from vegetative to reproductive growth, the young spikes of BW and *flo* mutants were dissected and characterized in several key developing stages, including double ridge (DR), triple mound (TM), glume primordium (GP), lemma primordium (LP), stamen primordium (SP), awn primordium (AP), white anther (WA) (Kirby and Appleyard, 1984). Developmental details of inflorescences in WTs and *flo* mutants were photographed using a stereomicroscope with a digital camera (Leica, MZ FLIII).

In the mature stage, all well-fruited spikes were harvested intact and characterized in BW and *flo* mutants. Using each triple-spikelet as the basic unit, observing the morphology and number in detail, and comparing the differences between wild-types and *flo* mutants. In addition, the other agronomic traits related to yield were investigated, including plant height, spikelet number per spike, node number per spike, spike length, grain number per spike, grain setting rate, grain length, grain width, thousand-grain weight, and grain area.

2.2.2 Genomic DNA isolation

Leaf tissues of two-week-old barley seedlings were harvested and used in this study. For obtaining high-quality genomic DNA, the method of genomic DNA isolation was modified based on published protocol (Doyle and Doyle, 1990). In brief, small pieces of young leaf were collected into a 2 ml labeled Eppendorf tube with two steel balls inside, which quickly got frozen in liquid nitrogen. Frozen samples were homogenized by grinding for 30 seconds at 30 spins/sec. Subsequently, 800 µl of the extraction buffer [55 mM cetyl-trimethylammonium bromide (CTAB); 20 mM Ethylenediaminetetraacetic acid (EDTA), pH=8.0; 100 mM Tris-HCl, pH=8.0; 1.4 M NaCl; 0.28 M β-Mercaptoethanol] was added into the 2 ml reaction tube, followed by vortexing at high speed until all lumps have disappeared. Then 800 µl of phenol/chloroform/isoamyl alcohol (25:24:1) was added to the tube and shaken for 5 min. The supernatant was transferred into a new 1.5 ml Eppendorf tube after centrifuging with 10,000 g for 10 min, followed by adding 60 µl 3 M NaAc, pH 5.2 and 600 µl Isopropanol (-20°C) into the new Eppendorf tube. The DNA streak was visible

by gently inverting precipitated by centrifuged with 10,000g for 10 min at 4°C. The washed DNA with 75% ethanol was re-precipitated by using the centrifuge with 10,000g for 10 min at 4°C again. Finally, the DNA was completely dried at room temperature and dissolved by adding 100 µl water and 2 µl RNase followed by incubating for 1 hour at 37°C and stored at -20°C.

2.2.3 Whole-genome sequencing and introgression identification

The genomic DNA of *flo.a* mutant was extracted by using fresh leaves (protocol described previously; see 2.2.2) and the quality and concentration by agarose gel electrophoresis and Qubit 2.0 were determined, respectively. Subsequently, DNA was used for whole-genome sequencing (WGS) by using Illumina sequencing platform at Novogene Co., Ltd (Cambridge, UK) to obtain 150 bp paired-end reads with 10X coverage of the ~5.1 Gb barley genome. The high-quality reads were used for further analysis. A total of 55.3 Gb (184,469,857 short reads >Q30) raw data was obtained.

The process of read alignment and variant calling was referred from (Milner *et al.*, 2019). In brief, raw reads were trimmed using Cutadapt (Martin, 2011) and aligned to barley reference genome of *cv.* Morex Version 2 (V2) (Monat *et al.*, 2019) using BWA-MEM version 0.7.12a (Li, 2013). Alignment records were converted into binary alignment map (BAM) files and sorted by reference position and indexed using Samtools (Li *et al.*, 2009). Variants were called between BW and *flo.a* mutant (the WGS data is unpublished) using SAMtools/BCFtools version 1.6 (Li, 2011) to generate VCF files. Subsequently, the heterozygous SNPs were removed and homozygous SNPs were filtered with Minimum allele frequency (MAF) >0.5 to obtain SNPs only exist between BW and *flo.a* mutant using VCFtools (Danecek *et al.*, 2011). Finally, the number and density of SNPs were calculated in bins of size with 100Kbp with VCFtools and visualized with R. Continuous bins with high density of SNPs can be regarded as introgression from *flo.a* mutant.

2.2.4 Genetic analysis of *Flo.a* locus in the F2 population

For the genetic analysis, the *flo.a* mutant was initially crossed with BW to generate F1 hybrids, for which genuine hybrids were identified by polymorphic molecular markers. The '*flo*' phenotype was investigated in the population. A chi-square test was performed to estimate whether the ratio of observed mutant type and observed wild type is in line with the single gene segregation (1:3).

2.2.5 Map-based cloning of *Flo.a*

After identifying three introgressions on chromosomes 3H (1x) and 6H (2x) in the *flo.a* mutant, molecular markers were designed based on the previously obtained SNPs matrix by WGS, to determine the phenotype-genotype linkage relationship. Since the *Flo.a* allele has been reported previously to locate on chromosome 6H (Druka *et al.*, 2011; Koppolu *et al.*, 2021), molecular markers on 6H were designed for initial linkage analysis. *Flo.a* was preliminarily mapped into an interval between two markers FB-74.4 and FB-115.0 on the short arm of chromosome 6H using F2 population. For high-resolution mapping within the *Flo.a* genomic interval, a large F3 segregating population was generated derived from the self-pollination of recombinants from F2 population and around 3,800 individuals were used for fine mapping with newly developed CAPS and Indel markers. The sequences of all markers for mapping are listed in (Appendix Table S1).

2.2.6 Identification of new *flo.a* alleles through allelism tests

Due to the three BW-NILs, including *flo.a*, *flo.b* and *flo.c* having 'flo' phenotypes, allelism tests between these three mutants were performed to identify any potential new allele for the *Flo.a* locus. Pairwise crosses were conducted between the three mutants, followed by investigating the phenotype of the positive F1 hybrids.

2.2.7 Inducing knock-out (KO) mutation by CRISPR-Cas9 gene-editing system

A robust barley transformation platform established in IPK-Gatersleben was used to create the barley transgenic plants (Marthe *et al.*, 2015). For inducing KO mutation of *HvALOG1* and its closest paralog on 7H (*HvALOG2*) mediated by CRISPR-Cas9 gene-editing engineering, The coding region of *HvALOG1* and *HvALOG2* of two-rowed barley cv. Golden Promise, which has higher transformation efficiency, was sequenced and used for guide RNA (gRNA) design. The target sequences for each gene were selected within or near the ALOG domain. Two 20-bp gene-specific guide RNA sequences targeting *HvALOG1* or *HvALOG2* were selected using the online prediction tool (<https://www.deskgen.com/guidebook/>) and detected the targeting specificity in barley genome using blast search (https://apex.ipk-gatersleben.de/apex/f?p=284:10:::HOME_LINK#) (Colmsee *et al.*, 2015), respectively. The secondary structures of gRNA were predicted by RNAfold (<http://rna.tbi.univie.ac.at/cgi-bin/RNAWebSuite/RNAfold.cgi>) to determine the most

suitable targets for selection. The oligonucleotides of gene-specific gRNA sequences were synthesized, annealed, and ligated into the monocot-compatible intermediate vector pSH91 (Budhagatapalli *et al.*, 2016). Subsequently, the expression unit containing gRNAs and Cas9 was subcloned into the binary vector p6i-d35S-TE9 (DNA Cloning Service e.K., Germany) by using the *SfiI* restriction sites. The construct was transformed into Golden Promise immature embryos by *Agrobacterium tumefaciens* AGL1-mediated co-transformation to generate transgenic T0 plants. A total of 34 independent lines were generated and grown in normal greenhouse conditions. PCR-based Sanger-sequencing was performed to detect the presence/absence of the T-DNA and the mutation sites in the target genes. The sequence of oligonucleotides and all primers for detecting transgenic plants are listed in (Appendix Table S1).

2.2.8 Construction of GFP report plants

To analyze HvALOG1 protein accumulation and regulation, GFP-reporter plants were produced by fusing HvALOG1 and GFP. The *HvALOG1-p::HvALOG1:GFP* construct was created by fusing the 2,550 bp *HvALOG1* promoter, full-length (780 bp without TAG) *HvALOG1* cDNA, enhanced green fluorescent protein (eGFP) and 1,065 bp 3' untranslated region (UTR) of *HvALOG1*, followed by cloning into the binary vector p6i-d35S-TE9 (DNA Cloning Service e.K., Germany). The vector was transformed into barley Golden Promise using *Agrobacterium tumefaciens* AGL1-mediated co-transformation as described above. The primers used for construction are listed in (Appendix Table S1).

2.2.9 Scanning Electron Microscopy (SEM) analysis

Immature spike tissues from seven stages, including DR, TM, GP, LP, SP, AP, WA as well as mature spikelets from BW and *flo.a* mutant growing in the greenhouse were collected. The fixation, processing and photographing of samples mainly refer to published literature (Poursarebani *et al.*, 2020). SEM was conducted by following a protocol established in IPK-Gatersleben (Lolas *et al.*, 2010). Probes were examined using a Zeiss Gemini30 scanning electron microscope (Carl Zeiss Microscopy GmbH). All images were recorded digitally.

2.2.10 mRNA isolation and qRT-PCR

For analyzing the expression pattern of the *Flo.a* gene in barley, the developing spike tissues of *flo.a* mutant and BW were collected for mRNA isolation from DR, TM, GP, LP, SP, AP, WA stages using the stereoscopic microscope (Kirby and Appleyard, 1984). Total RNA was extracted using TRIzol according to the manufacturer's instructions (Invitrogen), followed by quantifying the amount of total RNA using a NanoDrop 2000 (Thermo Fisher Scientific). The total RNA was treated with DNase I (Fermentas) to remove genomic DNA contamination. The cDNA was synthesized from 2µg RNA using SuperScript III reverse transcriptase and oligo (dT) primer, according to the manufacturer's instructions (Invitrogen). Diluted cDNA was used as a PCR template. Transcript levels of target genes were measured by quantitative real-time RT-PCR (qRT-PCR) using ABI Prism 7900HT sequence detection system machine (Applied Biosystems) and QuantiTect SYBR green PCR kit (Qiagen) according to the manufacturer's instructions. All primers for qRT-PCR are listed in (Appendix Table S1). qRT-PCR of each sample, which was collected three times independently, was performed technically three times. The average value of each sample was used to represent the transcription levels, which were normalized by the barley actin gene. Significance tests were calculated by using the Student's *t*-test (two-tailed).

2.2.11 RNA sequencing

Immature spike samples of BW and *flo.a* mutant plants were collected at Waddington stages W2.0 (DR), W3.0 (LP), W4.5 (AP) and W5.5 (WA) (Waddington *et al.*, 1983). Due to the '*flo*' spikelet phenotype only existing in the upper-mid portion of spike, the whole spike was cross-sectioned into two parts (upper-mid and basal) at stages W3.0, W4.5 and W5.5 under a stereoscopic microscope. A total of 15-48 spikes per sample and three biological replicates were harvested and used for RNA extraction (protocol described previously). The integrity and quantities of RNA were determined using an Agilent 2100 Bioanalyzer (Agilent Technologies) and Qubit (Invitrogen), respectively. A total of 1 µg of high-integrity RNA was used for the construction of sequencing libraries. Strand-specific RNA libraries were generated using TruSeq Stranded mRNA Sample Prep Kit (Illumina) according to the instructions of the manufacturer. High-throughput paired-end sequencing was conducted using a NovaSeq 6000 PE150 Platform (Illumina) at Novogene Co., Ltd (Cambridge, UK).

2.2.12 RNA-seq data analysis

The raw reads were assessed for quality initially using FastQC (version 0.11.9) (<http://www.bioinformatics.babraham.ac.uk/projects/fastqc/>), following conducted automated quality, adapters trimming and quality control using Trim Galore (version 0.6.5) (https://www.bioinformatics.babraham.ac.uk/projects/trim_galore/) to harvest high-quality reads. Subsequently, the sequences were aligned to the barley reference genome cv. Morex V2 (Monat *et al.*, 2019) using HISAT2 (version 2.2.1) (Pertea *et al.*, 2016). The read counts that reflect the level of gene transcription were obtained by featureCounts (version 1.22.2) (Liao *et al.*, 2014). The raw read counts were normalized to Transcripts Per Kilobase Million (TPM) expression levels. Differential gene expression analysis was performed using DESeq2 (version 3.13) package in R (Love *et al.*, 2014). Differentially expressed genes (DEGs) were called in pairwise comparisons of each of the stages and positions. The Benjamini-Hochberg method was implemented to calculate *P-values* and adjusted *P-values* by False Discovery Rate (FDR) for the significant test. The DEGs were identified by using the threshold of adjusted *P-values* < 0.05 and log₂ fold change ≥ 0.5845 or ≤ -0.5845.

The high-confidence (HC) genes in identified DEGs were used for further analysis. Heatmap for HC DEGs was produced using ComplexHeatmap package in R (Gu *et al.*, 2016). Cluster analysis for HC DEGs was performed using Z-scored normalized TPM by the K-medoids method with the PAM algorithm function. For GO term enrichment analysis, *Arabidopsis* homologs were identified by BLASTp in TAIR10 using the deduced sequences of barley HC protein (e-value < 1e⁻⁵). The corresponding *Arabidopsis* homologs to HC DEGs from clusters 1 to 8 were applied to GO term enrichment, summarization and visualization using Metascape with the default parameters (<http://metascape.org>) (Zhou *et al.*, 2019).

2.2.13 Phylogenetic analysis

The phylogenetic analysis of ALOG proteins is based on the amino acid sequence of the ALOG domain. The domain of *Hv*ALOG1 is initially used as query in BLASTp with a cutoff E-value of 1e⁻³⁰ in proteomes from 14 plant species including 8 monocots and 6 eudicots. Subsequently, all sequences of the retrieved proteins within the ALOG family were aligned using Clustal Omega (<https://www.ebi.ac.uk/Tools/msa/clustalo/>). The phylogenetic analysis was constructed based on maximum likelihood (ML) criterion by using IQ-tree v2.1.3 with the recommended parameter '-m MFP -B 1000 -

bnni' (Minh *et al.*, 2020). Finally, the phylogenetic tree was visualized and modified by iTOL (<https://itol.embl.de/itol.cgi>) (Letunic and Bork, 2021).

2.2.14 Phytohormone measurements

For phytohormone (auxin, CK, GAs and ABA) measurements, immature spikes at Waddington stage W2.0 (DR), W3.0 (LP), W4.5 (AP) and W5.5 (WA) were collected from BW and *flo.a* mutant plants. The immature spikes were cross-sectioned into the upper-mid and basal parts for sampling according to the tipping point of the '*flo*' phenotype among the rachis node on the spike under a stereoscopic microscope. Each sample contains four to six biological replicates, and each replicate contains approximately 10 mg of immature sectioned spikes tissues. All collected samples were quickly frozen and stored at -80 °C; the following samples were prepared and further subjected to the UPLC-MS platform (IPK-Gatersleben, Germany) for phytohormone quantification. Data from replicates of each sample were analyzed, and significance tests were calculated by two-way ANOVA tests.

2.2.15 Subcellular localization

The subcellular localization experiment was referred to (Rajaraman *et al.*, 2018). In brief, the full-length of *HvALOG1* CDS, PCR amplified from BW spikes was fused with eGFP to produce an *HvALOG1*-GFP transient expression construct based on P35S-EGFP expression vector driven by CaMV 35S promoter (Appendix Figure S2.1). Subsequently, the vector was transferred into barley leaf epidermis by microparticle bombardment. After two days of cultivation, the fluorescence signal was detected under an LSM780 confocal laser scanning microscope (Carl Zeiss MicroImaging). Primers for vector construction for subcellular localization were listed in (Appendix Table S1).

2.2.16 3D-reconstruction

For 3D reconstruction, spikes after pollination from BW and *flo.a* mutant were harvested and used for sectioning. Serial sections (1 µm) were collected at a 10 µm interval on the spike. After recording on a Zeiss Axio Scan Z1slidereader (Carl Zeiss, Jena, Germany). Image stacks were aligned with open source Fiji-ImageJ2 software after which segmentation was carried out with Amira software (Thermo Fischer Scientific, Waltham, USA).

2.2.17 Light microscopy

Immature spikes from BW and *flo.a* mutant were harvested and fixed with 1% glutaraldehyde and 4% formaldehyde in 50 mM phosphate buffer pH 7.0. After dehydration and embedding in Spurr resin, semithin sections (1.0 µm) were cut on a Reichert-Jung Ultracut S (Leica, Vienna, Austria) and stained with crystal violet. Digital recordings were made on a Zeiss Axiocam light microscope (Carl Zeiss, Jena, Germany) and stored as TIFF files.

2.2.18 mRNA *in situ* hybridization

For mRNA *in situ* hybridization analysis, the immature spikes tissues of BW and *flo.a* mutant at the DR, LP, SP, AP stages were collected under the observation of stereoscopic microscope and fixed in FAA (50% ethanol, 5% acetic acid and 3.7% formaldehyde) at 4°C, overnight. After alcohol dehydration with a series of ethanol (50, 70, 85, 95 and 100%), the samples were embedded into Paraplast Plus (Kendall, Mansfield, MA). RNA probes were developed based on gene-specific fragments (200 - 500 bp). The purified DNA product of *HvALOG1*, *HvALOG4* and *histone H4* was PCR-amplified from cDNA of BW spikes and was cloned into pGEM-T cloning vector, respectively. The PCR products were obtained by using the vector without mutations in the inserted fragment as templates and using fusion primers containing the T7 promoter sequence (5`-TAATACGACTCACTATAGGG-3`) before the forward primers of sense probes or reversed primer of antisense probes to amplify. The fusion primers are listed in (Appendix Table S1). The sense and antisense probes were synthesized by using PCR products generated in the previous step with the T7 RNA polymerase (Roche), according to the manufacturer's instructions. For hybridization, 8 µm thick sections were prepared using a microtome. The following steps, including pre-treatment, hybridization, washing and coloration were conducted as described in (JACKSON, 1991).

2.3. Data contribution by the author and the collaborators toward the present thesis

The author (Guojing Jiang) of the thesis generated most of the data of this work in the research group Plant architecture (PBP, Prof. Dr. Thorsten Schnurbusch), IPK-Gatersleben. Besides, other experiments, such as barley transformation,

phytohormone measurements and microscopy imaging, were carried out in partnership with other research teams from IPK, including Plant Reproductive Biology (PRB, Dr. Jochen Kumlehn), Molecular Plant Nutrition (MPE, Prof. Dr. Nicolaus von Wirén) and Structural Cell Biology (SZB, Dr. Michael Melzer). To make this thesis thorough and understandable, our collaborators have contributed considerably towards the results. The following provides a thorough description of the various efforts completed by the author (Guojing Jiang) and the other collaborators to accomplish the goals of the current thesis.

Barley materials

- The F2 mapping population with 192 individuals derived from BW and *flo.a* was generated by PBP technician team. The F3 fine-mapping population derived from recombinants of F2 was generated and managed by Guojing Jiang.
- The vectors for barley transgenic plants, including CRISPR-Cas9 knock-out and HvALOG1-p::HvALOG1:GFP report lines were prepared by Guojing Jiang and Dr. Yongyu Huang. The transformations were performed by the PRB team (Dr. Goetz Hensel, Robert Hoffie and Dr. Jochen Kumlehn).

Morphological analyses

- The phenotyping work for spike and spikelet traits of wild-types, mutants (*flo.a*, *flo.b*, *flo.c*, *flo-like*), mapping populations (F2 and F3) as well as the transgenic plants was carried out by Guojing Jiang and Dr. Ravi Koppolu.
- Sample collection for SEM, confocal imaging and 3D reconstruction for immature spikes and spikelets from BW, *flo.a* and HvALOG1-GFP report lines was done by Guojing Jiang. The SEM, confocal imaging and 3D reconstruction preparation and image recordings were performed by Dr. Twan Rutten.

Genetic and physical mapping of *Flo.a* locus

- WGS data analysis and SNP and indels retrieval were done by Guojing Jiang, Dr. Yongyu Huang and Dr. Martin Mascher.
- Marker development based on SNP and indels was carried out by Guojing Jiang.

- The preliminary mapping and fine-mapping for *Flo.a* locus in F2 and F3 populations were implemented by Guojing Jiang. Part of molecular markers was provided by Dr. Naser Poursarebani.

Mutant analyses

- Resequencing of *flo.a* mutant alleles and data analyses were done by Guojing Jiang.
- Allelism tests for *flo.a* and *flo.c* were carried out by Guojing Jiang.

RNA sequencing and data analysis

The spike samples from BW and *flo.a* for RNA sequencing were collected by Guojing Jiang. The RNA sequencing data analysis was conducted by Guojing Jiang with the support of Dr. Martin Mascher and Dr. Yongyu Huang.

Gene expression pattern analyses

- immature spikes sample collection, RNA extraction and purification, cDNA synthesis, and qRT-PCR for *HvALOG1* in BW were carried out by Guojing Jiang with the support of Dr. Yongyu Huang.
- The mRNA *in situ* hybridization assays (probes design and preparation, sample collection and fixation of immature spikes, hybridization, and staining) for *HvALOG1* and *HvALOG4* and *HvHistone4* were conducted by Guojing Jiang with the guide from Dr. Shuangshuang Zhao.

Subcellular localization

The vector for subcellular localization of *HvALOG1* was prepared by Guojing Jiang. Microparticle bombardment and confocal imaging were performed by Dr. Jeyaraman Rajaraman.

Phytohormone measurement assay

The immature spike samples for the phytohormone measurement assay were collected by Guojing Jiang. The phytohormone measurement assay was conducted in the UPLC-MS platform (IPK-Gatersleben, Germany) with the support of Dr. Yudelsy Antonia Tandron Moya and Prof. Dr. Nicolaus von Wirén.

3. Results

3.1 Morphological differences between wild-type and *flo.a* mutant

3.1.1 *flo.a* mutant produces extra spikelets

A spike with sessile, single-floreted spikelets is a common feature of barley inflorescence. Another distinguishing whole genus-defining feature in the inflorescence is that three spikelets are born on the same rachis node, generating a so-called spikelet triplet that is distichously organized and formed directly from the main inflorescence axis (Figure 3.1A). The spikelet triplet arises from the so-called triple spikelet meristem (TSM) which is the upper axillary primordial ridge of the spike at the DR stage and subsequently differentiates into three distinct meristematic mounds during the TM stage. Each mound develops a SM, i.e., one central spikelet meristem (CSM) and two lateral spikelet meristems (LSMs).

The TSMs differentiate continuously from the indeterminate IM and are accumulated over the reproductive growth stages, causing the spike to prolong until the maximum SM number is reached. Therefore, an immature spike contains multiple spikelets at different developmental stages, including DR, TM, GP, LP, SP, and AP (Figure 3.1B). Each SM matures into a single spikelet that contains a single fertile or sterile floret flanked by one pair of glumes in wild-type barley (Figure 3.2C).

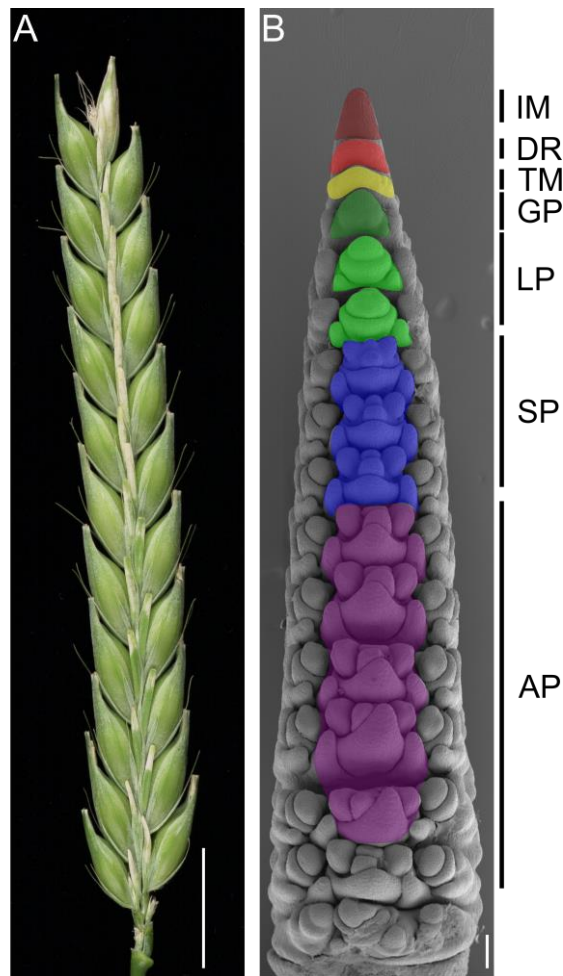


Figure 3.1. Spike morphology in two-rowed wild-type barley cv. Bowman (BW). (A) The morphology of a mature barley spike (lateral view). Awns of the CS have been removed. (B) SEM imaging of an immature spike at the Awn primordium (AP) stage showcasing the developmental gradient (dorsal view). From the top: IM, inflorescence meristem; DR, double ridge; TM, triple mound; GP, glume primordium; LP, lemma primordium; SP, stamen primordium. The meristems at the different developing stages are shown in different colors. Bar = 100 μ m.

To further understand the genetic basis of inflorescence shaping in barley, we performed a phenotypic examination of a spike mutant, *extra floret.a* (*flo.a*), showing the production of extra organs abaxially to the primary CSs. The original *flo.a* mutant was created in cv. Foma via ethyleneimine-induced mutagenesis. Other mutagenic mutants with spike morphologies similar to *flo.a* were also classified as *flo* mutants. The *flo.a* mutant was later backcrossed five times into a two-rowed barley cv. Bowman (BW, WT in this study) to form a near-isogenic line, BW-NIL-*flo.a*, displaying a spike phenotype identical to the ancestral mutant (Druka *et al.*, 2011). Therefore, we used BW-NIL-*flo.a* as material for this study and refer to it as the *flo.a* mutant in the following description.

The *flo.a* mutant was initially characterized as having extra floral bracts, growing from the same rachis node as the spikelet triplets, and was thus named *extra floret* (Druka *et al.*, 2011). However, in our observation, compared with BW, *flo.a* mutant not only produces extra florets but also develops two extra glumes (Figure 3.2 and 3.3), indicating that the supernumerary organs acquire spikelet identity. The extra spikelets lost the activity to become fertile due to the degeneration of the inner floral organs, i.e., stamens, pistil, and ovary, during later spikelet developmental stages, which is comparable to the phenotype of LS (Figure 3.2 G). Therefore, paired spikelets (one fertile CS, and one sterile extra spikelet in the central position) produced from the same rachis node were one of the distinct features in the *flo.a* mutant (Figure 3.2D and E). Interestingly, the development of floral organs within the CS's outermost whorl was also affected. Some pairs of glumes from CSs were fused to form a leaf-like structure, suggesting that the glumes lost their organ boundary (Figure 3.2E to F). In addition, the floral organs of the extra spikelets appeared to be distorted to varying degrees (Figure 3.3 and Appendix Figure S3.1), indicating that the development of extra spikelet-related organs was enhanced. It is worth noting that all the observed phenotypic defects in *flo.a* mutant (extra spikelets, fused glumes) only existed in the upper and middle parts of the spike but not in the basal part (Figure 3.2B and Figure 3.4), implying a position-specific developmental regulation by the *Flo.a* locus across the mutant spike.

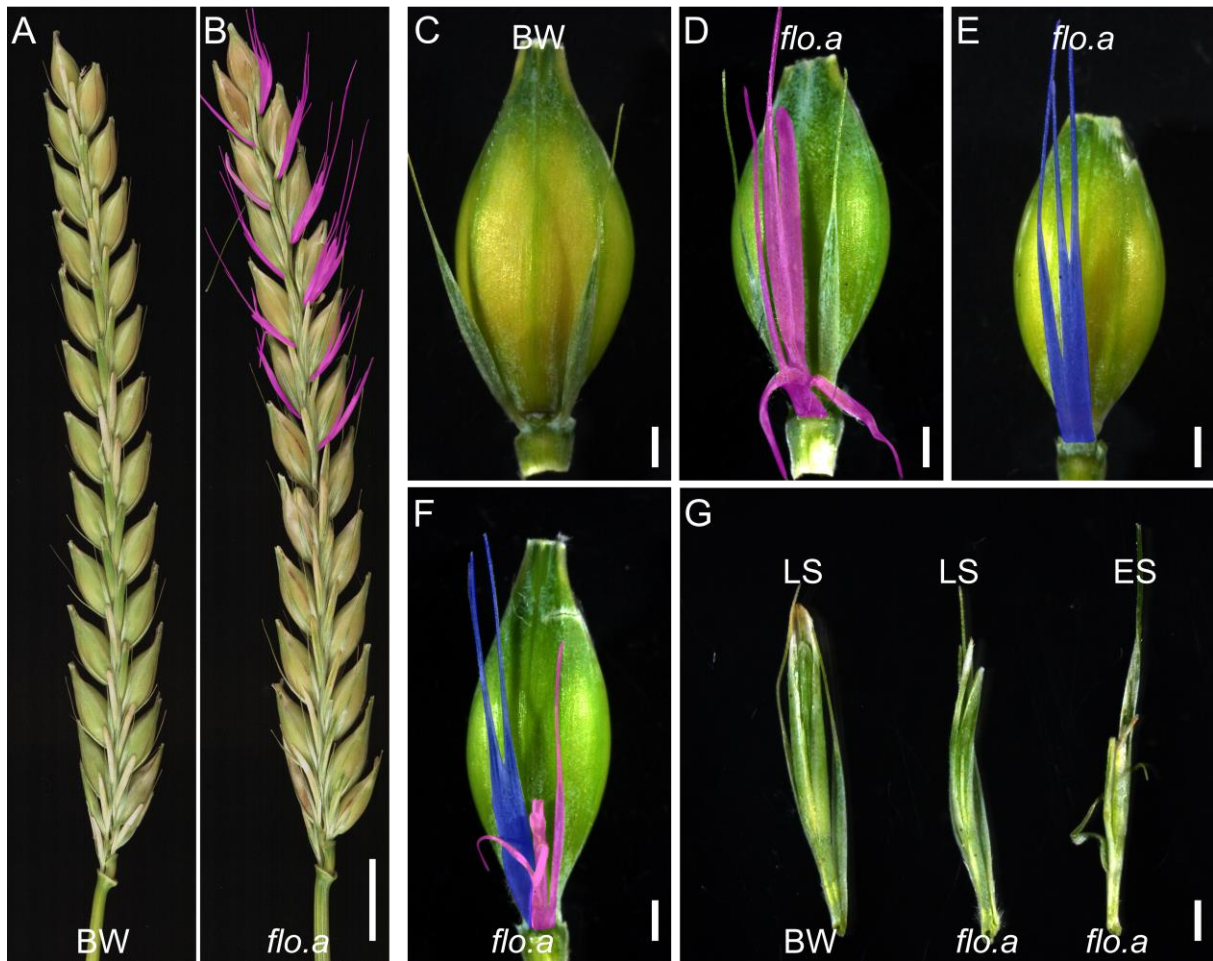


Figure 3.2. Phenotypic characterization of spikelets in *flo.a* mutant. (A) and (B) The morphology of spike of BW and *flo.a* mutant, respectively. (C) Central spikelet phenotype of BW. (D) to (F) Central spikelet phenotype of *flo.a* mutant. (G) Phenotypic comparison of lateral spikelet and extra spikelet in BW and *flo.a* mutant. The awns of the central spikelet have been removed. The lateral spikelets in (C to E) have been removed. The purple and dark blue areas represent extra spikelet and fused glume, respectively. Bar: (A) and (B) = 1 cm; (C) to (G) = 1mm.

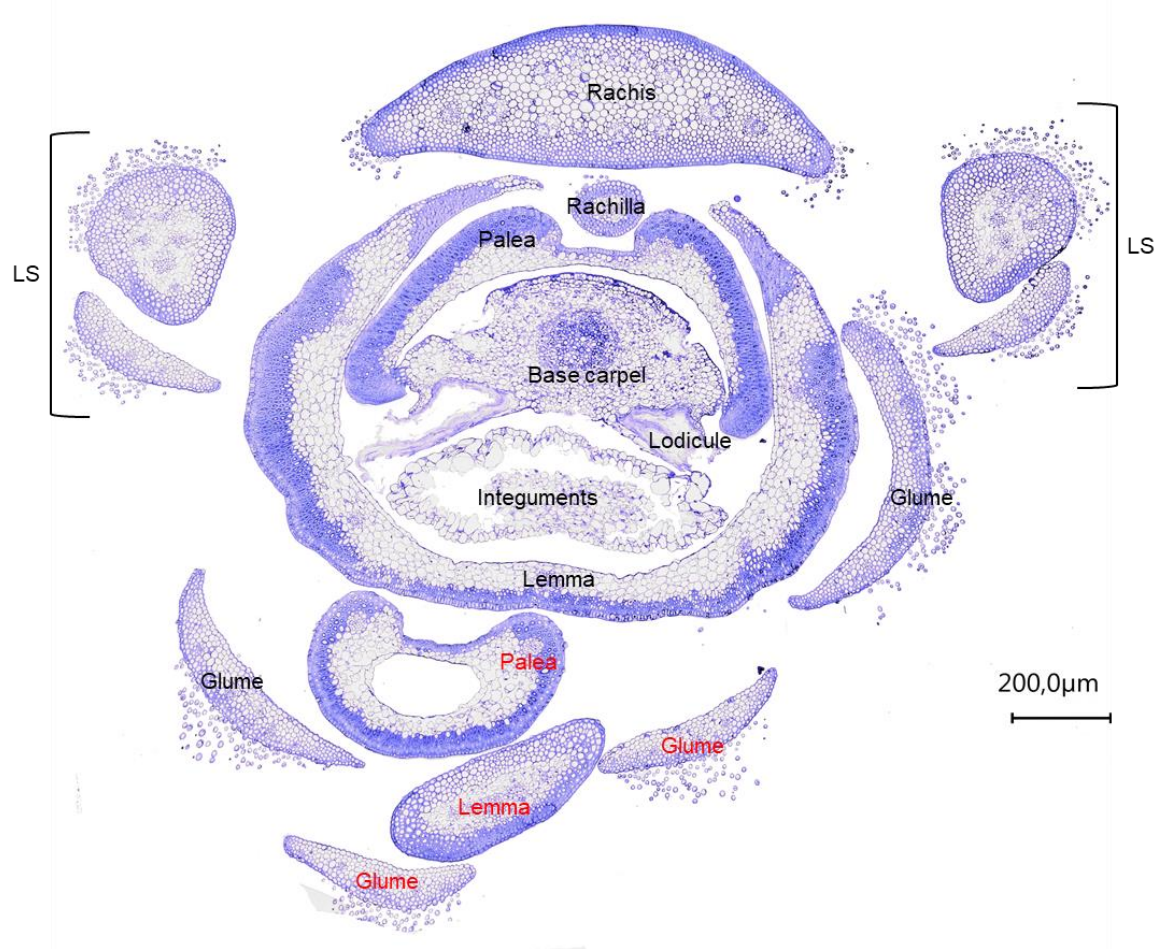


Figure 3.3. Morphological analysis of extra spikelet formation in the *flo.a* mutant. Cross-section details of spike phenotype of *flo.a*. The red terms indicate floral organs of the extra spikelet. LS, Lateral spikelet. Bar = 200 μ m.

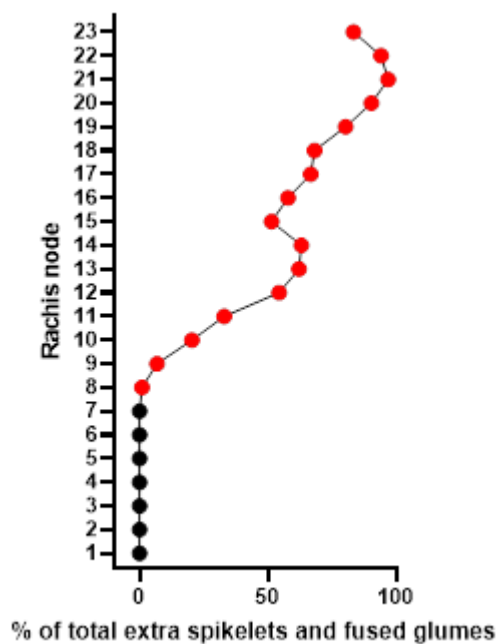


Figure 3.4. Position effect of the phenotypic defect in the *flo.a* mutant. Quantification of extra spikelet formation and fused glumes across rachis nodes of *flo.a*. The number of investigated spikes = 103. The black dot and red dot represent the percentage of total extra spikelets and fused glumes in the basal and upper-mid portion part of rachis nodes of *flo.a*, respectively.

In addition to producing extra spikelets, *flo.a* plants also displayed significant differences for several agronomic traits except for the spike number (Figure 3.5B). The *flo.a* plants were taller (Figure 3.5A) while showing a significant decrease in yield component traits, including node number per spike, grain number per spike, grain setting rate, spikelet length, grain area, grain length, grain width, and thousand-grain weight (Figures 3.5C to J). These data suggest that the production of extra spikelets influences spike and regular spikelet development in *flo.a* mutant.

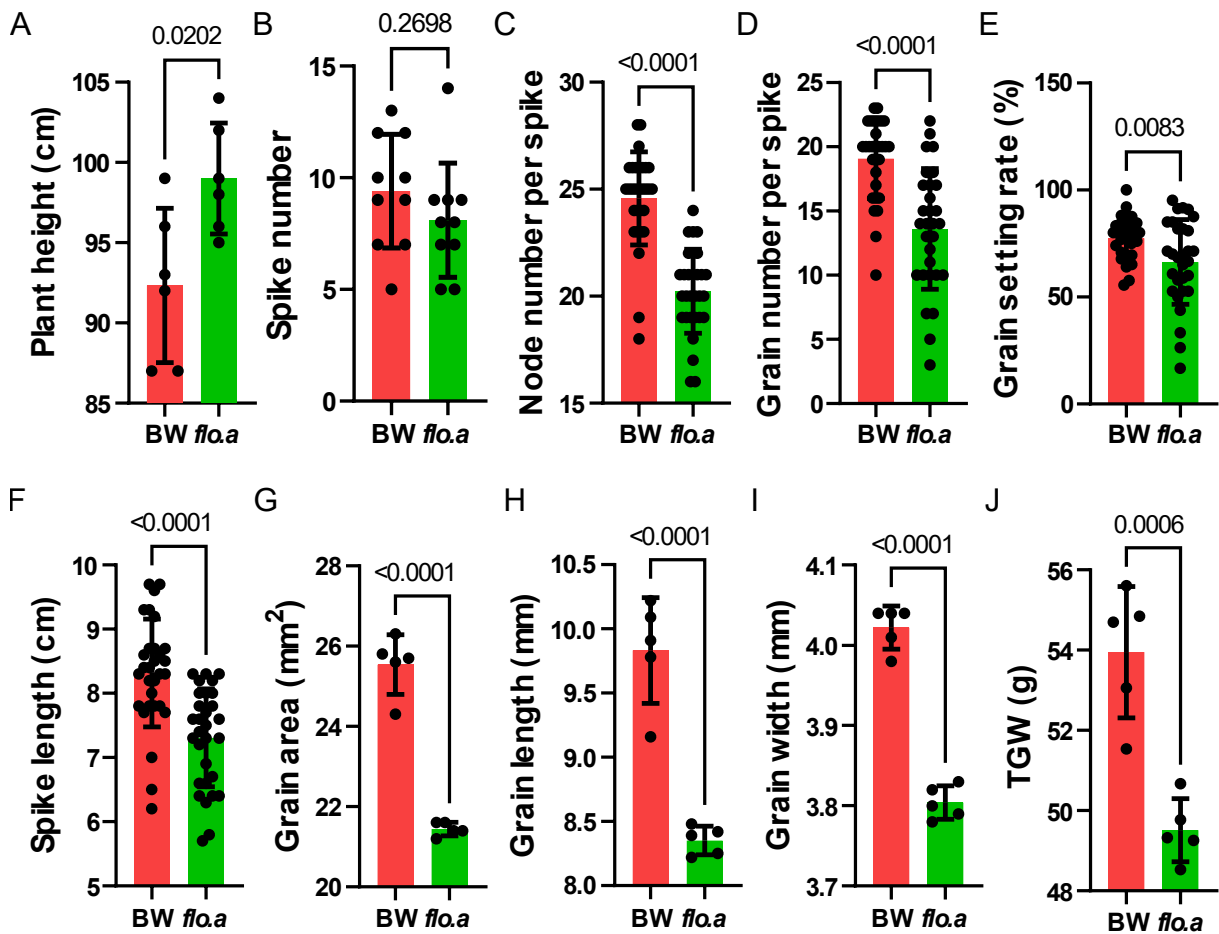


Figure 3.5. Phenotypic differences of agronomic traits between BW and *flo.a* mutant plants. Statistical analysis of (A) Plant height, (B) Spike number, (C) Node number per spike, (D) Grain number per spike, (E) Grain setting rate, (F) Spikelet length, (G) Grain area, (H) grain length, (I) Grain width, and (J) thousand-grain weight of BW and *flo.a* mutant. Error bars represent mean values ± SD, and the *P* values indicate statistically significant differences and were determined according to the two-tailed Student's *t*-test.

3.1.2 The development of lateral spikelets is suppressed in *flo.a* mutant

Another spikelet phenotype featured in the *flo.a* mutant was the extremely suppressed LS. In barley, the development of LS is mainly regulated by a set of *VRS* genes. The LSs of two-rowed barley are suppressed by functional *VRS* genes. In both BW and *flo.a*, the size of the later developed apical LSs is smaller than the basal LSs (Figure 3.6) Interestingly, in *flo.a* mutant, the development of the florets both in apical and basal parts was more strongly inhibited, resulting in significantly smaller sizes of the LSs (Figure 3.6B and C). The phenotype of suppressed LS is genetically linked to extra spikelets in segregating populations derived from BW and *flo.a*, indicating that inhibited LSs are partly regulated by the *Flo.a* locus.

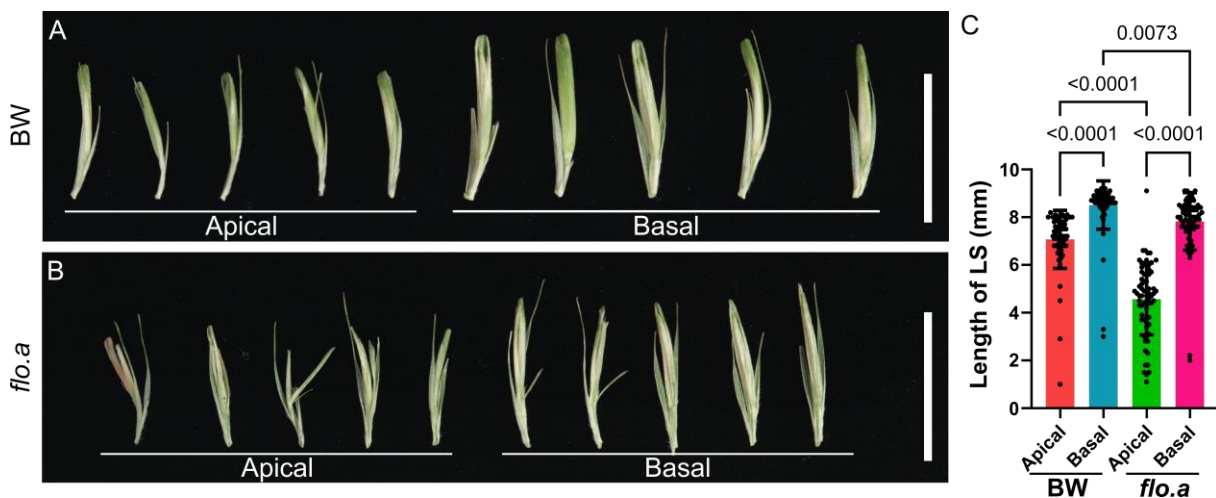


Figure 3.6. Phenotypic difference of lateral spikelet growth between BW and *flo.a*. (A) and (B) The phenotype of five apical and five basal LSs in the BW and *flo.a*, respectively. Bar = 10 mm. (C) Statistical analysis of length of the apical and basal lateral spikelet of BW and *flo.a*. Error bars represent mean values \pm SD, and the *P-values* indicate statistically significant differences and were determined according to ordinary one-way ANOVA.

3.1.3 The fertility of extra spikelets in *flo.a* mutant is inhibited

To better understand the developmental details of extra spikelet formation, we dissected immature spikes at different stages from BW and *flo.a*. In BW spikelet, a pair of glumes (inner and outer) with a clear boundary and spacing in between grew from the rachis node on the flanked side of the single floret (Figure 3.7A to C). At the WA Waddington scale 5.0 (W5.0) stage, the “*flo*” phenotypes were first visible under the stereomicroscope (Figure 3.7D). Compared with BW, the extra spikelet meristem of

the *flo.a* mutant differentiated at the rachis node on the abaxial face of the CS (Figure 3.7D and E). Additionally, the two glumes of the CS partly lost their boundary and fused from the base, close to a newly formed primordium with an unknown identity (Figure 3.7D). Notably, the extra spikelet developed later than the canonical triple spikelets (Figure 3.7D). At the WA (W6.0) stage, the extra spikelet meristem differentiated into FM and produced the inner floral organ (e.g., stamen) primordia (Figure 3.7E; red arrow). However, these inner floral organs remained undifferentiated and were eventually degenerated, resulting in the production of a sterile spikelet in the GA (W8.0) stage (Figure 3.7F). Taken together, extra spikelets are not part of the canonical spikelet triplet; in fact, they are unable to be fertile, which is similar to the fate of LSs.

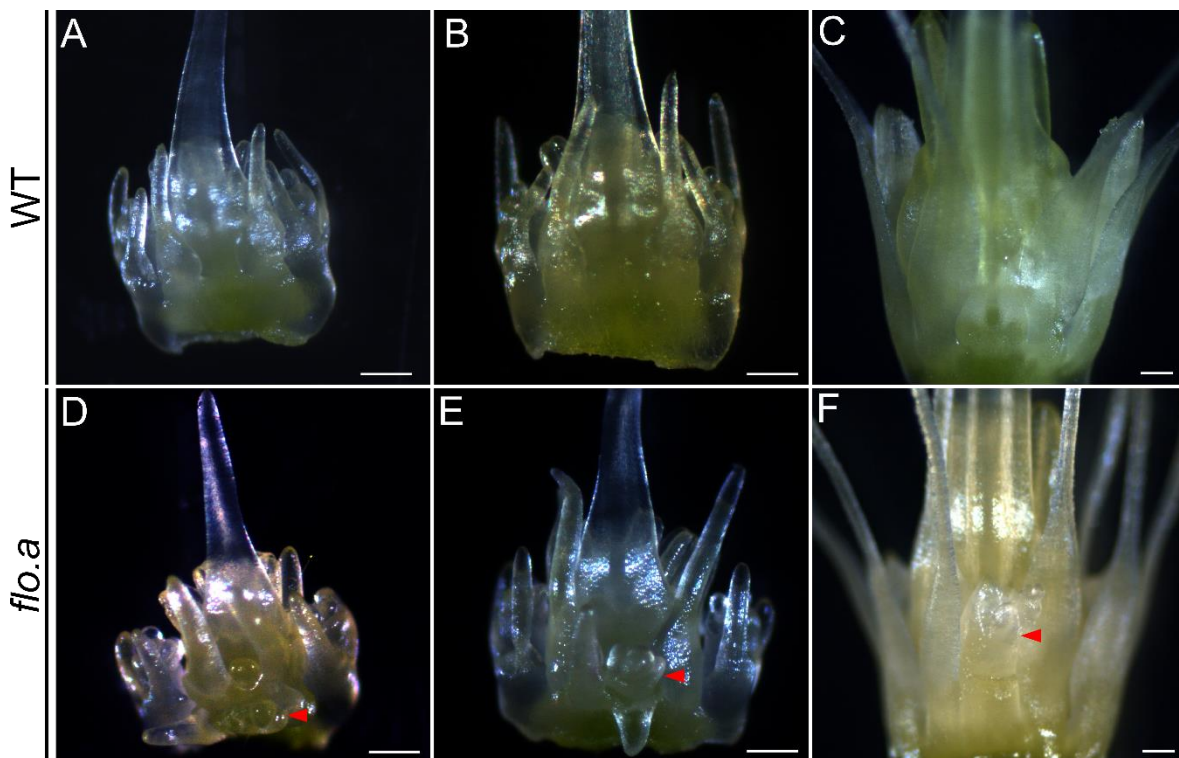


Figure 3.7. Stereomicroscope imaging for the extra spikelet in *flo.a*. (A to C) Developing spikelets of BW. (D to E) Developing spikelets of *flo.a*. The red triangles indicate the extra spikelet. Bar = 200 μ m.

3.1.4 Determinacy loss of the spikelet meristem in *flo.a* mutant

The extra spikelets generated on the upper-mid portion of the *flo.a* spike had an impact on the development of the corresponding CSs. In BW spike, the SM transformed into FM, which subsequently differentiated into floral organ primordia and eventually formed a complete spikelet (Figure 3.8A to I). During the DR stage, the TSMs differentiated from spikelet ridges similarly between BW and *flo.a* (Figure 3.8J).

However, with spike development, extra spikelets were detectable at the middle part towards the tip of the *flo.a* spike starting from the LP stage. Extra spikelet meristems started initiating from the rachis node and grew on the abaxial plane of the CSMs (Figure 3.8K and L), suggesting the phenotypic positional effects of *flo.a* may be related to the timing of extra spikelet formation in the upper-mid spike (Figure 3.8M to P). Notably, the emergence of extra spikelet meristems was after the formation of the spikelet triplets. While the CS was already at the WA stage, the extra spikelets in *flo.a* reached the SP stage, which is characterized by the appearance of stamen primordium (Figure 3.8Q and R). These results indicate that the CSM lost its determinacy and enabled the production of an additional SM, whereas the determinacy of the LSMs remained unaffected.

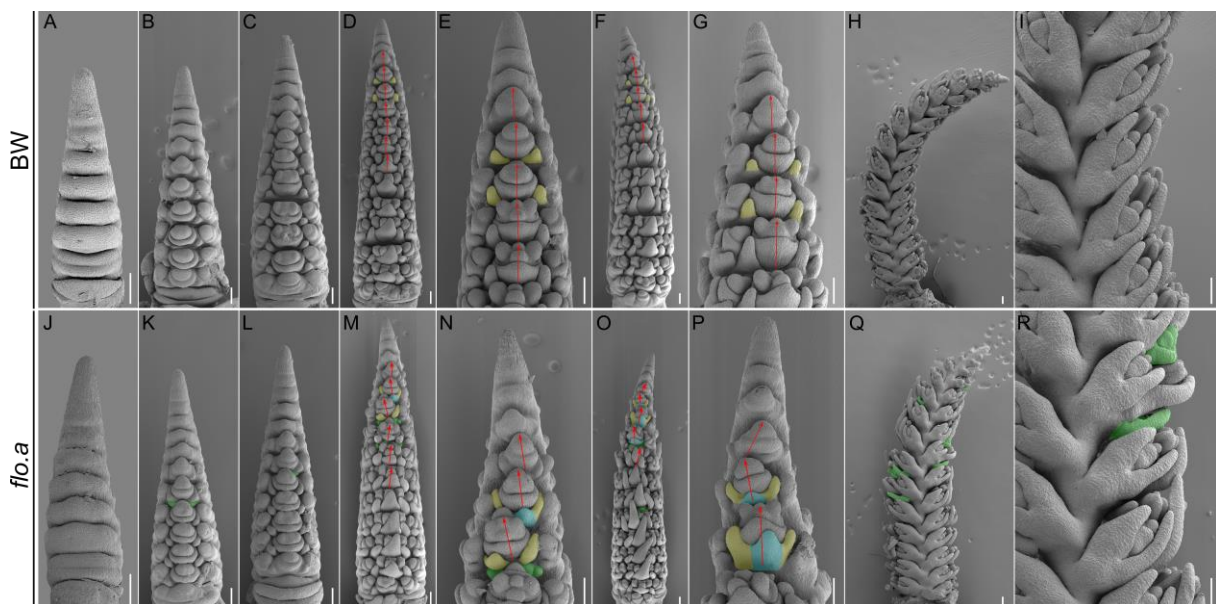


Figure 3.8. Scanning Electron Micrographs of the immature spike in BW and *flo.a*. (A to I) The immature spike of BW. (J to R) The immature spike of *flo.a*. The green area represents the extra spikelet meristem/primordia. The yellow areas represent glume primordia. The blue areas represent newly formed primordia from glume primordia. The red arrows indicate the direction of CS development. The awns of central spikelets in (H, I, Q, and R) were removed. Bar = 100 μ m.

3.1.5 The organ boundary and identity of glumes in the central spikelets are affected in *flo.a* mutant

Glume development of CS was affected by the appearance of extra spikelets. In the BW spikelet, glume primordia grew in parallel on either side of the developing floret (Figure 3.8B to G and 3.9A). However, this patterning was broken in the upper-mid

spike parts of *flo.a*, showing that glume initiation sites were not fixed (Figure 3.8M and N). In the most severe cases, two glume primordia were fused and produced a new glume primordium in the middle part (Figure 3.8M to P), indicating that the boundary and partial identity of the glume from the CS were lost. In addition, compared with BW, the growth direction of CSs in *flo.a* on the rachis changed, most likely affected by the newly generated extra spikelets (Figure 3.8M to P). These data showed that *flo.a* not only produced extra spikelets but that also boundary and identity of CS glumes were affected in *flo.a* mutant.

At the GrA stage, extra spikelets in *flo.a* produced one pair of glumes and one floret, having a similar morphological structure as LSs (Figure 3.9E). However, while the spikelet identity was established, in some severe cases, the extra spikelet meristem formed two FMs, which were consumed into two florets, resulting in a paired floret-spikelet phenotype (Figure 3.9D). In addition, the glumes of CSs were fused from their base while some primordia or organs of unknown identity were produced in the adaxial part of CS glumes (Figure 3.9B to D and F).

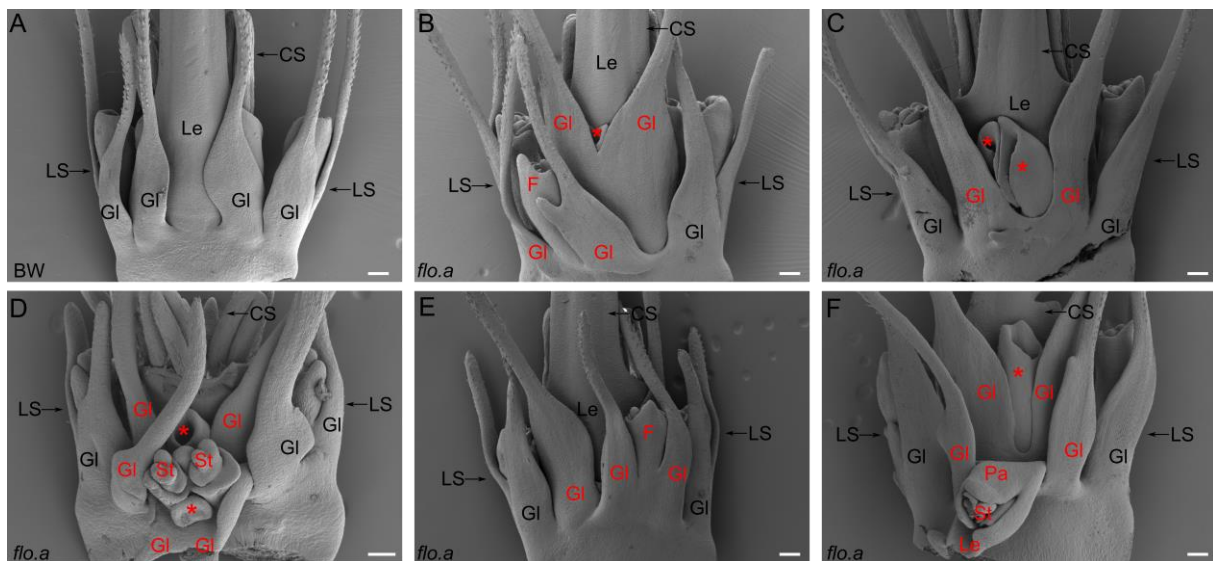


Figure 3.9. Scanning Electron Micrographs of the spikelet in BW and *flo.a*. (A) The immature spikelet triplet of BW (dorsal view). (B to F) The immature spikelet triplet and extra spikelets of *flo.a*. The black letters indicate the regular floral organs of the spikelet triplet. The red letters indicate the supernumerary or defective floral organs of the CS. Asterisks indicate those primordia or organs with unknown identity. F, floret. Gl, Glume. Le, lemma. Pa, Palea. St, stamen. Bar = 100 μ m.

3.1.6 The formation of extra spikelets interferes with the normal vascular patterning

To explore the connection status of extra spikelets to the rachis and its potential impact on the development of the spikelet triplet, we inspected one rachis node from *flo.a* bearing a spikelet triplet and one extra spikelet. Subsequently, we performed three-dimensional (3D) reconstruction using continuous serial cross-sections to obtain the internal structural characteristics of the entire rachis nodes (Figure 3.10 to 3.14). A total of 210 slices with 10 μm spacing were collected in BW and *flo.a* by cross-cutting across an integral rachis node (Figure 3.10).

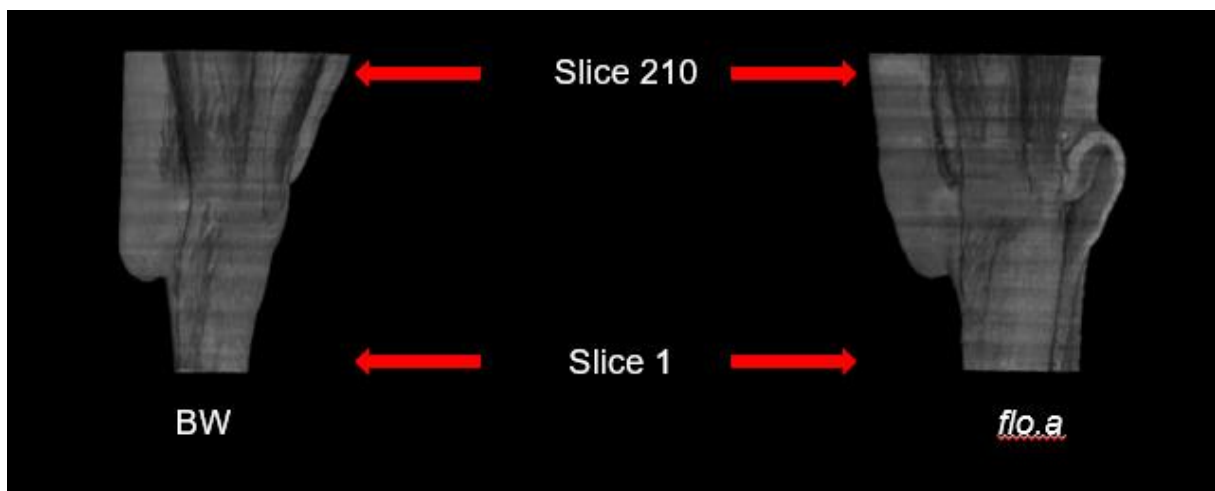


Figure 3.10. Schematic diagram of serial sections of nodal complexes in BW and *flo.a*. The sectioning starts from the lower internode and gradually goes up to the upper internode.

In comparison to BW, the altered morphology of the *flo.a* rachis node was evident in the 3D images (Figure 3.11A). Additional organs (glumes and lemma) in *flo.a* initiated abaxially of the CS and connected to the rachis node. Nearly 50 individual vascular bundles were identified in the section of the mutated rachis node belonging to different organs, including glume, lemma, palea, and rachis (Figure 3.11B). Only two types of extra floral organs were detectable and showed identical numbers to that in lemma (5 veins) and glumes (3 veins) of normal CS, demonstrating that these organs may have obtained lemma and glume identity, respectively (Figure 3.11B). However, at this stage, it may not be adequate to assume that the newly formed organs possess spikelet identity because palea and rachilla were underdeveloped or prematurely degenerated (Figure 3.10 and 3.11).

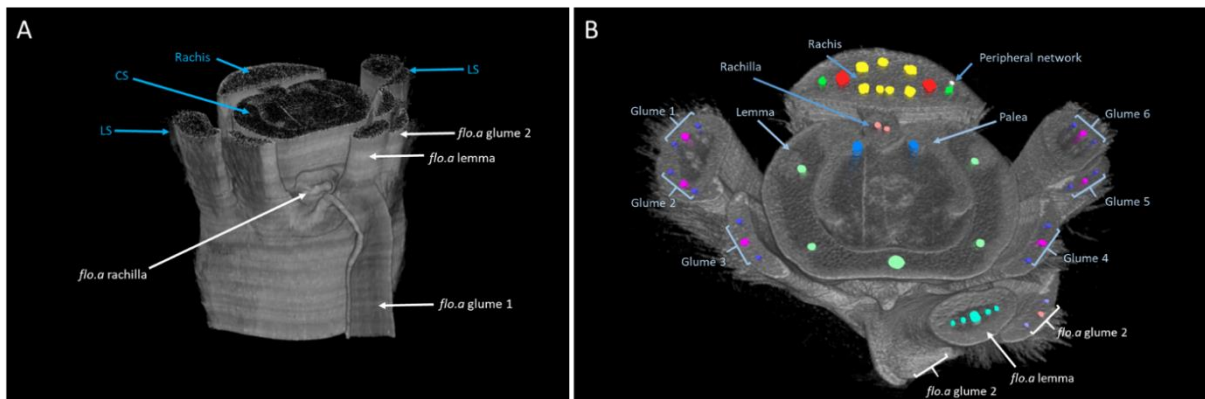


Figure 3.11. 3D reconstruction of *flo.a* rachis node. (A) Stereo imaging of *flo.a* rachis node. (B) Top-view of *flo.a* rachis node with all relevant vascular bundles. The areas marked in different colors indicate vascular bundles in different organs.

Meanwhile, the patterning of vascular bundles of the CS organs was affected by supernumerary organ formation in *flo.a*. Considering the critical role of vascular tissues in supplying assimilation to promote organ development, we firstly analyzed the patterning for the lemma, which showed the maximum number of veins in the CS to the rachis node. In BW spikes, the rachis node displayed a regular bilateral symmetry of vascular organization (Figure 3.12). In the upper part of the rachis node (Slice 136), these five vascular bundles (L1 to L5) were evenly spaced, while towards the base of the node (Slice 110), the bundles were coming closer together but still showing a strict bilateral symmetry of organization to connect to the rachis node (Figure 3.12). In *flo.a*, extra lemma vascular bundles (*flo.a* Lemma, fL1 to fL5) were able to access the nodal complex despite being different from that in regular CS lemma in size and distribution pattern (Figure 3.12). The strict symmetry of CS lemma vascular bundles was broken and arranged linearly.

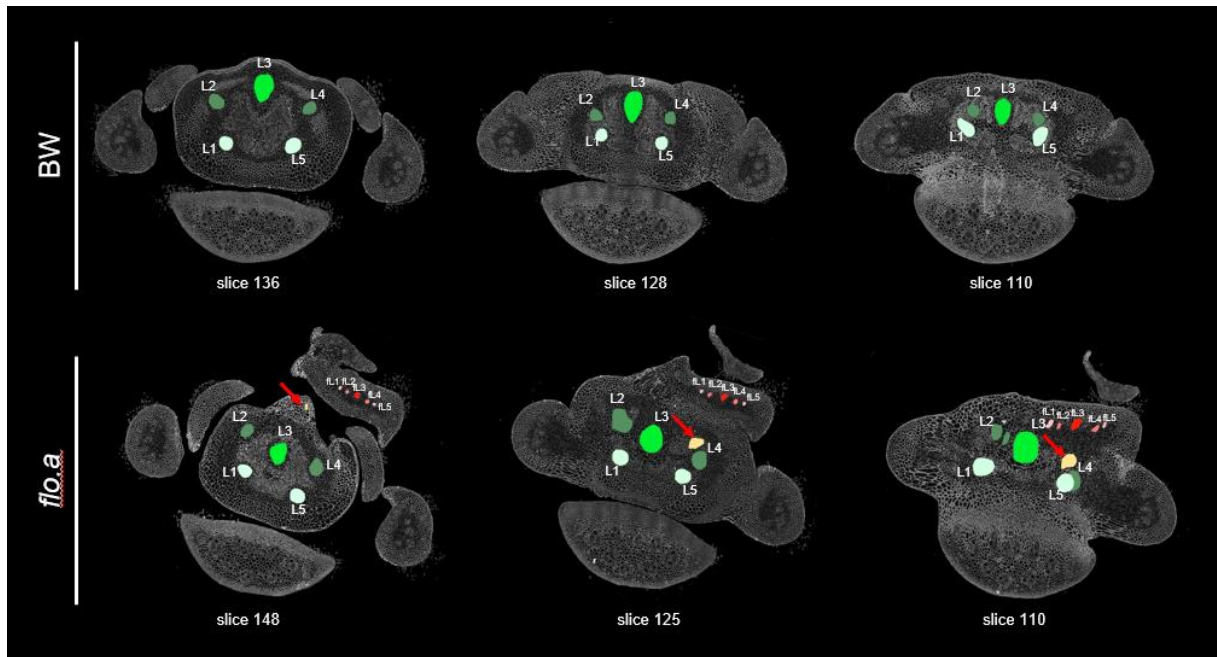


Figure 3.12. Top views of serial sections of nodal complexes in BW and *flo.a*. Regions marked by different degrees of green and pink indicate vascular bundles of CS lemma (L1 to L5) and extra spikelet lemma (fl1 to fl5), respectively. Regions marked by orange and red arrows indicate vascular bundles of extra spikelet rachilla. The image from left to right represents the position of the section surface from top to bottom in nodal complex.

The L4 position of the CS lemma was not fixed, gradually approaching, and eventually fusing with L5 from top to bottom of the rachis. Interestingly, the position vacated by the fusion of L4 and L5 was not occupied by lemma vascular bundles from the extra spikelet but was replaced by the newly formed rachilla (Figure 3.12; see arrow). The reconstructed 3D model also showed that L4 and L5 fuse near the nodal complex and provided the position for the connection of the vascular bundles of organs from extra spikelets (Figure 3.13).

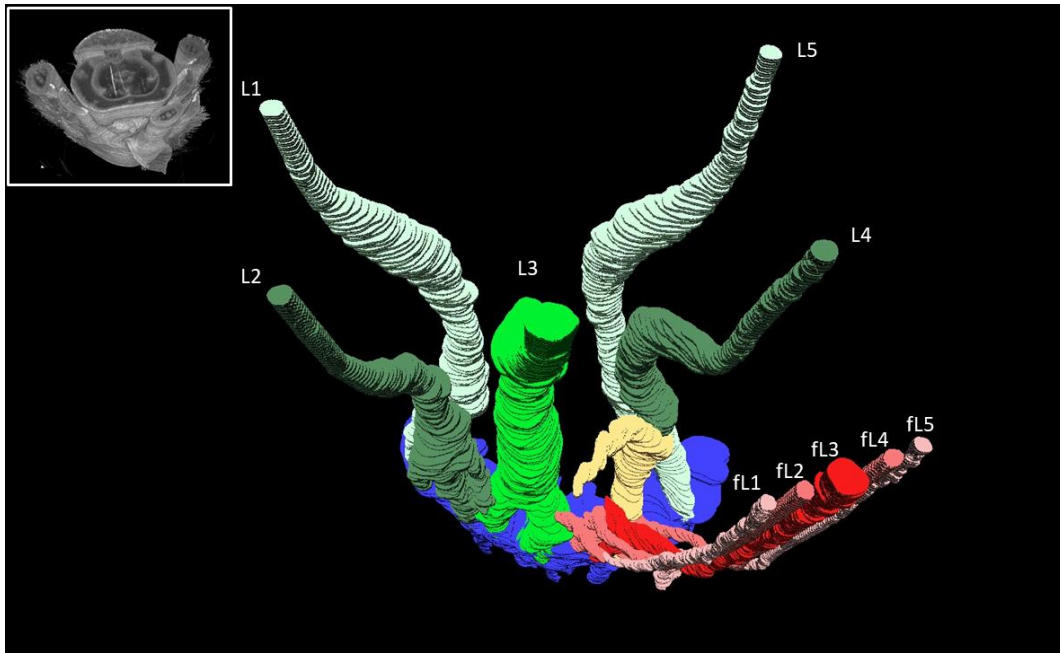


Figure 3.13. Schematic diagram and 3D reconstruction of lemma vascular bundles of CS and extra spikelet in *flo.a*. Bundle structure marked by different degrees of green (L1-5) and pink (fL1-5) indicate lemma vascular bundles of CS and extra spikelet, respectively. The bundle structure marked by orange indicates the rachilla vascular bundle of the extra spikelet. The blue structure represents the nodal complex. The image in the top left corner is the top view of the section within the *flo.a* spike.

The glume, as the diagnostic component of the spikelet, is considered to be a bract structure (Kellogg, 2022; Wang *et al.*, 2021). The barley spikelet contains one inner and one outer glume, each with three vascular bundles (one central and two lateral) attached to the rachis (Figure 3.14A and B). Notably, in BW barley glumes the central vascular bundles always merge with the nodal complex and the lateral vascular bundles almost always merge with the peripheral network. Thus, a total of 6 and 12 vascular bundles are connected to the nodal complex and peripheral network within the spikelet triplet, respectively (data not shown).

3D modeling for glumes showed that the vascular bundles in BW glumes were able to strictly enforce the specification of distribution patterns. In *flo.a*, however, this norm is broken; the formation of supernumerary spikelet not only added some extra glume vascular bundles to the nodal system but also appeared to cause disturbances for glumes of the spikelet triplet. Although all the six central vascular bundles of the glumes from the spikelet triplet and the two extra spikelet glumes merged with the nodal complex, out of a total of 16 lateral vascular bundles, no less than 5 were not connected to the peripheral network, especially the 3 vascular bundles from the glumes from CS

(Figure 3.14 C to D and Appendix Figure S3.2), suggesting that the formation of additional vascular bundles has a distance effect on the development of organs from spikelet triplet, perturbing the vascular patterning of adjacent organs. This result is consistent with our phenotypic observations that the identity of organs was not affected in LS but significantly in CS (Figure 3.2B to I and 3.6).

The above data shows that the initiation of the extra spikelets also occupies the nodal connecting point of developing organs; and thus, they affect the development of CS. This impact is mutual because the space of the nodal complex does not seem to be sufficient to support the complete development of quadruple-spikelets, causing various types of shapes in extra spikelets. And this seems to eventually lead to a significant difference in spikelet/grain size between BW and *flo.a* (Figure 3.5G to I and 3.6).

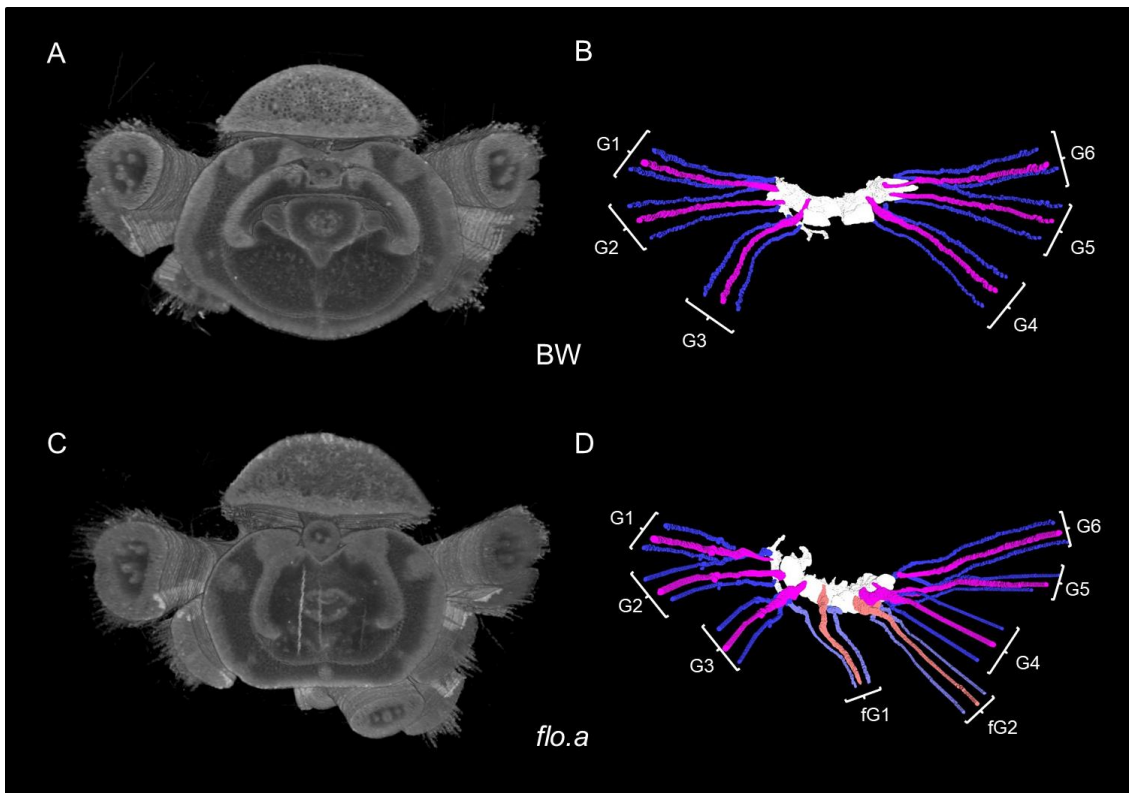


Figure 3.14. Schematic diagram of 3D reconstruction of glume vascular bundles in BW and *flo.a*. (A and C) the cross-section view of spikelet in BW and *flo.a*, respectively. (B and D) The connection status of glume vascular bundles to the rachis node in BW and *flo.a*, respectively. The glume central and lateral vascular bundles from spikelet triplet are marked by purple and dark blue, respectively. The central and lateral vascular bundles of the extra spikelet glumes are represented by pink and light blue, respectively. The white structure represents the nodal complex. (G1 to G6) indicate the glume vascular bundles of the spikelet triplet. (fG1 and fG2) indicate the glume vascular bundles of the extra spikelet.

3.2 Map-based cloning of *Flo.a*

3.2.1 *flo.a* is a recessive mutant

To identify the underlying gene responsible for the *flo.a* phenotypes, we performed whole-genome sequencing (WGS) of *flo.a*. Sequence analysis showed only three introgressed fragments from the original donor line (*cv. Foma*) present in *flo.a* because of the backcrosses into BW five times (Figure 3.15A). An F2 population with 190 individuals derived from a cross between BW and *flo.a* (BW × *flo.a*) was firstly constructed and carefully counted the mutated phenotypes, including extra spikelet formation and fused glumes. From our phenotypic analysis, the phenotypes followed a ratio of wild type (144) to mutant type (46) approximately fitting the expected 3:1 ratio ($\chi^2 = 0.06$, $p\text{-value} = 0.80$) (Figure 3.15B). Thus, the *flo.a* phenotypes display single nuclear monogenic recessive inheritance.

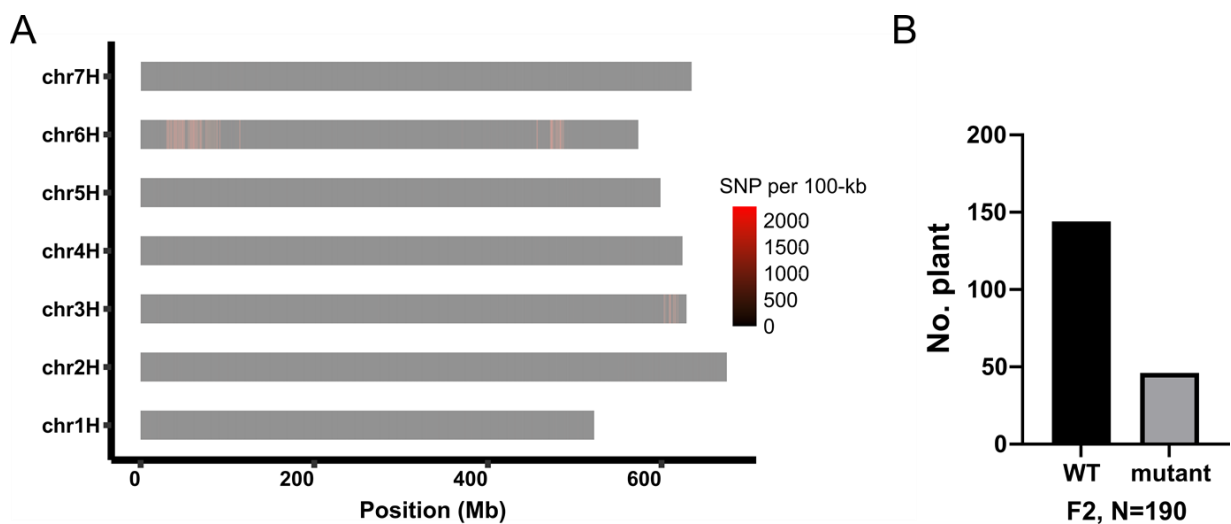


Figure 3.15. Genetic analysis in F2 population (BW × *flo.a*). (A) Graphical genotypes of *flo.a*. The SNPs were retrieved between BW and *flo.a*. The red box indicates the introgression from the original donor line (*cv. Foma*). The gray box indicates the BW background. (B) Distribution of the WT and *flo.a* phenotypes in the F2 population.

3.2.2 Fine-Mapping of the *Flo.a* locus

In previous reports, the *Flo.a* locus was determined to be on chromosome 6H (Druka *et al.*, 2011; Koppolu *et al.*, 2021). Therefore, we focused our attention on the introgressions on chromosome 6H in *flo.a* (Figure 3.15A). For identifying the genomic interval harboring the *flo.a* mutation, we developed a set of polymorphic molecular markers based on the genomic differences [insertion/deletion (indel) and single

nucleotide polymorphism (SNP)] between BW and *flo.a* on chromosome 6H to genotype the F2 population. Linkage analysis revealed that the *Flo.a* locus was associated with two molecular markers FB74.4 and FB110.0 on the short arm of chromosome 6H, covering the region also partially overlapping with the introgression from the original mutant. Fine-mapping using 3,794 plants generated from recombinants in the F2 population delimited the *Flo.a* locus to a 12.2-Mbp physical interval (Figure 3.16A). Sequence analysis based on WGS data revealed that one ~477 kb genomic region exhibited fairly low read coverage in *flo.a* compared to BW and Foma (Figure 3.16B), indicating that this candidate region had a large genomic deletion. The deleted interval contained only one High Confidence (HC) gene and three Low Confidence (LC) genes. Further inspection of all four genes with annotation revealed the HC gene, *HORVU.MOREX.r2.6HG0469780*, is a member of the *Arabidopsis* **L**SH1 and *Oryza* **G**1 (**A**LOG) family (Figure 3.16C and D). Several ALOG genes in *Arabidopsis*, rice, sorghum and tomato have been shown to play important roles in inflorescence and floral organ development (Bencivenga *et al.*, 2016; Cho and Zambryski, 2011; Huang *et al.*, 2021; Huang *et al.*, 2022; Li *et al.*, 2012; Macalister *et al.*, 2012; Peng *et al.*, 2017; Sato *et al.*, 2014; Takeda *et al.*, 2011; Xu *et al.*, 2016; Yoshida *et al.*, 2013; Yoshida *et al.*, 2009; Zhao *et al.*, 2004a; Zhou *et al.*, 2021). Subsequent PCR amplification also showed that the gene is absent in *flo.a* but present in three wild-type genotypes (Morex, BW and Foma) (Figure 3.16E). Therefore, *HORVU.MOREX.r2.6HG0469780* was the best plausible candidate for the *Flo.a* locus.

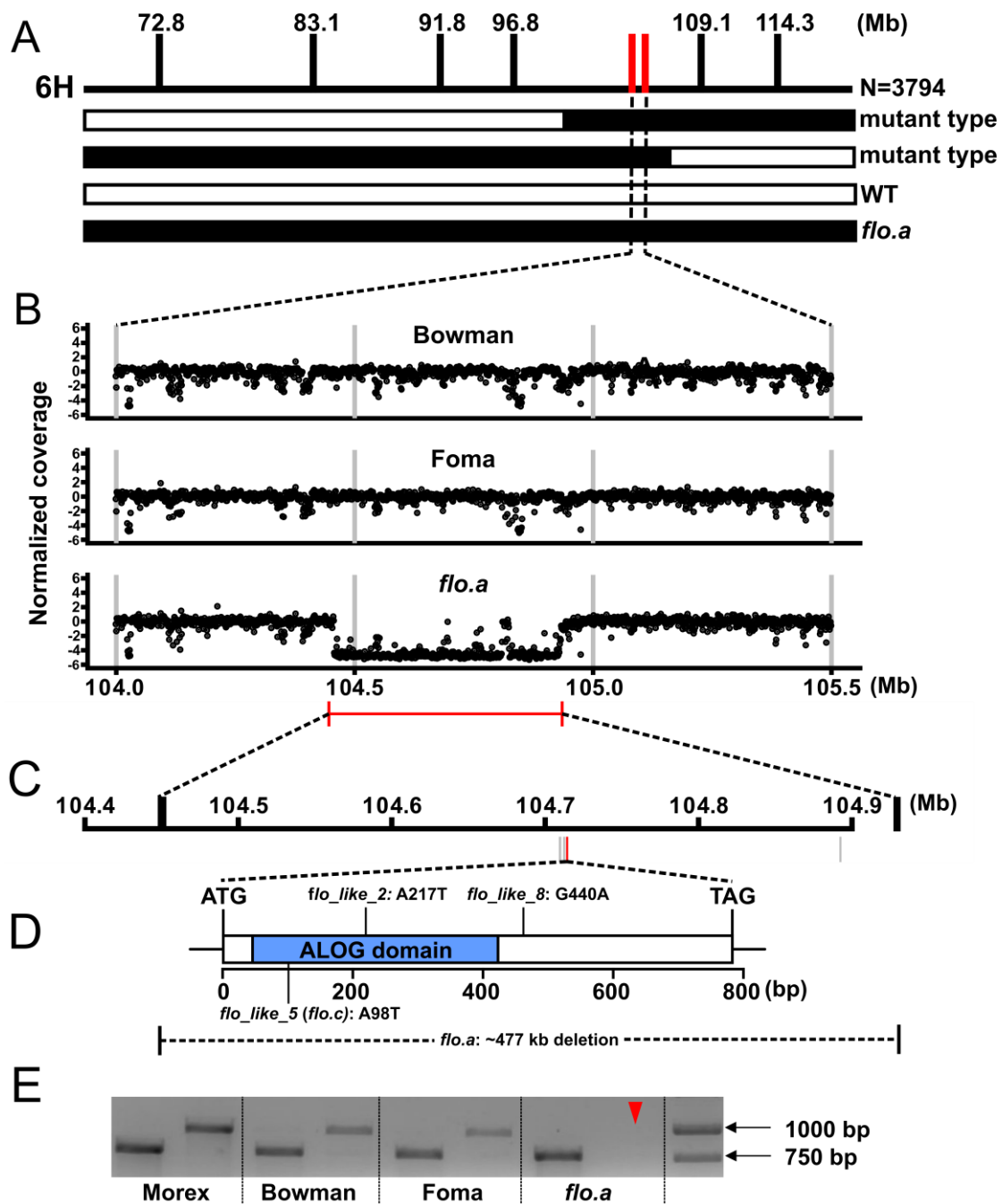


Figure 3.16. Map-based cloning of *Flo.a*. (A) *Flo.a* was narrowed down to a 12.2-Mbp interval on the short arm of chromosome 6H. The number of plants used for mapping and the recombinants is indicated. WT, wild-type. (B) Normalized coverage of whole-genome sequencing in 1.5-Mbp region between Bowman, Foma and *flo.a*. The ~477-kb deleted interval is marked by the red line. (C) Gene number in the deleted interval. The red and gray lines indicate high confidence (HC) and low confidence (LC) genes, respectively. (D) *Flo.a* gene model containing one ALOG domain (blue box). The mutation positions in the *Flo.a* gene from four barley mutants showing *flo.a* phenotypes are indicated. (E) PCR amplification by primer pairs covering the *flo.a* candidate (*HORVU.MOREX.r2.6HG0469780*) (right) and flanking gene (*HORVU.MOREX.r2.6HG0469830*) (left) outside of the deletion in Morex, Bowman, Foma and *flo.a* mutant.

3.2.3 Validation of *Flo.a* candidate in allelic *flo-like* mutants

To validate that the candidate gene (*HORVU.MOREX.r2.6HG0469780*) is responsible for the *flo.a* phenotypes, we sequenced it in two other known *flo* (*flo.b* and *flo.c*) mutants considering that they have the same background and similar phenotypes to *flo.a* mutant (Druka *et al.*, 2011). Interestingly, *flo.c* was found to carry a non-synonymous mutation in the candidate gene (Figure 3.16D). Allelism test showed that F1 plants (*F1_flo.a/flo.c*) derived from *flo.a* and *flo.c* produced extra spikelets, indicating that *flo.c* is another allele to the *Flo.a* locus (Figure 3.17). Furthermore, we collected a set of nine *flo*-like (*flo_like_1* to 9) induced mutants that came from different backgrounds, showing extra spikelets in the upper-mid part of the spike that resembled *flo.a* (Figure 3.18B to E). Sanger-sequencing of these mutants, using primer pairs covering CDS and promoter region (Appendix Table S1), revealed that three of them, i.e., *flo_like_2*, *flo_like_5* (identical to *flo.c*), *flo_like_8*, harbored three non-synonymous mutations, possessed amino acid (aa) substitutions or premature stop codon leading to protein truncation, respectively (Figure 3.16D and 3.18A). Thus, three mutants within *HORVU.MOREX.r2.6HG0469780* strongly supported that it is causative for the *Flo.a* locus.



Figure 3.17. Allelism test between *flo.a* and *flo.c*. (A to D) The spike phenotype of BW, *flo.a*, *flo.c* and *F1_flo.a/flo.c*, respectively. The red triangle represents the extra spikelet. Bar = 1 cm.

A

```

Flo_like_8      MDMSGVSAVDSPPGGSSASSAVAAPRPSRYESQKRRDWQTFGGYLRNHRPPELARCSCGAH 60
Flo_like_5(flo.c) MDMSGVSAVDSPPGGSSASSAVAAPRPSRYESQKRRDWQTFGGYLRNHRPPELARCSCGAH 60
Flo_like_2      MDMSGVSAVDSPPGGSSASSAVAAPRPSRYESQKRRDWQTFGGYLRNHRPPELARCSCGAH 60
Morex          MDMSGVSAVDSPPGGSSASSAVAAPRPSRYESQKRRDWQTFGGYLRNHRPPELARCSCGAH 60
Bowman         MDMSGVSAVDSPPGGSSASSAVAAPRPSRYESQKRRDWQTFGGYLRNHRPPELARCSCGAH 60
Foma           MDMSGVSAVDSPPGGSSASSAVAAPRPSRYESQKRRDWQTFGGYLRNHRPPELARCSCGAH 60
Bonus         MDMSGVSAVDSPPGGSSASSAVAAPRPSRYESQKRRDWQTFGGYLRNHRPPELARCSCGAH 60

Flo_like_8      VLEFLRYLDQFGKTKVHAAGCPSGHPSPAPCPCLKQWGSLDALVGRLLRAAFEEENG 120
Flo_like_5(flo.c) VLEFLRYLDQFGKTKVHAAGCPSGHPSPAPCPCLKQWGSLDALVGRLLRAAFEEENG 120
Flo_like_2      VLEFLRYLDQFGKTKVHAAGCPSGHPSPAPCPCLKQWGSLDALVGRLLRAAFEEENG 119
Morex          VLEFLRYLDQFGKTKVHAAGCPSGHPSPAPCPCLKQWGSLDALVGRLLRAAFEEENG 120
Bowman         VLEFLRYLDQFGKTKVHAAGCPSGHPSPAPCPCLKQWGSLDALVGRLLRAAFEEENG 120
Foma           VLEFLRYLDQFGKTKVHAAGCPSGHPSPAPCPCLKQWGSLDALVGRLLRAAFEEENG 120
Bonus         VLEFLRYLDQFGKTKVHAAGCPSGHPSPAPCPCLKQWGSLDALVGRLLRAAFEEENG 120
*****

Flo_like_8      RPEANPFGARAVRLYL RDVRDQQAAGIAYEKRRKRHPQTSKQKQAAAAATAANPA 180
Flo_like_5(flo.c) RPEANPFGARAVRLYL RDVRDQQAAGIAYEKRRKRHPQTSKQKQAAAAATAANPA 180
Flo_like_2      RPEANPFGARAVRLYL RDVRDQQAAGIAYEKRRKRHPQTSKQKQAAAAATAANPA 179
Morex          RPEANPFGARAVRLYL RDVRDQQAAGIAYEKRRKRHPQTSKQKQAAAAATAANPA 180
Bowman         RPEANPFGARAVRLYL RDVRDQQAAGIAYEKRRKRHPQTSKQKQAAAAATAANPA 180
Foma           RPEANPFGARAVRLYL RDVRDQQAAGIAYEKRRKRHPQTSKQKQAAAAATAANPA 180
Bonus         RPEANPFGARAVRLYL RDVRDQQAAGIAYEKRRKRHPQTSKQKQAAAAATAANPA 180
*****

Flo_like_8      PVDRPDMRHDMLEQTHYLFPMHAHLFQGHFLAPADGDPVGLDGVVPAPGDDIVVMMAA 240
Flo_like_5(flo.c) PVDRPDMRHDMLEQTHYLFPMHAHLFQGHFLAPADGDPVGLDGVVPAPGDDIVVMMAA 240
Flo_like_2      PVDRPDMRHDMLEQTHYLFPMHAHLFQGHFLAPADGDPVGLDGVVPAPGDDIVVMMAA 239
Morex          PVDRPDMRHDMLEQTHYLFPMHAHLFQGHFLAPADGDPVGLDGVVPAPGDDIVVMMAA 240
Bowman         PVDRPDMRHDMLEQTHYLFPMHAHLFQGHFLAPADGDPVGLDGVVPAPGDDIVVMMAA 240
Foma           PVDRPDMRHDMLEQTHYLFPMHAHLFQGHFLAPADGDPVGLDGVVPAPGDDIVVMMAA 240
Bonus         PVDRPDMRHDMLEQTHYLFPMHAHLFQGHFLAPADGDPVGLDGVVPAPGDDIVVMMAA 240
*****

Flo_like_8      AAAAAEAHAAGCMPLSVFH* 260
Flo_like_5(flo.c) AAAAAEAHAAGCMPLSVFH* 260
Flo_like_2      AAAAAEAHAAGCMPLSVFH* 259
Morex          AAAAAEAHAAGCMPLSVFH* 260
Bowman         AAAAAEAHAAGCMPLSVFH* 260
Foma           AAAAAEAHAAGCMPLSVFH* 260
Bonus         AAAAAEAHAAGCMPLSVFH* 260
*****

```

B



Figure 3.18. Barley *flo.a* alleles show extra spikelets phenotype. (A) Alignment of the amino acid sequence of *Flo.a* in three *flo*-like induced mutants. (B) The spike phenotype of two wild-types (Foma and Bonus), *flo_like_2*, *flo_like_5* (*flo.c*) and *flo_like_8*. The red triangles represent the extra spikelets. Bar = 1 cm.

3.3 *Flo.a* encodes an ALOG protein

Flo.a encodes a plant-specific transcription factor harboring an ALOG domain starting from aa 21 to 155, which is derived from the XerC/D-like recombinases (Figure 3.19A) (Iyer and Aravind, 2012). Here, we defined the *Flo.a* gene as *HvALOG1*. The proteins of the ALOG family have been reported to be key regulators of inflorescence architecture in several plant species. In grasses, rice *LONG STERILE LEMMA1* (*G1*) is thought to specify the sterile lemma by repressing lemma identity and preventing its development; the loss-of-function mutant *g1* produces abnormally enlarged sterile lemma due to the establishment of lemma identity (Yoshida *et al.*, 2009). Rice *TAWAWA1* (*TAW1*) is proposed to be a unique regulator for meristem activity in the inflorescence; the activity of the IM is extended and the specification of spikelet identity is delayed in a dominant gain-of-function mutant *tawawa1-D*, promoting increased branching phenotypes (Yoshida *et al.*, 2013). Rice *TRIANGULAR HULL1/BEAK LIKE SPIKELET1/ABNORMAL FLOWER AND DWARF1* (*TH1/BLS1/ADF1*) is an important gene regulating floral organ development; the mutations in this gene induce abnormal floral organs possibly suppressing genes involved in the development and

identification of palea and lemma (Li *et al.*, 2012; Ma *et al.*, 2013; Ren *et al.*, 2016). In tomato, *TERMINATING FLOWER* (*TMF*) maintains the phase of vegetative growth and represses meristem maturation. *TMF* senses H₂O₂ signaling to form transcriptional condensates to repress the expression of floral identity gene *ANANTHA* (*AN*) by binding and sequestering its promoter. The loss of *TMF* in tomato leads to premature activation of *AN*, which speeds up the acquisition of floral identity in some meristems in the vegetative stage, resulting in a single flower of primary inflorescence (Huang *et al.*, 2021; Macalister *et al.*, 2012; Xu *et al.*, 2016). In *Arabidopsis* and other eudicots, studies have reported that *ALOG* genes play key roles in light signaling, organ specification and boundary formation (Cho and Zambryski, 2011; Lee *et al.*, 2020; Lei *et al.*, 2019; Takeda *et al.*, 2011; Xiao *et al.*, 2019; Zhao *et al.*, 2004a).

Barley has ten *ALOG* genes (*HvALOG1* to *HvALOG10*) in the genome (Figure 3.19B and Appendix Table S2). Protein alignment analysis showed that these ten *ALOG* family members in barley can be divided into three clades. *HvALOG1* and its closest paralog *HvALOG2* (*HORVU.MOREX.r2.7HG0610530*) on chromosome 7H clustered into clade 1 (Figure 3.19B) and shared a similar mRNA expression pattern in young spike tissues based on tissue-specific profiling data (Appendix Figure S3.3) (Thiel *et al.*, 2021), suggesting that their proteins may have comparable functions in regulating barley inflorescence development. In addition, although *HvALOG10* differs greatly from other *ALOG* members in phylogenetic branches (Figure 3.19B), its ortholog (*G1*) in rice has an important role in specifying the identity of the sterile lemma, suggesting that many *ALOG* family members have conserved functions.

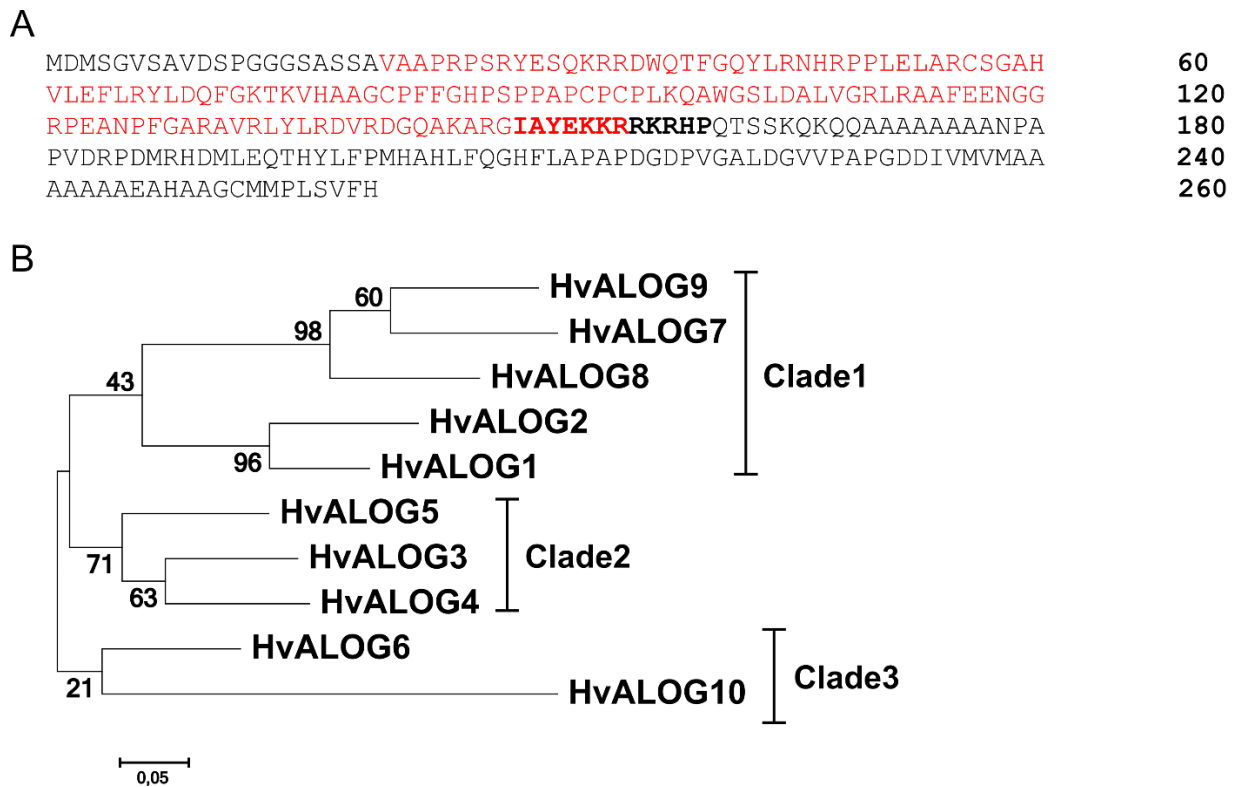


Figure 3.19. Protein similarity analysis among ALOG family members. (A) The amino acid sequence of HvALOG1. The ALOG domain is indicated with red letters. The sequence of the nuclear localization signal is indicated in bold letters. (B) Tree alignment of ALOG proteins in barley. The numbers indicate the percentage of bootstrap values calculated from 1,000 replicates.

3.4 Site-directed mutagenesis of *HvALOG1* and *HvALOG2* by RNA-guided CRISPR-Cas9

Considering that *HvALOG1* and *HvALOG2* have the highest similarity in amino acid sequences and comparable expression patterns (Figure 3.19B and Appendix Figure S3.3), we next asked whether there was functional redundancy or a phenotypic dosage effect for these two paralogs. Loss-of-function mutations of these two genes were generated in two-rowed barley cv. Golden Promise via clustered regularly interspaced short palindromic repeats (CRISPR) associated protein 9 (Cas9). The two sites of single-guide RNAs that targeted the exon region of *HvALOG1* and *HvALOG2* respectively were engineered into the same binary vector to generate single and double mutants (Figure 3.20A and B). In second-generation (T1) transgenic plants, we detected homozygous indel mutations in *HvALOG1* and *HvALOG2* by Sanger-sequencing, even though target 1 in *HvALOG1* displayed low editing efficiency (Figure 3.20 C and D). In single knock-out *Hvalog2* transgenics (i.e., *HvALOG1/Hvalog2^{CR}*),

spike and spikelet phenotypes did not change significantly compared to Golden Promise (Figure 3.20 E, F, J and K), indicating that *HvALOG2* has a negligible impact on the suppression of extra spikelets. However, the knock-out plants carrying *Hvalog1* homozygous mutations [(*Hvalog1^{CR} Hvalog2^{CR}*, double mutant) and (*Hvalog1^{CR} Hvalog2^{CR/+}*, homozygous in *HvALOG1* and heterozygotes in *HvALOG2*)] displayed stronger 'flo' phenotypes in the upper and middle parts of spike: here, not only one extra spikelet was produced, but also CS glumes developed various degrees of organs from fused leaf-like state to floret with lemma, palea, stamens and ovary (Figure 3.20 M to N and Appendix Figure S3.4 A to B, F to G). Moreover, the CS produced two independent florets but shared the same lemma (Figure 3.20 O to P and Appendix Figure S3.4 C to E). Notably, out of 190 transgenic plants, no single mutant of *HvALOG1* (*Hvalog1^{CR} / HvALOG2*) was detected. This was mainly due to the high gene editing efficiency of target 1 and target 2 for *HvALOG2* (99 heterozygotes *Hvalog2^{CR/+}* and 91 homozygotes *Hvalog2^{CR}*). Taken together, mutations in *HvALOG1* cause determinacy loss of the SM. The enhancement of "flo" phenotypes may be derived from the additive effect contributed by mutations in *HvALOG2*.

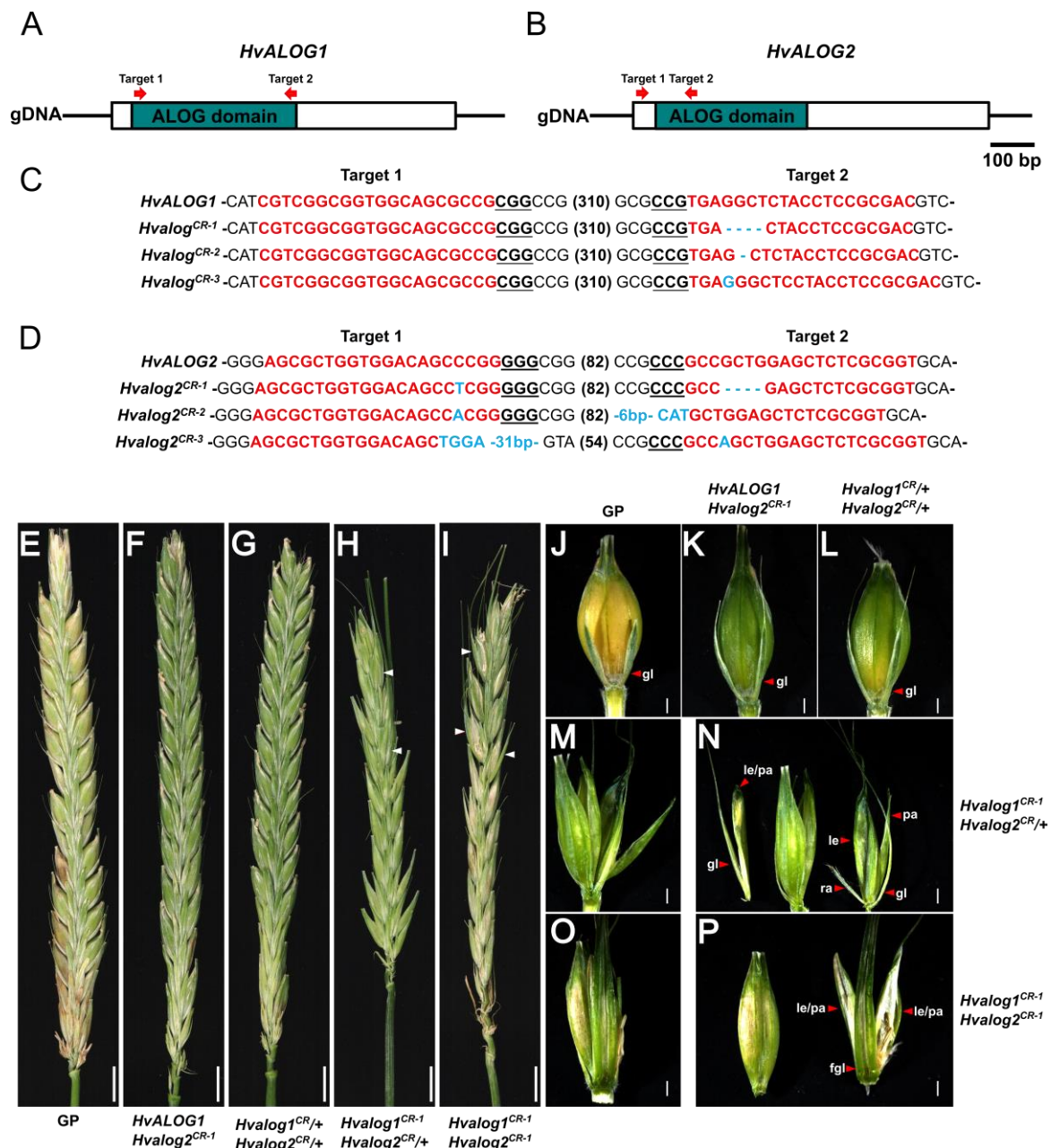


Figure 3.20. The phenotypes of the induced mutants by CRISPR-Cas9 in *HvALOG1* and *HvALOG2*. (A and B) Gene structure of *HvALOG1* (A) and *HvALOG2* (B) with two single-guide RNA targets. The targets are indicated by red arrowheads. (C and D) CRISPR-Cas9 -induced mutations in *HvALOG1* (C) and *HvALOG2* (B) were identified by Sanger-sequencing. The sequence of sgRNA targets and protospacer-adjacent motifs (PAM) are marked in red and bold letters, underlined and bold letters, respectively; deletions are represented by blue dashes; insertions are indicated with blue and bold letters; the number in the parenthesis represents the length of sequence gap. (F to I) Representative inflorescence images from Golden Promise and engineered *Hvalog1* and *Hvalog2* mutant combinations. White arrowheads indicate extra organ events. Bar = 1 cm. (E to I) Representative spikelet images from Golden Promise and engineered *Hvalog1* and *Hvalog2* mutant combinations. The dissected floral organs of the spikelet in M and N are shown in N and P, respectively. fgl, fused glumes; gl, glume; le, lemma; le/pa, lemma- or palea-like organ; pa, palea; ra, rachilla. Bar = 1 mm.

3.5 The conserved role of ALOG proteins across grasses and eudicots lineages

ALOG proteins first appeared before the evolution of land plants and have shown functional conservation and diversification as land plants have evolved (Naramoto *et al.*, 2020). The proteins containing an ALOG domain were found in the genome of basal land plants, i.e., *Physcomitrella patens*, *Selaginella moellendorffii*, *Sphagnum fallax* and *Marchantia polymorpha* (Naramoto *et al.*, 2019; Xiao *et al.*, 2018; Yoshida *et al.*, 2009). Notably, ALOG proteins tend to be evolved in a lineage-specific manner even though their aa sequences are extremely conserved (Naramoto *et al.*, 2020; Naramoto *et al.*, 2019).

To elucidate the phylogenetic relationships among the ALOG protein family from various grass and eudicot species, we conducted a genomic database search for available aa sequences of ALOG proteins from fourteen representative species across grasses and eudicots (Appendix Table S3) using BLASTp (e-value cut-off: $1e^{-30}$). A total of 220 ALOG proteins were retrieved and used for phylogenetic analysis. The phylogenetic tree generated showed that ALOG family members are structurally separable in grasses and eudicots (Figure 3.21), suggesting the independent evolutionary events and functional diversification between these two large plant lineages. However, several identified ALOG genes in different species showed conserved functions in controlling inflorescence development (Huang *et al.*, 2021; Huang *et al.*, 2022; Li *et al.*, 2012; Macalister *et al.*, 2012; Yoshida *et al.*, 2013; Yoshida *et al.*, 2009; Zhou *et al.*, 2021). Both rice *TAW1* gene and tomato *TMF*, for example, play a critical role in maintaining meristematic activity and timing the transition of the fate between different meristems (Macalister *et al.*, 2012; Yoshida *et al.*, 2009). Interestingly, a liverwort (*Marchantia polymorpha*) *LATERAL ORGAN SUPPRESSOR 1* (*MpLOS1*), a member of the ALOG protein family, regulates lateral organ development and apical meristem activity; loss-of-function of *MpLOS1* results in misspecified identity in lateral organs and defects in apical meristem maintenance. Expressed *MpLOS1* in the rice *g1* mutant rescues the lemma-like sterile lemma phenotype, suggesting a conserved role of ALOG proteins in the convergent evolution of lateral organogenesis among diversified plant lineages (Naramoto *et al.*, 2019). Moreover, independent duplication or deletion events occurred repeatedly within grass and eudicot species (Figure 3.21). The inconsistency in the number of ALOG proteins among species suggests potential effects on the complexity of plant architecture.

Among the proteins, which are phylogenetically close to *HvALOG2*, sorghum *AWN1* was functionally identified and plays an essential role in awn development (Zhou *et al.*, 2021) (Figure 3.21), however, the single mutant of *Hvalog2* did not show significant differences in spike and spikelet development compared with Golden Promise (Figure 3.20 E to F, J and K).

The functions of the closest orthologs of *HvALOG1* are not identified in grasses. We extracted ten aa sequences of *HvALOG1* orthologs from seven grass species by BLASTp (e-value cut-off: $1e^{-30}$). Sequence alignment revealed that the ALOG domain is highly conserved across grasses, especially within the *Triticeae* (wheat, barley and rye) with only three aa differences, suggesting that *HvALOG1* is likely to perform a conserved function in grasses (Figure 3.22).

Taken together, these results suggest that although ALOG proteins evolve in a lineage-specific manner, they most likely retained conserved functions in the regulation of plant reproductive growth.

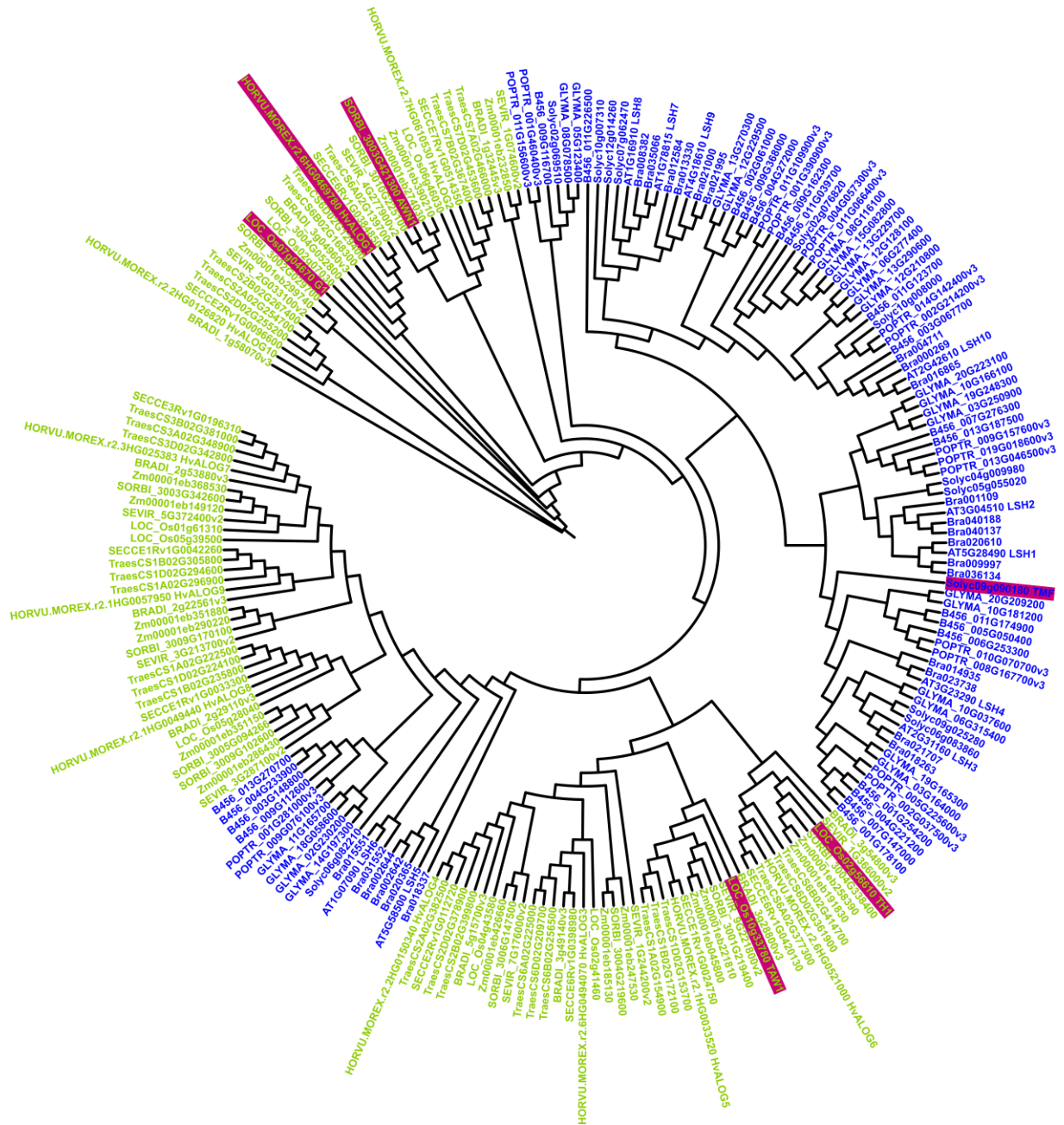


Figure 3.21. Phylogenetic tree of ALOG family proteins. Amino acids of ALOG proteins from 14 grass and eudicot plant species were used for phylogenetic analysis. The phylogenetic tree was constructed using the maximum likelihood (ML) method. Bootstrap support values were calculated from 1,000 replicates and given at the branch nodes. The Monocot and eudicot species are marked in blue and green, respectively. Blue Previously identified genes are highlighted in purple. The details of species and proteins are listed in **(Appendix Table S3)**.

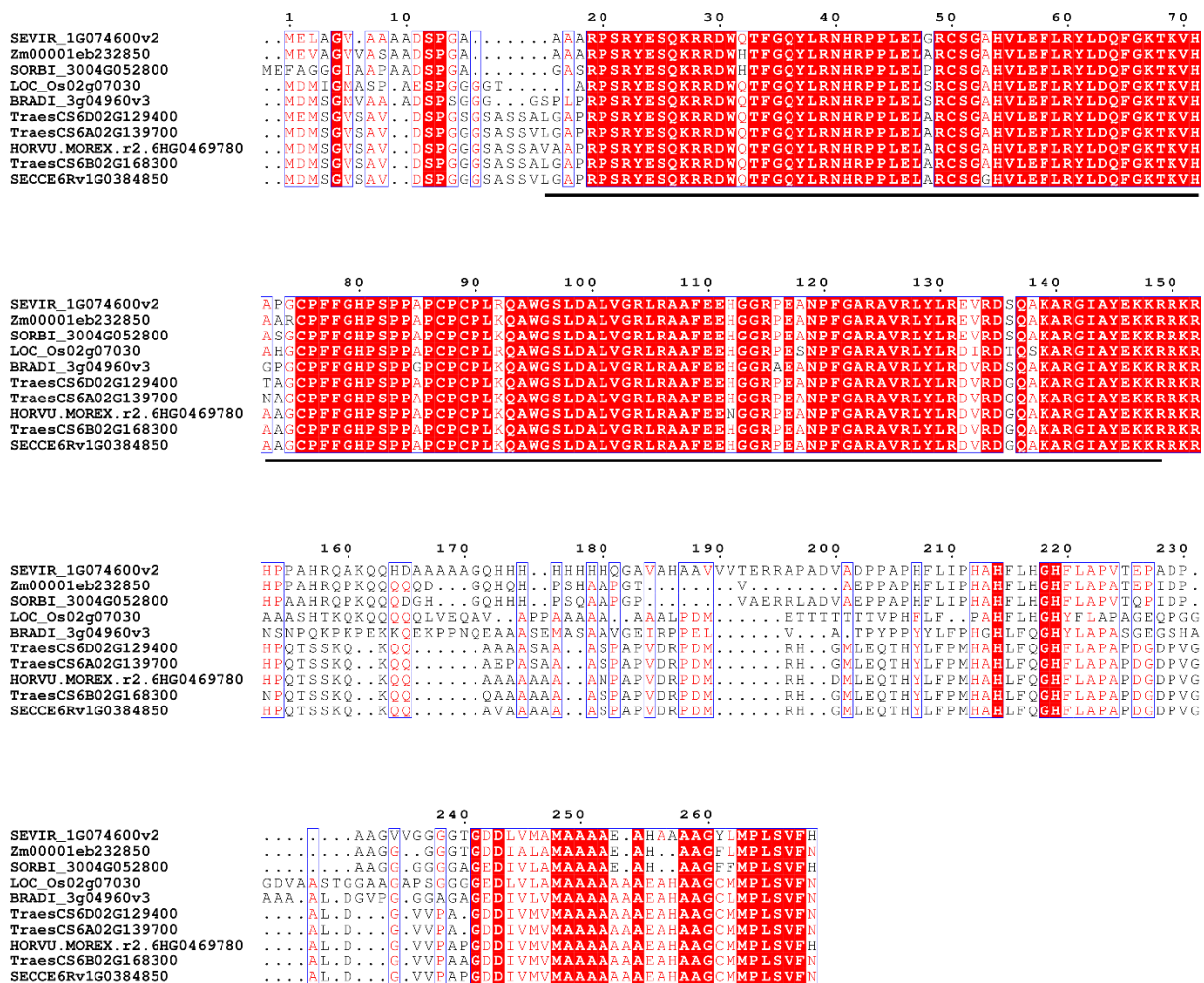


Figure 3.22. The HvALOG1 protein alignment in grasses. The alignment was based on the proteins from barley (HORVU.MOREX.r2.6HG0469780), rice (LOC_Os02g07030), sorghum (SORBI_3004G052800), maize (Zm00001eb232850), *Brachypodium* (BRADI_3g04960v3), wheat (TraesCS6B02G168300, TraesCS6D02G129400 and TraesCS6A02G139700), rye (SECCE6Rv1G0384850) and green foxtail (SEVIR_1G074600v2). The conserved ALOG domain was indicated by the black line.

3.6 HvALOG1 protein localizes to the nucleus

ALOG family proteins have been reported as transcriptional factors in plants. To further characterize the function of *HvALOG1* in barley, we investigated the subcellular localization of *HvALOG1* protein in barley leaf cells. The construct was made by using the full-length CDS sequence of BW *HvALOG1* fused with GFP (Figure 3.23A), which subsequently was subjected to detect the transient expression of the fused protein in barley leaf cells by biolistic bombardment. The *HvALOG1*-GFP fused protein was localized to the nucleus of barley leaf cells (Figure 3.23C), whereas the fluorescent signals of control GFP protein were distributed throughout the leaf cells (Figure 3.23B),

suggesting that HvALOG1 is a nucleus-targeted protein and most likely a transcriptional regulator in barley.

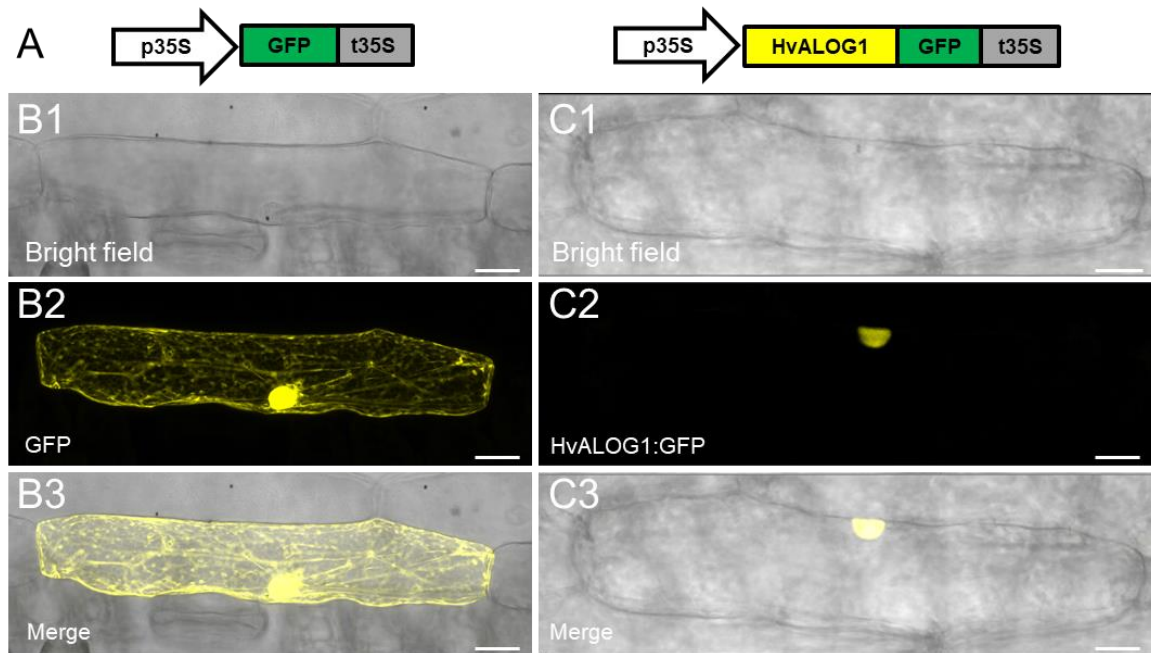


Figure 3.23. Subcellular localization of HvALOG1-GFP fusion protein. (A) Schematic diagram of GFP expression constructs. (B) and (C) Subcellular localization of GFP and HvALOG1-GFP in barley leaf cells by particle bombardment, respectively. All bar scale = 20 μm.

3.7 Temporal and spatial expression pattern of *HvALOG1*

To explore the expression pattern of *HvALOG1* in barley, we first examined the transcript levels of *HvALOG1* in the barley developing spike transcriptome atlas (Morex V2 reference) (Appendix Figure S3.3) (Thiel *et al.*, 2021); *HvALOG1* was highly expressed in the SAM sample during the vegetative stage and the spike during the DR stage, especially peak in the regions of the leaf ridge (LR), followed by expressions in CSs and LSs. Subsequently, we examined the spatiotemporal expression pattern of *HvALOG1* in BW developing spikes by real-time quantitative PCR (qRT-PCR). Consistent with the above result, *HvALOG1* had the highest expressional level in spike tissues at the DR stage and gradually decreased at next several developing stages, whereas it was hardly detectable in vegetative organs (flag leaves and leaf sheath) (Figure 3.24A), indicating that *HvALOG1* may play a role predominantly during reproductive growth and development.

We then performed mRNA *in situ* hybridizations on young spike tissues from BW and *flo.a* at different developing stages (DR, LP and AP). After barley enters the reproductive growth, the IM continues to differentiate LR and SR primordia (Koppolu and Schnurbusch, 2019). During spike development, the LR primordia degenerate and disappear, while the SR primordia develop into the TSMs (Koppolu and Schnurbusch, 2019). In BW spikes, the accumulation of *HvALOG1* mRNA signals was initially detected in the LR primordia but not in the SR primordia (Figure 3.24B to G and K). Intriguingly, all reproductive meristems, i.e., IM, TSM, SM and FM throughout the spikelet differentiation phase, were devoid of any *HvALOG1* signals (Figure 3.24D to K). During spikelet differentiation, *HvALOG1* showed signals in leaf-like floral organs, such as glume, lemma and palea primordia (Figure 3.24H and I). After floral organ formation, *HvALOG1* was specifically expressed at the base of floral organs (Figure 3.24J to M). Expectedly, no accumulation of *HvALOG1* mRNA was detected at any stage or tissue in *flo.a* (Figure 3.24N to Q), consistent with *flo.a* gene deletion in.

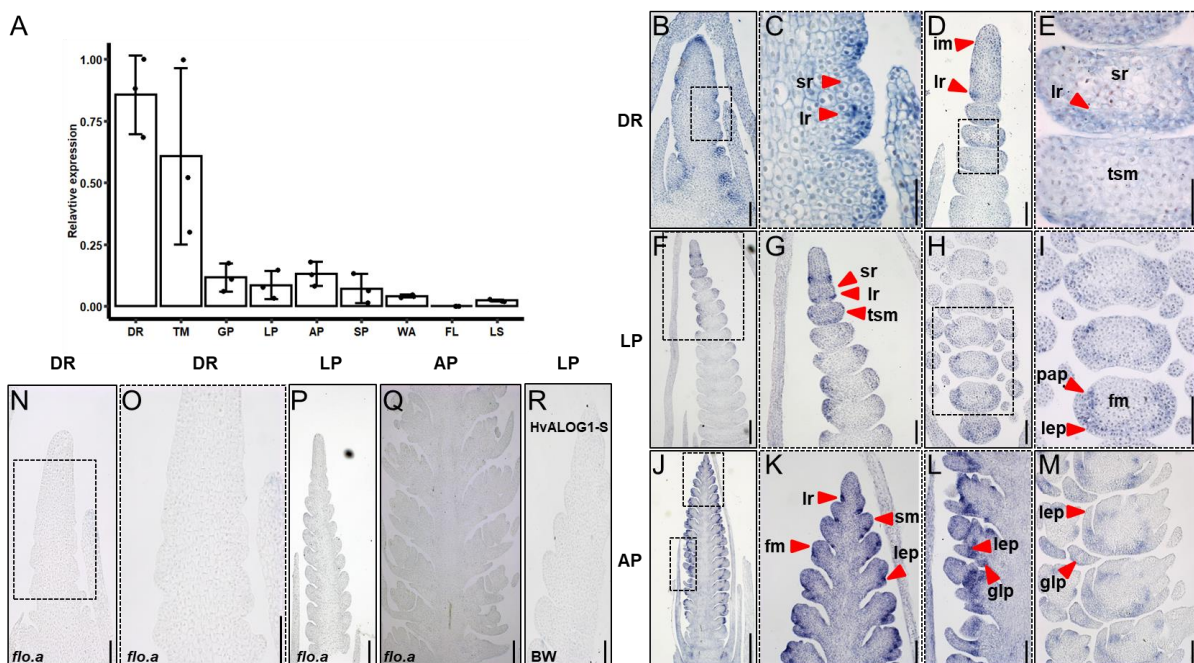


Figure 3.24. Expression pattern of *HvALOG1*. (A) Relative expression by qRT-PCR of *HvALOG1* in different tissues. *HvActin* was used for expression normalization. Data are shown as mean \pm s.d.; biological replicates = 3; DR, Double ridge; TM, Triple mound; GP, Glume primordium; LP, Lemma primordium; SP, Stamen primordium; AP, Awn primordium; WA, White anther; FL, flag leaf in Awn primordium stage; LS, leaf sheath in Awn primordium stage. (B to M) Representative images of *HvALOG1* expression domains in BW young spike by mRNA *in situ* hybridization. (N to Q) Representative images of *HvALOG1* expression domains in *flo.a* young spike by mRNA *in situ* hybridization. (R) the sense-probe of *HvALOG1* in BW young spike. (C, E, G, I, K, M and O) is an

enlarged image of the dotted box in the corresponding image on the left. fm, floral meristem; glp, glume primordium; lep, lemma primordium; lr, leaf ridge; pap, palea primordium; sr, spike ridge. Bar: 100 μ m in (B, D, G, H, I, K to O); 50 μ m in (C and E); 200 μ m in (F, P, and Q); 500 μ m in (J).

Subsequently, we produced a GFP reporter line to investigate the protein expression pattern of HvALOG1-GFP during different stages of barley spike development (Figure 3.25A). Consistent with our mRNA *in situ* hybridization results, the GFP signals were undetectable in reproductive meristems, including IM, SR primordia, TSM, SM (CSM and LSM) and FM but strong GFP signals were observed in the LR primordia and rachis tissue (Figure 3.25B to C and 3.26, Appendix Figure S3.5). Moreover, during spikelet initiation, GFP signals were detected at the base of developing floral organs demarcating possible organ boundaries (Figure 3.25B to C and 3.26). In addition, the GFP signals were limited in the rachis and boundary domain of floral organs after spikelet formation (Appendix Figure S3.6).

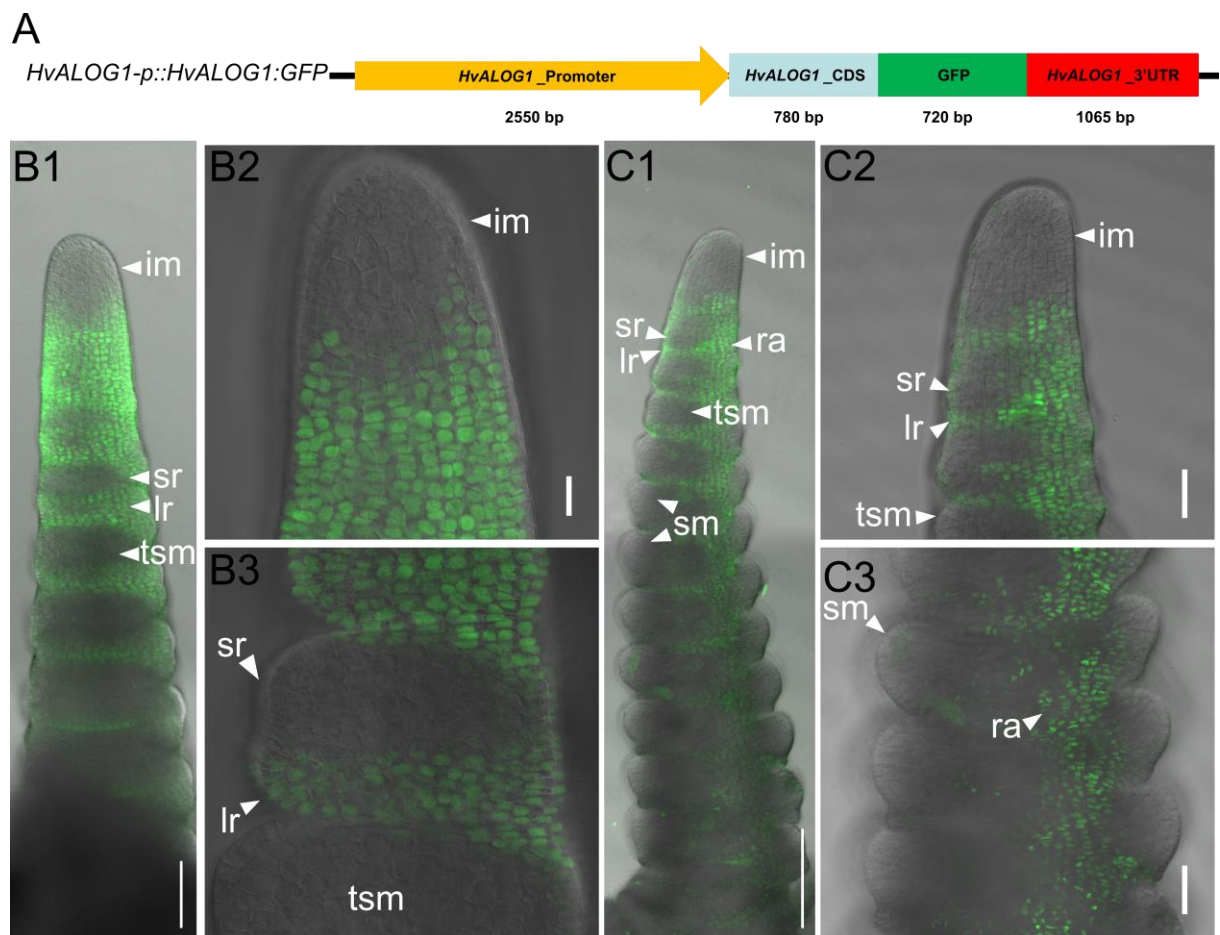


Figure 3.25. Expression pattern of the HvALOG1 protein in the spike tissues at the DR and TM stages. (A) Schematic image of engineering fused DNA for *HvALOG1-p::HvALOG1:GFP* construct. (B and C) Accumulation of the HvALOG1 protein in spikes from DR (B) and TM (C) stages in *HvALOG1-p::HvALOG1:GFP* transgenic lines. Partially enlarged details in B1 and C1 are shown in (B2 and 3) and

(C2 and 3), respectively. glp, glume primordium; im, inflorescence meristem; lep, lemma primordium; lr, leaf ridge; pap, palea primordium; ra, rachilla; sm, spikelet meristem; sr, spike ridge; tsm, triple-spikelet meristem. Bar: 20 μm in (B2 and 3); 50 μm in (C2 and 3); 100 μm in (B1); 200 μm in (C1).

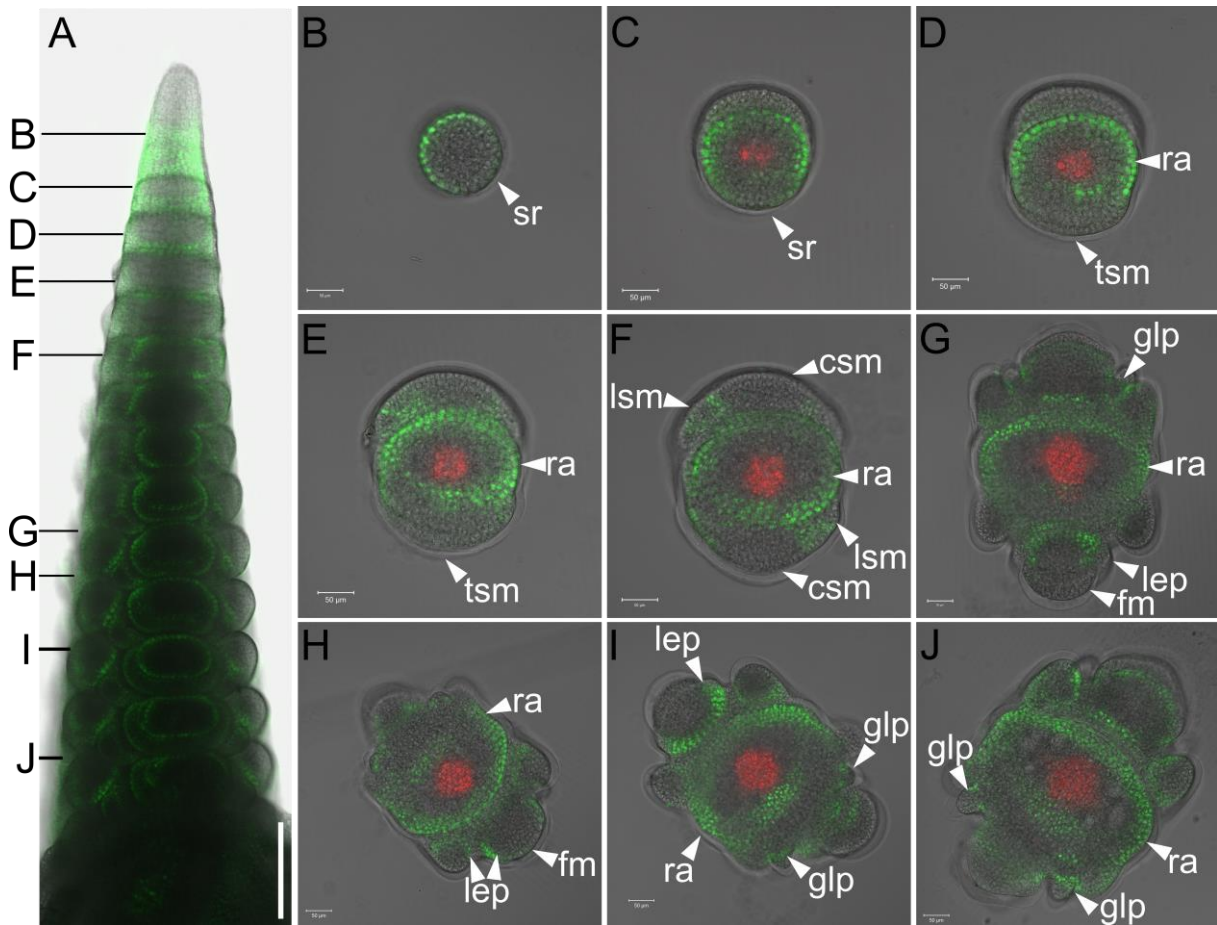


Figure 3.26. Expression pattern of the HvALOG1 protein in the spike tissues at the LP stages. (A) Accumulation of the HvALOG1 protein in whole spikes in *HvALOG1-p::HvALOG1:GFP* transgenic lines. (B to J) Accumulation of the HvALOG1 protein in different sections of spike from apical to basal in (A). csm, central spikelet meristem; glp, glume primordium; lep, lemma primordium; lsm, lateral spikelet meristem; ra, rachis; sm, spikelet meristem; sr, spike ridge; tsm, triple-spikelet meristem. Bar: 50 μm in (B to J); 200 μm in (A).

These results suggest that *HvALOG1* is consistently expressed in non-meristematic reproductive tissues during spike development and at the base of floral organs during spikelet development. Therefore, *HvALOG1* may play an important role in specifying the determinacy of the barley SM in a non-cell autonomous manner by modulating proper boundary establishment and by regulating floral organ development in a cell autonomous way.

3.8 *HvALOG1* involves in the regulation of organ boundary formation and development

Our phenotypic and expression analyses suggested that *HvALOG1* is involved in specifying meristem determinacy as well as establishing floral organ boundaries. To further understand the molecular function of extra spikelet initiation and glume fusion in the upper-mid part of the inflorescence induced by the absence of *HvALOG1*, we performed transcriptome analysis (RNA-seq) for the whole spike at the DR (W2.0) stage and separated spike (upper-mid and basal) at the LP (W3.0), AP (W4.5) and WA (5.5) stages from BW and *flo.a* (Appendix Figure S3.7 and S3.8). Consistent with the emergence of extra organs from *flo.a* at the LP stage, principal component analysis (PCA) using all 42 samples revealed drastic transcriptome modulation starting from the LP stage (Figure 3.27A). The distribution of samples follows the trajectory of inflorescence development (DR to WA) and positional effects (upper-mid to basal). Transcriptomes of all BW and *flo.a* samples were clustered together at the DR and WA stages but were separated at the LP and AP stages, indicating the remarkable gene expressional variance from upper-mid and basal parts of spike between BW and *flo.a* (Figure 3.27A).

A total number of 3,158 differentially expressed genes (DEGs) were identified in *flo.a* vs. BW using a cut-off [absolute (\log_2 Fold-Change) > 0.5845; adjusted $P < 0.05$] (Figure 3.27B). Of these, most DEGs were identified at the LP stage, supporting the strong ectopic meristematic activity promoting extra spikelet formation in *flo.a*. Notably, the number of up-regulated DEGs was significantly higher than the down-regulated DEGs in the pairwise sample comparison, indicating that *HvALOG1* may function as a transcriptional repressor (Figure 3.27B). Interestingly, *HvALOG1* was expressed throughout the BW spike in mRNA and protein level (Figure 3.24 to 3.26 and Appendix Figure S3.9), but no extra spikelets were observed in the basal part of *flo.a* spikes when the gene is deleted (Figure 3.2B). Moreover, 1,061 and 664 genes were differentially expressed among groups of LP-Basal and AP-Basal, respectively, suggesting that *HvALOG1* may also be involved in other pathways regulating spike development (Figure 3.27B).

Expression clustering analysis revealed that all DEGs can be classified into 8 groups (C1 to C8) (Figure 3.27C and Appendix Figure S3.10). Among them, genes in C4 and C6 were specifically differentially expressed in the upper-mid and basal parts of spikes

at the LP stage, respectively. Gene ontology (GO) enrichment analysis showed that DEGs at C4 from the upper-mid part were enriched in activities associated with shoot system development, plant organ development, floral whorl development and auxin homeostasis; whereas DEGs at C6 from the basal part were largely involved in stress responses and metabolite biosynthesis (Figure 3.27D and Appendix Figure S3.11).

The most prominent expression difference occurred at the LP and AP stages, where expressions of a set of genes, including *CUC2* (Hibara *et al.*, 2006), *KNAT1/BP-like 1* (Douglas *et al.*, 2002), *KNAT1/BP-like 2*, *HvLG1* (Poursarebani *et al.*, 2020), *SUP-like* (Xu *et al.*, 2018), *ATHB1* (Miguel *et al.*, 2020), *PAN* (Lohmann *et al.*, 2011) and *LOF2* (Lee *et al.*, 2009), associated with organ boundary establishment was down-regulated in *flo.a*, consistent with the inability to correctly establish boundaries in meristems or primordia in *flo.a* spikelets (Figure 3.27E and Appendix Table S4). Moreover, expressions of genes including *Vrs4/HvRA2* (Koppolu *et al.*, 2013), *Arabidopsis ABNORMAL FLORAL ORGANS/FILAMENTOUS FLOWER (AFO/FIL)* (Kumaran *et al.*, 1999; Sawa *et al.*, 1999), *HvAP2L-5H* (Zhong *et al.*, 2021), and *INT-C/HvTB1* (Ramsay *et al.*, 2011), involved in the specification of spikelet identity or determinacy were similarly down-regulated in the upper-mid part of the *flo.a* spike (Figure 3.27E and Appendix Table S4). In contrast, the expression of genes involved in auxin signaling pathway, including *Auxin response factor 16 (ARF16)*, *Auxin/Indole-3-Acetic Acid (Aux/IAA)*, *small auxin up-regulated RNA (SAUR)*, *Gretchen Hagen3 (GH3)* and *PIN-FORMED 3 (PIN3)* were specifically up-regulated in the upper-mid spike of *flo.a*. In addition, another group of genes such as *MADS-boxs* (Kuijter *et al.*, 2021), *PACLOBUTRAZOL-RESISTANCE 5 and 6 (PRE5 and 6)* (Shin *et al.*, 2019) and *FD* (Gorham *et al.*, 2018) related to organ development, was also specifically highly expressed in the upper-mid part of spike of *flo.a*, possibly due to the absence of repression from down-regulated genes mentioned above (Figure 3.27E and Appendix Table S4).

We therefore conclude that *HvALOG1* specifies the correct growth of spikelets by promoting spikelet identity/determinacy and proper boundary formation and therefore inhibits ectopic organ development during barley spike development.

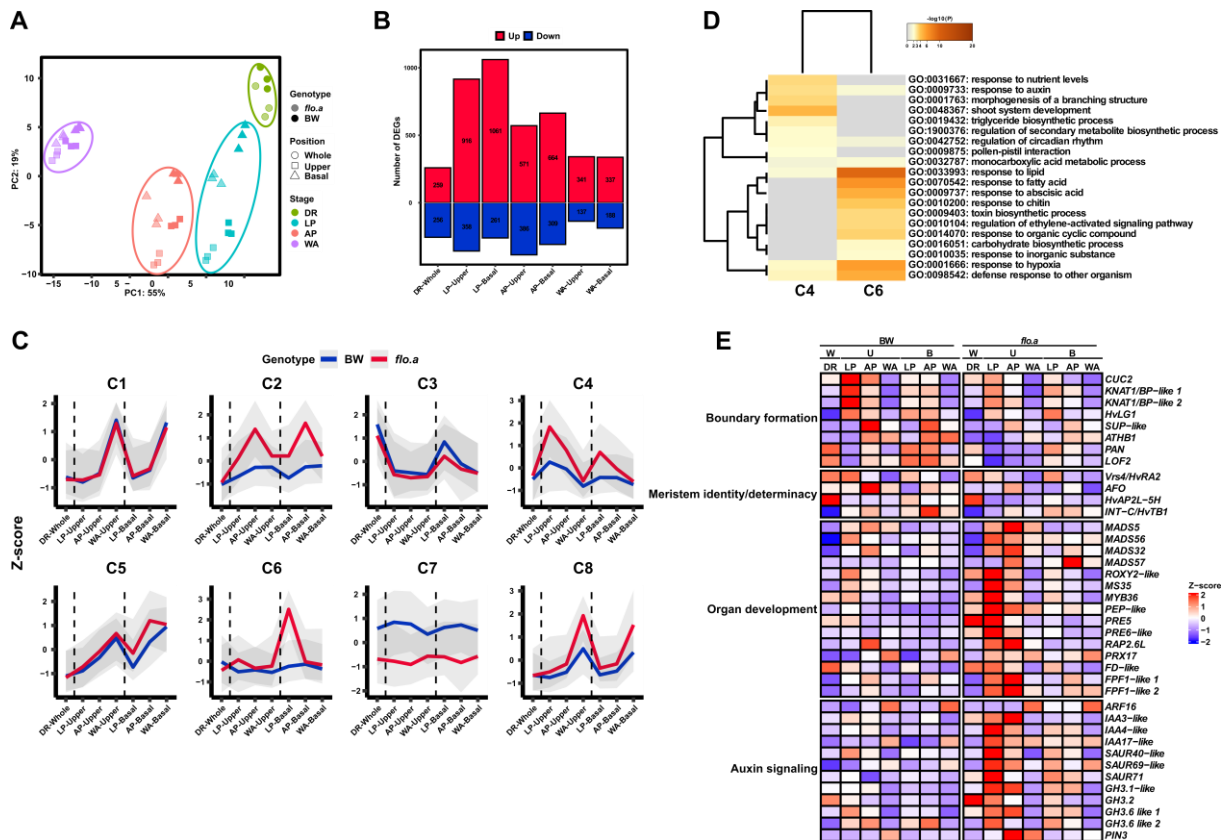


Figure 3.27. *HvALOG1*-related transcriptional changes affect the boundary formation of floral organs. (A) Principal component analysis (PCA) on the expression-filtered transcriptomes illustrates the variation between BW and *flo.a* from different spike sections at the DR, LP, AP, WA stages. (B) The number of up- and down-regulated differentially expressed genes (DEGs) of pairwise sample comparisons between BW and *flo.a*. (C) Clustering analysis of DEGs in (B) based on Partition Around Medoids (PAM) using normalized expression value (Z-score). The blue and red lines indicate median expression; the gray area represents the 5th and 95th quantile. (D) Gene Ontology (GO) analysis of Cluster 4 (C4) and 6 (C6) shows specific expression in the upper-mid and basal parts of spikes at the LP stage. (E) Heatmap of the selected candidate genes with roles in organ boundary formation, meristem identity/determinacy, auxin homeostasis, organ development using Z-score value. W, whole spike; U, upper-mid; B, basal.

3.9 *HvALOG1* represses ectopic activity of cell division in meristems

Maintaining inflorescence shape is guided by meristem determinacy through concerted cell division and differentiation (Bommert and Whipple, 2017; Li *et al.*, 2021a; Wang *et al.*, 2021; Zhang and Yuan, 2014). In our observations, *HvALOG1* is expressed in boundaries of the reproductive meristems to specify determinacy to the SM non-cell autonomously (Figure 3.24 to 3.26) while deletion of *HvALOG1* induced extra spikelet formation. To further dissect how *HvALOG1* affects cellular activity, we examined the

mRNA accumulation level of the cell division marker gene *HvHistone4* (*H4*) in young spikes by *in situ* hybridization. As we expected, *H4* was expressed in all meristems, including SR and LR in both BW and *flo.a* spikes at the DR stage (Figure 3.28A1 and B1). Subsequently, at the SP and AP stages, we observed a strong expression signal of *H4* in the domain below the CS from the upper-mid part of *flo.a* spike, indicating that new meristems were forming in the mutant compared to the limited expressional domain in meristems/primordia of the BW CS (Figure 3.28A2 to A6 and B2 to B6). Thus, our data suggest that *HvALOG1* regulates cell division and meristem activity during barley spike development.

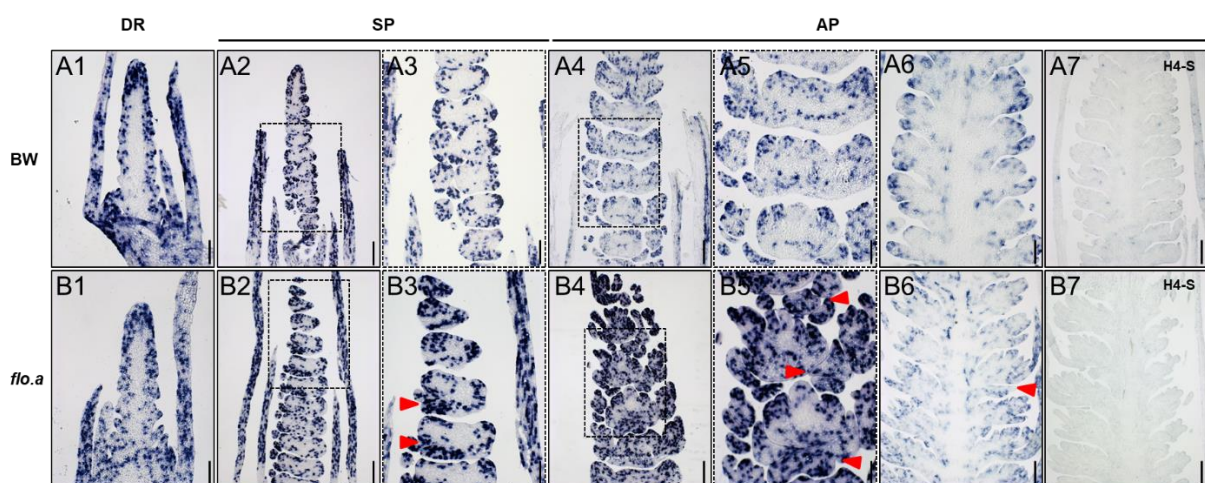


Figure 3.28. Extra organs display cell division activity. (A and B) Representative images of *Histone4* (*H4*) expression pattern in young spike of BW and *flo.a* by mRNA *in situ* hybridization at the DR, SP and AP stages. The signals in (1 to 6) and (7) were using anti-sense and sense probes of *H4*, respectively. Red arrowheads indicate extra meristem/primordium events. Bar: 100 μ m in (1, 3, 5 and 6); 200 μ m in (2, 4 and 7).

3.10 Potential functional redundancy of ALOG protein family members occurs early during spike development

The ability of a system to maintain its function in the presence of environmental or genetic perturbations is called robustness, which is genetically achieved notably by partial redundancy derived from gene duplication (Diss *et al.*, 2014). Functional overlap between paralogs within a gene family confers genetic robustness to compensate for each other's loss. It has been reported that members of the ALOG family are functionally redundant in tomato to precisely control SAM maturation, thereby synchronizing flowering and compound inflorescence production (Huang *et al.*, 2022).

Here, we hypothesized that ALOG genes in barley have a redundant function but with spatiotemporal specificity to regulate the SM determinacy and organ boundary formation. We first investigated the phylogeny of ALOG genes and their expression patterns in diverse spike tissues at different developmental stages. The ten members of the barley ALOG family were divided into three clades (Figure 3.19B). Among them, only *HvALOG1* was expressed in all BW spike tissues with the highest levels in whole spikes during the DR stage, suggesting that *HvALOG1* is one key regulatory gene for SM activity and boundary establishment at all developing stages among ALOG family (Figure 3.29A). However, the genes, except for *HvALOG1* in Clade 1 and 2, had spatiotemporal and tissue-specific expression patterns in spike samples of BW and *flo.a* during early developmental stages, featuring high levels in whole spikes (DR stage) but very low levels in the upper-mid part at the LP stage (Figure 3.29A). Moreover, *in situ* hybridization results revealed that mRNA accumulation of a Clade 2 representative, e.g., *HvALOG4*, was highly expressed in whole spike tissues during the DR stage, while it decreased during LP and SP stages (Figure 3.29B). These data suggest that the positional distribution of ‘*flo*’ phenotypes across the spike may be derived from imbalances in spatiotemporal expression dynamics of ALOG family members: eventually, different ALOG members, including *HvALOG1*, can synergistically regulate SM activity and confer SM determinacy at early developmental stage (DR); however, the absence of *HvALOG1* expression leads to an indeterminate SM, but only in the upper-mid portion of the spike during later stages (LP and AP) when *HvALOG1* is the only expressed gene. Notably, although *HvALOG1* and *HvALOG2* shared the highest protein similarity, their expression patterns in our transcriptome profiling data were not comparable (Figure 3.29A). In addition, the transgenic knock-out mutants of *Hvalog2* did not show any extra spikelets, resembling wild-type plants, further suggesting a functional differentiation between *HvALOG1* and *HvALOG2* (Figure 3.20 F, G, K and L).

Therefore, we propose that the ALOG protein family may work synergistically to regulate barley inflorescence shape. *HvALOG1* may play a dominant role in specifying the SM determinacy and maintaining boundary formation in barley inflorescence across ALOG family members; the loss of *HvALOG1* may be rescued by other ALOG proteins, producing the positional effect of “*flo*” phenotypes in the *flo.a* spike.

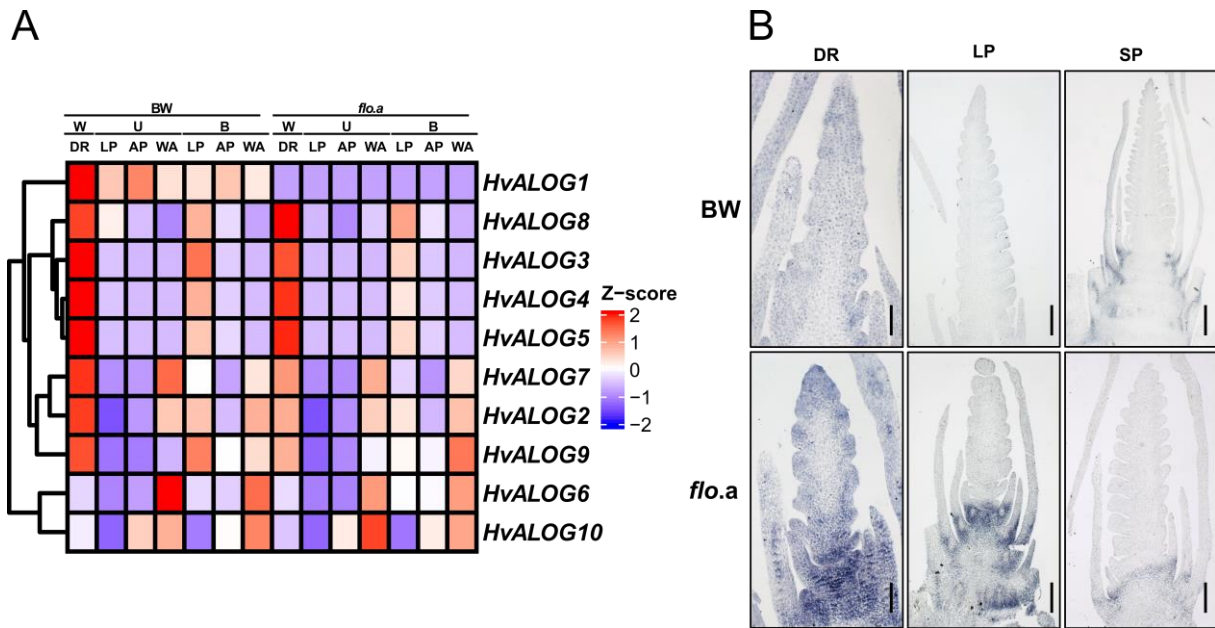


Figure 3.29. Potential functional redundancy of the ALOG gene family. (A) Expression pattern of ten members of ALOG family using RNA-Seq data. (B) Representative images of *HvALOG4* expression pattern in young spikes of BW and *flo.a* by mRNA *in situ* hybridization, at the DR, LP and SP stages. Bar: 100 μ m in (B and E); 200 μ m in (C, D, F and G).

3.11 Dysregulation of hormonal homeostasis involves extra organ formation

Plant hormones, including auxins, gibberellic acid (GA), cytokinins (CK), and abscisic acid (ABA), are involved in the regulation of plant architecture and inflorescence meristem activity in barley (Boussora *et al.*, 2019; Li *et al.*, 2021a; Thiel *et al.*, 2021; Youssef *et al.*, 2017). To further examine how hormones affect barley inflorescence development, we measured the concentration of endogenous auxin, GA, CK, and ABA in different spike parts between BW and *flo.a* at three different developmental stages (LP, AP and WA) using liquid chromatography-tandem mass spectrometry (LCMS) (Figure 3.30).

We found that in terms of the whole spike, the accumulation level of auxin was not significantly different in *flo.a* for all three stages compared with BW; but in different parts of the spike, *flo.a* showed a marked auxin increase, especially in the upper-mid part at the LP stage (Figure 3.30A). Notably, in our transcriptomic profiling data, a group of genes involved in response to auxin, including *IAA*, *GH3*, and *SAUR* family members, were significantly upregulated in the upper-mid part of *flo.a* spike (Figure 3.27E). Considering that high local auxin maxima drive the initiation of new

meristems/primordia, the meristems of the extra spikelets might originate from high auxin accumulation in the more upper-mid spikelets of *flo.a* (Zhu and Wagner, 2020).

We also detected distinct accumulation patterns for the two bio-inactive forms of GA (GA8 and GA19) (Figure 3.30B and Appendix Figure S3.12B). Interestingly, the level of GA8 was affected by developmental progression. At the early developmental stage (LP), the level of GA8 in the upper-mid and basal parts of the *flo.a* spike was significantly higher than in BW, but during the AP and WA stages, the level of GA8 showed the opposite trend, indicating that the accumulation of GA8 in *flo.a* underwent a rapidly changing process (Figure 3.30B).

The accumulation of CK levels in BW and *flo.a* had different trends between upper-mid and basal portions of the spike. The accumulation of the active CK form (isopentenyladenine, IP) in the upper-mid part of the *flo.a* spike was lower than that in BW; whereas, in the basal part of the spike, the opposite pattern was detected (Figure 3.30C).

Furthermore, ABA, a hormone responding to stress, was strongly accumulated in all parts of spike tissues from *flo.a* at the WA stage, suggesting that *flo.a* experienced a potential growth inhibition at the late-developing stages of the inflorescence (Appendix Figure S3.12A).

Therefore, the above data suggest that the concentration of these four key phytohormones is significantly altered in BW and *flo.a*, resulting in the disruption of hormonal homeostasis.

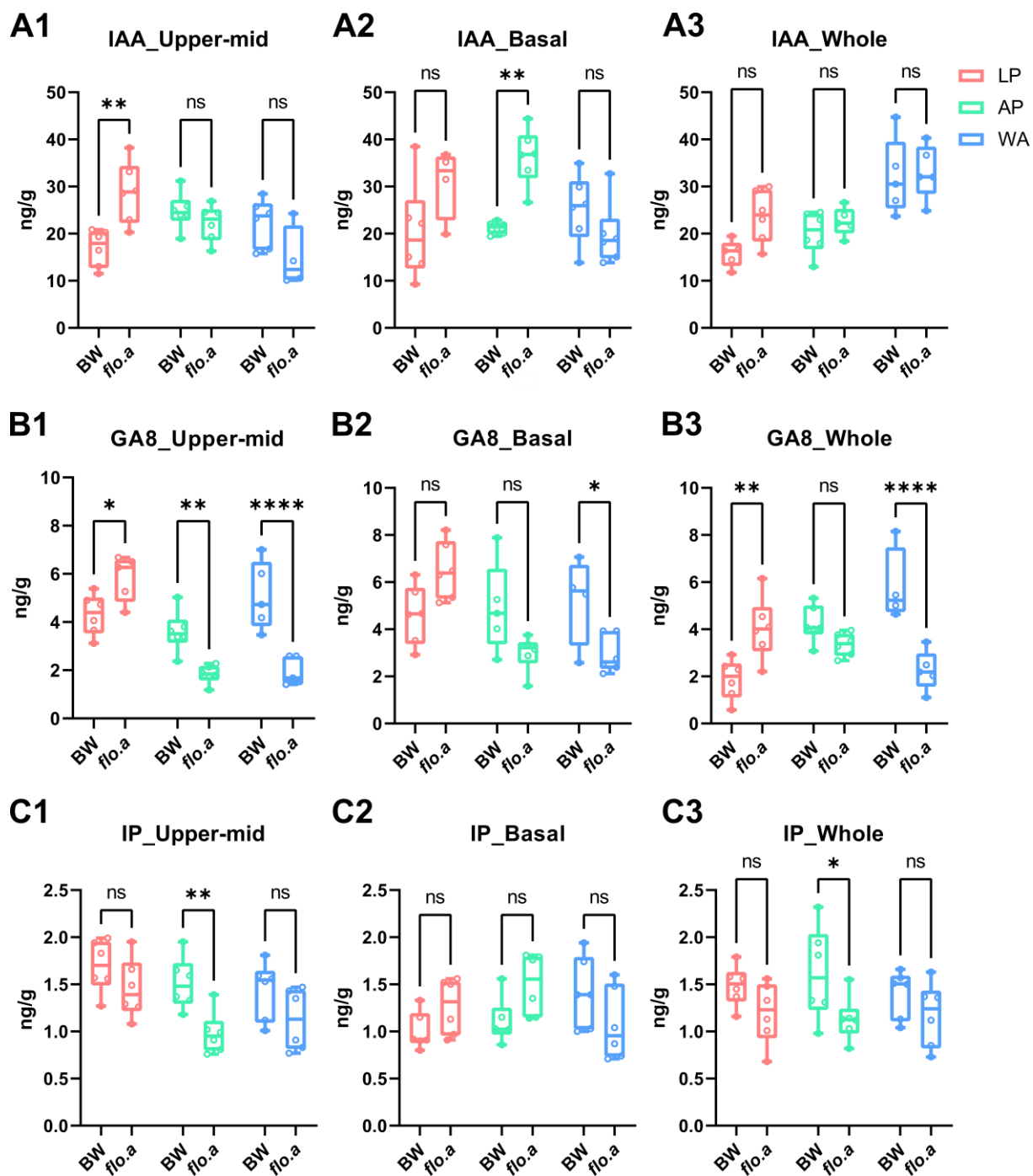


Figure 3.30. Endogenous hormone levels in upper-mid, Basal and Whole spikes between BW and flo.a. N = 4 to 6 biological replicates. The *P-values* indicate the results from pairwise comparisons using two-way ANOVA tests.

4. Discussion

Plant inflorescences are the major determinant of crop yield (Meyer and Purugganan, 2013; Soyk *et al.*, 2017). The plasticity of inflorescences is critical for optimizing the source-sink metabolic allocation balance in response to a continuously changing external environment. Improved inflorescence plasticity is one of the main goals during crop domestication, especially in cereal crops, including barley, maize, rice and wheat, for which humans have selected variants with larger branches to obtain higher numbers of grains (Chen and Gallavotti, 2021; Wang *et al.*, 2021; Yuan *et al.*, 2020; Zhang and Yuan, 2014). Inflorescence architectures are mainly defined by the duration of meristem activity, the number of meristems and their arrangement (Koppolu and Schnurbusch, 2019). Although inflorescence architectures of these crops have been known and described for a long time, the regulatory network underpinning inflorescence development remains to be further elucidated.

The work in this thesis utilized barley *flo.a* induced mutant to identify the *HvALOG1* gene by map-based cloning, which is involved in formation of inflorescence architecture. A typical feature of the *flo.a* mutant is the emergence of extra sterile spikelets and fused glumes on the abaxial face of the CS in the upper-mid portion of spike. The production of an extra spikelet leads to spikelet quadruplets on the same rachis node, potentially increasing barley sink size to produce more grains. Thus, this work sheds light on the genetic basis of the specification of the SM, perhaps paving the way for unlocking the genetic potential of extra spikelets to increase grain yields in barley.

4.1 *flo.a* is an ‘extra spikelet’ mutant but not an ‘extra floret’ mutant

In barley, extensive and well-characterized mutants by physical and chemical mutagens have been collected and used as a valuable resource for exploring complex and fundamental biological processes (Druka *et al.*, 2011) In particular, a series of genes related to inflorescence development were previously identified thereby greatly deepening our understanding of barley spike morphogenesis (Houston *et al.*, 2012; Houston *et al.*, 2013; Koppolu *et al.*, 2013; Koppolu *et al.*, 2021; Poursarebani *et al.*, 2015; Poursarebani *et al.*, 2020; Ramsay *et al.*, 2011; Sakuma *et al.*, 2017; van Esse *et al.*, 2017; Youssef *et al.*, 2017; Zhong *et al.*, 2021). In the present study, we identified a set of mutagenized spike development defect mutants that exhibited extra floral organ formation and fused CS glumes on the abaxial face of the CS (Figure 3.2, 3.3

and 3.7). The additional and distorted organs were initially characterized as extra floral bracts and therefore the mutant was previously named *Extra floret (flo)* (Druka *et al.*, 2011). However, in this study, the naming of the '*Extra floret*' does not accommodate characteristics of *flo* mutants' phenotypes. One or more florets subtended by two glumes constitute the spikelet, the basic structural unit of all grass inflorescences (Bommert and Whipple, 2017; Tanaka *et al.*, 2013; Whipple, 2017; Zhang and Yuan, 2014). The barley spikelet has a single-floreted (determinant) identity, by which the rachilla is suppressed and only one floret is developed (Koppolu *et al.*, 2021; Koppolu and Schnurbusch, 2019). Our observations proved that supernumerary organs not only contain one floret but also two extra glumes in *flo.a*, indicating that extra organs acquired the identity of a spikelet (Figure 3.2, 3.3 and 3.7). The extra spikelets produced in *flo.a* are developed from the SM and contain all the floral whorl structures, however, the inner floral organs degenerate prematurely, resulting in leaf-like morphological features (Figure 3.7 to 3.9). Moreover, vascular bundles derived from extra lemma and glumes can connect to the nodal complex of the rachis, thereby affecting the vascular patterning and altering the growth patterns of CS bundles (Figure 3.13 and 3.14). Therefore, we propose that *flo.a* is an '*extra spikelet*' mutant but not an '*extra floret*' mutant.

Barley inflorescence mutants, such as *vrs4*, *com1*, *com2*, and *Hvmads1* (Koppolu *et al.*, 2013; Li *et al.*, 2021a; Poursarebani *et al.*, 2015; Poursarebani *et al.*, 2020), lose the identity and/or determinacy of the SM, and thus radically change the morphological structure of the inflorescence, producing additional spikelets/florets or branching. Different from these barley spike mutants, the identity of the spikelet triplet in *flo.a* was not altered, but extra spikelet sharing the same rachis node with triple spikelets is produced, forming quadruplet spikelets, suggesting SM determinacy is lost. Therefore, *HvALOG1* is necessary for the specification of SM determinacy during reproductive growth. However, the formation of extra spikelets in *flo.a* may be independent of the SM identity pathway.

4.2 *Hv*ALOG1 is involved in the regulation of spikelet meristem activity and the establishment of floral organ boundary

4.2.1 Conserved roles of ALOG genes in the regulation of plant inflorescence formation

In this study, we identified a plant-specific TF, *Hv*ALOG1, which plays a critical role in regulating the shape of barley inflorescence. The influence of mutations in *Hv*ALOG1 on meristem activity and spikelet organ boundary establishment provides more insights into the role of the ALOG protein family in plants. *Hv*ALOG1 is one member of the barley ALOG family, in which orthologs have been widely reported as key regulators of inflorescence development in model plants (Bencivenga *et al.*, 2016; Cho and Zambryski, 2011; Huang *et al.*, 2021; Huang *et al.*, 2022; Li *et al.*, 2012; Macalister *et al.*, 2012; Peng *et al.*, 2017; Sato *et al.*, 2014; Takeda *et al.*, 2011; Xu *et al.*, 2016; Yoshida *et al.*, 2013; Yoshida *et al.*, 2009; Zhao *et al.*, 2004a; Zhou *et al.*, 2021). In *Arabidopsis*, members of the ALOG family play important roles in light signaling and specifying organ boundaries (Cho and Zambryski, 2011; Takeda *et al.*, 2011; Zhao *et al.*, 2004a). In grasses, such as rice and sorghum, several ALOG family members have been found to be involved in the regulation of the transition from indeterminate to determinate meristems, spikelet/floret specification and development (Li *et al.*, 2012; Peng *et al.*, 2017; Sato *et al.*, 2014; Yoshida *et al.*, 2013; Yoshida *et al.*, 2009; Zhou *et al.*, 2021). In particular, the rice *OsG1* gene is involved in suppressing lemma identity to specify sterile lemmas. According to the three-floret hypothesis (one central and two lateral) spikelets, during the evolution of rice, *OsG1* activity was designated to repress the development of the lemma of the lateral floret, which is now completely degenerated in modern rice compared with the ancestral state, leaving only sterile lemmas significantly reduced in size (Ren *et al.*, 2020; Yuan *et al.*, 2020; Zhang *et al.*, 2017). The loss-of-function *Osg1* mutation converted the sterile lemma into a lemma-like structure, which is interpreted as restoring the lemma from lateral florets in the hypothesized ancestral three-flowered spikelet structure (Yoshida *et al.*, 2009). Formally, *Hv*ALOG1 may also play a similar role in the development of lateral floral organs in barley. In the WT, the formation of extra spikelets and the development of sterile LSs are suppressed by the functional *Hv*ALOG1 (Figure 3.2 and 3.6). In particular, fused glumes of CSs were converted into lemma- or leaf-like structures, suggesting a possible change in the identity of glumes (Figure 3.2 and 3.9). The

inhibition of lateral floral organs by *HvALOG1* and *OsG1* suggests a conserved function for the ALOG family in grasses. Recently in tomato, proteins of the ALOG family were reported to synergistically control the developmental program of SAM maturation for flowering and production of the composite inflorescence through phase separation (Huang *et al.*, 2021; Huang *et al.*, 2022; Macalister *et al.*, 2012; Xu *et al.*, 2016). Notably, *MpLOS1*, a member of the ALOG family in *Marchantia polymorpha*, plays a role in integrating meristem activity and lateral organ differentiation, contributing to the diversification of lateral organs in shoot systems during land plant evolution (Naramoto *et al.*, 2019).

The phylogenetic analysis revealed that ALOG family members are structurally separable in grasses and eudicots (Figure 3.21), suggesting ALOG genes evolve in a lineage-specific way. Moreover, the number of ALOG proteins is diverse among grass and eudicot species, suggesting that independent duplication or deletion events occurred repeatedly within species. There are a total of 10 ALOG family proteins in the barley genome. Here, we identified and carefully characterized the first member of this family, *HvALOG1*, as *Flo.a* locus. The function of closest orthologs of *HvALOG1* is not identified in grasses. *HvALOG1* is highly conserved across grasses suggesting that this gene is likely to perform a conserved function in grasses (Figure 3.22). Considering similar roles of identified genes in inflorescence development, proteins of the ALOG family have conserved functions across these taxa and likely functioned in their last common ancestor (Naramoto *et al.*, 2019).

4.2.2 *HvALOG1* specifies the spikelet meristem determinacy in a non-cell autonomous manner

The discovery of *HvALOG1* adds to our knowledge of how the paired spikelet architecture develops in grasses. Our phenotypic analysis revealed that *flo.a* produced extra spikelets arising from the boundary between the CSs and the rachis (Figure 3.2 and 3.9). The extra spikelet and CS constitute the paired spikelet phenotype in *flo.a*. In addition, the vascular bundles of the extra spikelets were able to connect to the same rachis nodal complex as the canonical spikelet triplet but interfered with the distribution pattern of the vascular bundles from the CSs, affecting the development of the CSs and ultimately changing grain size (Figure 3.5G to J, 3.13 to 3.14). The paired or supernumerary spikelet spike architecture is a polygenic trait and several genes in wheat have been identified to regulate the formation of secondary spikelet. Mutations

in wheat floral activating genes, *Photoperiod-1 (Ppd-1)* and *FLOWERING LOCUS T1 (FT1)* result in the formation of secondary spikelet by reducing the expression of meristem identity genes to delay the inflorescence and lateral meristems development (Boden *et al.*, 2015; Dixon *et al.*, 2018). The induction of secondary spikelet can also be promoted by increased expression of *TB1* and *HOMEODOMAIN-2 (HB-2)* (Dixon *et al.*, 2018; Dixon *et al.*, 2022). Moreover, wheat *DUO-B1* affects spike inflorescence architecture; *duo-B1* mutations lead to the production of two to three spikelets at a single rachis node to form a multi-row spikelets phenotype (Wang *et al.*, 2022). These genes mainly control the formation of extra spikelets by regulating the activity of AxM (Boden *et al.*, 2015; Dixon *et al.*, 2018; Dixon *et al.*, 2022; Wang *et al.*, 2022). Our results show that at the cellular level, *HvALOG1* plays its role by regulating cell proliferation. In *flo.a* mutant, strong signals of cell division were observed at basal parts where extra SMs initiated (Figure 3.28 and Appendix Figure S3.9). Our ISH expression analysis revealed that the mRNA of *HvALOG1* was restricted to the LR and basal parts of spikelet organs in all spike developmental stages, whereas the *HvALOG1*-GFP fusion protein had more extensive-expression signals extending to other rachis tissues, and specifically circumvented reproductive meristems, including IM, spikelet ridges, TSM, SM and FM (Figure 3.24 and 3.26). Therefore, we propose that *HvALOG1* is not expressed in the reproductive meristems but provides developmental signals from their peripheral regions to regulate meristem activity.

Genes that are specifically expressed in domains between plant organs are required for the establishment and maintenance of the boundaries, and the synergy of these genes establishes signaling centers critical for morphogenesis (Whipple, 2017). In grasses, a set of genes specific for meristem identity and determinacy is expressed at organ boundaries and provides developmental signals for fate and activity to adjacent meristems, directing meristem normative growth (Whipple, 2017). For example, *branchless silk 1 (bd1)* (Chuck *et al.*, 2002) in maize and *FRIZZY PANICLE (FZP)* (Bai *et al.*, 2017; Huang *et al.*, 2018; Komatsu *et al.*, 2003; Wang *et al.*, 2020) in rice, are not expressed in the SM itself, but in a narrow band between the glume and the SM, providing a signal specifying the identity/determinacy of the SM. Loss of *bd1/FZP* results in the production of additional glumes (loss of SM determinacy) and initiation of spikelets from the axils of normally sterile glumes (partial loss of spikelet identity). Another typical example of specifying SM identity is the barley *COM1 (COMPOSITUM 1)*, whose expression is restricted to the IM to SM boundary and purposefully affects

the identity of neighboring SMs (Poursarebani *et al.*, 2020). Failure of signaling from the boundaries leads to the loss of SM identity and eventual reversion to an IM-like meristem that forms a branch-like structure. Spikelet activity of maize *ids1* (*indeterminate spikelet1*) mutants is capable of indeterminately generating multiple FMs rather than terminating in one FM. The expression of *ids1* is not located in the meristem, but in a narrow band opposite the SM, providing the signals to regulate meristem determinacy (Chuck *et al.*, 1998). Similar to the above gene, *HvALOG1* is not expressed in any reproductive meristem but instead forms an expression domain around it to produce signals of limitation for ectopic growth activity (Figure 3.24 and 3.25). This regulatory mechanism is non-cell autonomous. Unlike *BD1/FZP* and *IDS1*, mutations in the *HvALOG1* gene do not affect the identity but dispossess the determinacy of SM in barley, enabling the formation of additional spikelets that manifest as spikelet quartets in *flo.a*. Here, we thus propose that *HvALOG1* non-cell autonomously regulates meristem activity to specify SM determinacy.

4.2.3 *HvALOG1* cell autonomously regulates the establishment of floral organ boundary

Organ boundaries are cellular domains that restrict growth between different cell identities and therefore play an important role in plant organogenesis (Hepworth and Pautot, 2015). After plants enter reproductive growth, the formation of meristem-organ (M-O) boundaries drives the initiation of new floral primordia, while the establishment of organ-organ (O-O) boundaries specifies floral organ development (Yu and Huang, 2016). In this study, we found besides the production of extra spikelet, the glumes of the CSs were extended or fused to form a leaf-like structure in *flo.a*, indicating that the establishment of floral organ boundaries is disturbed and the identity of CS glume is partially lost (Figure 3.8 and 3.9).

Another expression feature of *HvALOG1* is the localization at the base of floral organs. After floral organs start to differentiate, both the mRNA and GFP protein signals of *HvALOG1* were localized at the junction of the newly formed floral organs and the floral meristems (Figure 3.24 and 3.26). Loss-of-function of *HvALOG1* resulted in the fusion of two glumes of CSs, which is consistent with boundary formation-deficient phenotypes in other plant species. In addition, the activity of fused glume primordium was promoted and produced additional organs with unknown identities adaxial to fused glumes (Figure 3.9). 3D reconstruction of the *flo.a* spikelet also indicated that the

vascular development of CS glumes interfered with the formation of an additional spikelet (Figure 3.14). In the transgenic knock-out mutants, the glume-deficient phenotypes were further enhanced, and the feature with glume identity was completely lost, resulting in homeotic transformation into a floret consisting of lemma, palea, stamens and carpel (Figure 3.20 and Appendix Figure S3.4). Thus, we speculate that regulation of boundary establishment and development of CS glumes by *HvALOG1* is performed in a cell autonomous manner.

In *Arabidopsis*, the canonical mechanisms for floral organ boundary establishment and maintenance are defined by a regulatory network centered on *NO APICAL MERISTEM/CUP-SHAPED COTYLEDON (NAM/CUC1, 2 and 3)* genes (Aida *et al.*, 1997; Aida *et al.*, 1999; Hepworth and Pautot, 2015; Hibara *et al.*, 2006; Ishida *et al.*, 2000; Raman *et al.*, 2008; Takada *et al.*, 2001; Takeda *et al.*, 2011; Taoka *et al.*, 2004; Vroemen *et al.*, 2003; Wang *et al.*, 2016b). The *CUC* genes are expressed in boundary regions between organs/primordia, and the inactivation of any two *CUC* genes results in the fusion of normally separated adjacent organs (Aida *et al.*, 1997; Takada *et al.*, 2001; Vroemen *et al.*, 2003; Wang *et al.*, 2016b). Two *ALOG* family members, *ORGAN BOUNDARY1/LIGHT-DEPENDENT SHORT HYPOCOTYL (OBO1/LSH3)* and *OBO4/LSH4* act downstream of *CUC1* and are specifically expressed at the boundary of shoot organs/primordia, involved in inhibiting border cell differentiation (Cho and Zambryski, 2011; Hepworth and Pautot, 2015; Takeda *et al.*, 2011; Wang *et al.*, 2016b). Ablation of *OBO1*-expressing cells results in defects in the formation of SAM and lateral organs (Cho and Zambryski, 2011). Characterization of boundary-specific expression patterns in floral organs and prominent organ fusions in *HvALOG1* loss-of-function mutants allowed us to speculate that *HvALOG1* and other boundary genes share similar functions for involvement in the regulation of boundary formation of barley glumes after spikelet differentiation. Interestingly, fused glumes were not always accompanied by extra spikelets (Figure 3.9), suggesting that the mechanisms regulating these two phenotypes are not identical.

In conclusion, we propose that the function of *HvALOG1* can be divided into two aspects: before SM initiation, by limiting the growth domain of the SM to provide a signal to specify its determinacy in a non-cell autonomous manner; after spikelet formation, *HvALOG1* is expressed at the base of floral organ primordia directing the formation of boundaries between floral organs in a cell autonomous way.

4.3 Putative regulatory factors of spikelet meristem determinacy and floral organ boundary formation in barley

4.3.1 *HvALOG1* may integrate the boundary genes to regulate the development of lateral organs

Reduced cell division in boundary domains is crucial for separation of newly formed organs from the central meristematic tissues, as well as the maintenance and organization of the meristem/primordia (Hepworth and Pautot, 2015). A specific group of genes is expressed in boundary cells to restrict cell division and auxin efflux carrier activity (Yu and Huang, 2016; Zadnikova and Simon, 2014). Here, we provided transcriptome profiling evidence for a function of *HvALOG1* in the regulation of the boundary genes, which might operate as cell-specific repressors for cell proliferation in boundary between meristems/primordia in the barley spike. Clearly, a group of genes, including *CUC2* (Aida *et al.*, 1997; Aida *et al.*, 1999; Hibara *et al.*, 2006; Ishida *et al.*, 2000; Takada *et al.*, 2001; Takeda *et al.*, 2011; Vroemen *et al.*, 2003), *KNAT1/BP-like 1* (Douglas *et al.*, 2002), *KNAT1/BP-like 2*, *HvLG1* (Lee *et al.*, 2007; Liu *et al.*, 2019; Moreno *et al.*, 1997; Poursarebani *et al.*, 2020), *SUP-like* (Bowman *et al.*, 1992; Gaiser *et al.*, 1995; Nibau *et al.*, 2011; Sakai *et al.*, 1995; Xu *et al.*, 2018), *ATHB1* (Capella *et al.*, 2015; Miguel *et al.*, 2020), *PAN* (Chuang *et al.*, 1999; Lohmann *et al.*, 2011; Running and Meyerowitz, 1996) and *LOF2* (Lee *et al.*, 2009) were down-regulated in the young spike tissues of *flo.a*. The reduction in expression of these genes may provide inhibition for division activity of boundary cells, bringing absence or delay in boundary establishment between CS glumes.

These key regulators involved in boundary formation have a feature of boundary-specific expression patterns in plants; their loss-of-function mutants typically produce fused organs (Yu and Huang, 2016). Our expression analysis revealed that *HvALOG1* is not expressed in the reproductive meristems but boundaries and other spike tissues (Figure 3.24 and 3.25). Consistent with this, *LSH3/OBO1*, one member of the *Arabidopsis* ALOG family has unique expression at the boundaries between the apical meristems and lateral organs, overlapping with other key genes related to boundary formation (Cho and Zambryski, 2011). Therefore, *HvALOG1* may be a critical factor to integrate the boundary genes to control the development of lateral organs. In addition, *LSH3/OBO1* and *LSH4* have been identified as direct targets of the *CUC1* in *Arabidopsis* (Cho and Zambryski, 2011; Hepworth and Pautot, 2015; Takeda *et al.*,

2011; Wang *et al.*, 2016b), implying that a possible feedback regulatory loop between ALOGs and CUCs is responsible for boundary formation.

4.3.2 Putative role for low auxin during barley boundary formation

Genes relative to boundary establishment function through various mechanisms, including interaction with the phytohormone auxin to regulate the number and location of floral organs (Zadnikova and Simon, 2014). *CUC* genes are negatively regulated by auxin-dependent signaling pathways involved in boundary establishment (Daimon *et al.*, 2003; Takada *et al.*, 2001). In *Arabidopsis* SAM, new floral primordia are initiated in peripheral regions where auxin concentrations are highest; subsequently, auxin is depleted from the potential boundary between the emerging primordium and meristem and flows concurrently to the starting domain of the next primordium (Heisler *et al.*, 2005; Xu *et al.*, 2018). The expression regions of the *CUC* genes are restricted to coincide with the boundaries with low auxin activity. Endogenous hormone assays in this study revealed that auxin accumulation was higher in the upper-middle spikes of *flo.a*, consistent with the extra spikelets and glumes fusion phenotypes. In addition, a group of auxin-related genes such as *ARF16*, *Aux/IAA*, *SAUR*, *GH3* and *PIN3* was specifically highly expressed in the middle-upper spikes of *flo.a*. These genes functions in auxin signaling, transport and homeostasis, indicating that auxin signaling is involved in organogenesis and boundary formation during barley inflorescence development (Chapman and Estelle, 2009; Keuskamp *et al.*, 2010; Leyser, 2018; Stortenbeker and Bemer, 2019; Sun *et al.*, 2019).

4.3.3 Potential effect of meristem identity/determinacy genes

One feature of the *flo.a* spike phenotypes is the production of extra spikelets from the rachis node bearing spikelet triplet. The mutations in *HvALOG1* cases the loss of SM determinacy, resulting in the formation of ectopic organs. Our transcriptome profiling data showed that a group of genes, including *Vrs4/HvRA2*, *AFO*, *HvAP2L-5H*, and *INT-C/HvTB1*, related to meristem identity or determinacy were down-regulated in the young spike of *flo.a*. The misexpression of these genes disrupts the maintenance for meristem stability, enabling the changing status of proliferation or differentiation of the meristematic cells.

In barley, *VRS4*, a key row-type gene encodes a TF containing a LOB domain, involved in the regulation of LS fertility and SM determinacy. The *vrs4* mutants lose SM

determinacy and cause strong supernumerary spikelets/florets phenotypes (Koppolu *et al.*, 2013) and might contribute to the extra spikelet phenotype in *flo.a*. *AFO*, a member of YABBY family TF, is involved in abaxial cell type specification in leaves and fruits, and is required for normal flower development (Kumaran *et al.*, 1999; Sawa *et al.*, 1999). The null *afo/fil* mutant shows defects in all four floral whorls featured by a various number of organs (Kumaran *et al.*, 1999; Sawa *et al.*, 1999). The closely related *AFO/FIL* in rice called *TONGARI-BOUSHI1(TOB1)* is not expressed in the meristem and may have a non-cell autonomous role in maintaining normal meristem organization. The mutation of *TOB1* showcases pleiotropic phenotypes in spikelets derived from failure in the growth of the lateral organs and defects in the maintenance and organization of meristems (Tanaka *et al.*, 2012). In addition, three rice YABBY genes (*TOB1*, *TOB2*, *TOB3*) have a conserved function to maintain the proper activity of meristems in rice spikelets (Tanaka *et al.*, 2017). The expression of *TOB1* is similar to *HvALOG1*, the down-regulation of *TBO1* in *flo.a* might induce the formation of extra spikelets. Moreover, two other critical genes for barley spike development, *HvAP2L-H5* and *INT-C/HvTB1*, were also down-regulated in *flo.a*. *HvAP2L-H5* suppresses the identity shift of IM to a terminal SM. Mutations in *HvAP2L-H5* resemble wheat spike phenotypes with terminal spikelet and extra florets per spikelet (Zhong *et al.*, 2021). *INT-C/HvTB1* plays a key role in barley inflorescence development, specifically in inhibiting the growth of LS (Ramsay *et al.*, 2011). These genes function downstream of *HvALOG1* to maintain meristem activity.

The MADS-box family of transcription factors has been reported to be extensively related to the determination of floral organ development based on the ABCDE model (Ciaffi *et al.*, 2011). In barley, specific grouping members of the MIKCC MADS-box family may be involved in developmental events that drive inflorescence meristem initiation, floral meristem identity, and floral organ determination (Kuijjer *et al.*, 2021). In our transcriptome profiling data, several classes of MADS-box genes were differentially expressed in BW and *flo.a* (adjusted P < 0.05), although some of them did not reach the cut-off threshold [absolute (log₂Fold-Change) > 0.5845], suggesting their involvement in specification and maintenance of inflorescence-, spikelet- and floral meristems (Appendix Figure S3.13). In particular, mRNA levels of *MADS5*, *MADS32*, and *MADS56* were specifically accumulated in the upper-mid parts of *flo.a* spike, suggesting that these three proteins might contribute to the specification of identity to the extra spikelets.

4.3.4 Promotion of organ development genes may induce extra spikelet organs

Compared with BW, a set of genes that relate to cell division, shoot development and floral organogenesis were induced with the upper-middle-specific expression pattern in *flo.a* spike tissues. Among them, *ROXY2*-like plays a role in controlling anther development together with *ROXY1* in *Arabidopsis* (Murmu *et al.*, 2010; Wang *et al.*, 2012; Xing and Zachgo, 2008). *Arabidopsis RAP2.6L* was initially reported to be required for shoot regeneration in tissue culture (Che *et al.*, 2006). Overexpression of *RAP2.6L* in WT enhances the capacity of *de novo* shoot formation, producing phenotypes similar to the mutant of *ALTERED MERISTEM PROGRAM1 (AMP1)*, characterized by enlarged shoot apical meristem, excess stem cell pool and a higher rate of leaf formation (Yang *et al.*, 2018b). Up-regulation of *ROXY2-like* and *RAP2.6L* are associated with the organogenesis of extra spikelets in upper-middle spikes of *flo.a*.

The genes encoding the bHLH domain were up-regulated in upper-middle spikes of *flo.a*, including *PRE5* and *PRE6*. In *Arabidopsis*, the *PRE* family includes 6 genes, and they are related to growth regulation via several signaling pathways, including auxin, GA, BR, high temperature and light. Elevated expression from any *PRE* genes promotes an elongated hypocotyl/petiole phenotype, whereas downregulation of multiple *PRE* genes results in dwarf phenotypes, suggesting a functionally redundant role of *PRE* family members in promoting cell elongation (Bai *et al.*, 2013; Chapman *et al.*, 2012; Lee *et al.*, 2006; Oh *et al.*, 2012; Wang *et al.*, 2010; Zhang *et al.*, 2010). Additionally, the *PRE* genes are involved in the coordinated growth of floral organs and contribute to successful autogamous reproduction in *Arabidopsis* (Shin *et al.*, 2019).

In addition, several genes putatively involved in flowering time regulation, including *MADS14 (VRN1)*, *PEP-like*, *FD-like*, *FPF1-like 1* and *FPF1-like 2*, also appear to be involved in the formation of extra spikelets and floral organ development in *flo.a*. The expression levels of these genes were significantly increased in *flo.a*. *VRN1* is a known vernalization gene that regulates the temperature response and controls flowering time in barley; *VRN1* exhibits high transcript levels during early inflorescence development before spikelet differentiation, suggesting a possible role in the establishment and maintenance of IM and SM identity in barley (Kuijjer *et al.*, 2021; Trevaskis *et al.*, 2007). In wheat, *VRN1* is involved in regulating the acquisition and termination of IM identity. The formation of the terminal spikelet is delayed in the *vrn1* null mutant, ending with an increased number of spikelets per spike (Li *et al.*, 2019). *Arabidopsis PEPPER*

(*PEP*), a K-homologous nuclear ribonucleoprotein was reported to affect vegetative and gynoecium development (José Ripoll *et al.*, 2006), and interact antagonistically with its paralog FLK as a central floral suppressor of *FLOWERING LOCUS C* expression (Ripoll *et al.*, 2009). *PEP* also plays an important role in maintaining FLC function during flower morphogenesis (Rodríguez-Cazorla *et al.*, 2015). *Arabidopsis* *FD* and *FLOWERING PROMOTING FACTOR 1 (FPF1)* are key regulatory factors in the flowering pathway and are required for the positive regulation of flowering (Gorham *et al.*, 2018; Kania *et al.*, 1997). Thus, our results suggest that flowering regulatory pathways play critical roles in spikelet and inflorescence development.

Taken together, our data suggest that HvALOG1 maintains the stability of the SM by coordinating the expressional balance between genes associated with boundary formation, hormonal homeostasis, meristem identity/determinacy and organ development.

4.4 Barley ALOG family members are functionally redundant in early spike development

Position effects of *flo.a* phenotypes may be related to incomplete redundancy in ALOG family. Recently, tomato *TMF* and five other *TMF FAMILY MEMBERS (TFAMs)* paralogs have been reported to synergistically regulate SAM maturation to determine flowering transition and production of compound inflorescences (Huang *et al.*, 2021; Huang *et al.*, 2022). Individual or higher-order mutant combinations from *tmf* and *tfams* produced continuous flowering transition defects, with a feature of flower number spanning fewer to single with sterile floral organs (Huang *et al.*, 2022). The ALOG paralogs play unequal roles with different transcriptional abundances in the shoot meristem and act together to suppress the precocious activation of floral identity genes *ANANTHA* (Huang *et al.*, 2022).

The ingenious regulatory mechanism from tomato ALOG genes enables us to imagine that phenotypic effects in *flo.a* may also arise from the unequal functional redundancy of ALOG family members in barley. The phenotypes of the extra spikelet formation and glume fusion of the CS occurred only in the upper and middle parts of spike from *flo.a* mutant, while the basal approximately 10 spikelets were not significantly different from WT (Figure 3.4), indicating that SM determinacy and CS glume identity were not

altered. Considering that *HvALOG1* is completely deleted in *flo.a*, its function for maintenance of meristem activity may be complemented by other basally expressed ALOG paralogs which rescue the mutant phenotypes. We speculate that the formation of extra spikelets in *flo.a* mutant may be related to differences in the spatiotemporal expression of ALOG genes (Figure 3.29).

Interestingly, a total of seven ALOG genes were specifically highly expressed both in the whole spike of BW and *flo.a* at the DR stage, when the first several SRs formed; but less expressed in spike tissues at the later developing stages (Figure 3.29 and 3.31), indicating they only affect the activity of first few SMs that are formed. In contrast, *HvALOG1* was specifically expressed throughout the developmental stages of the spikelet and floral organs in BW (Figure 3.29 and 3.31). Deletion of *HvALOG1* and only weak expression of other paralogs may lead to a gap of determinacy signals during the formation and differentiation of SMs in the upper and middle parts of *flo.a* spike, resulting in extra spikelets and organ fusion phenotypes (Figure 3.31).

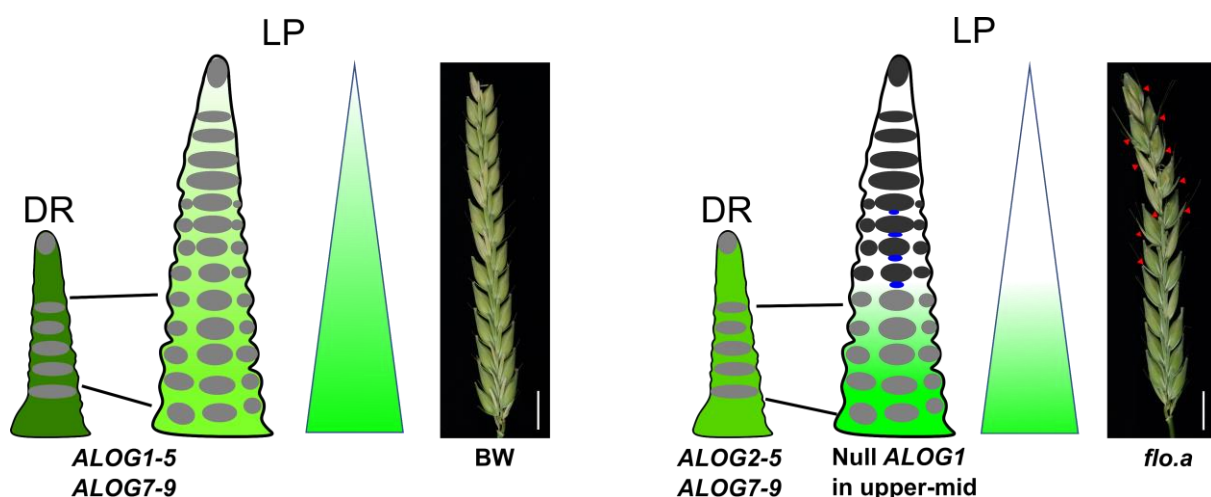


Figure 3.31 The regulatory mechanism of ALOG family members for SM determinacy. Different degrees of green indicate expression levels of ALOG members in spike tissues. The red triangles indicate the *flo.a* events. Light and dark grey ovals represent unaffected and affected reproductive meristems, respectively. Blue ovals represent additional spikelet meristems. DR, double ridge. LP, lemma primordium. Bar = 1 cm.

Therefore, we hypothesize that barley ALOG family members may provide yet unidentified genetic redundancy to maintain the meristem activity to specify SM determinacy, especially during early spike development.

4.5 Application of extra spikelets in breeding

Rapid and large-scale changes in the environment and society place higher demands on crop productivity and diversity (Eshed and Lippman, 2019). The flowering and shoot systems of classic crops are constantly being adjusted in response to environmental changes (Eshed and Lippman, 2019). The pursuit of high yield has always been the main goal of breeders. The grain yield of small grain cereals, such as barley and wheat, is mainly determined by the number of grains produced per unit area (Koppolu *et al.*, 2021). Improving the number of grains by increasing the number of spikelets per spike, the number of florets per spikelet, and increasing the fertility of the florets within the spikelet are proven ways to increase the number of grains (Koppolu *et al.*, 2021).

Here, we characterize a barley *flo.a* mutant that shows the production of extra spikelets and thus exhibits the phenotype of paired spikelets. Extra spikelets in the upper-mid part of the spikes derived from loss-of-function of *HvALOG1* are sterile, mainly because the development of inner floral organs is inhibited during the later stages of spikelet development. The degenerated extra spikelets are similar to the LS of two-rowed barley. Therefore, we speculate that the suppression of the development of extra spikelets may also be regulated by row-typed genes (*VRS1* to *5*). Indeed, several key factors controlling row-type from our transcriptome profiling data set, including *VRS1*, *VRS4*, and *INT-C*, were differentially expressed in BW and *flo.a* (Figure 3.27 and Appendix Figure S3.9). In particular, *VRS1*, a domestication gene majorly inhibiting fertility of lateral spikelets (Sakuma *et al.*, 2017), was elevated in *flo.a* (Appendix Figure S3.9), which may similarly contribute to suppressing the development of extra spikelets. Phenotypic analysis showed the size of LSs in *flo.a* was significantly smaller than that of WT, further implying that row-type genes may also affect the formation and development of extra spikelets. In conclusion, our study shows that loss-of-function of *HvALOG1* leads to extra spikelet formation and confers the possibility of increased grain number in six-rowed barley background by genetic improvement, despite the fertility of extra spikelet remains to be shown.

However, we also have to consider the downsides that come with the formation of extra spikelets. Essentially, the formation of extra spikelets expands the sink of barley inflorescence. Altered source-sink balances can have effects on the development of the regular spikelet triplet. Our phenotypic analysis revealed that yield-related traits, such as grain number per spike, grain size and weight, were significantly decreased in

flo.a (Figure 3.5). In this regard, these extra sterile spikelets appear to be an unfavorable trait in breeding. Inhibition of extra spikelet formation by *HvALOG1* ensures normal development of spikelet triplets, thereby maintaining canonical barley spike architecture. We found that only a single amino acid substitution was present in *HvALOG1* across 20 accessions (7/13) from the barley pan-genome dataset (Appendix table S5) (Jayakodi *et al.*, 2020). However, we did not observe the clear '*flo*' phenotype in these accessions, despite in natural populations, we did find the presence of extra spikelets in a small amount of six-rowed barley (data not shown). Taken together, *HvALOG1* loci have not been utilized during barley genetic improvement.

Recently, the creation of targeted genetic variation through CRISPR-Cas9-mediated gene editing is a new and powerful addition to existing conventional crossbreeding or mutagenesis breeding to improve crops (Eshed and Lippman, 2019). One of the most straightforward options possible is to generate defined and favorable mutations of *HvALOG1* in the genetic background of six-rowed barley to produce extra fertile spikelets without affecting the development of normal spikelet triplets.

Overall, how to balance the effects of extra spikelet and regular triple spikelet to genetic improvement of barley yield needs further study.

5. Outlook

This study reveals that the barley HvALOG1 acts as an important regulator of plant architecture, responsible for suppressing the production of additional spikelets and driving organ boundary formation, thereby maintaining the stability of spike development. Compared to wild-type plants, the *flo.a* produces extra spikelets instead of florets on the dorsal side of the upper-middle spike, and in addition, the boundary between the glumes of the central spikelet is lost, forming a fused leaf-like organ. What has been elusive, however, is how HvALOG1 affects both the formation of extra spikelets and the boundary of the glumes. Phenotypic analysis revealed these two typical features of *flo.a* do not appear to be congruent. Both or only one of the two may be present in *flo.a*, suggesting that their regulatory mechanisms seem to be different. In addition, new organs with unknown identity were generated with the glume fusion phenotype. Therefore, how to define these newly formed organs and dissect the underlying regulatory networks will be the focus of future research.

ALOG proteins are key transcriptional factors regulating inflorescence morphology in land plants, and they share a highly conserved ALOG domain. However, functional studies of ALOG proteins have only been performed in a few limited species, including rice, sorghum, *Arabidopsis*, and tomato. Recently, the function of *TMF* in tomato, as well as its paralogs as transcriptional repressors, has been carefully characterized. Five ALOG proteins with different phase-separation capabilities and transcriptional activities interact and assemble into heterotypic condensates to isolate the promoter region of the floral identity gene and inhibit its precocious activation (Huang *et al.*, 2021; Huang *et al.*, 2022). In the present study, we confirmed that HvALOG1 is expressed in the nucleus, suggesting that it acts as a potential transcription factor. Moreover, transcriptome profiling data revealed that a set of genes involved in inflorescence development, spikelet identity/determinacy and organ development were differentially expressed between wild-type and *flo.a*, implying that these genes may be directly or indirectly regulated by HvALOG1. However, as a candidate for a transcription factor, its function in barley still needs to be further elucidated. Therefore, a series of experiments centered on DNA-protein interaction, such as transcriptional activity assay, chromatin immunoprecipitation (ChIP) sequencing and Electrophoretic mobility shift assay (EMSA), can be used to verify the regulation mechanism of HvALOG1 to downstream genes.

In this study, we found that the extra spikelets and fused glumes occurred only on the dorsal side of the upper-mid CS. We propose the positional spike effect of the *flo.a* phenotype may be associated with functional redundancies with other ALOG family proteins. These proteins may function together specifically during early spike developmental stages to rescue the *flo.a* phenotype. Although transcriptome profiling data and mRNA *in situ* hybridization experiments showed that other ALOG proteins were specifically expressed at the DR stage, which partially confirmed our conjecture, we still lack more direct evidence to prove that other ALOG proteins are involved in the suppression of extra spikelets and formation of glume boundaries. A possible solution is to construct single and higher-order mutants of ALOG proteins mediated by the CRISPR-Cas9 system to resolve their redundant functions. At the same time, exploring whether these transcription factors can interact to jointly regulate the expression of downstream genes.

Taken together, our results shed new light on how HvALOG1 non-cell autonomously specifies the determinacy of the SM and autonomously regulates the boundary formation of the glumes of the CS in barley. Exploration for ALOG family-mediated regulatory mechanism of barley inflorescence morphogenesis must await future studies and would also be interesting.

6. Summary

The inflorescence architecture determines the distribution of the grains and ultimately has a decisive impact on yield in cereals and therefore is one of the most important agricultural traits to be modified for production and harvesting during breeding. The induced genetic variations provide generous gains for crop improvement. However, the genes that control inflorescence development in crops are largely unknown.

Here, we investigated the genetic and molecular basis of “paired spikelet” phenotypes in barley recessive mutant previously named *extra floret.a* (*flo.a*). Detailed phenotypic analysis showed the phenotypes of the *flo.a* mutant rely on three aspects: (i) production of extra spikelets adaxial to the primary central spikelets; (ii) modulation of inner and outer glume boundary establishment, resulting in a fused leaf-like organ; and (iii) the extra spikelets and fused glumes were developed starting from the upper-mid portion to the tip of the spike.

By constructing segregating populations and using map-based cloning, we mapped the candidate gene within a 12.2 Mb interval on the short arm of chromosome 6H. A deletion fragment of approximately 477 kb was identified in the mapping interval of the *flo.a* mutant. The independent allelic and induced transgenic mutant plants, using CRISPR-Cas9, strongly supported *HORVU.MOREX.r2.6HG0469780* as the *Flo.a* locus. *Flo.a* encodes an ALOG1 transcription factor (*HvALOG1*), a close homolog of *Arabidopsis thaliana* *LSH1* and *Oryza* *G1*. ALOG proteins have been reported to be involved in light signaling, floral organ specification, spikelet development and inflorescence branching in several plant species.

A subcellular localization assay revealed that *HvALOG1* is a nucleus-targeted protein and most likely functions as a transcriptional factor in barley. By mRNA *in situ* hybridization and ectopic expression of an *HvALOG1-p::HvALOG1:GFP* construct, we show that *HvALOG1* is not expressed in reproductive meristems during early spike development but is expressed at the base of the floral organ primordia after spikelet initiation. Transcriptome profiling suggested that *HvALOG1* regulates other known regulators of inflorescence architecture. In particular, genes involved in boundary formation, meristem maintenance and organization were down-regulated while those involved in auxin-dependent signaling pathways and organ development were up-regulated in *flo.a* mutant. Moreover, auxin accumulation in the upper-middle spike of *flo.a* mutant appears to promote extra spikelet formation and modulate glume boundary establishment. We propose that *HvALOG1* provides signals from the

meristem boundaries to specify the spikelet meristem determinacy by non-cell autonomously regulating the spikelet meristem; however, the boundary established between the two glumes of central spikelet appears to be cell autonomous. Furthermore, phylogenetic analysis showed that ALOG family members share a conserved domain and can be distinguished into different lineages, suggesting ALOG proteins evolved in a lineage-specific manner, but may play a conserved role in the regulation of plant reproductive growth.

Position effects of *flo.a* phenotypes may be related to incomplete redundancy in the ALOG family. Spikelets with normal development in the basal part of *flo.a* spike might benefit from the effect of seven ALOG family members during early spike development; however, Deletion of *HvALOG1* and weak expression of the seven paralogs in *flo.a* mutant lead to a gap of determinacy signals during the differentiation of spikelet meristems in the upper-mid parts spike at the later developing stages, resulting in extra spikelets and organ fusion phenotypes. Therefore, we hypothesize that barley ALOG family members may provide yet unidentified genetic redundancy to maintain the meristem activity to specify spikelet meristem determinacy, especially during early spike development.

Taken together, the present study shows *HvALOG1* is critical in maintaining inflorescence architecture in barley by non-cell autonomously specifying the determinacy of spikelet meristem and autonomously regulating the boundary formation of the floral organs. Our results provide a novel insight into the function of ALOG transcription factors during the development of cereal inflorescence and the potential for genetic improvement in Breeding.

7. Zusammenfassung

Der Blütenstandsarchitektur bestimmt die Verteilung der Körner und hat letztendlich entscheidenden Einfluss auf den Getreideertrag und ist daher eines der wichtigsten landwirtschaftlichen Merkmale, das für Produktion und Ernte während der Züchtung modifiziert werden muss. Die induzierten genetischen Variationen sind ein großer Gewinn für die Verbesserung von Kulturpflanzen. Dabei sind die Gene, die die Entwicklung der Blütenstände bei Kulturpflanzen steuern, jedoch weitgehend unbekannt.

Hier untersuchten wir die genetischen und molekularen Grundlagen von „gepaarten Ährchen“-Phänotypen in der rezessiven Gerstenmutante, die zuvor als *extra floret.a* (*flo.a*) bezeichnet wurde. Eine detaillierte phänotypische Analyse zeigte, dass die Phänotypen der *flo.a*-Mutante auf drei Aspekten beruhen: (i) Produktion zusätzlicher Ährchen, die an die primären zentralen Ährchen angrenzen; (ii) Modulation der Festlegung der inneren und äußeren Hüllspelzengrenze, was zu einem verschmolzenen blattähnlichen Organ führt; und (iii) die zusätzlichen Ährchen und verschmolzenen Hüllspelzen wurden ausgehend vom oberen mittleren Teil bis zur Spitze des Ährchens entwickelt.

Durch die Konstruktion von segregierenden Populationen und die Verwendung von kartenbasiertem Klonen kartierten wir das Kandidatengen innerhalb eines 12.2-Mb-Intervalls auf dem kurzen Arm von Chromosom 6H. Im Kartierungsintervall der *flo.a*-Mutante wurde ein Deletionsfragment von etwa 477 kb identifiziert. Die unabhängigen allelischen und induzierten transgenen Mutantpflanzen unter Verwendung von CRISPR-Cas9 unterstützten stark *HORVU.MOREX.r2.6HG0469780* als *Flo.a*-Locus. *Flo.a* codiert einen ALOG1-Transkriptionsfaktor (*HvALOG1*), ein enges Homolog von *Arabidopsis thaliana* **L**SH1 und *Oryza* **G**1. Es wurde berichtet, dass ALOG-Proteine an der Lichtsignalisierung, der Spezifikation der Blütenorgane, der Ährchenentwicklung und der Blütenstandsverzweigung in mehreren Pflanzenarten beteiligt sind.

Ein Test zur subzellulären Lokalisierung zeigte, dass *HvALOG1* ein auf den Zellkern ausgerichtetes Protein ist und höchstwahrscheinlich als Transkriptionsfaktor in Gerste fungiert. Durch mRNA-in-situ-Hybridisierung und ektopische Expression eines *HvALOG1-p::HvALOG1:GFP*-Konstrukts zeigen wir, dass *HvALOG1* während der frühen Ährenentwicklung nicht in reproduktiven Meristemen exprimiert wird, sondern

an der Basis der Blütenorgan-Primordien nach Ährcheninitiation exprimiert wird. Die Erstellung von Transkriptomprofilen legte nahe, dass *HvALOG1* andere bekannte Regulatoren der Blütenstandsarchitektur reguliert. Insbesondere Gene, die an der Grenzbildung, Meristemerhaltung und -organisation beteiligt sind, wurden herunterreguliert, während diejenigen, die an Auxin-abhängigen Signalwegen und der Organentwicklung beteiligt sind, in der *flo.a*-Mutante hochreguliert wurden. Darüber hinaus scheint die Akkumulation von Auxin in der oberen mittleren Ähre der *flo.a*-Mutante die Bildung zusätzlicher Ährchen zu fördern und die Etablierung der Hüllspelzengrenze zu modulieren. Wir schlagen vor, dass *HvALOG1* Signale von den Meristemgrenzen liefert, um die Determiniertheit des Ährchenmeristems zu spezifizieren, indem das Ährchen-Meristem nicht von der Zelle autonom reguliert wird; die Grenze zwischen den beiden Hüllspelzen des zentralen Ährchens scheint jedoch zellautonom zu sein. Darüber hinaus zeigte die phylogenetische Analyse, dass Mitglieder der ALOG-Familie eine konservierte Domäne teilen und in verschiedene Linien unterschieden werden können, was darauf hindeutet, dass sich ALOG-Proteine auf eine Linien-spezifische Weise entwickelt haben, aber möglicherweise eine konservierte Rolle bei der Regulierung des reproduktiven Wachstums von Pflanzen spielen.

Positionseffekte von *flo.a*-Phänotypen können mit unvollständiger Redundanz in der ALOG-Familie zusammenhängen. Ährchen mit normaler Entwicklung im basalen Teil der *flo.a*-Ähre könnten von der Wirkung von sieben Mitgliedern der ALOG-Familie während der frühen Ährenentwicklung profitieren; die Deletion von *HvALOG1* und die schwache Expression der sieben Paraloge in der *flo.a*-Mutante führen jedoch zu einer Lücke von Determinationssignalen während der Differenzierung von Ährchenmeristemen in den Ähren im oberen Mittelteil in den späteren Entwicklungsstadien, was zu zusätzlichen Ährchen und Organfusionphänotypen führt. Daher stellen wir die Hypothese auf, dass Mitglieder der ALOG-Familie bei Gerste eine noch nicht identifizierte genetische Redundanz zur Aufrechterhaltung der Meristemaktivität bieten, um die Determination des Ährchenmeristems zu spezifizieren, insbesondere während der frühen Ährenentwicklung.

Zusammengenommen zeigt die vorliegende Studie, dass *HvALOG1* entscheidend für die Aufrechterhaltung der Blütenstandsarchitektur in Gerste ist, indem es nicht-zellautonom die Determiniertheit des Ährchenmeristems spezifiziert und die

Grenzbildung der Blütenorgane autonom reguliert. Unsere Ergebnisse liefern einen neuen Einblick in die Funktion von ALOG-Transkriptionsfaktoren während der Entwicklung von Getreideblütenständen und das Potenzial genetischer Verbesserung in der Züchtung.

8. References

- Aida M, Ishida T, Fukaki H, Fujisawa H, Tasaka M.** 1997. Genes involved in organ separation in Arabidopsis: an analysis of the cup-shaped cotyledon mutant. *The Plant Cell* **9**, 841-857.
- Aida M, Ishida T, Tasaka M.** 1999. Shoot apical meristem and cotyledon formation during Arabidopsis embryogenesis: interaction among the CUP-SHAPED COTYLEDON and SHOOT MERISTEMLESS genes. *Development* **126**, 1563-1570.
- Aida M, Tasaka M.** 2006. Morphogenesis and Patterning at the Organ Boundaries in the Higher Plant Shoot Apex. *Plant Molecular Biology* **60**, 915-928.
- Aida M, Tsubakimoto Y, Shimizu S, Ogisu H, Kamiya M, Iwamoto R, Takeda S, Karim M, Mizutani M, Lenhard M, Tasaka M.** 2020. Establishment of the Embryonic Shoot Meristem Involves Activation of Two Classes of Genes with Opposing Functions for Meristem Activities. *International Journal of Molecular Sciences* **21**, 5864.
- Aida M, Vernoux T, Furutani M, Traas J, Tasaka M.** 2002. Roles of PIN-FORMED1 and MONOPTEROS in pattern formation of the apical region of the Arabidopsis embryo. *Development* **129**, 3965-3974.
- Alejandra Mandel M, Gustafson-Brown C, Savidge B, Yanofsky MF.** 1992. Molecular characterization of the Arabidopsis floral homeotic gene APETALA1. *Nature* **360**, 273-277.
- Andres F, Romera-Branchat M, Martínez-Gallegos R, Patel V, Schneeberger K, Jang S, Altmüller J, Nürnberg P, Coupland G.** 2015. Floral induction in Arabidopsis thaliana by FLOWERING LOCUS T requires direct repression of BLADE-ON-PETIOLE genes by homeodomain protein PENNYWISE. *Plant Physiology*, pp.00960.02015.
- Bai M-Y, Fan M, Oh E, Wang Z-Y.** 2013. A Triple Helix-Loop-Helix/Basic Helix-Loop-Helix Cascade Controls Cell Elongation Downstream of Multiple Hormonal and Environmental Signaling Pathways in Arabidopsis. *The Plant Cell* **24**, 4917-4929.
- Bai X, Huang Y, Hu Y, Liu H, Zhang B, Smaczniak C, Hu G, Han Z, Xing Y.** 2017. Duplication of an upstream silencer of FZP increases grain yield in rice. *Nat Plants*.
- Bailey-Serres J, Parker JE, Ainsworth EA, Oldroyd GED, Schroeder JI.** 2019. Genetic strategies for improving crop yields. *Nature* **575**, 109-118.
- Baker CC, Sieber P, Wellmer F, Meyerowitz EM.** 2005. The early extra petals1 Mutant Uncovers a Role for MicroRNA miR164c in Regulating Petal Number in Arabidopsis. *Current Biology* **15**, 303-315.
- Balkunde R, Kitagawa M, Xu XM, Wang J, Jackson D.** 2017. SHOOT MERISTEMLESS trafficking controls axillary meristem formation, meristem size and organ boundaries in Arabidopsis. *The Plant Journal* **90**, 435-446.
- Barlow P.** 2002. McManus, M.T. and Veit, B.E. eds. Meristematic tissues in plant growth and development. *Annals of Botany* **90**, 546-547.

-
- Barton MK, Poethig RS.** 1993. Formation of the shoot apical meristem in *Arabidopsis thaliana*: an analysis of development in the wild type and in the shoot meristemless mutant. *Development* **119**, 823-831.
- Bell EM, Lin W-C, Husbands AY, Yu L, Jaganatha V, Jablonska B, Mangeon A, Neff MM, Girke T, Springer PS.** 2012. *Arabidopsis* LATERAL ORGAN BOUNDARIES negatively regulates brassinosteroid accumulation to limit growth in organ boundaries. *Proceedings of the National Academy of Sciences* **109**, 21146-21151.
- Belles-Boix E, Hamant O, Witiak SM, Morin H, Traas J, Pautot VR.** 2006. KNAT6: An *Arabidopsis* Homeobox Gene Involved in Meristem Activity and Organ Separation. *The Plant Cell* **18**, 1900-1907.
- Bencivenga S, Serrano-Mislata A, Bush M, Fox S, Sablowski R.** 2016. Control of Oriented Tissue Growth through Repression of Organ Boundary Genes Promotes Stem Morphogenesis. *Dev Cell* **39**, 198-208.
- Benlloch R, Berbel A, Ali L, Gohari G, Millán T, Madueño F.** 2015. Genetic control of inflorescence architecture in legumes. *Frontiers in plant science* **6**.
- Benlloch R, Berbel A, Serrano-Mislata A, Madueno F.** 2007. Floral Initiation and Inflorescence Architecture: A Comparative View. *Annals of Botany* **100**, 659-676.
- Blazquez MA, Soowal LN, Lee I, Weigel D.** 1997. LEAFY expression and flower initiation in *Arabidopsis*. *Development* **124**, 3835-3844.
- Boden SA, Cavanagh C, Cullis BR, Ramm K, Greenwood J, Jean Finnegan E, Trevaskis B, Swain SM.** 2015. Ppd-1 is a key regulator of inflorescence architecture and paired spikelet development in wheat. *Nat Plants* **1**, 14016.
- Bommert P, Satoh-Nagasawa N, Jackson D, Hirano H-Y.** 2005. Genetics and Evolution of Inflorescence and Flower Development in Grasses. *Plant and cell physiology* **46**, 69-78.
- Bommert P, Whipple C.** 2017. Grass inflorescence architecture and meristem determinacy. *Semin Cell Dev Biol.*
- Borghi L, Bureau M, Simon RD.** 2007. *Arabidopsis* JAGGED LATERAL ORGANS Is Expressed in Boundaries and Coordinates KNOX and PIN Activity. *The Plant Cell* **19**, 1795-1808.
- Bortiri E, Chuck G, Vollbrecht E, Rocheford T, Martienssen R, Hake S.** 2006. *ramosa2* encodes a LATERAL ORGAN BOUNDARY domain protein that determines the fate of stem cells in branch meristems of maize. *Plant Cell* **18**, 574.
- Bossinger G, Lundqvist U, Rohde W, Salamini F.** 1992. Genetics of plant development in barley. *Barley Genetics* **6**, 989-1022.
- Boussora F, Allam M, Guasmi F, Ferchichi A, Rutten T, Hansson M, Youssef HM, Börner A.** 2019. Spike developmental stages and ABA role in spikelet primordia abortion contribute to the final yield in barley (*Hordeum vulgare* L.). *Botanical Studies* **60**.

-
- Bowman JL, Alvarez J, Weigel D, Meyerowitz EM, Smyth DR.** 1993. Control of flower development in *Arabidopsis thaliana* by APETALA1 and interacting genes. *Development* **119**, 721-743.
- Bowman JL, Sakai H, Jack T, Weigel D, Mayer U, Meyerowitz EM.** 1992. SUPERMAN, a regulator of floral homeotic genes in *Arabidopsis*. *Development* **114**, 599-615.
- Bradley D, Ratcliffe O, Vincent C, Carpenter R, Coen E.** 1997. Inflorescence Commitment and Architecture in *Arabidopsis*. *Science* **275**, 80-83.
- Brown RH, Bregitzer P.** 2011. A Ds Insertional Mutant of a Barley miR172 Gene Results in Indeterminate Spikelet Development. *Crop Science* **51**, 1664-1672.
- Budhagatapalli N, Schedel S, Gurushidze M, Pencs S, Hiekel S, Rutten T, Kusch S, Morbitzer R, Lahaye T, Panstruga R, Kumlehn J, Hensel G.** 2016. A simple test for the cleavage activity of customized endonucleases in plants. *Plant Methods* **12**.
- Bull H, Casao MC, Zwirek M, Flavell AJ, Thomas WTB, Guo W, Zhang R, Rapazote-Flores P, Kyriakidis S, Russell J, Druka A, McKim SM, Waugh R.** 2017. Barley SIX-ROWED SPIKE3 encodes a putative Jumonji C-type H3K9me2/me3 demethylase that represses lateral spikelet fertility. *Nat Commun* **8**, 936.
- Byrne ME, Simorowski J, Martienssen RA.** 2002. ASYMMETRIC LEAVES1 reveals knox gene redundancy in *Arabidopsis*. *Development* **129**, 1957-1965.
- Capella M, Ribone PA, Arce AL, Chan RL.** 2015. *Arabidopsis thaliana* HomeoBox 1 (AtHB1), a Homeodomain-Leucine Zipper I (HD-Zip I) transcription factor, is regulated by PHYTOCHROME-INTERACTING FACTOR 1 to promote hypocotyl elongation. *New Phytologist* **207**, 669-682.
- Chapman EJ, Estelle M.** 2009. Mechanism of Auxin-Regulated Gene Expression in Plants. *Annual Review of Genetics* **43**, 265-285.
- Chapman EJ, Greenham K, Castillejo C, Sartor R, Bialy A, Sun T-P, Estelle M.** 2012. Hypocotyl Transcriptome Reveals Auxin Regulation of Growth-Promoting Genes through GA-Dependent and -Independent Pathways. *PLoS ONE* **7**, e36210.
- Che P, Lall S, Nettleton D, Howell SH.** 2006. Gene Expression Programs during Shoot, Root, and Callus Development in *Arabidopsis* Tissue Culture. *Plant Physiology* **141**, 620-637.
- Chen Z, Gallavotti A.** 2021. Improving architectural traits of maize inflorescences. *Molecular Breeding* **41**.
- Cho E, Zambryski PC.** 2011. ORGAN BOUNDARY1 defines a gene expressed at the junction between the shoot apical meristem and lateral organs. *Proceedings of the National Academy of Sciences* **108**, 2154-2159.

-
- Chuang C-F, Running MP, Williams RW, Meyerowitz EM.** 1999. The PERIANTHIA gene encodes a bZIP protein involved in the determination of floral organ number in *Arabidopsis thaliana*. *Genes & Development* **13**, 334-344.
- Chuck G, Meeley R, Hake S.** 2008. Floral meristem initiation and meristem cell fate are regulated by the maize AP2 genes *ids1* and *sid1*. *Development* **135**, 3013-3019.
- Chuck G, Meeley R, Irish E, Sakai H, Hake S.** 2007. The maize tasselseed4 microRNA controls sex determination and meristem cell fate by targeting Tasselseed6/indeterminate spikelet1. *Nature Genetics* **39**, 1517.
- Chuck G, Meeley RB, Hake S.** 1998. The control of maize spikelet meristem fate by the APETALA2-like gene indeterminate spikelet1. *Genes & Development* **12**, 1145-1154.
- Chuck G, Muszynski M, Kellogg E, Hake S, Schmidt RJ.** 2002. The Control of Spikelet Meristem Identity by the *branched silkless1* Gene in Maize. *Science* **298**, 1238-1241.
- Ciaffi M, Paolacci AR, Tanzarella OA, Porceddu E.** 2011. Molecular aspects of flower development in grasses. *Sex Plant Reprod* **24**, 247-282.
- Clark SE, Williams RW, Meyerowitz EM.** 1997. The CLAVATA1 Gene Encodes a Putative Receptor Kinase That Controls Shoot and Floral Meristem Size in *Arabidopsis*. *Cell* **89**, 575-585.
- Colmsee C, Beier S, Himmelbach A, Schmutzer T, Stein N, Scholz U, Mascher M.** 2015. BARLEX – the Barley Draft Genome Explorer. *Molecular Plant* **8**, 964-966.
- Conti L, Bradley D.** 2007. TERMINAL FLOWER1 Is a Mobile Signal Controlling *Arabidopsis* Architecture. *The Plant Cell* **19**, 767-778.
- Dabbert T, Okagaki RJ, Cho S, Heinen S, Boddu J, Muehlbauer GJ.** 2010. The genetics of barley low-tillering mutants: low number of tillers-1 (*lnt1*). *Theoretical and Applied Genetics* **121**, 705-715.
- Daimon Y, Takabe K, Tasaka M.** 2003. The CUP-SHAPED COTYLEDON Genes Promote Adventitious Shoot Formation on Calli. *Plant and cell physiology* **44**, 113-121.
- Danecek P, Auton A, Abecasis G, Albers CA, Banks E, Depristo MA, Handsaker RE, Lunter G, Marth GT, Sherry ST, Mcvean G, Durbin R.** 2011. The variant call format and VCFtools. *Bioinformatics* **27**, 2156-2158.
- Dawson IK, Russell J, Powell W, Steffenson B, Thomas WT, Waugh R.** 2015. Barley: a translational model for adaptation to climate change. *New Phytol* **206**, 913-931.
- Debernardi JM, Greenwood JR, Jean Finnegan E, Jernstedt J, Dubcovsky J.** 2020. APETALA 2-like genes AP2L2 and Q specify lemma identity and axillary floral meristem development in wheat. *The Plant Journal* **101**, 171-187.
- Debernardi JM, Lin H, Faris JD, Dubcovsky J.** 2017. microRNA172 plays a critical role in wheat spike morphology and grain threshability. *Development* **144**, 1966-1975.

-
- Derbyshire P, Byrne ME.** 2013. *MORE SPIKELETS1* Is Required for Spikelet Fate in the Inflorescence of *Brachypodium*. *Plant Physiology* **161**, 1291-1302.
- Ding L, Yan S, Jiang L, Zhao W, Ning K, Zhao J, Liu X, Zhang J, Wang Q, Zhang X.** 2015. HANABA TARANU (HAN) Bridges Meristem and Organ Primordia Boundaries through PINHEAD, JAGGED, BLADE-ON-PETIOLE2 and CYTOKININ OXIDASE 3 during Flower Development in *Arabidopsis*. *PLOS Genetics* **11**, e1005479.
- Dinneny JR, Weigel D, Yanofsky MF.** 2006. NUBBIN and JAGGED define stamen and carpel shape in *Arabidopsis*. *Development* **133**, 1645-1655.
- Dinneny JR, Yadegari R, Fischer RL, Yanofsky MF, Weigel D.** 2004. The role of JAGGED in shaping lateral organs. *Development* **131**, 1101-1110.
- Diss G, Ascencio D, Deluna A, Landry CR.** 2014. Molecular mechanisms of paralogous compensation and the robustness of cellular networks. *Journal of Experimental Zoology Part B: Molecular and Developmental Evolution* **322**, 488-499.
- Dixon LE, Greenwood JR, Bencivenga S, Zhang P, Cockram J, Mellers G, Ramm K, Cavanagh C, Swain SM, Boden SA.** 2018. TEOSINTE BRANCHED1 Regulates Inflorescence Architecture and Development in Bread Wheat (*Triticum aestivum*). *The Plant Cell* **30**, 563-581.
- Dixon LE, Pasquariello M, Badgami R, Levin KA, Poschet G, Ng PQ, Orford S, Chayut N, Adamski NM, Brinton J, Simmonds J, Steuernagel B, Searle IR, Uauy C, Boden SA.** 2022. MicroRNA-resistant alleles of *HOMEBOX DOMAIN-2* modify inflorescence branching and increase grain protein content of wheat. *Science Advances* **8**, eabn5907.
- Dobrovolskaya O, Pont C, Sibout R, Martinek P, Badaeva E, Murat F, Chosson A, Watanabe N, Prat E, Gautier N, Gautier V, Poncet C, Orlov YL, Krasnikov AA, Bergès H, Salina E, Laikova L, Salse J.** 2014. FRIZZY PANICLE Drives Supernumerary Spikelets in Bread Wheat. *Plant Physiology* **167**, 189-199.
- Doebley J, Stec A, Hubbard L.** 1997. The evolution of apical dominance in maize. *Nature* **386**, 485-488.
- Douglas SJ, Chuck G, Dengler RE, Pelecanda L, Riggs CD.** 2002. KNAT1 and ERECTA Regulate Inflorescence Architecture in *Arabidopsis*. *The Plant Cell* **14**, 547-558.
- Doyle JJ, Doyle JL.** 1990. Isolation of plant DNA from fresh tissue. *Focus* **12**, 13-15.
- Druka A, Franckowiak J, Lundqvist U, Bonar N, Alexander J, Houston K, Radovic S, Shahinnia F, Vendramin V, Morgante M, Stein N, Waugh R.** 2011. Genetic Dissection of Barley Morphology and Development. *Plant Physiology* **155**, 617-627.
- Endrizzi K, Moussian B, Haecker A, Levin JZ, Laux T.** 1996. The SHOOT MERISTEMLESS gene is required for maintenance of undifferentiated cells in *Arabidopsis* shoot and floral meristems and acts at a different regulatory level than the meristem genes WUSCHEL and ZWILLE. *The Plant Journal* **10**, 967-979.

-
- Eshed Y, Lippman ZB.** 2019. Revolutions in agriculture chart a course for targeted breeding of old and new crops. *Science* **366**, eaax0025.
- Espinosa-Ruiz A, Martínez C, De Lucas M, Fàbregas N, Bosch N, Caño-Delgado AI, Prat S.** 2017. TOPLESS mediates brassinosteroid control of shoot boundaries and root meristem development in *Arabidopsis thaliana*. *Development* **144**, 1619-1628.
- FAO.** 2022. Food and Agriculture Organization Corporate Statistical Database. <https://www.fao.org/faostat/en/#data/QCL/visualize>.
- Ferrandiz C, Gu Q, Martienssen R, Yanofsky MF.** 2000. Redundant regulation of meristem identity and plant architecture by FRUITFULL, APETALA1 and CAULIFLOWER. *Development* **127**, 725-734.
- Fletcher J.** 2018. The CLV-WUS Stem Cell Signaling Pathway: A Roadmap to Crop Yield Optimization. *Plants* **7**, 87.
- Fletcher JC.** 1999. Signaling of Cell Fate Decisions by CLAVATA3 in *Arabidopsis* Shoot Meristems. *Science* **283**, 1911-1914.
- Franckowiak JD LU.** 2011. Descriptions of barley genetic stocks for 2011. *Barley Genet Newsl*, 41:197.
- Fujishiro Y, Agata A, Ota S, Ishihara R, Takeda Y, Kunishima T, Ikeda M, Kyojuka J, Hobo T, Kitano H.** 2018. Comprehensive panicle phenotyping reveals that qSrn7/FZP influences higher-order branching. *Scientific Reports* **8**.
- Gaiser JC, Robinson-Beers K, Gasser CS.** 1995. The *Arabidopsis* SUPERMAN gene mediates asymmetric growth of the outer integument of ovules. *The Plant Cell* **7**, 333-345.
- Gallavotti A, Long JA, Stanfield S, Yang X, Jackson D, Vollbrecht E, Schmidt RJ.** 2010. The control of axillary meristem fate in the maize ramosa pathway. *Development* **137**, 2849-2856.
- Gendron JM, Liu J-S, Fan M, Bai M-Y, Wenkel S, Springer PS, Barton MK, Wang Z-Y.** 2012. Brassinosteroids regulate organ boundary formation in the shoot apical meristem of *Arabidopsis*. *Proceedings of the National Academy of Sciences* **109**, 21152-21157.
- Geng L, Li M, Zhang G, Ye L.** 2022. Barley: a potential cereal for producing healthy and functional foods. *Food Quality and Safety* **6**.
- Gibson DJ.** 2009. *Grasses and grassland ecology*. Oxford University Press.
- Gómez-Mena CN, Sablowski R.** 2008. ARABIDOPSIS THALIANA HOMEODOMAIN GENE1 Establishes the Basal Boundaries of Shoot Organs and Controls Stem Growth. *The Plant Cell* **20**, 2059-2072.
- Gomez MD, Urbez C, Perez-Amador MA, Carbonell J.** 2011. Characterization of constricted fruit (ctf) Mutant Uncovers a Role for AtMYB117/LOF1 in Ovule and Fruit Development in *Arabidopsis thaliana*. *PLoS ONE* **6**, e18760.

-
- González-Carranza ZH, Rompa U, Peters JL, Bhatt AM, Wagstaff C, Stead AD, Roberts JA.** 2007. HAWAIIAN SKIRT: An F-Box Gene That Regulates Organ Fusion and Growth in Arabidopsis. *Plant Physiology* **144**, 1370-1382.
- González-Carranza ZH, Zhang X, Peters JL, Boltz V, Szecsi J, Bendahmane M, Roberts JA.** 2017. HAWAIIAN SKIRT controls size and floral organ number by modulating CUC1 and CUC2 expression. *PLoS ONE* **12**, e0185106.
- Gorham SR, Weiner AI, Yamadi M, Krogan NT.** 2018. HISTONE DEACETYLASE 19 and the flowering time gene FD maintain reproductive meristem identity in an age-dependent manner. *Journal of experimental botany* **69**, 4757-4771.
- Greb T, Clarenz O, Schäfer E, Müller D, Herrero R, Schmitz G, Theres K.** 2003. Molecular analysis of the LATERAL SUPPRESSOR gene in Arabidopsis reveals a conserved control mechanism for axillary meristem formation. *Genes & Development* **17**, 1175-1187.
- Gu Z, Eils R, Schlesner M.** 2016. Complex heatmaps reveal patterns and correlations in multidimensional genomic data. *Bioinformatics* **32**, 2847-2849.
- Ha CM, Jun JH, Nam HG, Fletcher JC.** 2004. BLADE-ON-PETIOLE1 Encodes a BTB/POZ Domain Protein Required for Leaf Morphogenesis in Arabidopsis thaliana. *Plant and cell physiology* **45**, 1361-1370.
- Ha CM, Jun JH, Nam HG, Fletcher JC.** 2007. BLADE-ON-PETIOLE1 and 2 Control Arabidopsis Lateral Organ Fate through Regulation of LOB Domain and Adaxial-Abaxial Polarity Genes. *The Plant Cell* **19**, 1809-1825.
- Hake S.** 2008. Inflorescence Architecture: The Transition from Branches to Flowers. *Current Biology* **18**, R1106-R1108.
- Han Y, Yang H, Jiao Y.** 2014. Regulation of inflorescence architecture by cytokinins. *Frontiers in plant science* **5**.
- Harrington HD.** 1977. How to identify grasses and grasslike plants (sedges and rushes).
- Hay A, Tsiantis M.** 2010. KNOX genes: versatile regulators of plant development and diversity. *Development* **137**, 3153-3165.
- Heisler MG, Ohno C, Das P, Sieber P, Reddy GV, Long JA, Meyerowitz EM.** 2005. Patterns of Auxin Transport and Gene Expression during Primordium Development Revealed by Live Imaging of the Arabidopsis Inflorescence Meristem. *Current Biology* **15**, 1899-1911.
- Hempel FD, Weigel D, Mandel MA, Ditta G, Zambryski PC, Feldman LJ, Yanofsky MF.** 1997. Floral determination and expression of floral regulatory genes in Arabidopsis. *Development* **124**, 3845-3853.
- Hepworth SR, Pautot VA.** 2015. Beyond the Divide: Boundaries for Patterning and Stem Cell Regulation in Plants. *Front Plant Sci* **6**, 1052.

-
- Hepworth SR, Zhang Y, Mckim S, Li X, Haughn GW.** 2005. BLADE-ON-PETIOLE–Dependent Signaling Controls Leaf and Floral Patterning in Arabidopsis. *The Plant Cell* **17**, 1434-1448.
- Hibara K-I, Karim MR, Takada S, Taoka K-I, Furutani M, Aida M, Tasaka M.** 2006. Arabidopsis CUP-SHAPED COTYLEDON3 Regulates Postembryonic Shoot Meristem and Organ Boundary Formation. *The Plant Cell* **18**, 2946-2957.
- Houston K, Druka A, Bonar N, Macaulay M, Lundqvist U, Franckowiak J, Morgante M, Stein N, Waugh R.** 2012. Analysis of the barley bract suppression gene Trd1. *Theoretical and Applied Genetics* **125**, 33-45.
- Houston K, McKim SM, Comadran J, Bonar N, Druka I, Uzrek N, Cirillo E, Guzy-Wrobelska J, Collins NC, Halpin C, Hansson M, Dockter C, Druka A, Waugh R.** 2013. Variation in the interaction between alleles of *HvAPETALA2* and microRNA172 determines the density of grains on the barley inflorescence. *Proceedings of the National Academy of Sciences* **110**, 16675-16680.
- Huang T, López-Giráldez F, Townsend JP, Irish VF.** 2012. RBE controls microRNA164 expression to effect floral organogenesis. *Development* **139**, 2161-2169.
- Huang X, Chen S, Li W, Tang L, Zhang Y, Yang N, Zou Y, Zhai X, Xiao N, Liu W, Li P, Xu C.** 2021. ROS regulated reversible protein phase separation synchronizes plant flowering. *Nature Chemical Biology* **17**, 549-557.
- Huang X, Xiao N, Zou Y, Xie Y, Tang L, Zhang Y, Yu Y, Li Y, Xu C.** 2022. Heterotypic transcriptional condensates formed by prion-like paralogous proteins canalize flowering transition in tomato. *Genome Biology* **23**.
- Huang Y, Zhao S, Fu Y, Sun H, Ma X, Tan L, Liu F, Sun X, Sun H, Gu P, Xie D, Sun C, Zhu Z.** 2018. Variation in the regulatory region of FZP causes increases in secondary inflorescence branching and grain yield in rice domestication. *The Plant Journal* **96**, 716-733.
- Irish VF.** 2010. The flowering of Arabidopsis flower development. *The Plant Journal* **61**, 1014-1028.
- Ishida T, Aida M, Takada S, Tasaka M.** 2000. Involvement of CUP-SHAPED COTYLEDON Genes in Gynoecium and Ovule Development in Arabidopsis thaliana. *Plant and cell physiology* **41**, 60-67.
- Iyer LM, Aravind L.** 2012. ALOG domains: provenance of plant homeotic and developmental regulators from the DNA-binding domain of a novel class of DIRS1-type retroposons. *Biology Direct* **7**, 39.
- JACKSON D.** 1991. In situ hybridization in plants. *Molecular plant pathology: a practical approach*.

-
- Jasinski S, Piazza P, Craft J, Hay A, Woolley L, Rieu I, Phillips A, Hedden P, Tsiantis M.** 2005. KNOX Action in Arabidopsis Is Mediated by Coordinate Regulation of Cytokinin and Gibberellin Activities. *Current Biology* **15**, 1560-1565.
- Jayakodi M, Padmarasu S, Haberer G, Bonthala VS, Gundlach H, Monat C, Lux T, Kamal N, Lang D, Himmelbach A, Ens J, Zhang X-Q, Angessa TT, Zhou G, Tan C, Hill C, Wang P, Schreiber M, Boston LB, Plott C, Jenkins J, Guo Y, Fiebig A, Budak H, Xu D, Zhang J, Wang C, Grimwood J, Schmutz J, Guo G, Zhang G, Mochida K, Hirayama T, Sato K, Chalmers KJ, Langridge P, Waugh R, Pozniak CJ, Scholz U, Mayer KFX, Spannagl M, Li C, Mascher M, Stein N.** 2020. The barley pan-genome reveals the hidden legacy of mutation breeding. *Nature* **588**, 284-289.
- Jeong S, Trotochaud AE, Clark SE.** 1999. The Arabidopsis CLAVATA2 Gene Encodes a Receptor-like Protein Required for the Stability of the CLAVATA1 Receptor-like Kinase. *The Plant Cell* **11**, 1925-1933.
- Ji L, Liu X, Yan J, Wang W, Yumul RE, Kim YJ, Dinh TT, Liu J, Cui X, Zheng B, Agarwal M, Liu C, Cao X, Tang G, Chen X.** 2011. ARGONAUTE10 and ARGONAUTE1 Regulate the Termination of Floral Stem Cells through Two MicroRNAs in Arabidopsis. *PLOS Genetics* **7**, e1001358.
- José Ripoll J, Ferrándiz C, Martínez-Laborda A, Vera A.** 2006. PEPPER, a novel K-homology domain gene, regulates vegetative and gynoecium development in Arabidopsis. *Developmental Biology* **289**, 346-359.
- Jost M, Taketa S, Mascher M, Himmelbach A, Yuo T, Shahinnia F, Rutten T, Druka A, Schmutzer T, Steuernagel B, Beier S, Taudien S, Scholz U, Morgante M, Waugh R, Stein N.** 2016. A homolog of Blade-On-Petiole 1 and 2 (BOP1/2) controls internode length and homeotic changes of the barley inflorescence. *Plant Physiology*, pp.00124.02016.
- Jun JH, Ha CM, Fletcher JC.** 2010. BLADE-ON-PETIOLE1 Coordinates Organ Determinacy and Axial Polarity in Arabidopsis by Directly Activating ASYMMETRIC LEAVES2. *The Plant Cell* **22**, 62-76.
- Kania T, Russenberger D, Peng S, Apel K, Melzer S.** 1997. FPF1 promotes flowering in Arabidopsis. *The Plant Cell* **9**, 1327-1338.
- Kaufmann K, Pajoro A, Angenent GC.** 2010a. Regulation of transcription in plants: mechanisms controlling developmental switches. *Nature Reviews Genetics* **11**, 830-842.
- Kaufmann K, Wellmer F, Muiño JM, Ferrier T, Wuest SE, Kumar V, Serrano-Mislata A, Madueño F, Krajewski P, Meyerowitz EM, Angenent GC, Riechmann JL.** 2010b. Orchestration of Floral Initiation by APETALA1. *Science* **328**, 85-89.
- Kellogg EA.** 2022. Genetic control of branching patterns in grass inflorescences. *The Plant Cell*.

-
- Kellogg EA, Camara PE, Rudall PJ, Ladd P, Malcomber ST, Whipple CJ, Doust AN.** 2013. Early inflorescence development in the grasses (Poaceae). *Frontiers in plant science* **4**.
- Keuskamp DH, Pollmann S, Voeselek LACJ, Peeters AJM, Pierik R.** 2010. Auxin transport through PIN-FORMED 3 (PIN3) controls shade avoidance and fitness during competition. *Proceedings of the National Academy of Sciences* **107**, 22740-22744.
- Khan M, Ragni L, Tabb P, Salasini BC, Chatfield S, Datla R, Lock J, Kuai X, Despres C, Proveniers M, Yongguo C, Xiang D, Morin H, Rullière J-P, Citerne S, Hepworth SR, Pautot V.** 2015. Repression of lateral organ boundary genes by PENNYWISE and POUND-FOOLISH is essential for meristem maintenance and flowering in *Arabidopsis thaliana*. *Plant Physiology*, pp.00915.02015.
- Khan M, Tabb P, Hepworth SR.** 2012a. BLADE-ON-PETIOLE1 and 2 regulate *Arabidopsis* inflorescence architecture in conjunction with homeobox genes KNAT6 and ATH1. *Plant Signaling & Behavior* **7**, 788-792.
- Khan M, Xu M, Murmu J, Tabb P, Liu Y, Storey K, Mckim SM, Douglas CJ, Hepworth SR.** 2012b. Antagonistic Interaction of BLADE-ON-PETIOLE1 and 2 with BREVIPEDICELLUS and PENNYWISE Regulates *Arabidopsis* Inflorescence Architecture. *Plant Physiology* **158**, 946-960.
- Kirby E, Appleyard M.** 1984. Cereal development guide. 2nd Edition.
- Komatsu M, Chujo A, Nagato Y, Shimamoto K, Kyojuka J.** 2003. *FRIZZY PANICLE* is required to prevent the formation of axillary meristems and to establish floral meristem identity in rice spikelets. *Development* **130**, 3841-3850.
- Komatsuda T, Pourkheirandish M, He C, Azhaguvel P, Kanamori H, Perovic D, Stein N, Graner A, Wicker T, Tagiri A, Lundqvist U, Fujimura T, Matsuoka M, Matsumoto T, Yano M.** 2007. Six-rowed barley originated from a mutation in a homeodomain-leucine zipper I-class homeobox gene. *Proc Natl Acad Sci U S A* **104**, 1424-1429.
- Koppolu R, Anwar N, Sakuma S, Tagiri A, Lundqvist U, Pourkheirandish M, Rutten T, Seiler C, Himmelbach A, Ariyadasa R.** 2013. Six-rowed spike4 (Vrs4) controls spikelet determinacy and row-type in barley. *Proceedings of the National Academy of Sciences* **110**, 13198-13203.
- Koppolu R, Jiang G, Milner SG, Muqaddasi QH, Rutten T, Himmelbach A, Guo Y, Stein N, Mascher M, Schnurbusch T.** 2021. The barley mutant multiflorus2.b reveals quantitative genetic variation for new spikelet architecture. *Theoretical and Applied Genetics*.
- Koppolu R, Schnurbusch T.** 2019. Developmental pathways for shaping spike inflorescence architecture in barley and wheat. *Journal of Integrative Plant Biology* **61**, 278-295.

-
- Kuijjer HNJ, Shirley NJ, Khor SF, Shi J, Schwerdt J, Zhang D, Li G, Burton RA.** 2021. Transcript Profiling of MIKCC MADS-Box Genes Reveals Conserved and Novel Roles in Barley Inflorescence Development. *Frontiers in plant science* **12**.
- Kumaran MK, Ye D, Yang W-C, Griffith ME, Chaudhury AM, Sundaresan V.** 1999. Molecular cloning of ABNORMAL FLORAL ORGANS: a gene required for flower development in Arabidopsis. *Sexual plant reproduction* **12**, 118-122.
- Kyojuka J.** 2014. Grass Inflorescence: Basic Structure and Diversity. *The Molecular Genetics of Floral Transition and Flower Development* **72**, 191.
- Larson SR, Kellogg EA, Jensen KB.** 2013. Genes and QTLs controlling inflorescence and stem branch architecture in *Leymus* (Poaceae: Triticeae) Wildrye. *J Hered* **104**, 678-691.
- Laufs P, Peaucelle A, Morin H, Traas J.** 2004. MicroRNA regulation of the CUC genes is required for boundary size control in Arabidopsis meristems. *Development* **131**, 4311-4322.
- Lee D-K, Geisler M, Springer PS.** 2009. LATERAL ORGAN FUSION1 and LATERAL ORGAN FUSION2 function in lateral organ separation and axillary meristem formation in Arabidopsis. *Development* **136**, 2423-2432.
- Lee D-Y, An G.** 2012. Two AP2 family genes, SUPERNUMERARY BRACT (SNB) and OsINDETERMINATE SPIKELET 1 (OsIDS1), synergistically control inflorescence architecture and floral meristem establishment in rice. *The Plant Journal* **69**, 445-461.
- Lee J, Park J-J, Kim SL, Yim J, An G.** 2007. Mutations in the rice liguleless gene result in a complete loss of the auricle, ligule, and laminar joint. *Plant Molecular Biology* **65**, 487-499.
- Lee M, Dong X, Song H, Yang JY, Kim S, Hur Y.** 2020. Molecular characterization of Arabidopsis thaliana LSH1 and LSH2 genes. *Genes & Genomics* **42**, 1151-1162.
- Lee S, Lee S, Yang K-Y, Kim Y-M, Park S-Y, Kim SY, Soh M-S.** 2006. Overexpression of PRE1 and its Homologous Genes Activates Gibberellin-dependent Responses in Arabidopsis thaliana. *Plant and cell physiology* **47**, 591-600.
- Lei Y, Su S, He L, Hu X, Luo D.** 2019. A member of the ALOG gene family has a novel role in regulating nodulation in *Lotus japonicus*. *Journal of Integrative Plant Biology* **61**, 463-477.
- Lenhard M, Jürgens G, Laux T.** 2002. The WUSCHEL and SHOOTMERISTEMLESS genes fulfil complementary roles in Arabidopsis shoot meristem regulation. *Development* **129**, 3195-3206.
- Letunic I, Bork P.** 2021. Interactive Tree Of Life (iTOL) v5: an online tool for phylogenetic tree display and annotation. *Nucleic Acids Research* **49**, W293-W296.
- Levin JZ, Fletcher JC, Chen X, Meyerowitz EM.** 1998. A Genetic Screen for Modifiers of UFO Meristem Activity Identifies Three Novel FUSED FLORAL ORGANS Genes Required for Early Flower Development in Arabidopsis. *Genetics* **149**, 579-595.
- Lewis MW, Bolduc N, Hake K, Htike Y, Hay A, Candela H, Hake S.** 2014. Gene regulatory interactions at lateral organ boundaries in maize. *Development* **141**, 4590-4597.

-
- Leyser O.** 2018. Auxin Signaling. *Plant Physiology* **176**, 465-479.
- Li C, Lin H, Chen A, Lau M, Jernstedt J, Dubcovsky J.** 2019. Wheat VRN1, FUL2 and FUL3 play critical and redundant roles in spikelet development and spike determinacy. *Development* **146**, dev175398.
- Li G, Kuijter HNJ, Yang X, Liu H, Shen C, Shi J, Betts N, Tucker MR, Liang W, Waugh R, Burton RA, Zhang D.** 2021a. MADS1 maintains barley spike morphology at high ambient temperatures. *Nature Plants* **7**, 1093-1107.
- Li G, Zhang H, Li J, Zhang Z, Li Z.** 2021b. Genetic control of panicle architecture in rice. *The Crop Journal* **9**, 590-597.
- Li H.** 2011. A statistical framework for SNP calling, mutation discovery, association mapping and population genetical parameter estimation from sequencing data. *Bioinformatics* **27**, 2987-2993.
- Li H.** 2013. Aligning sequence reads, clone sequences and assembly contigs with BWA-MEM. *ArXiv13033997 Q-Bio* Available: <http://arxiv.org/abs/1303.3997>.
- Li H, Handsaker B, Wysoker A, Fennell T, Ruan J, Homer N, Marth G, Abecasis G, Durbin R.** 2009. The Sequence Alignment/Map format and SAMtools. *Bioinformatics* **25**, 2078-2079.
- Li X, Sun L, Tan L, Liu F, Zhu Z, Fu Y, Sun X, Sun X, Xie D, Sun C.** 2012. TH1, a DUF640 domain-like gene controls lemma and palea development in rice. *Plant Molecular Biology* **78**, 351-359.
- Li Y, Li L, Zhao M, Guo L, Guo X, Zhao D, Batool A, Dong B, Xu H, Cui S, Zhang A, Fu X, Li J, Jing R, Liu X.** 2021c. Wheat FRIZZYPANICLE activates VERNALIZATION1-A and HOMEBOX4-A to regulate spike development in wheat. *Plant Biotechnology Journal* **19**, 1141-1154.
- Li Z, He Y.** 2020. Roles of Brassinosteroids in Plant Reproduction. *International Journal of Molecular Sciences* **21**, 872.
- Liao Y, Smyth GK, Shi W.** 2014. featureCounts: an efficient general purpose program for assigning sequence reads to genomic features. *Bioinformatics* **30**, 923-930.
- Liljegren SJ, Gustafson-Brown C, Pinyopich A, Ditta GS, Yanofsky MF.** 1999. Interactions among APETALA1, LEAFY, and TERMINAL FLOWER1 Specify Meristem Fate. *The Plant Cell* **11**, 1007-1018.
- Liu K, Cao J, Yu K, Liu X, Gao Y, Chen Q, Zhang W, Peng H, Du J, Xin M, Hu Z, Guo W, Rossi V, Ni Z, Sun Q, Yao Y.** 2019. Wheat TaSPL8 Modulates Leaf Angle Through Auxin and Brassinosteroid Signaling. *Plant Physiology* **181**, 179-194.
- Liu L, Lindsay PL, Jackson D.** 2021. Next Generation Cereal Crop Yield Enhancement: From Knowledge of Inflorescence Development to Practical Engineering by Genome Editing. *International Journal of Molecular Sciences* **22**, 5167.

-
- Liu Q, Yao X, Pi L, Wang H, Cui X, Huang H.** 2009. The ARGONAUTE10 gene modulates shoot apical meristem maintenance and establishment of leaf polarity by repressing miR165/166 in Arabidopsis. *The Plant Journal* **58**, 27-40.
- Lohmann J, Maier A, Stehling-Sun S, Offenburger S-L.** 2011. The bZIP Transcription Factor PERIANTHIA: A Multifunctional Hub for Meristem Control. *Frontiers in plant science* **2**.
- Lolas IB, Himanen K, Grønlund JT, Lynggaard C, Houben A, Melzer M, Van Lijsebettens M, Grasser KD.** 2010. The transcript elongation factor FACT affects Arabidopsis vegetative and reproductive development and genetically interacts with HUB1/2. *The Plant Journal* **61**, 686-697.
- Long J, Barton MK.** 2000. Initiation of Axillary and Floral Meristems in Arabidopsis. *Developmental Biology* **218**, 341-353.
- Long JA, Moan EI, Medford JI, Barton MK.** 1996. A member of the KNOTTED class of homeodomain proteins encoded by the STM gene of Arabidopsis. *Nature* **379**, 66-69.
- Love MI, Huber W, Anders S.** 2014. Moderated estimation of fold change and dispersion for RNA-seq data with DESeq2. *Genome Biology* **15**.
- Lundqvist U.** 2014. Scandinavian mutation research in barley – a historical review. *Hereditas* **151**, 123-131.
- Luo Z, Janssen BJ, Snowden KC.** 2021. The molecular and genetic regulation of shoot branching. *Plant Physiology*.
- Lyu J, Huang L, Zhang S, Zhang Y, He W, Zeng P, Zeng Y, Huang G, Zhang J, Ning M, Bao Y, Zhao S, Fu Q, Wade LJ, Chen H, Wang W, Hu F.** 2020. Neo-functionalization of a Teosinte branched 1 homologue mediates adaptations of upland rice. *Nature Communications* **11**.
- Ma X, Cheng Z, Wu F, Jin M, Zhang L, Zhou F, Wang J, Zhou K, Ma J, Lin Q, Lei C, Wan J.** 2013. BEAK LIKE SPIKELET1 is Required for Lateral Development of Lemma and Palea in Rice. *Plant Molecular Biology Reporter* **31**, 98-108.
- Macalister CA, Park SJ, Jiang K, Marcel F, Bendahmane A, Izkovich Y, Eshed Y, Lippman ZB.** 2012. Synchronization of the flowering transition by the tomato TERMINATING FLOWER gene. *Nature Genetics* **44**, 1393-1398.
- Maizel A, Busch MA, Tanahashi T, Perkovic J, Kato M, Hasebe M, Weigel D.** 2005. The floral regulator LEAFY evolves by substitutions in the DNA binding domain. *Science* **308**, 260-263.
- Marthe C, Kumlehn J, Hensel G.** 2015. Barley (*Hordeum vulgare* L.) transformation using immature embryos. *Methods Mol Biol* **1223**, 71-83.
- Martin M.** 2011. Cutadapt removes adapter sequences from high-throughput sequencing reads. *EMBnet.journal* **17**, 10.

-
- Matsoukas IG.** 2014. Interplay between sugar and hormone signaling pathways modulate floral signal transduction. *Frontiers in Genetics* **5**.
- McKim S, Koppolu R, Schnurbusch T.** 2018. *Barley inflorescence architecture*. In: Stein N, Muehlbauer GJ, eds. *The barley genome*. Berlin Heidelberg: Springer.
- McKim SM, Stenvik G-E, Butenko MA, Kristiansen W, Cho SK, Hepworth SR, Aalen RB, Haughn GW.** 2008. The BLADE-ON-PETIOLE genes are essential for abscission zone formation in Arabidopsis. *Development* **135**, 1537-1546.
- Meyer RS, Purugganan MD.** 2013. Evolution of crop species: genetics of domestication and diversification. *Nature Reviews Genetics* **14**, 840-852.
- Miguel VN, Manavella PA, Chan RL, Capella MA.** 2020. The AtHB1 Transcription Factor Controls the miR164-CUC2 Regulatory Node to Modulate Leaf Development. *Plant and cell physiology* **61**, 659-670.
- Milner SG, Jost M, Taketa S, Mazón ER, Himmelbach A, Oppermann M, Weise S, Knüpffer H, Basterrechea M, König P, Schüler D, Sharma R, Pasam RK, Rutten T, Guo G, Xu D, Zhang J, Herren G, Müller T, Krattinger SG, Keller B, Jiang Y, González MY, Zhao Y, Habekuß A, Färber S, Ordon F, Lange M, Börner A, Graner A, Reif JC, Scholz U, Mascher M, Stein N.** 2019. Genebank genomics highlights the diversity of a global barley collection. *Nature Genetics* **51**, 319-326.
- Minh BQ, Schmidt HA, Chernomor O, Schrempf D, Woodhams MD, Von Haeseler A, Lanfear R.** 2020. IQ-TREE 2: New Models and Efficient Methods for Phylogenetic Inference in the Genomic Era. *Molecular Biology and Evolution* **37**, 1530-1534.
- Monat C, Padmarasu S, Lux T, Wicker T, Gundlach H, Himmelbach A, Ens J, Li C, Muehlbauer GJ, Schulman AH, Waugh R, Braumann I, Pozniak C, Scholz U, Mayer KFX, Spannagl M, Stein N, Mascher M.** 2019. TRITEX: chromosome-scale sequence assembly of Triticeae genomes with open-source tools. *Genome Biology* **20**.
- Moreno MA, Harper LC, Krueger RW, Dellaporta SL, Freeling M.** 1997. *liguleless1* encodes a nuclear-localized protein required for induction of ligules and auricles during maize leaf organogenesis. *Genes & Development* **11**, 616-628.
- Murmu J, Bush MJ, DeLong C, Li S, Xu M, Khan M, Malcolmson C, Fobert PR, Zachgo S, Hepworth SR.** 2010. Arabidopsis Basic Leucine-Zipper Transcription Factors TGA9 and TGA10 Interact with Floral Glutaredoxins ROXY1 and ROXY2 and Are Redundantly Required for Anther Development. *Plant Physiology* **154**, 1492-1504.
- Nair SK, Wang N, Turuspekov Y, Pourkheirandish M, Sinsuwongwat S, Chen G, Sameri M, Tagiri A, Honda I, Watanabe Y, Kanamori H, Wicker T, Stein N, Nagamura Y, Matsumoto T, Komatsuda T.** 2010. Cleistogamous flowering in barley arises from the suppression of microRNA-guided HvAP2 mRNA cleavage. *Proceedings of the National Academy of Sciences* **107**, 490-495.

-
- Naramoto S, Hata Y, Kyojuka J.** 2020. The origin and evolution of the ALOG proteins, members of a plant-specific transcription factor family, in land plants. *Journal of Plant Research* **133**, 323-329.
- Naramoto S, Jones VAS, Trozzi N, Sato M, Toyooka K, Shimamura M, Ishida S, Nishitani K, Ishizaki K, Nishihama R, Kohchi T, Dolan L, Kyojuka J.** 2019. A conserved regulatory mechanism mediates the convergent evolution of plant shoot lateral organs. *PLOS Biology* **17**, e3000560.
- Nibau C, Di Stilio VS, Wu H-m, Cheung AY.** 2011. Arabidopsis and Tobacco SUPERMAN regulate hormone signalling and mediate cell proliferation and differentiation. *Journal of experimental botany* **62**, 949-961.
- Nidhi S, Preciado J, Tie L.** 2021. Knox homologs shoot meristemless (STM) and KNAT6 are epistatic to CLAVATA3 (CLV3) during shoot meristem development in Arabidopsis thaliana. *Molecular Biology Reports*.
- Nolan TM, Vukašinović N, Liu D, Russinova E, Yin Y.** 2020. Brassinosteroids: Multidimensional Regulators of Plant Growth, Development, and Stress Responses. *The Plant Cell* **32**, 295-318.
- Norberg M, Holmlund M, Nilsson O.** 2005. The BLADE ON PETIOLE genes act redundantly to control the growth and development of lateral organs. *Development* **132**, 2203-2213.
- Nordström A, Tarkowski P, Tarkowska D, Norbaek R, Åstot C, Dolezal K, Sandberg G.** 2004. Auxin regulation of cytokinin biosynthesis in Arabidopsis thaliana: A factor of potential importance for auxin–cytokinin-regulated development. *Proceedings of the National Academy of Sciences of the United States of America* **101**, 8039-8044.
- Oh E, Zhu J-Y, Wang Z-Y.** 2012. Interaction between BZR1 and PIF4 integrates brassinosteroid and environmental responses. *Nature Cell Biology* **14**, 802-809.
- Ohno CK, Reddy GV, Heisler MGB, Meyerowitz EM.** 2004. The Arabidopsis JAGGED gene encodes a zinc finger protein that promotes leaf tissue development. *Development* **131**, 1111-1122.
- Palmer S, Moore J, Clapham A, Rose P, Allaby R.** 2009. Archaeogenetic Evidence of Ancient Nubian Barley Evolution from Six to Two-Row Indicates Local Adaptation. *PLoS ONE* **4**, e6301.
- Parcy F, Nilsson O, Busch MA, Lee I, Weigel D.** 1998. A genetic framework for floral patterning. *Nature* **395**, 561-566.
- Peng P, Liu L, Fang J, Zhao J, Yuan S, Li X.** 2017. The rice TRIANGULAR HULL1 protein acts as a transcriptional repressor in regulating lateral development of spikelet. *Scientific Reports* **7**.

-
- Pertea M, Kim D, Pertea GM, Leek JT, Salzberg SL.** 2016. Transcript-level expression analysis of RNA-seq experiments with HISAT, StringTie and Ballgown. *Nature Protocols* **11**, 1650-1667.
- Pourkheirandish M, Kanamori H, Wu J, Sakuma S, Blattner FR, Komatsuda T.** 2018. Elucidation of the origin of 'agriocrithon' based on domestication genes questions the hypothesis that Tibet is one of the centers of barley domestication. *The Plant Journal* **94**, 525-534.
- Poursarebani N, Seidensticker T, Koppolu R, Trautewig C, Gawronski P, Bini F, Govind G, Rutten T, Sakuma S, Tagiri A, Wolde GM, Youssef HM, Battal A, Ciannamea S, Fusca T, Nussbaumer T, Pozzi C, Borner A, Lundqvist U, Komatsuda T, Salvi S, Tuberosa R, Uauy C, Sreenivasulu N, Rossini L, Schnurbusch T.** 2015. The Genetic Basis of Composite Spike Form in Barley and 'Miracle-Wheat'. *Genetics* **201**, 155-165.
- Poursarebani N, Trautewig C, Melzer M, Nussbaumer T, Lundqvist U, Rutten T, Schmutzer T, Brandt R, Himmelbach A, Altschmied L, Koppolu R, Youssef HM, Sibout R, Dalmais M, Bendahmane A, Stein N, Xin Z, Schnurbusch T.** 2020. COMPOSITUM 1 contributes to the architectural simplification of barley inflorescence via meristem identity signals. *Nature Communications* **11**.
- Przemeck GH, Mattsson J, Hardtke C, Sung ZR, Berleth T.** 1996. Studies on the role of the Arabidopsis gene MONOPTEROS in vascular development and plant cell axialization. *Planta* **200**.
- Ragni L, Belles-Boix E, Günl M, Pautot VR.** 2008. Interaction of KNAT6 and KNAT2 with BREVIPEDICELLUS and PENNYWISE in Arabidopsis Inflorescences. *The Plant Cell* **20**, 888-900.
- Rajaraman J, Douchkov D, Lück S, Hensel G, Nowara D, Pogoda M, Rutten T, Meitzel T, Brassac J, Höfle C, Hückelhoven R, Klinkenberg J, Trujillo M, Bauer E, Schmutzer T, Himmelbach A, Mascher M, Lazzari B, Stein N, Kumlehn J, Schweizer P.** 2018. Evolutionarily conserved partial gene duplication in the Triticeae tribe of grasses confers pathogen resistance. *Genome Biology* **19**.
- Raman S, Greb T, Peaucelle A, Blein T, Laufs P, Theres K.** 2008. Interplay of miR164, CUP-SHAPED COTYLEDON genes and LATERAL SUPPRESSOR controls axillary meristem formation in Arabidopsis thaliana. *The Plant Journal* **55**, 65-76.
- Ramsay L, Comadran J, Druka A, Marshall DF, Thomas WT, Macaulay M, MacKenzie K, Simpson C, Fuller J, Bonar N, Hayes PM, Lundqvist U, Franckowiak JD, Close TJ, Muehlbauer GJ, Waugh R.** 2011. INTERMEDIUM-C, a modifier of lateral spikelet fertility in barley, is an ortholog of the maize domestication gene TEOSINTE BRANCHED 1. *Nat Genet* **43**, 169-172.

Ren D, Li Y, He G, Qian Q. 2020. Multifloret spikelet improves rice yield. *New Phytologist* **225**, 2301-2306.

Ren D, Li Y, Zhao F, Sang X, Shi J, Wang N, Guo S, Ling Y, Zhang C, Yang Z, He G. 2013. MULTI-FLORET SPIKELET1, Which Encodes an AP2/ERF Protein, Determines Spikelet Meristem Fate and Sterile Lemma Identity in Rice. *Plant Physiology* **162**, 872-884.

Ren D, Rao Y, Wu L, Xu Q, Li Z, Yu H, Zhang Y, Leng Y, Hu J, Zhu L, Gao Z, Dong G, Zhang G, Guo L, Zeng D, Qian Q. 2016. The pleiotropic ABNORMAL FLOWER AND DWARF1

affects plant height, floral development and grain yield in rice. *Journal of Integrative Plant Biology* **58**, 529-539.

Richardson AE, Hake S. 2019. Drawing a Line: Grasses and Boundaries. *Plants* **8**, 4.

Ripoll JJ, Rodríguez-Cazorla E, González-Reig S, Andújar A, Alonso-Cantabrana H, Perez-Amador MA, Carbonell J, Martínez-Laborda A, Vera A. 2009. Antagonistic interactions between Arabidopsis K-homology domain genes uncover PEPPER as a positive regulator of the central floral repressor FLOWERING LOCUS C. *Developmental Biology* **333**, 251-262.

Rodríguez-Cazorla E, Ripoll JJ, Andújar A, Bailey LJ, Martínez-Laborda A, Yanofsky MF, Vera A. 2015. K-homology Nuclear Ribonucleoproteins Regulate Floral Organ Identity and Determinacy in Arabidopsis. *PLOS Genetics* **11**, e1004983.

Running MP, Meyerowitz EM. 1996. Mutations in the PERIANTHIA gene of Arabidopsis specifically alter floral organ number and initiation pattern. *Development* **122**, 1261-1269.

Sakai H, Krizek BA, Jacobsen SE, Meyerowitz EM. 2000. Regulation of SUP Expression Identifies Multiple Regulators Involved in Arabidopsis Floral Meristem Development. *The Plant Cell* **12**, 1607-1618.

Sakai H, Medrano LJ, Meyerowitz EM. 1995. Role of SUPERMAN in maintaining Arabidopsis floral whorl boundaries. *Nature* **378**, 199-203.

Sakamoto T, Kamiya N, Ueguchi-Tanaka M, Iwahori S, Matsuoka M. 2001. KNOX homeodomain protein directly suppresses the expression of a gibberellin biosynthetic gene in the tobacco shoot apical meristem. *Genes & Development* **15**, 581-590.

Sakuma S, Golan G, Guo Z, Ogawa T, Tagiri A, Sugimoto K, Bernhardt N, Brassac J, Mascher M, Hensel G, Ohnishi S, Jinno H, Yamashita Y, Ayalon I, Peleg Z, Schnurbusch T, Komatsuda T. 2019. Unleashing floret fertility in wheat through the mutation of a homeobox gene. *Proceedings of the National Academy of Sciences* **116**, 5182-5187.

Sakuma S, Lundqvist U, Kakei Y, Thirulogachandar V, Suzuki T, Hori K, Wu J, Tagiri A, Rutten T, Koppolu R, Shimada Y, Houston K, Thomas WTB, Waugh R, Schnurbusch T,

-
- Komatsuda T.** 2017. Extreme Suppression of Lateral Floret Development by a Single Amino Acid Change in the VRS1 Transcription Factor. *Plant Physiology* **175**, 1720-1731.
- Sakuma S, Pourkheirandish M, Hensel G, Kumlehn J, Stein N, Tagiri A, Yamaji N, Ma JF, Sassa H, Koba T, Komatsuda T.** 2013. Divergence of expression pattern contributed to neofunctionalization of duplicated HD-Zip I transcription factor in barley. *New Phytologist* **197**, 939-948.
- Sakuma S, Salomon B, Komatsuda T.** 2011. The domestication syndrome genes responsible for the major changes in plant form in the Triticeae crops. *Plant and cell physiology* **52**, 738-749.
- Sakuma S, Schnurbusch T.** 2020. Of floral fortune: tinkering with the grain yield potential of cereal crops. *New Phytologist* **225**, 1873-1882.
- Sato D-S, Ohmori Y, Nagashima H, Toriba T, Hirano H-Y.** 2014. A role for TRIANGULAR HULL1 in fine-tuning spikelet morphogenesis in rice. *Genes & genetic systems* **89**, 61-69.
- Sawa S, Watanabe K, Goto K, Kanaya E, Morita EH, Okada K.** 1999. FILAMENTOUS FLOWER, a meristem and organ identity gene of Arabidopsis, encodes a protein with a zinc finger and HMG-related domains. *Genes & Development* **13**, 1079-1088.
- Scofield S, Murison A, Jones A, Fozard J, Aida M, Band LR, Bennett M, Murray JAH.** 2018. Coordination of meristem and boundary functions by transcription factors in the SHOOT MERISTEMLESS regulatory network. *Development* **145**, dev157081.
- Shang Y, Yuan L, Di Z, Jia Y, Zhang Z, Li S, Xing L, Qi Z, Wang X, Zhu J, Hua W, Wu X, Zhu M, Li G, Li C.** 2020. A CYC/TB1-type TCP transcription factor controls spikelet meristem identity in barley. *Journal of experimental botany* **71**, 7118-7131.
- Shin K, Lee I, Kim E, Park S, Soh M-S, Lee S.** 2019. PACLOBUTRAZOL-RESISTANCE Gene Family Regulates Floral Organ Growth with Unequal Genetic Redundancy in Arabidopsis thaliana. *International Journal of Molecular Sciences* **20**, 869.
- Shuai B, Reynaga-Peña CG, Springer PS.** 2002. The Lateral Organ Boundaries Gene Defines a Novel, Plant-Specific Gene Family. *Plant Physiology* **129**, 747-761.
- Simons KJ, Fellers JP, Trick HN, Zhang Z, Tai Y-S, Gill BS, Faris JD.** 2006. Molecular Characterization of the Major Wheat Domestication Gene Q. *Genetics* **172**, 547-555.
- Smith HMS, Hake S.** 2003. The Interaction of Two Homeobox Genes, BREVIPEDICELLUS and PENNYWISE, Regulates Internode Patterning in the Arabidopsis Inflorescence. *The Plant Cell* **15**, 1717-1727.
- Soyk S, Lemmon ZH, Oved M, Fisher J, Liberatore KL, Park SJ, Goren A, Jiang K, Ramos A, van der Knaap E.** 2017. Bypassing negative epistasis on yield in tomato imposed by a domestication gene. *Cell* **169**, 1142-1155. e1112.

-
- Spinelli SV, Martin AP, Viola IL, Gonzalez DH, Palatnik JF.** 2011. A Mechanistic Link between STM and CUC1 during Arabidopsis Development. *Plant Physiology* **156**, 1894-1904.
- Stortenbeker N, Bemer M.** 2019. The SAUR gene family: the plant's toolbox for adaptation of growth and development. *Journal of experimental botany* **70**, 17-27.
- Su Y-H, Liu Y-B, Zhang X-S.** 2011. Auxin–Cytokinin Interaction Regulates Meristem Development. *Molecular Plant* **4**, 616-625.
- Sun, Wang, Ma, Li, Liu.** 2019. Genome-Wide Analysis of Cotton Auxin Early Response Gene Families and Their Roles in Somatic Embryogenesis. *Genes* **10**, 730.
- Sun Q, Zhou D-X.** 2008. Rice jmjC domain-containing gene JMJ706 encodes H3K9 demethylase required for floral organ development. *Proceedings of the National Academy of Sciences* **105**, 13679-13684.
- Takada S, Hibara K-i, Ishida T, Tasaka M.** 2001. The CUP-SHAPED COTYLEDON1 gene of Arabidopsis regulates shoot apical meristem formation. *Development* **128**, 1127-1135.
- Takeda S, Hanano K, Kariya A, Shimizu S, Zhao L, Matsui M, Tasaka M, Aida M.** 2011. CUP-SHAPED COTYLEDON1 transcription factor activates the expression of LSH4 and LSH3, two members of the ALOG gene family, in shoot organ boundary cells. *Plant J* **66**, 1066-1077.
- Takeda S, Matsumoto N, Okada K.** 2004. RABBIT EARS, encoding a SUPERMAN-like zinc finger protein, regulates petal development in Arabidopsis thaliana. *Development* **131**, 425-434.
- Tanaka W, Pautler M, Jackson D, Hirano HY.** 2013. Grass meristems II: inflorescence architecture, flower development and meristem fate. *Plant Cell Physiol* **54**, 313-324.
- Tanaka W, Toriba T, Hirano HY.** 2017. Three *TOB1*-related *YABBY* genes are required to maintain proper function of the spikelet and branch meristems in rice. *New Phytologist* **215**, 825-839.
- Tanaka W, Toriba T, Ohmori Y, Yoshida A, Kawai A, Mayama-Tsuchida T, Ichikawa H, Mitsuda N, Ohme-Takagi M, Hirano H-Y.** 2012. The *YABBY* Gene *TONGARI-BOUSHI1* Is Involved in Lateral Organ Development and Maintenance of Meristem Organization in the Rice Spikelet. *The Plant Cell* **24**, 80-95.
- Taoka K-i, Yanagimoto Y, Daimon Y, Hibara K-i, Aida M, Tasaka M.** 2004. The NAC domain mediates functional specificity of CUP-SHAPED COTYLEDON proteins. *The Plant Journal* **40**, 462-473.
- Tavakol E, Okagaki R, Verderio G, Shariati J. V, Hussien A, Bilgic H, Scanlon MJ, Todt NR, Close TJ, Druka A, Waugh R, Steuernagel B, Ariyadasa R, Himmelbach A, Stein N, Muehlbauer GJ, Rossini L.** 2015. The Barley Uniculme4 Gene Encodes a BLADE-ON-

-
- PETIOLE-Like Protein That Controls Tillering and Leaf Patterning. *Plant Physiology* **168**, 164-174.
- Teo ZWN, Song S, Wang Y-Q, Liu J, Yu H.** 2014. New insights into the regulation of inflorescence architecture. *Trends in Plant Science* **19**, 158-165.
- Thiel J, Koppolu R, Trautewig C, Hertig C, Kale S, Erbe S, Mascher M, Himmelbach A, Rutten T, Esteban E.** 2021. Transcriptional landscapes of floral meristems in barley. *Science Advances* **7**, eabf0832.
- Thirulogachandar V, Alqudah AM, Koppolu R, Rutten T, Graner A, Hensel G, Kumlehn J, Bräutigam A, Sreenivasulu N, Schnurbusch T, Kuhlmann M.** 2017. Leaf primordium size specifies leaf width and vein number among row-type classes in barley. *The Plant Journal* **91**, 601-612.
- Trevaskis B, Hemming MN, Dennis ES, Peacock WJ.** 2007. The molecular basis of vernalization-induced flowering in cereals. *Trends in Plant Science* **12**, 352-357.
- van Esse GW, Walla A, Finke A, Koornneef M, Pecinka A, von Korff M.** 2017. Six-Rowed Spike3 (VRS3) Is a Histone Demethylase That Controls Lateral Spikelet Development in Barley. *Plant Physiol* **174**, 2397-2408.
- Venglat SP, Dumonceaux T, Rozwadowski K, Parnell L, Babic V, Keller W, Martienssen R, Selvaraj G, Datla R.** 2002. The homeobox gene BREVIPEDICELLUS is a key regulator of inflorescence architecture in Arabidopsis. *Proceedings of the National Academy of Sciences* **99**, 4730-4735.
- Vernoux T, Kronenberger J, Grandjean O, Laufs P, Traas J.** 2000. PIN-FORMED 1 regulates cell fate at the periphery of the shoot apical meristem. *Development* **127**, 5157-5165.
- Vroemen CW, Mordhorst AP, Albrecht C, Kwaaitaal MACJ, De Vries SC.** 2003. The CUP-SHAPED COTYLEDON3 Gene Is Required for Boundary and Shoot Meristem Formation in Arabidopsis. *The Plant Cell* **15**, 1563-1577.
- Waddington SR, Cartwright PM, Wall PC.** 1983. A Quantitative Scale of Spike Initial and Pistil Development in Barley and Wheat. *Annals of Botany* **51**, 119-130.
- Wagner D.** 2017. Key developmental transitions during flower morphogenesis and their regulation. *Curr Opin Genet Dev* **45**, 44-50.
- Wagner D, Sablowski RW, Meyerowitz EM.** 1999. Transcriptional activation of APETALA1 by LEAFY. *Science* **285**, 582-584.
- Wang B, Smith SM, Li J.** 2018. Genetic Regulation of Shoot Architecture. *Annual Review of Plant Biology* **69**, 437-468.
- Wang C, Yang X, Li G.** 2021. Molecular Insights into Inflorescence Meristem Specification for Yield Potential in Cereal Crops. *International Journal of Molecular Sciences* **22**, 3508.

-
- Wang H, Zhu Y, Fujioka S, Asami T, Li J, Li J.** 2010. Regulation of Arabidopsis Brassinosteroid Signaling by Atypical Basic Helix-Loop-Helix Proteins. *The Plant Cell* **21**, 3781-3791.
- Wang J, Lin Z, Zhang X, Liu H, Zhou L, Zhong S, Li Y, Zhu C, Lin Z.** 2019. *krn1*, a major quantitative trait locus for kernel row number in maize. *New Phytologist* **223**, 1634-1646.
- Wang L, Sun S, Jin J, Fu D, Yang X, Weng X, Xu C, Li X, Xiao J, Zhang Q.** 2015. Coordinated regulation of vegetative and reproductive branching in rice. *Proceedings of the National Academy of Sciences* **112**, 15504-15509.
- Wang Q, Hasson A, Rossmann S, Theres K.** 2016a. Divide et impera: boundaries shape the plant body and initiate new meristems. *New Phytologist* **209**, 485-498.
- Wang Q, Hasson A, Rossmann S, Theres K.** 2016b. Divide et impera: boundaries shape the plant body and initiate new meristems. *New Phytol* **209**, 485-498.
- Wang S-S, Chung C-L, Chen K-Y, Chen R-K.** 2020. A Novel Variation in the FRIZZLE PANICLE (FZP) Gene Promoter Improves Grain Number and Yield in Rice. *Genetics* **215**, 243-252.
- Wang X-T, Yuan C, Yuan T-T, Cui S-J.** 2012. The Arabidopsis LFR Gene Is Required for the Formation of Anther Cell Layers and Normal Expression of Key Regulatory Genes. *Molecular Plant* **5**, 993-1000.
- Wang Y, Du F, Wang J, Wang K, Tian C, Qi X, Lu F, Liu X, Ye X, Jiao Y.** 2022. Improving bread wheat yield through modulating an unselected AP2/ERF gene. *Nature Plants*.
- Weberling F.** 1992. *Morphology of flowers and inflorescences*: CUP Archive.
- Weigel D, Alvarez J, Smyth DR, Yanofsky MF, Meyerowitz EM.** 1992. LEAFY controls floral meristem identity in Arabidopsis. *Cell* **69**, 843-859.
- Weigel D, Meyerowitz EM.** 1993. Activation of floral homeotic genes in Arabidopsis. *Science* **261**, 1723-1726.
- Whipple CJ.** 2017. Grass inflorescence architecture and evolution: the origin of novel signaling centers. *New Phytologist* **216**, 367-372.
- Wyatt R.** 1982. INFLORESCENCE ARCHITECTURE: HOW FLOWER NUMBER, ARRANGEMENT, AND PHENOLOGY AFFECT POLLINATION AND FRUIT-SET. *American Journal of Botany* **69**, 585-594.
- Xiao W, Su S, Higashiyama T, Luo D.** 2019. A homolog of the ALOG family controls corolla tube differentiation in *Torenia fournieri*. *Development* **146**, dev177410.
- Xiao W, Ye Z, Yao X, He L, Lei Y, Luo D, Su S.** 2018. Evolution of ALOG gene family suggests various roles in establishing plant architecture of *Torenia fournieri*. *BMC Plant Biology* **18**.
- Xing S, Zachgo S.** 2008. ROXY1 and ROXY2, two Arabidopsis glutaredoxin genes, are required for anther development. *The Plant Journal* **53**, 790-801.

-
- Xu C, Park SJ, Van Eck J, Lippman ZB.** 2016. Control of inflorescence architecture in tomato by BTB/POZ transcriptional regulators. *Genes Dev* **30**, 2048-2061.
- Xu M, Hu T, Mckim SM, Murmu J, Haughn GW, Hepworth SR.** 2010. Arabidopsis BLADE-ON-PETIOLE1 and 2 promote floral meristem fate and determinacy in a previously undefined pathway targeting APETALA1 and AGAMOUS-LIKE24. *The Plant Journal* **63**, 974-989.
- Xu Y, Prunet N, Gan ES, Wang Y, Stewart D, Wellmer F, Huang J, Yamaguchi N, Tatsumi Y, Kojima M, Kiba T, Sakakibara H, Jack TP, Meyerowitz EM, Ito T.** 2018. SUPERMAN regulates floral whorl boundaries through control of auxin biosynthesis. *The EMBO Journal* **37**, e97499.
- Xue Z, Liu L, Zhang C.** 2020. Regulation of Shoot Apical Meristem and Axillary Meristem Development in Plants. *International Journal of Molecular Sciences* **21**, 2917.
- Yamaguchi N, Wu M-F, Winter M, Cara, Berns C, Markus, Nole-Wilson S, Yamaguchi A, Coupland G, Krizek A, Beth, Wagner D.** 2013. A Molecular Framework for Auxin-Mediated Initiation of Flower Primordia. *Developmental cell* **24**, 271-282.
- Yanai O, Shani E, Dolezal K, Tarkowski P, Sablowski R, Sandberg G, Samach A, Ori N.** 2005. Arabidopsis KNOX1 Proteins Activate Cytokinin Biosynthesis. *Current Biology* **15**, 1566-1571.
- Yang J, Thames S, Best NB, Jiang H, Huang P, Dilkes BP, Eveland AL.** 2018a. Brassinosteroids Modulate Meristem Fate and Differentiation of Unique Inflorescence Morphology in *Setaria viridis*. *The Plant Cell* **30**, 48-66.
- Yang S, Poretska O, Sieberer T.** 2018b. ALTERED MERISTEM PROGRAM1 Restricts Shoot Meristem Proliferation and Regeneration by Limiting HD-ZIP III-Mediated Expression of RAP2.6L. *Plant Physiology* **177**, 1580-1594.
- Yoshida A, Sasao M, Yasuno N, Takagi K, Daimon Y, Chen R, Yamazaki R, Tokunaga H, Kitaguchi Y, Sato Y, Nagamura Y, Ushijima T, Kumamaru T, Iida S, Maekawa M, Kyojuka J.** 2013. TAWAWA1, a regulator of rice inflorescence architecture, functions through the suppression of meristem phase transition. *Proceedings of the National Academy of Sciences* **110**, 767-772.
- Yoshida A, Suzaki T, Tanaka W, Hirano H-Y.** 2009. The homeotic gene long sterile lemma (G1) specifies sterile lemma identity in the rice spikelet. *Proceedings of the National Academy of Sciences* **106**, 20103-20108.
- Youssef HM, Eggert K, Koppolu R, Alqudah AM, Poursarebani N, Fazeli A, Sakuma S, Tagiri A, Rutten T, Govind G, Lundqvist U, Graner A, Komatsuda T, Sreenivasulu N, Schnurbusch T.** 2017. VRS2 regulates hormone-mediated inflorescence patterning in barley. *Nat Genet* **49**, 157-161.
- Yu H, Huang T.** 2016. Molecular Mechanisms of Floral Boundary Formation in Arabidopsis. *International Journal of Molecular Sciences* **17**, 317.

-
- Yu H, Li J.** 2021. Short- and long-term challenges in crop breeding. *National Science Review* **8**.
- Yuan Z, Gao S, Xue D-W, Luo D, Li L-T, Ding S-Y, Yao X, Wilson ZA, Qian Q, Zhang D-B.** 2009. RETARDED PALEA1 Controls Palea Development and Floral Zygomorphy in Rice. *Plant Physiology* **149**, 235-244.
- Yuan Z, Persson S, Zhang D.** 2020. Molecular and genetic pathways for optimizing spikelet development and grain yield. *aBIOTECH* **1**, 276-292.
- Zadnikova P, Simon R.** 2014. How boundaries control plant development. *Curr Opin Plant Biol* **17**, 116-125.
- Žádníková P, Simon R.** 2014. How boundaries control plant development. *Current opinion in plant biology* **17**, 116-125.
- Zhang D, Yuan Z.** 2014. Molecular Control of Grass Inflorescence Development. *Annual Review of Plant Biology* **65**, 553-578.
- Zhang L-Y, Bai M-Y, Wu J, Zhu J-Y, Wang H, Zhang Z, Wang W, Sun Y, Zhao J, Sun X, Yang H, Xu Y, Kim S-H, Fujioka S, Lin W-H, Chong K, Lu T, Wang Z-Y.** 2010. Antagonistic HLH/bHLH Transcription Factors Mediate Brassinosteroid Regulation of Cell Elongation and Plant Development in Rice and Arabidopsis. *The Plant Cell* **21**, 3767-3780.
- Zhang T, Li Y, Ma L, Sang X, Ling Y, Wang Y, Yu P, Zhuang H, Huang J, Wang N, Zhao F, Zhang C, Yang Z, Fang L, He G.** 2017. *LATERAL FLORET 1* induced the three-florets spikelet in rice. *Proceedings of the National Academy of Sciences* **114**, 9984-9989.
- Zhao L, Nakazawa M, Takase T, Manabe K, Kobayashi M, Seki M, Shinozaki K, Matsui M.** 2004a. Overexpression of LSH1, a member of an uncharacterised gene family, causes enhanced light regulation of seedling development. *The Plant Journal* **37**, 694-706.
- Zhao M, Yang S, Chen C-Y, Li C, Shan W, Lu W, Cui Y, Liu X, Wu K.** 2015. Arabidopsis BREVIPEDICELLUS Interacts with the SWI2/SNF2 Chromatin Remodeling ATPase BRAHMA to Regulate KNAT2 and KNAT6 Expression in Control of Inflorescence Architecture. *PLOS Genetics* **11**, e1005125.
- Zhao Y, Medrano L, Ohashi K, Fletcher JC, Yu H, Sakai H, Meyerowitz EM.** 2004b. HANABA TARANU Is a GATA Transcription Factor That Regulates Shoot Apical Meristem and Flower Development in Arabidopsis[W]. *The Plant Cell* **16**, 2586-2600.
- Zhong J, van Esse GW, Bi X, Lan T, Walla A, Sang Q, Franzen R, von Korff M.** 2021. INTERMEDIUM-M encodes an HvAP2L-H5 ortholog and is required for inflorescence indeterminacy and spikelet determinacy in barley. *Proc Natl Acad Sci U S A* **118**.
- Zhou L, Zhu C, Fang X, Liu H, Zhong S, Li Y, Liu J, Song Y, Jian X, Lin Z.** 2021. Gene duplication drove the loss of awn in sorghum. *Molecular Plant* **14**, 1831-1845.

-
- Zhou Y, Zhou B, Pache L, Chang M, Khodabakhshi AH, Tanaseichuk O, Benner C, Chanda SK.** 2019. Metascape provides a biologist-oriented resource for the analysis of systems-level datasets. *Nature Communications* **10**.
- Zhu H, Hu F, Wang R, Zhou X, Sze S-H, Liou W, Lisa, Barefoot A, Dickman M, Zhang X.** 2011. Arabidopsis Argonaute10 Specifically Sequesters miR166/165 to Regulate Shoot Apical Meristem Development. *Cell* **145**, 242-256.
- Zhu Y, Wagner D.** 2020. Plant Inflorescence Architecture: The Formation, Activity, and Fate of Axillary Meristems. *Cold Spring Harbor Perspectives in Biology* **12**, a034652.
- Zwitek M, Waugh R, Mckim SM.** 2019. Interaction between row-type genes in barley controls meristem determinacy and reveals novel routes to improved grain. *New Phytologist* **221**, 1950-1965.

9. Appendix

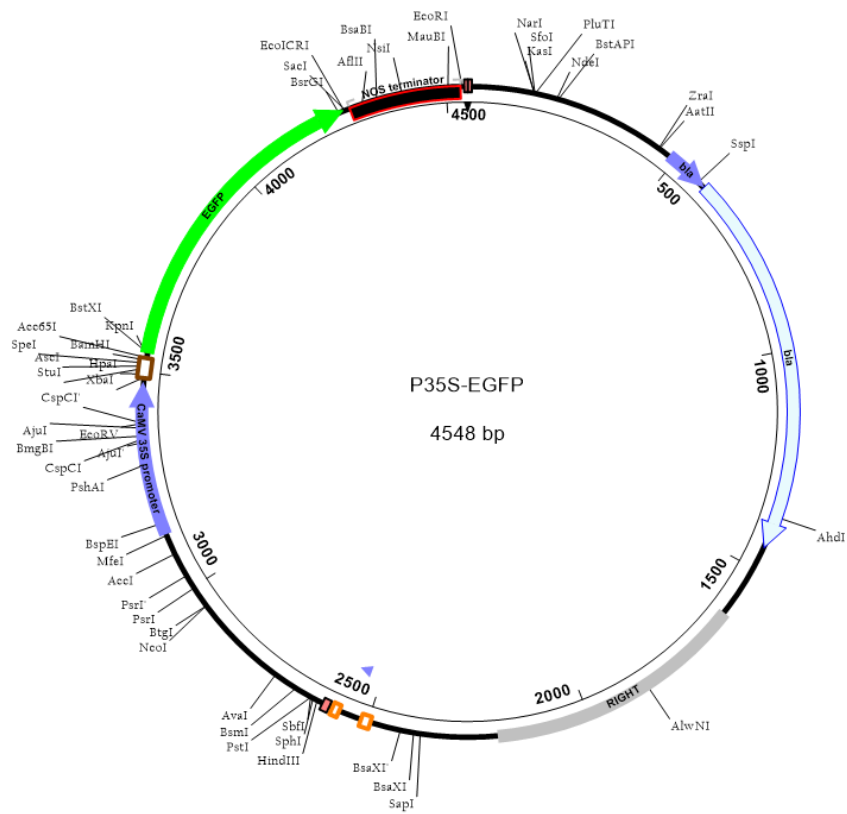


Figure S2.1. The vector model of P35S-EGFP was used to generate a HvALOG1-GFP transient expression construct. CaMV 35S promoter and EGFP are represented by blue and green.



Figure S3.1. The extra spikelets with different degrees of floral organ distortion. Bar=10 mm.

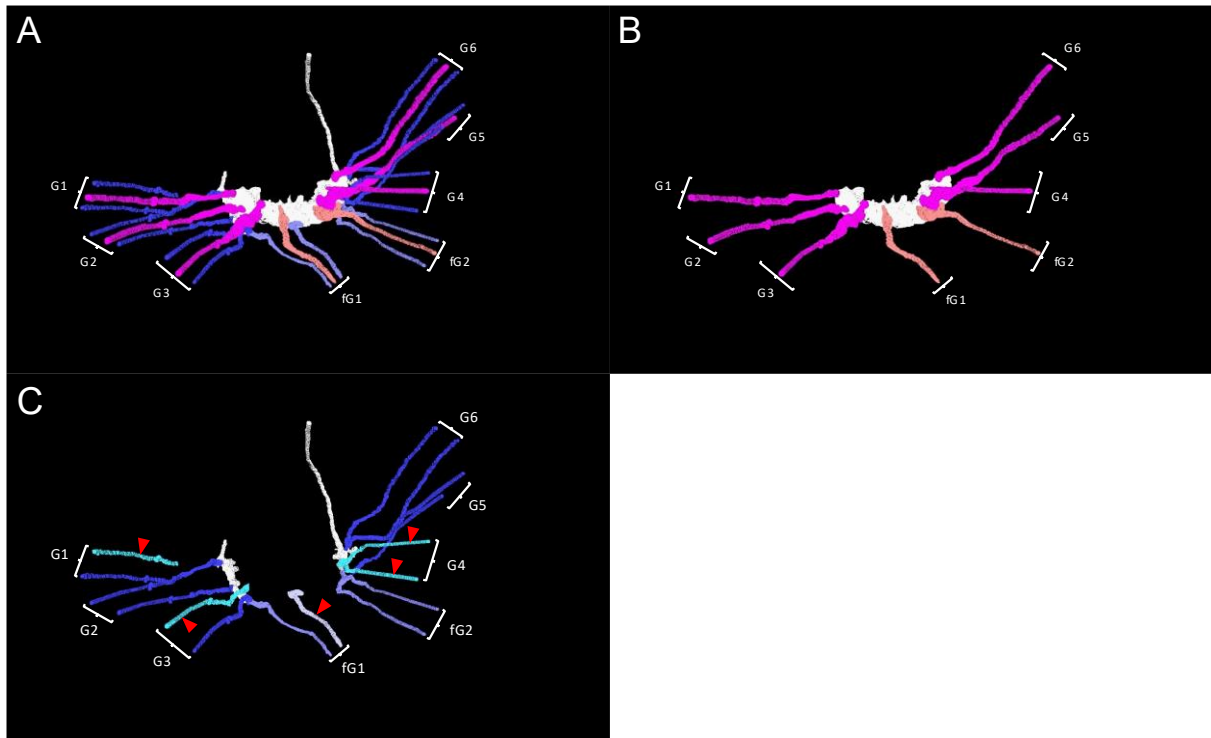
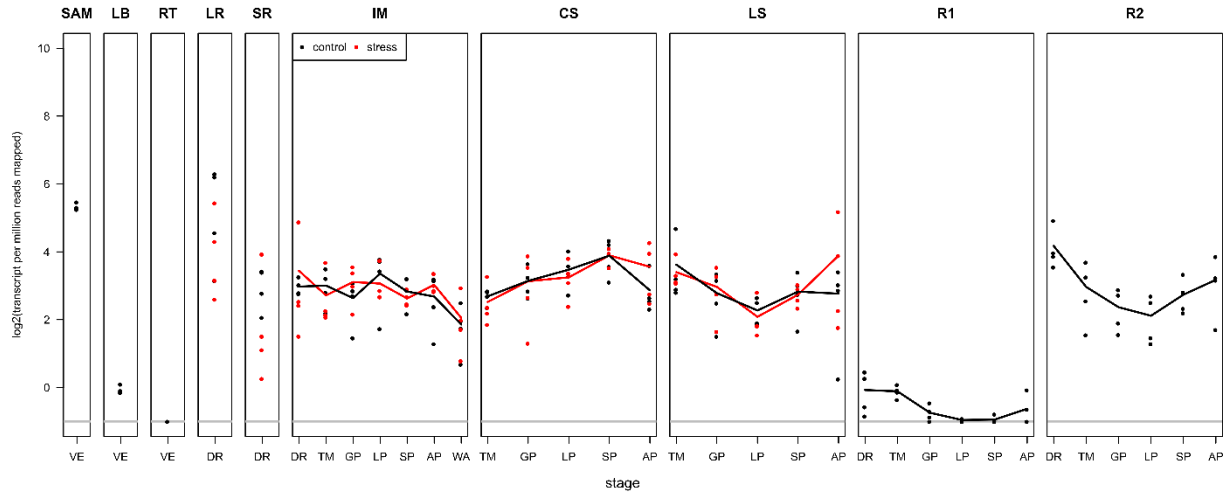


Figure S3.2. The connection status of vascular bundles of glumes to the rachis node in *flo.a* mutant. (A) The overall model of vascular bundles of glumes connected to rachis node system. (B) The model of central vascular bundles of glumes connected to the nodal complex. (C) The lateral vascular bundles of glumes connected to the peripheral network. The normal central and lateral vascular bundles of glumes from triple spikelets are marked by purple and dark blue, respectively. The central and lateral vascular bundles of glumes from extra spikelets are represented by pink and light blue, respectively. the unconnected vascular bundles of glumes from triple spikelets and extra spikelet are marked by blue and gray, respectively as well as by red triangles. The white structure represents the node complex. (G1 to G6) indicate the glume vascular bundles of the triple spikelet. (fG2 and fG2) indicate the glume vascular bundles of the extra spikelet.

*Hv*ALOG1



*Hv*ALOG2

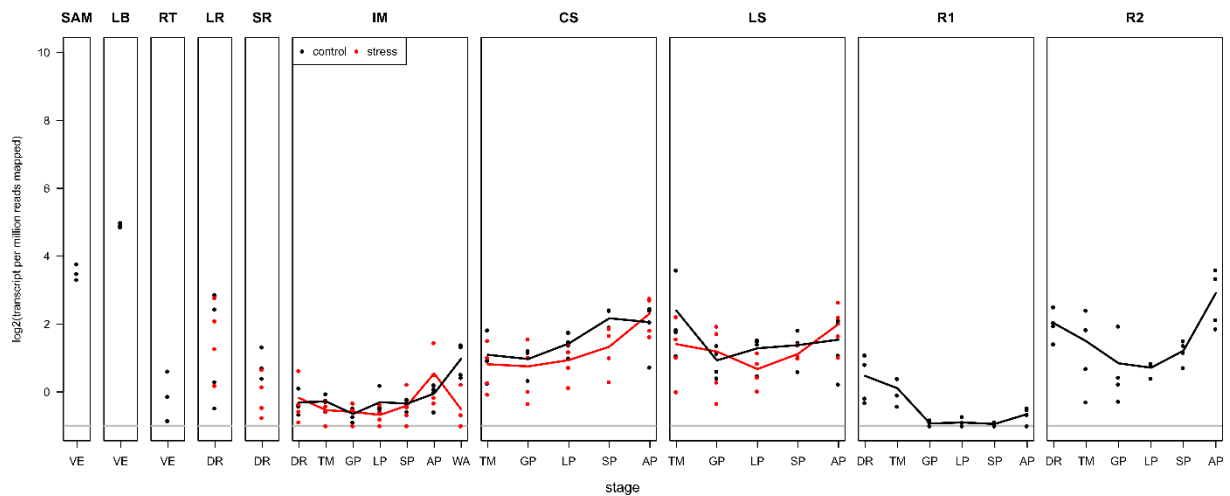


Figure S3.3. The expression pattern of *Hv*ALOG1 and *Hv*ALOG2, respectively. SAM, Shoot apical meristem; LB, Leaf blade; RT, Root tips; SR, Spikelet ridge; LR, Leaf ridge; IM, Inflorescence meristem; CS, Central spikelet; LS, Lateral spikelet; R1, Control 1 (Rachis tissue); R2, Control 2 (Whole spikelet tissue); VE, Vegetative stage; DR, Double ridge; TM, Triple mound; GP, Glume primordium; LP, Lemma primordium; SP, Stamen primordium; AP, Awn primordium; WA, White anther. The black and red line indicates the data from barley plants in normal and light shading conditions, respectively.

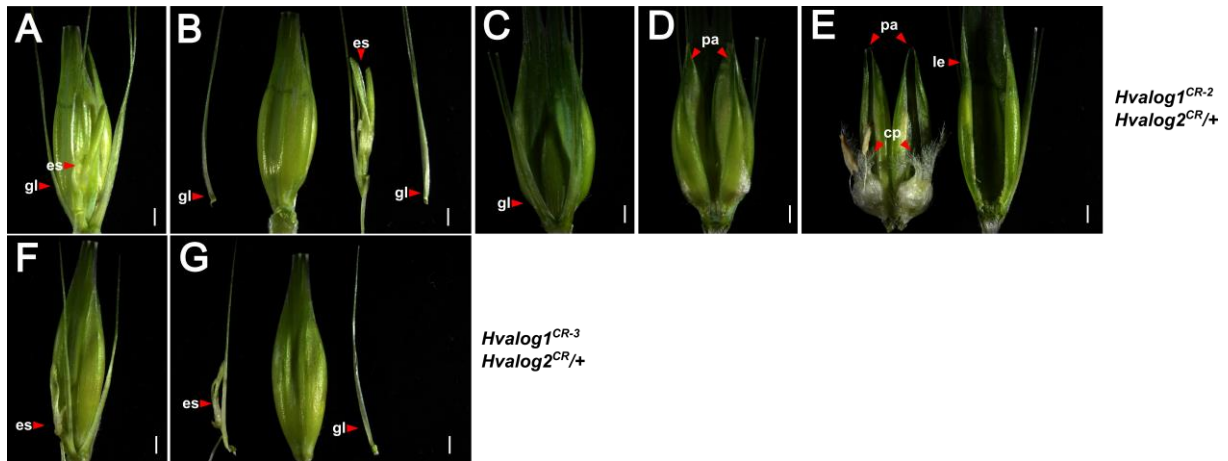


Figure S3.4. The phenotype of transgenic T1 plants of *Hvalog1* and *Hvalog2* by CRISPR-Cas9. (A to E) Representative spikelet images of homozygous *Hvalog1^{CR-2}* and heterozygous *Hvalog2* mutant combination; (C and D) are abaxial and adaxial views from the same spikelet, respectively. (F to G) Representative spikelet images of homozygous *Hvalog1^{CR-3}* and heterozygous *Hvalog2* mutant combination. The dissected floral organs of the spikelet in A, D and F are shown in B, E and G, respectively. es, extra spikelet; gl, glume; le, lemma; pa, palea; cp, carpel. Bar = 1 mm.

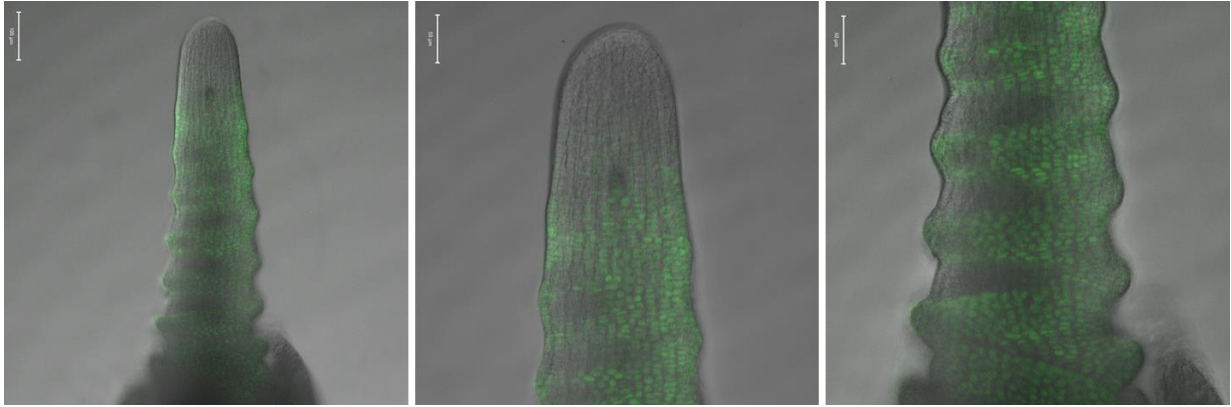


Figure S3.5. Expression pattern of HvALOG1 protein in early DR (W1.5) stage. Accumulation of the HvALOG1 protein in *HvALOG1-p::HvALOG1:GFP* transgenic lines. The middle and right images are partial enlargements of the left image.

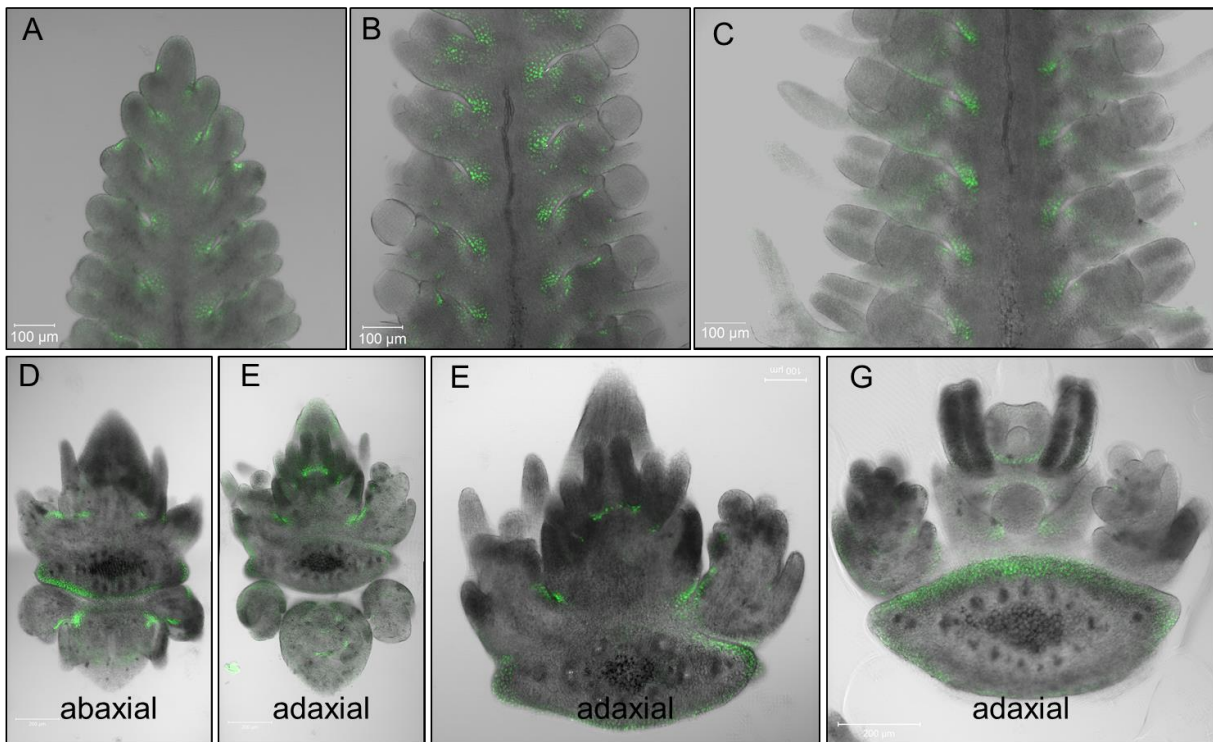


Figure S3.6. Expression pattern of HvALOG1 protein at the AP stage. (A to C) Accumulation of the HvALOG1 protein in different parts of spike from apical to basal in *HvALOG1-p::HvALOG1:GFP* transgenic lines. (D to G) Accumulation of the *HvALOG1* protein in floral organs of spikelet.

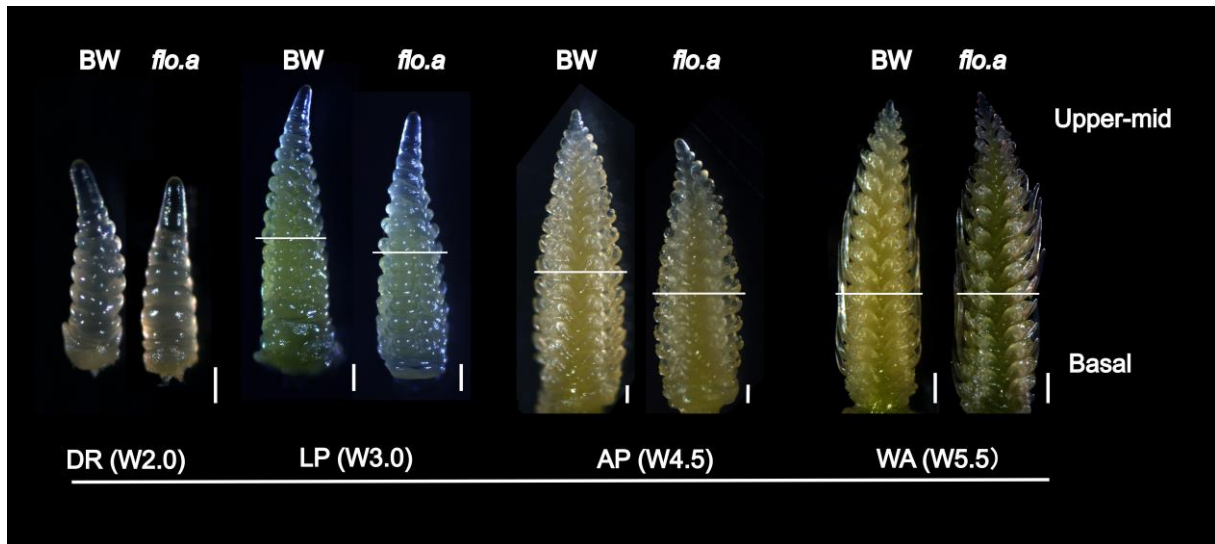


Figure S3.7. Sampling details in the transcriptomic study. Spike sections were hand-dissected with a scalpel based on the positional distribution of extra spikelets event. Bars: 200 μm at the DR, LP and AP stages; 500 μm at the WA stage.

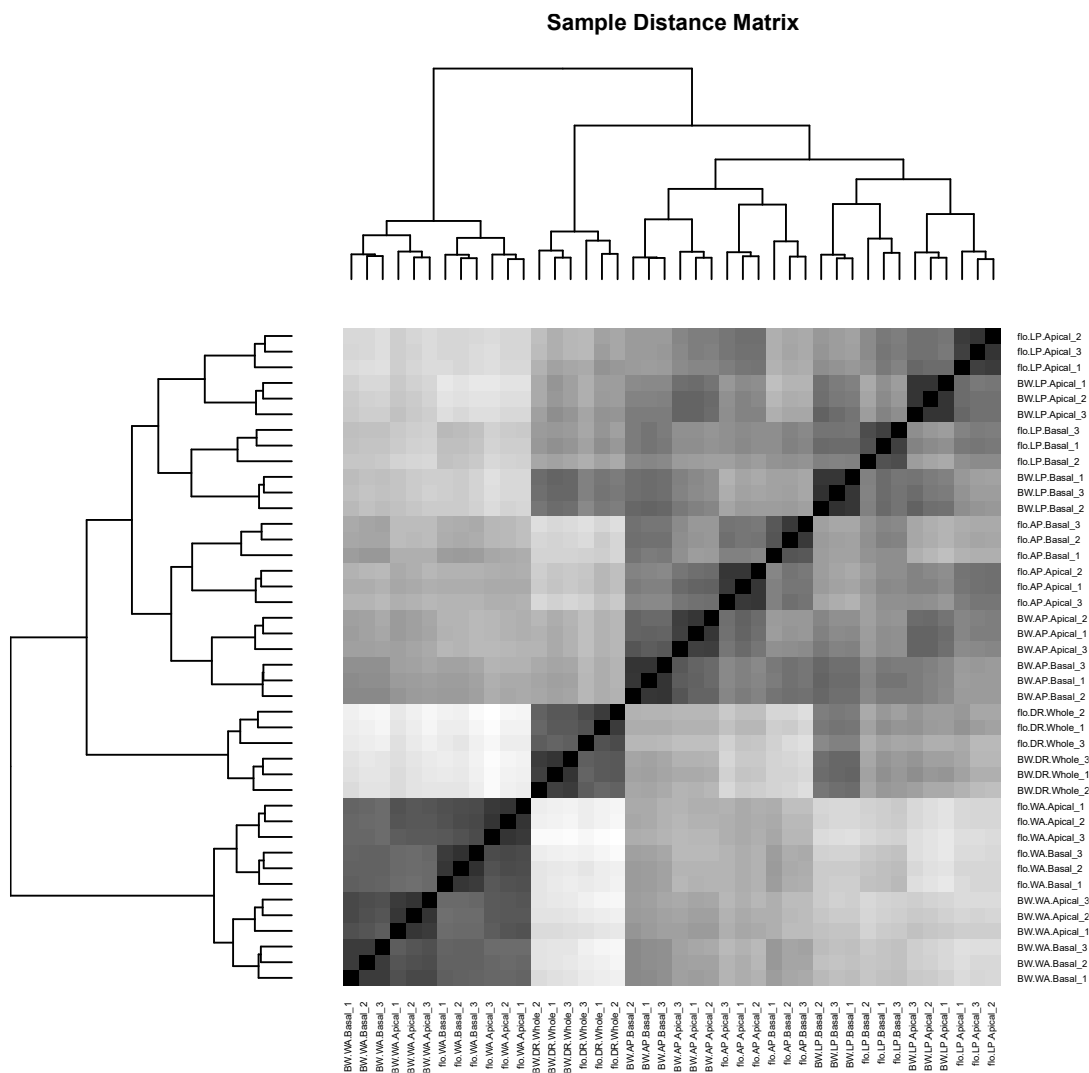


Figure S3.8. Sample distance matrix of RNA seq data.

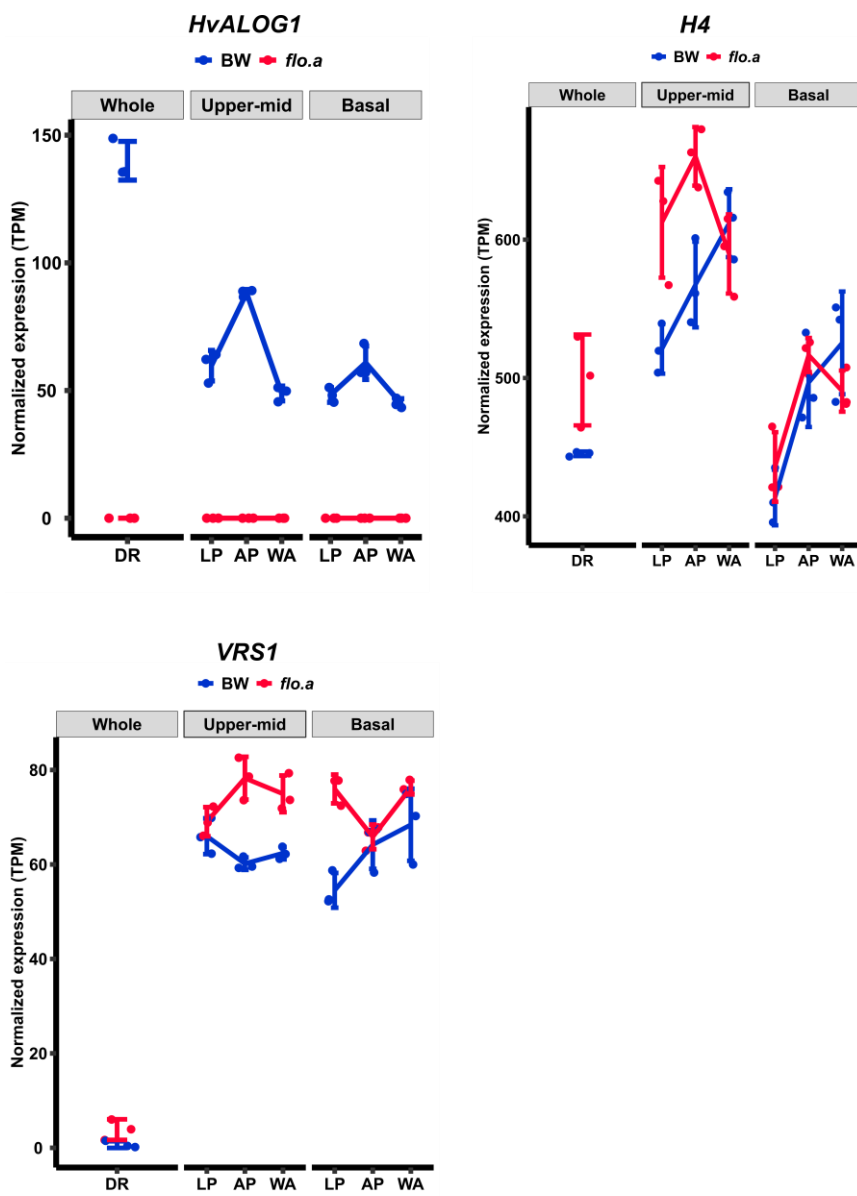


Figure S3.9. Expression pattern of *HvALOG1*, *H4* and *VRS1* in RNA-seq dataset.

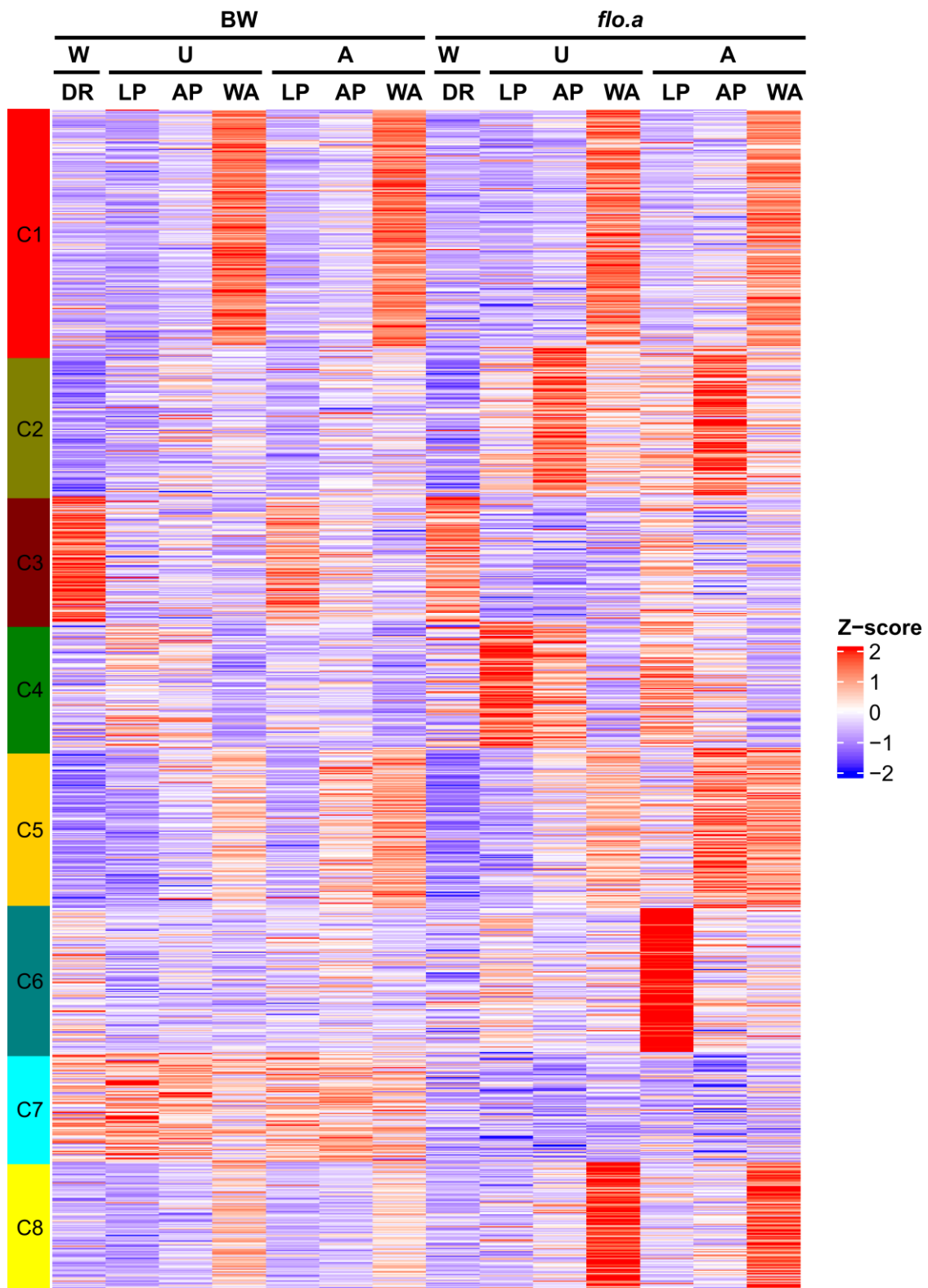
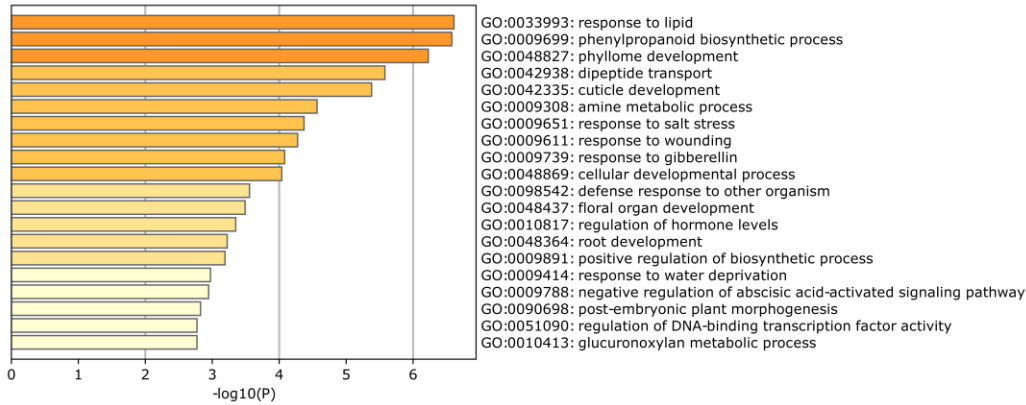
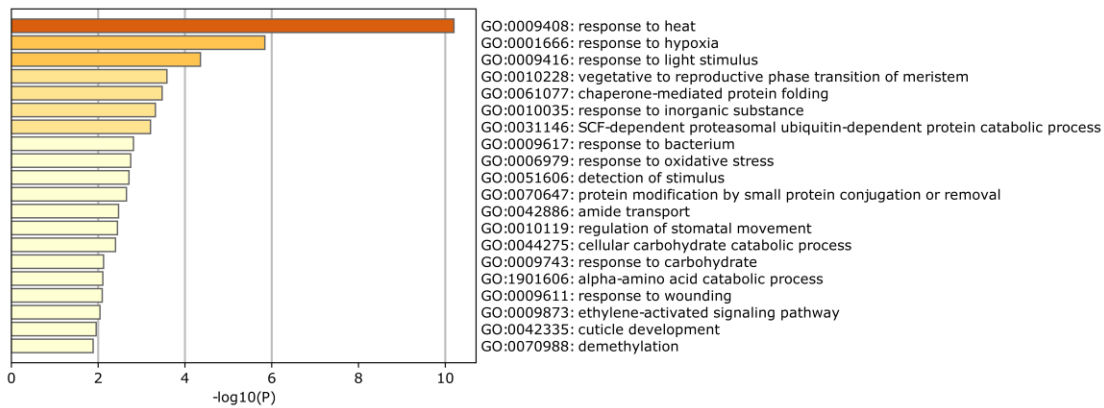


Figure S3.10. Heatmap of DEGs from the pairwise comparison between BW and *flo.a* mutant. The transcript levels were normalized by Z-score method. The blocks with different colors indicate eight clusters, respectively. W, whole spike; U, upper-mid; B, basal.

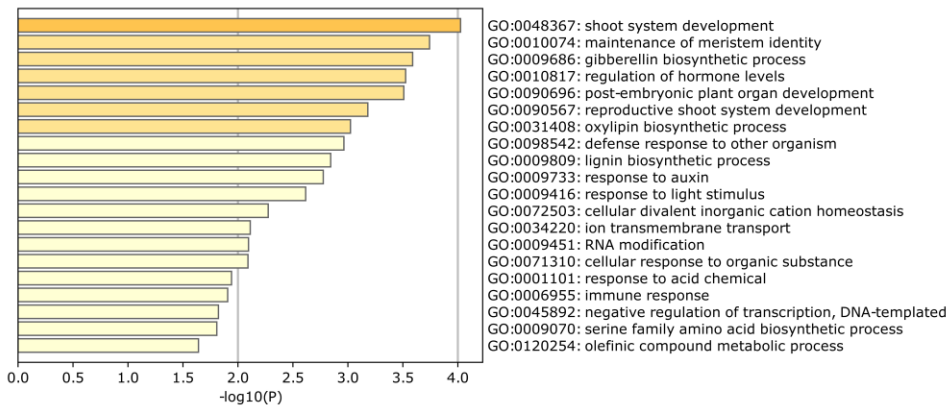
C1



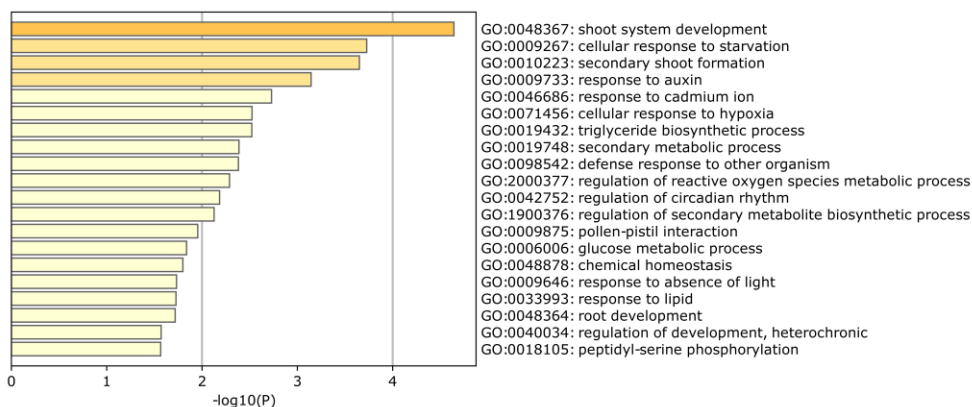
C2



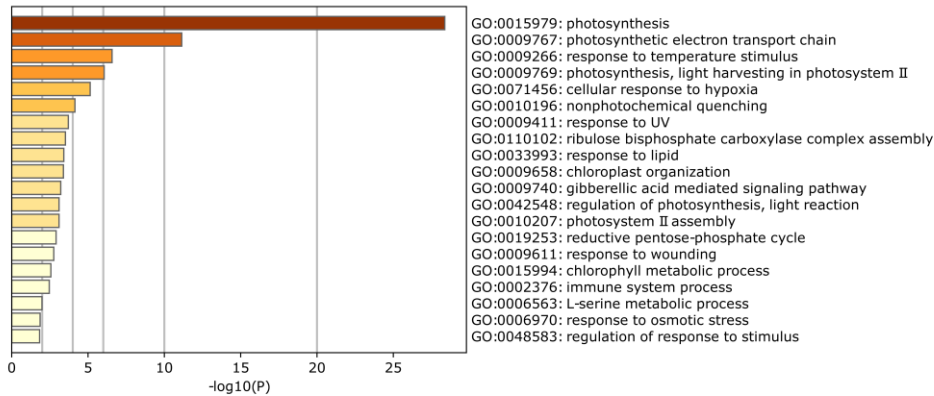
C3



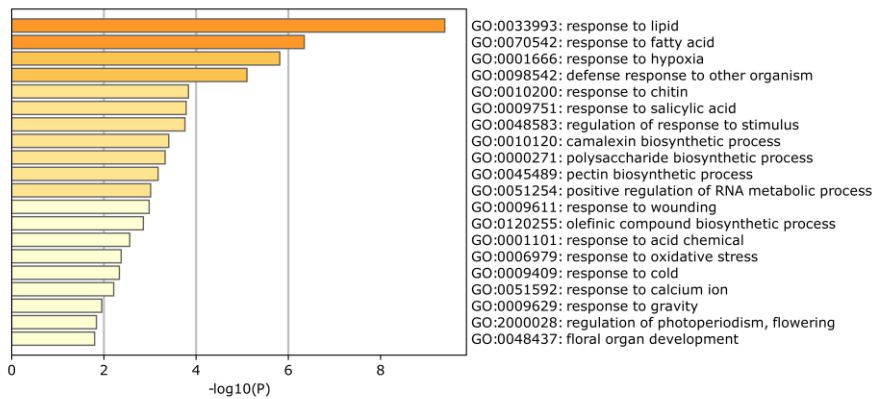
C4



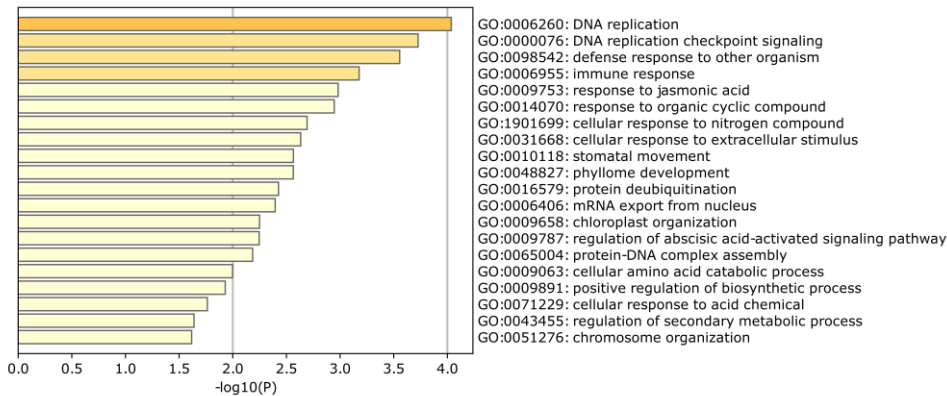
C5



C6



C7



C8

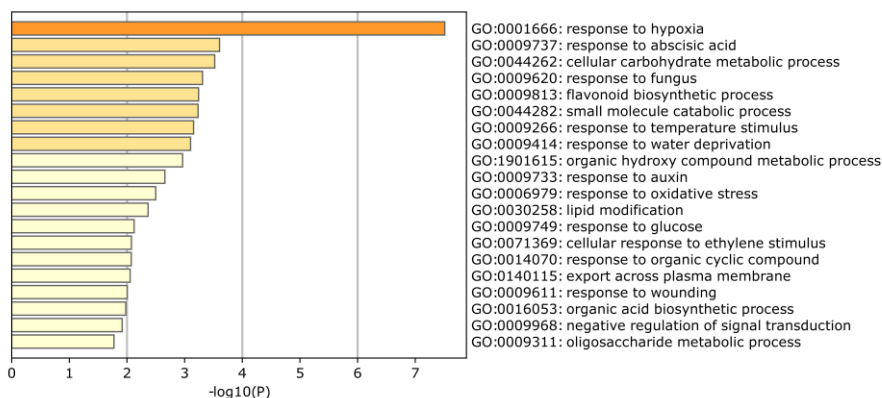


Figure S3.11. Selected GO terms of genes from all 8 clusters.

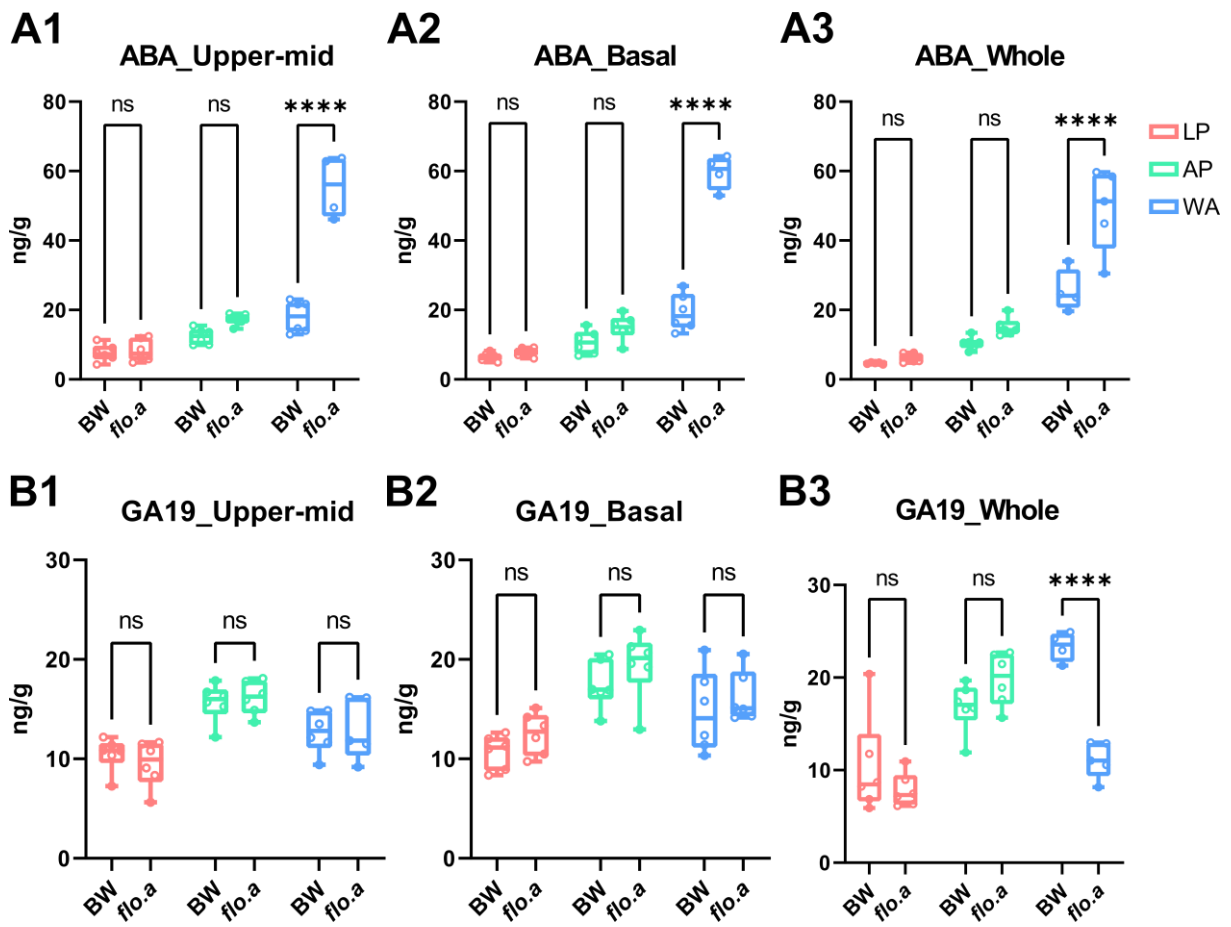


Figure S3.12. Accumulation of ABA and GA19 between BW and *flo.a*. N = 4 to 6 biological replicates. The P-values indicate the results from pairwise comparisons using two-way ANOVA tests.

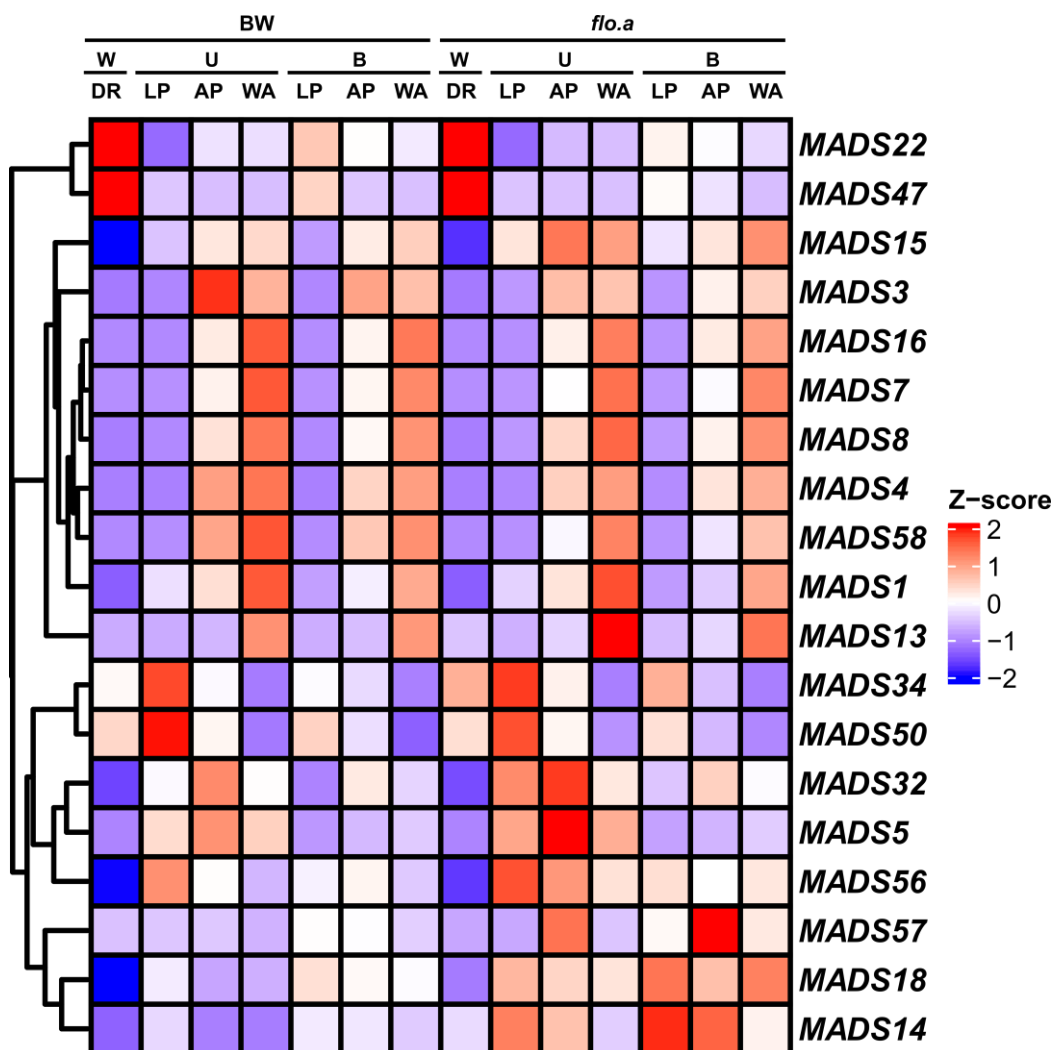


Figure S3.13. Expression pattern of MADS-Box genes in BW and *flo.a* mutant. W, whole spike; U, upper-mid; B, basal.

Table S1: List of the primers used in this study (shown from 5'- to 3'- ends)

Name	Sequence (5'-3')	Usage
bw-flo.a-115.0-F	TGCACTCTCGTGTGTGCAT	Mapping
bw-flo.a-115.0-R	TGGCTAGCTCGCAGCAATTA	Mapping
bw-flo.a-83.7-F	ACTGATCAGCCATCAAGTTGC	Mapping
bw-flo.a-83.7-R	ACACCTCAAGCACAACAAGTC	Mapping
bw-flo.a-105.2-F	GTGTGTTTGC GGAAGCGTAG	Mapping
bw-flo.a-105.2-R	GCATCGCTCCCTAAATCGGA	Mapping
bw-flo.a-74.4-F	GAGAAGCCAGCGAAACATCG	Mapping
bw-flo.a-74.4-R	CCGTTCTCTCGTGCTCTTT	Mapping
bw-flo.a-98.8-F	CAATCCCCTGACAGAGTCGG	Mapping
bw-flo.a-98.8-R	TCTCTATGCAGCACACGTCA	Mapping
bw-flo.a-91.4-F	AGCACGGAGTTGGTTACCTG	Mapping
bw-flo.a-91.4-R	TTACAAGGGCACAGCAAGCA	Mapping
bw-flo.a-110.4-F	TGGACACACATGGGCAATCA	Mapping
bw-flo.a-110.4-R	TGGACTCAGAACGGACAACG	Mapping
bw-flo.a-105-F	CAAATGGCGTGACGACCAAG	Mapping
bw-flo.a-105-R	TGGCATTTCATCGGTGCAGA	Mapping
bw-flo.a-97.4-F	CTGGGGAAACCGCATTGTTG	Mapping
bw-flo.a-97.4-R	TACCATCAAGGTCCCTGGCA	Mapping
bw-flo.a-92.3-F	CCTTCACCAGCCGAGATTGT	Mapping
bw-flo.a-92.3-R	TTGATGTCCCATGAGGGTGC	Mapping
bw-flo.a-99-F	CTAGCCCCATGTCACGC	Mapping
bw-flo.a-99-F-R	GTGCCAGTTCCTGCTTGTG	Mapping
bw-flo.a-100-F	GCCGTCTACTTTGGGGTTGA	Mapping
bw-flo.a-100-R	AAGTATACGAGGTGGCAGCG	Mapping
bw-flo.a-104.3-F	TGATGCTCCATAGCACTGCC	Mapping
bw-flo.a-104.3-R	GTGTGTTTGC GGAAGCGTAG	Mapping
Sense-HvALOG1-F	TAATACGACTCACTATAGGGATCGCCTACGAGAAGAAGCG	mRNA <i>in situ</i> hybridization
Sense-HvALOG1-R	AGTGTCCCTGGAAAAGGTGC	mRNA <i>in situ</i> hybridization
Anti-Sense-HvALOG1-F	ATCGCCTACGAGAAGAAGCG	mRNA <i>in situ</i> hybridization
Anti-Sense-HvALOG1-R	TAATACGACTCACTATAGGGAGTGTCCCTGGAAAAGGTGC	mRNA <i>in situ</i> hybridization
Sense-ALOG4-F	TAATACGACTCACTATAGGGTCACTCGCTTTCTGTGGTC	mRNA <i>in situ</i> hybridization
Sense-ALOG4-R	GTCAAGGTAGCGCAGGAACT	mRNA <i>in situ</i> hybridization
Anti-Sense-ALOG4-F	TCACCTCGCTTTCTGTGGTC	mRNA <i>in situ</i> hybridization
Anti-Sense-ALOG4-R	TAATACGACTCACTATAGGGGTCAAGGTAGCGCAGGAACT	mRNA <i>in situ</i> hybridization

Sense-HvHistone4-F	TAATACGACTCACTATAGGGATGTCTGGGCGTGGCAAGGG	mRNA <i>in situ</i> hybridization
Sense-HvHistone4-R	TCAGCCGCCGAAGCCGT	mRNA <i>in situ</i> hybridization
Anti-Sense-HvHistone4-F	ATGTCTGGGCGTGGCAAGGG	mRNA <i>in situ</i> hybridization
Anti-Sense-HvHistone4-R	TAATACGACTCACTATAGGGTCAGCCGCCGAAGCCGT	mRNA <i>in situ</i> hybridization
HvALOG1_3UTR-1F	GACCATGAGGCTGGGTCTC	Amplification
HvALOG1_3UTR-1R	CCGCCTGAAGATCATACGCT	Amplification
HvALOG1_3UTR-2F	AGCTTCCTTCTCCCTCCCTG	Amplification
HvALOG1_cds-F	ATGGACATGTCTGGGCGTGAG	Amplification
HvALOG1_cds-R	CTAATGGAACACGGACAGCG	Amplification
HvALOG4-1-F	GAGGTGAGATTCAGGCCGAC	Amplification
HvALOG4-1-R	CGCTTCTTCTCGTAGGCGAT	Amplification
HvALOG4-cds-F	CTTTTGGTTTCAGGCCGCTC	Amplification
HvALOG4-cds-R	TGCGATTGCATTTGCTAGGAT	Amplification
HvALOG1-pro-cds-seq-1-F	AACAGGTAGTGCGTCTGCTC	Amplification
HvALOG1-pro-cds-seq-2-F	GTGGTCCCGTAGGTAAGTCC	Amplification
HvALOG1-pro-cds-seq-3-F	CTCCACAGACGCACAGTGAT	Amplification
HvALOG1-pro-cds-seq-4-F	GGCACGATGGAGTTGAGTGA	Amplification
HvALOG1pro-cds-seq-5-F	AGCGTGTACGCAGAACTGA	Amplification
flo.a_qPCR_1-F	ATGGACATGTCTGGGCGTGAG	qRT-PCR
flo.a_qPCR_1-R	GTGGTCCCGTAGGTAAGTCC	qRT-PCR
q-HvActin-F	AAGTACAGTGTCTGGATTGGAGGG	qRT-PCR
q-HvActin-R	TCGCAACTTAGAAGCACTTCCG	qRT-PCR
HvALOG1-Guide1-F	TGGCGTCGGCGGTGGCAGCGCCG	CRISPR-cas9
HvALOG1-Guide1-R	AAACCGGCGCTGCCACCGCCGAC	CRISPR-cas9
HvALOG1-Guide2-F	TGGCGTCGGCGGAGGTAGAGCCTCA	CRISPR-cas9
HvALOG1-Guide2-R	AAACTGAGGCTCTACCTCCGCGAC	CRISPR-cas9
HvALOG2-Guide1-F	TGGCAGCGCTGGTGGACAGCCCGG	CRISPR-cas9
HvALOG2-Guide1-R	AAACCCGGGCTGTCCACCAGCGCT	CRISPR-cas9
HvALOG2-Guide2-F	TGGCACC GCGAGAGCTCCAGCGGC	CRISPR-cas9
HvALOG2-Guide2-R	AAACGCCGCTGGAGCTCTCGCGGT	CRISPR-cas9
flo.a-PUC_CMF4_GFP_F	TTGGAGAGAACACGGGGGACTCTAGAATGGACATGTCTGGCG TGAG	Subcellular localization
flo.a-PUC_CMF4_GFP_R	CTCACCATTGATATGGTACCGGATCCATGGAACACGGACAGC GGCA	Subcellular localization
mid-HvALOG1-GFP-F	cgctctagaactagtgatccCTTTCATGGTCTCGACGGG	GFP-fusion
mid-HvALOG1-GFP-R	gtcgacggtatcgataagcttTGGAAACACGGACAGCGGC	GFP-fusion
HvALOG1_CDS_GFP-F	ggcgccgcactagtgatccCTTTCATGGTCTCGACGGG	GFP-fusion
HvALOG1_CDS_GFP-R	ctctacgtcgagctagTTACTTGTACAGCTCGTCCATGCC	GFP-fusion
HvALOG1_CDS_GFP-3UTR-F	gtaaCTAGCTCGACGTAGAGAATTAAGTAAGTAG	GFP-fusion

HvALOG1_CDS_GFP-3UTR-R	acgacaatctgatcgggtaccTAGGCGTCACACATCTGCATG	GFP-fusion
------------------------	--	------------

Table S2: Gene information of the ALOG family members in barley

Gene id	name	Chromosome	CDS length
<i>HORVU.MOREX.r2.6HG0469780</i>	<i>HvALOG1</i>	6H	783
<i>HORVU.MOREX.r2.7HG0610530</i>	<i>HvALOG2</i>	7H	810
<i>HORVU.MOREX.r2.6HG0494070</i>	<i>HvALOG3</i>	6H	615
<i>HORVU.MOREX.r2.2HG0150340</i>	<i>HvALOG4</i>	2H	600
<i>HORVU.MOREX.r2.1HG0033520</i>	<i>HvALOG5</i>	1H	621
<i>HORVU.MOREX.r2.6HG0521000</i>	<i>HvALOG6</i>	6H	771
<i>HORVU.MOREX.r2.3HG0253830</i>	<i>HvALOG7</i>	3H	639
<i>HORVU.MOREX.r2.1HG0049440</i>	<i>HvALOG8</i>	1H	861
<i>HORVU.MOREX.r2.1HG0057950</i>	<i>HvALOG9</i>	1H	699
<i>HORVU.MOREX.r2.2HG0126820</i>	<i>HvALOG10</i>	2H	783

Table S3: List of the plant species used in phylogenetic analysis

Species	Lineage	Source	Usage
<i>Hordeum vulgare</i>	Monocots-Poaceae	IPK, Version 2	phylogenetics analysis
<i>Zea mays</i>	Monocots-Poaceae	Ensembl Plants	phylogenetics analysis
<i>Oryza sativa</i>	Monocots-Poaceae	Ensembl Plants	phylogenetics analysis
<i>Sorghum bicolor</i>	Monocots-Poaceae	Ensembl Plants	phylogenetics analysis
<i>Triticum aestivum</i>	Monocots-Poaceae	Ensembl Plants	phylogenetics analysis
<i>Brachypodium distachyon</i>	Monocots-Poaceae	Ensembl Plants	phylogenetics analysis
<i>Setaria viridis</i>	Monocots-Poaceae	Ensembl Plants	phylogenetics analysis
<i>Secale cereale</i>	Monocots-Poaceae	Ensembl Plants	phylogenetics analysis
<i>Gossypium raimondii</i>	Eudicots - Malvaceae	Ensembl Plants	phylogenetics analysis
<i>Glycine max</i>	Eudicots - Fabaceae	Ensembl Plants	phylogenetics analysis
<i>Arabidopsis thaliana</i>	Eudicots - Brassicaceae	Ensembl Plants	phylogenetics analysis
<i>Brassica rapa</i>	Eudicots - Brassicaceae	Ensembl Plants	phylogenetics analysis
<i>Populus trichocarpa</i>	Eudicots - Salicaceae	Ensembl Plants	phylogenetics analysis
<i>Solanum lycopersicum</i>	Eudicots - Solanaceae	Ensembl Plants	phylogenetics analysis

Table S4: List of the selected genes in DEGs.

Gene	<i>Arabidopsis</i> _id	More_V2 ID	Function
<i>CUC2</i>	AT5G53950	HORVU.MOREX.r2.7HG0590600	Organ boundary
<i>KNAT1/BP-like 1</i>	AT4G08150	HORVU.MOREX.r2.4HG0282910	Organ boundary
<i>KNAT1/BP-like 2</i>	AT4G08150	HORVU.MOREX.r2.5HG0426660	Organ boundary
<i>HvLG1</i>	AT1G02065	HORVU.MOREX.r2.2HG0168480	Organ boundary
<i>SUP-like</i>	AT3G23130	HORVU.MOREX.r2.1HG0070090	Organ boundary
<i>ATHB1</i>	AT4G32980	HORVU.MOREX.r2.7HG0595310	Organ boundary
<i>PAN</i>	AT1G68640	HORVU.MOREX.r2.3HG0246180	Organ boundary
<i>LOF2</i>	AT5G17800	HORVU.MOREX.r2.3HG0213150	Meristem identity and determinacy
<i>Vrs4/HvRA2</i>	AT5G63090	HORVU.MOREX.r2.3HG0194160	Meristem identity and determinacy
<i>AFO</i>	AT4G00180	HORVU.MOREX.r2.2HG0152680	Meristem identity and determinacy
<i>HvAP2L-5H</i>	AT4G36920	HORVU.MOREX.r2.5HG0437030	Meristem identity and determinacy
<i>INT-C/HvTB1</i>	AT1G68800	HORVU.MOREX.r2.4HG0280760	Meristem identity and determinacy
<i>MADS5</i>	AT5G15800	HORVU.MOREX.r2.7HG0543420	Meristem and organ development
<i>MADS56</i>	AT2G45660	HORVU.MOREX.r2.1HG0042540	Meristem and organ development
<i>MADS32</i>	AT3G57230	HORVU.MOREX.r2.3HG0237490	Meristem and organ development
<i>MADS57</i>	AT3G57230	HORVU.MOREX.r2.6HG0507700	Meristem and organ development
<i>ROXY2-like</i>	AT5G14070	HORVU.MOREX.r2.2HG0126030	Meristem and organ development
<i>MS35</i>	AT3G13890	HORVU.MOREX.r2.3HG0235620	Meristem and organ development
<i>MYB36</i>	AT5G57620	HORVU.MOREX.r2.7HG0602600	Meristem and organ development
<i>PEP-like</i>	AT4G26000	HORVU.MOREX.r2.6HG0458420	Meristem and organ development
<i>PRE5</i>	AT3G28857	HORVU.MOREX.r2.4HG0336070	Meristem and organ development
<i>PRE6-like</i>	AT1G26945	HORVU.MOREX.r2.7HG0552630	Meristem and organ development
<i>RAP2.6L</i>	AT5G13330	HORVU.MOREX.r2.2HG0135520	Meristem and organ development
<i>PRX17</i>	AT2G22420	HORVU.MOREX.r2.5HG0404500	Meristem and organ development
<i>FD-like</i>	AT4G35900	HORVU.MOREX.r2.2HG0167560	Meristem and organ development
<i>FPP1-like 1</i>	AT5G24860	HORVU.MOREX.r2.2HG0083830	Meristem and organ development
<i>FPP1-like 2</i>	AT5G24860	HORVU.MOREX.r2.2HG0083880	Meristem and organ development
<i>ARF16</i>	AT4G30080	HORVU.MOREX.r2.2HG0150790	Auxin signaling
<i>IAA3-like</i>	AT1G04240	HORVU.MOREX.r2.5HG0422780	Auxin signaling
<i>IAA4-like</i>	AT5G43700	HORVU.MOREX.r2.6HG0520360	Auxin signaling
<i>IAA17-like</i>	AT1G04250	HORVU.MOREX.r2.1HG0021490	Auxin signaling
<i>SAUR40-like</i>	AT1G79130	HORVU.MOREX.r2.2HG0157620	Auxin signaling
<i>SAUR69-like</i>	AT5G10990	HORVU.MOREX.r2.2HG0167490	Auxin signaling
<i>SAUR71</i>	AT1G56150	HORVU.MOREX.r2.4HG0277800	Auxin signaling
<i>GH3.1-like</i>	AT2G14960	HORVU.MOREX.r2.2HG0106420	Auxin signaling
<i>GH3.2</i>	AT4G37390	HORVU.MOREX.r2.3HG0242100	Auxin signaling
<i>GH3.6 like 1</i>	AT5G54510	HORVU.MOREX.r2.1HG0054200	Auxin signaling
<i>GH3.6 like 2</i>	AT5G54510	HORVU.MOREX.r2.3HG0244730	Auxin signaling
<i>PIN3</i>	AT1G70940	HORVU.MOREX.r2.1HG0059860	Auxin signaling

Table S5: Summary of amino acid variation in 20 pan-genome accessions.

Accession	Status	Row-type	Country of origin	aa position (175/261)
Akashinriki	cultivar	six-rowed	Japan	A
B1K_04_12	wild	two-rowed	Israel	A
Barke	cultivar	two-rowed	Germany	T
Golden Promise	cultivar	two-rowed	Europe	T
Hockett	cultivar	two-rowed	USA	T
HOR_10350	landrace	six-rowed	Ethiopia	T
HOR_13821	landrace	two-rowed	Turkey	A
HOR_13942	landrace	six-rowed	Southern Europe	A
HOR_21599	landrace	two-rowed	Syria	T
HOR_3081	cultivar	six-rowed	Poland	A
HOR_3365	landrace	six-rowed	Russia	A
HOR_7552	landrace	six-rowed	Pakistan	A
HOR_8148	landrace	two-rowed	Turkey	A
HOR_9043	landrace	six-rowed	Ethiopia	T
Igri	cultivar	two-rowed	Germany	A
Morex	cultivar	six-rowed	USA	A
OUN333	landrace	intermedium	Nepal	A
RGT_Planet	cultivar	two-rowed	Australia	T
ZDM01467	landrace	six-rowed	China	A
ZDM02064	landrace	six-rowed	China	A

10. Curriculum Vitae

Name: Guojing Jiang

Education

Ph.D. candidate for plant genetics (September 2017 – Present)
Leibniz Institute of Plant Genetics and Crop Plant Research (IPK), Germany

Major: plant genetics
Supervisor: Prof. Dr. Thorsten Schnurbusch

Thesis title: “HvALOG1, an ALOG Transcription Factor Regulates Spikelet Meristem Determinacy and Organ Boundary Formation in the Barley Inflorescence”.

Master of Agriculture (September 2014 - June 2017)

Rice Research Institute, Sichuan Agricultural University, China
Major: Crop Genetics and Breeding
Supervisor: Prof. Dr. Shigui Li

Thesis title: “QTL Analysis of Flag Leaf Shape and Fine Mapping of qFLW1 in Heavy Panicle Rice”.

Bachelor of Agriculture (September 2010- June 2014)

College of Animal Science and Technology, Sichuan Agricultural University, China
Major: Grassland Science

Publications

Guojing Jiang, Ravi Koppolu, Twan Rutten, Goetz Hensel, Udda Lundqvist, Yudelsy Antonia Tandron Moya, Yongyu Huang, Jeyaraman Rajaraman, Naser Poursarebani, Nicolaus von Wirén, Jochen Kumlehn, Martin Mascher, Thorsten Schnurbusch. Non-cell Autonomous Signaling Associated with Barley ALOG1 Specifies Spikelet Meristem Determinacy. *Current Biology*. (***Under review***)

Guojing Jiang, Yongyu Huang, Ravi Koppolu, Roop Kamal, Murukarthick Jayakodi, Martin Mascher, Thorsten Schnurbusch. Genome-Wide Association Study and Haplotype Analysis Reveal Genetic Control of Rachilla Extension in Barley. (***in preparation***)

Koppolu R, Jiang G, Milner SG, Muqaddasi QH, Rutten T, Himmelbach A, Guo Y, Stein N, Mascher M, Schnurbusch T. 2021. The barley mutant *multiflorus2.b* reveals

quantitative genetic variation for new spikelet architecture. *Theoretical and Applied Genetics*. # **co-first**

Wang S, Ma B, Gao Q, Jiang G, Zhou L, Tu B, Qin P, Tan X, Liu P, Kang Y, Wang Y, Chen W, Liang C, Li S. 2018. Dissecting the genetic basis of heavy panicle hybrid rice uncovered *Gn1a* and *GS3* as key genes. *Theoretical and Applied Genetics* 131, 1391-1403.

11. Eidesstattliche Erklärung/Declaration under Oath

Ich erkläre an Eides statt, dass ich die Arbeit selbstständig und ohne fremde Hilfe verfasst, keine anderen als die von mir angegebenen Quellen und Hilfsmittel benutzt und die den benutzten Werken wörtlich oder inhaltlich entnommenen Stellen als solche kenntlich gemacht habe.

I declare under penalty of perjury that this thesis is my own work entirely and has been written without any help from other people. I used only the sources mentioned and included all the citations correctly both in word or content.

Datum / Date

Unterschrift des Antragstellers /

Signature of the applicant

12. Erklärung über bestehende Vorstrafen und anhängige Ermittlungsverfahren/Declaration concerning Criminal Record and Pending Investigations

Hiermit erkläre ich, dass ich weder vorbestraft bin noch dass gegen mich Ermittlungsverfahren anhängig sind.

I hereby declare that I have no criminal record and that no preliminary investigations are pending against me.

Datum / Date

Unterschrift des Antragstellers /
Signature of the applicant